FRAGILE X-ASSOCIATED TREMOR/ATAXIA SYNDROME: RNA OR RAN?

Ronald Adrianus Maria Buijsen

The work described in this thesis was performed at the Department of Clinical Genetics, Erasmus MC, the Netherlands.

The studies presented in this thesis were financially supported by:
Dutch Brain Foundation project number F2012(1)-101

The production costs of this thesis were supported by:
Erasmus University, Rotterdam, the Netherlands
Department of Clinical Genetics, Erasmus MC, Rotterdam, the Netherlands
Fragiele X Vereniging Nederland

ISBN: 978-94-6182-685-5
Author: Ronald A.M. Buijsen
Cover: Lies-Anne Severijnen and Tom de Vries-Lentsch
Chapter illustrations: Sofie and Wouter Buijsen
Layout: Ronald A.M. Buijsen and Off Page, Amsterdam
Printing: Off Page, Amsterdam

FRAGILE X-ASSOCIATED TREMOR/ATAXIA SYNDROME: RNA OR RAN?

Fragiele X-geassocieerd tremor/ataxie syndroom:
RNA of RAN?

Proefschrift

ter verkrijging van de graad van doctor aan de
Erasmus Universiteit Rotterdam
op gezag van de
rector magnificus

Prof.dr. H.A.P. Pols
en volgens besluit van het College voor Promoties.

De openbare verdediging zal plaatsvinden op
woensdag 22 juni 2016 om 13:30 uur

door

Ronald Adrianus Maria Buijsen

geboren te Bergen op Zoom

Erasmus University Rotterdam

PROMOTIECOMMISSIE

Promotor:	Prof.dr. R. Willemsen
Overige leden:	Prof.dr. R.F. Kooy
	Prof.dr. J.M. Kros
	Dr. N. Charlet-Berguerand
Copromotor:	Dr. R.K. Hukema

TABLE OF CONTENTS

LIST OF ABBREVIATIONS

AAV	adeno-associated viral
ADHD	attention-deficit hyperactivity disorder
ALS	amyotrophic lateral sclerosis
AMPA	α-amino-3-hydroxy-5-methyl-4-isoxazole propionic acid
AON	antisense oligonucleotides
ASD	autism spectrum disorder
ATPB	β-subunit of ATP synthase
ATR	Ataxia-telangiectasia and rad3-related (ATR)
BDS	behavioural dyscontrol scale
C9FTD	chromosome 9 open reading frame 72 frontotemporal dementia
CamKII	Ca2+/calmodulin-dependent protein kinase II
Cas9	CRISPR-associated 9
CB	clustered burst
CCS	splenium of the corpus callosum
CNS	central nervous system
CRISPR	clustered, regularly interspaced, short palindromic repeat
CSF	cerebrospinal fluid
DBS	deep brain stimulation
DHPG	3,5-dihydroxyphenylglycine
DIV	days in vitro
DMI	myotonic muscular dystrophy type 1
DOX	doxycycline
EGFP	enhanced green fluorescent protein
ELISA	enzyme-linked immunosorbent assay
ES	embryonic stem
FAD	flavin adenine dinucleotide
FCS	fetal calf serum
FMR1	fragile X mental retardation 1
FMRP	fragile X mental retardation protein
FMRpolyA	alanine containing protein
FMRpolyG	polyglycine containing protein
FPM	fragile X premutation
FTD	frontotemporal dementia
FXPOI	fragile X-associated primary ovarian insufficiency
FXS	fragile X syndrome
FXTAS	fragile X-associated tremor/ataxia syndrome
GABA	*gamma*-aminobutyric acid
GFAP	glial fibrillary acidic protein
GPX1	glutathione oxidase
HD	Huntington's disease

HGPS	Hutchinson Gilford progeria syndrome
hnRNP	heterogeneous nuclear ribonucleoprotein
ICV	intracerebroventricular
IF	immunofluorescence
iPSC	induced pluripotent stem cells
IRES	internal ribosome entry site
IT	intrathecal
KI	knock-in
KO	knock-out
LTD	long-term depression
LTP	long-term potentiation
MAP2	microtubule-associated protein 2
MBNL	muscle blind-like protein
MCP	middle cerebellar peduncle
MEF	mouse embryonic fibroblast
mGluR	metabotropic glutamate receptors
miRNA	microRNA
MnSOD	manganese superoxide dismutase
MRCD	mitochondrial respiratory chain enzyme deficiencies
NAD	nicotinamide adenine dinucleotide
NMDA	N-methyl-d-aspartate
NPC	neural progenitor cells
OKR	optokinetic reflex
ORF	open reading frame
PCL	Purkinje cell layer
PLA_2	phospholipase A_2
PM	premutation
POI	premature ovarian insufficiency
PrP	prion protein
PSD95	postsynaptic density protein 95
RAN	repeat-associated non-AUG
RD	restrictive dermopathy
ROS	reactive oxygen species
rtTA	reverse tetracycline-controlled transactivator
SCA8	spinocerebellar ataxia type 8
TRE	tetracycline responsive element
UPS	ubiquitin proteasome system
UTR	untranslated region
VOR	vestibulo-ocular reflex
VZ	ventricular zone
WT	wild-type
YAC	yeast artificial chromosome

SCOPE OF THIS THESIS

Since the discovery of the fragile X-associated tremor/ataxia syndrome (FXTAS), a large number of studies have been performed in order to identify the underlying disease mechanism(s). Two disease mechanisms for FXTAS have been proposed. The first hypothesis is an RNA gain-of-function mechanism in which the *FMR1* RNA, containing an expanded CGG repeat, sequesters RNA-binding proteins. A second proposed mechanism is a repeat-associated non-AUG-initiated (RAN) protein gain-of-function mechanism in which the *FMR1* RNA, containing an expanded repeat, triggers RAN translation of a cryptic polyglycine-containing protein, FMRpolyG. Gaining more mechanistic insight is essential to develop potential targets for future therapeutic intervention studies and to identify new reliable biomarkers.

The general aim of this thesis is to advance our understanding of the molecular mechanisms underlying toxicity of both RNA and RAN in FXTAS using new cellular and FXTAS mouse models. To date, no targeted treatments exist for FXTAS. Thus translational research using mouse and cellular models, as generated and characterized in this thesis, will provide the critical information needed for the development and evaluation of effective therapeutic interventions for FXTAS.

MOUSE MODELS OF THE FRAGILE X PREMUTATION AND FRAGILE X-ASSOCIATED TREMOR/ATAXIA SYNDROME

R.F. Berman[1], **R.A.M. Buijsen**[2], K. Usdin[3], E. Pintado[4], R.F. Kooy[5], D. Pretto[6], I.N. Pessah[7], D.L. Nelson[8], Z. Zalewski[8], N. Charlet-Berguerand[9], R. Willemsen[2], R.K. Hukema[2]

[1] Department of Neurological Surgery, UC Davis, Davis, USA
[2] Department of Clinical Genetics, Erasmus MC, Rotterdam, the Netherlands
[3] NIDDK, National Institutes of Health, Bethesda, USA
[4] University of Seville, School of Medicine, Seville, Spain
[5] Department of Medical Genetics, University of Antwerp, Antwerp, Belgium
[6] UC Davis M.I.N.D. Institute, Sacramento, USA
[7] Molecular Biosciences, UC Davis, Davis, USA
[8] Department of Molecular and Human Genetics, Baylor College of Medicine, Houston, USA
[9] Department of Translational Medicine, IGBMC, Illkirch, France

Journal of Neurodevelopmental Disorders 2014 6(1):25
(adapted version)

ABSTRACT

Carriers of the fragile X premutation (PM) have CGG trinucleotide repeat expansions of between 55-200 in the 5'UTR of *FMR1*, compared to CGG repeat length of between 5-54 for the general population. Carriers were once thought to be without symptoms, but it is now recognized that they can develop a variety of early neurological symptoms as well as being at risk for developing the late onset neurodegenerative disorder fragile X-associated tremor/ataxia syndrome (FXTAS). Several mouse models have contributed to our understanding of PM and FXTAS. This chapter summarizes findings from studies using these mouse models and how this information is contributing to our understanding of the molecular and cellular abnormalities that contribute to neurobehavioral features seen in some PM carriers and in FXTAS patients. Mouse models show much of the pathology seen in PM carriers and in individuals with FXTAS, including the presence of elevated levels of *Fmr1* mRNA, decreased levels of FMRP, and ubiquitin- and FMRpolyG-positive intranuclear inclusions. Abnormalities in dendritic spine morphology in several brain regions are associated with neurocognitive deficits in spatial and temporal memory processes, impaired motor performance, and altered anxiety. *In vitro* studies have identified altered dendritic and synaptic architecture associated with abnormal Ca^{2+} dynamics and electrical network activity. PM mice have been particularly useful in understanding the roles of *Fmr1* mRNA, FMRP, and translation of a potentially toxic polyglycine peptide in pathology. The inducible mouse model enabled us to show that neuropathology and functional phenotype/deficit could be reversed at an early time-point. Finally, these and emerging mouse models are crucial for preclinical development of therapies to improve neurological function in FXTAS.

FMR1 gene and prevalence of FXTAS

The *fragile X mental retardation 1* gene (*FMR1*) is located on the long-arm of the X-chromosome at Xq27.3 and codes for the fragile X mental retardation protein (FMRP) which is necessary for normal brain development and synaptic plasticity [1-5]. The fragile X gene carries a variable number of CGG repeats in the 5'-untranslated region (5'-UTR) of between 5-54 in most individuals (modal value of 32-33) (**Figure 1**). However, due to instability of the repeat across generations there are large numbers of individuals who carry an expanded CGG repeat of between 55-200. These individuals are referred to as fragile X premutation (PM) carriers, and occur in the general population with an estimated frequency of 1 in 250 females and 1 in 400-800 males [6-8]. The chance of developing FXTAS increases dramatically with age, with approximately 40% of males and 8-16% of female PM carriers over the age of 50 developing FXTAS [7, 9, 10]. Indeed, FXTAS may be one of the more common causes of tremor/ataxia in older adults [11]. Besides age and CGG repeat length, the risk factors that lead to the development of FXTAS in PM carriers remains largely unknown, but are likely to include additional (epi) genetic and environmental factors (i.e., environmental toxins, chemotherapy, addictive substances and other illnesses) [3, 12-16]. The CGG repeat number negatively correlates with ages of onset of action tremor and cerebellar gait ataxia [17].

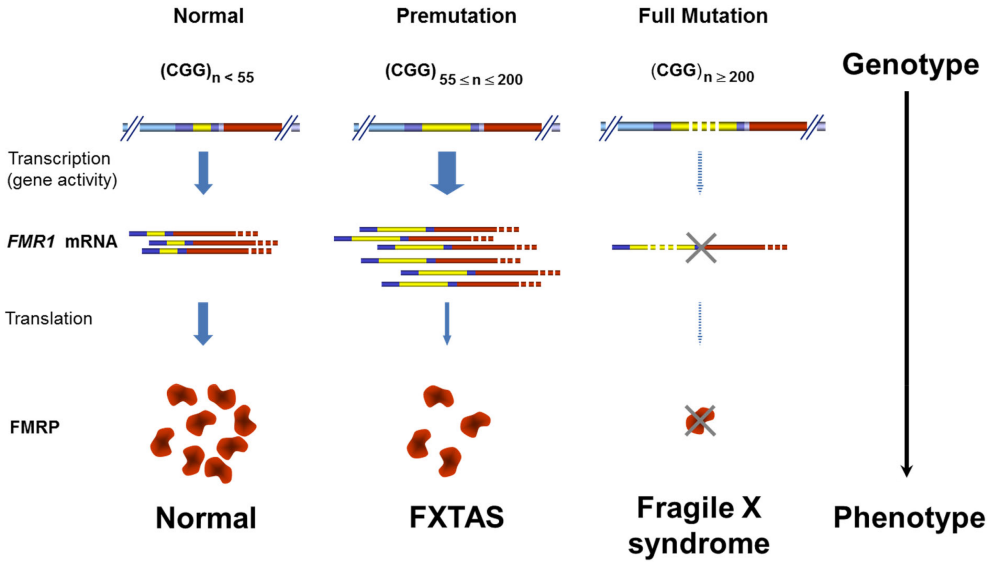

Figure 1. Most individuals in the general population have between 5-54 CGG trinucleotide repeats in the 5'-UTR of *FMR1*. Repeat length in the fragile X premutation (PM) range is 55-200, resulting in an elevation in *FMR1* mRNA levels, a moderate decrease in FMRP and an increased risk of developing FXTAS. Repeat size in the full mutation is >200, *FMR1* transcription is silenced due to DNA hypermethylation, and the absence of FMRP results in fragile X syndrome (adapted from [103]).

Because of the increase in the number of people reaching the age of 65 it is likely that the numbers of cases of FXTAS will increase accordingly, further highlighting the importance of unraveling the underlying molecular mechanisms of FXTAS, establish its developmental time course, and develop rational treatments to delay or halt progression of disease and improve neurological function [11].

Clinical features of FXTAS

Premutation carriers with 55-200 CGG repeats were originally thought to be clinically unaffected. However, it is now known that they can develop a variety of neurological symptoms, including memory problems, deficits in executive function, depression, anxiety and problems with numerical processing and magnitude estimates [3, 18, 19]. They are also at risk for developing the late onset neurodegenerative disorder fragile X-associated tremor/ataxia syndrome (FXTAS). Major clinical symptoms of FXTAS include action tremor and cerebellar gait ataxia. Minor clinical symptoms include impairments in executive function and memory, cognitive decline and dementia in some patients [20, 21].

Next to these core clinical features unexplained medical comorbidities have been reported, including thyroid disease [9, 22], fibromyalgia [22, 23], seizures [24], autoimmune disease [22], cardiac arrhythmias, hypertension [22], migraine [25], impotence [26, 27], and neuropathy [28] (Reviewed in [5, 29]. Females carrying the *FMR1* premutation are also at increased risk to develop fragile X-associated primary ovarian insufficiency (FXPOI) (reviewed in [30]). Premature ovarian insufficiency (POI) includes infertility due to cessation of ovarian function before the age of 40 [31]. FXPOI affects 12-28% of women carrying the PM [32, 33]. Very little is known about the underlying mechanisms of FXPOI, but recent studies suggests that the same molecular mechanisms involved in FXTAS might underlie FXPOI as well ([34-36] and Cohen, et al. Abstracts of the 2nd Premutation Meeting, Sitges, Spain, 2015).

Diagnostics

FXTAS only occurs in individuals who have an expanded CGG repeat in the 5'UTR of the *FMR1* gene. Therefore, it is essential that individuals being considered for this diagnosis are tested for and confirmed as a PM carrier. Diagnostic criteria were initially based on the first descriptions of patients with FXTAS [27, 28] and have been very helpful for the identification of affected individuals [37]. Since then additional features in individuals with FXTAS have been reported and new diagnostic criteria have been provided (reviewed in [38]). The revised major diagnostic criteria are: action tremor, cerebellar gait ataxia, and white matter lesions in middle cerebellar peduncle (MCP) or splenium of the corpus callosum (CCS). The main neuropathological hallmark in postmortem brain tissue are ubiquitin-positive intranuclear inclusions in both neurons and astrocytes. The revised

minor diagnostic criteria include: parkinsonism, moderate to severe short-term memory deficiency, executive function deficits, neuropathy, white matter lesions in cerebral white matter, and moderate to severe generalized atrophy [38]. For the definite diagnosis of FXTAS one major clinical criterion *and* one of the following criteria are required: one radiological major criterion or the presence of intranuclear inclusions. For the diagnosis of probable FXTAS two major clinical criteria or one radiological major criterion *and* one major clinical criterion are required. For the diagnosis of possible FXTAS one major clinical criterion *and* one radiological minor criterion are required [38].

(Neuro)pathology of FXTAS

The main neuropathological hallmark in FXTAS is the presence of ubiquitin-positive intranuclear inclusions present in both neurons and astrocytes throughout the brain in postmortem brain tissue [39-42]. Mass spectrometric and immunohistochemical analyses of these inclusions revealed over thirty inclusion-associated proteins, including a number of neurofilaments, lamin A/C, heterogeneous nuclear ribonucleoprotein A2 (hnRNP A2), muscle blind-like protein 1 (MBNLI), Sam68 and drosha [43-46]. Intranuclear inclusions were also found in non-CNS organs of FXTAS patients, including brain, kidney, adrenal gland, heart, thyroid, and pituitary [26, 29, 34, 42, 47, 48]. This suggests the involvement of the peripheral nervous system and systemic organs in the pathogenesis of FXTAS as well and might explain some of the observed comorbidities [29]. Furthermore degeneration of the cerebellum has been reported, including Purkinje neuronal cell loss, Bergman gliosis, spongiosis of the deep cerebellar white matter and axonal swelling in the granular cell layer of the cerebellum [39].

Mouse models and FXTAS

Pathology in affected PM carriers and in individuals with FXTAS is thought to be the result of RNA toxicity due to 2-8 fold elevated levels of a CGG-repeat bearing *FMR1* mRNA. As depicted in **Figure 2A**, elevated *FMR1* mRNA with a CGG repeat expansion is thought to sequester proteins critical for normal cell function resulting in pathology [43, 44, 49]. However, recent findings have suggested an additional model for toxicity, as depicted in **Figure 2B**, in which a potentially toxic polyglycine-containing peptide is produced as the result of a CGG repeat-mediated non-ATG translation (RAN) mechanism [41]. Research using animal models has provided much of the evidence supporting these theories as presented in this chapter.

Several mouse models have been developed to study the PM and FXTAS. These models show much of the pathology associated with CGG repeat expansions on *FMR1*. **Table 1** compares pathology seen in FXTAS with that reported in CGG KI mouse models. This includes molecular, histological and some behavioral deficits see in PM and

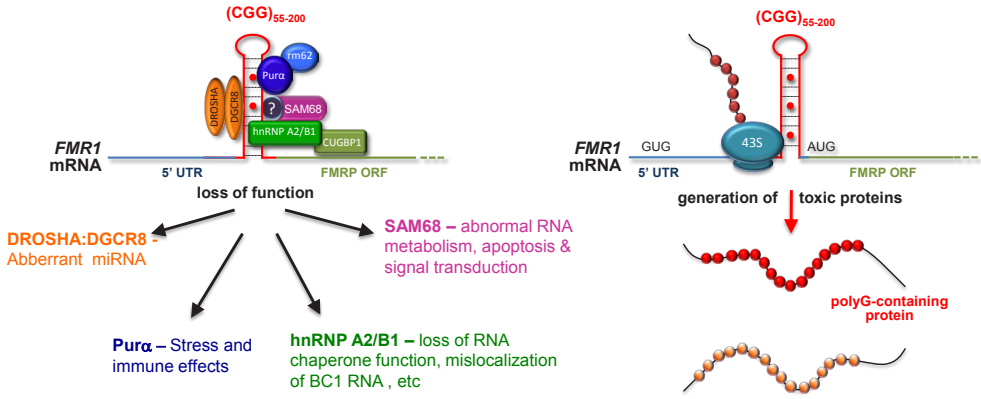

A. Protein sequestration

B. Repeat-associated non-ATG (RAN) translation model

Figure 2. Potential mechanisms of CGG-repeat RNA toxicity in FMP carriers. (**A**) Protein sequestration model: RNA binding proteins are sequestered through their interactions with the expanded CGG-repeat RNA. These proteins can in turn recruit other proteins. The net result of sequestration of these proteins being that they are unavailable to carry out their normal functions and critical cellular processes are thereby altered or blocked. (Sequestration of SAM68 by CGG expanded repeats is indirect, presumably through protein-protein interactions). (**B**) Toxic polypeptide model: The translation initiation complex stalls near the CGG repeat hairpin formed on the *FMR1* RNA. This promotes the repeat-associated non-AUG (RAN) translation of *FMR1* mRNA using a near-AUG start site. This results in a frame shift and the production of polyGlycine and/or polyAlanine containing polypeptides that somehow interferes with normal cell function or may be directly toxic.

FXTAS. However, none has been completely successful in reproducing all of the features reported in affected PM or individuals with FXTAS. An important example is the absence of any reports of obvious tremor in current mouse models, a defining neurological feature of FXTAS. Therefore, it is acknowledged at the outset that current mouse models only partially recapitulate features of the PM and FXTAS. The mouse models described below have been developed to study specific aspects of disease associated with CGG repeat expansions, each offers advantages and limitations, and each has already provided important insights into disease mechanisms.

1. The Dutch mouse

The study of FXS and FXTAS has been greatly facilitated by the development of animal models that mimic much of the pathology associated with these disorders. The first mouse model of FXTAS and the PM was a CGG knock-in (CGG KI) mouse model from the Willemsen lab in the Netherlands, the so called "Dutch" mouse (CGG_{dut} KI). This mouse model was generated by replacing the native murine CGG repeat 8 trinucleotides

Table 1. FXTAS compared to the CGG KI mouse model[a]

Pathology	Human FXTAS	CGG KI mouse
CGG trinucleotide repeat length	55-200 CGG repeat length, repeat instability	70-300 CGG repeats, modest repeat instability
Elevated FMR1 mRNA Expression	Increased 2-8 fold	Increased 1.5-3 fold
FMRP levels	Reduced in several brain regions	Reduced in several brain regions
Motor impairments	Tremor/ataxia, postural sway, parkinsonism	Impaired on rotarod and ladder rung task
Cognitive Impairments	Poor working memory, anxiety, depression, social phobia	Spatial memory deficits, altered anxiety- like behaviors
Intranuclear inclusions	Neurons and astrocytes, highly correlated with CGG repeat length, frequency increases with age	Neurons and astrocytes, related to length of CGG repeat, frequency increases with age

[a]Adapted from [163].

in length (i.e., CGG8) within the endogenous *Fmr1* gene with a human CGG98 repeat by homologous recombination in embryonic stem (ES) cells [50]. Importantly, while minimal changes to the murine *Fmr1* promoter were made when the targeting construct containing the human $(CGG)_{98}$ repeat was generated, the region flanking the repeat in the human *FMR1* was included. These CGG_{dut} KI mice show moderate instability of repeat length upon paternal and maternal transmission, with both small expansions and contractions (i.e., typically fewer than 10 repeats) [51, 52]. These CGG_{dut} KI mice have been bred onto a C57BL/6J background over several generations to establish lines with expanded alleles ranging from 70 to greater than 300 CGG repeats [50, 53]. Although expected, based on silencing of *FMR1* expression in FXS, no increased methylation of the *Fmr1* gene has been found even with longer CGG repeat expansions (e.g., >300). As described below these mice model much of the pathology seen in affected PM carriers and in FXTAS, including increased expression of *Fmr1* mRNA, decreased FMRP, ubiquitin-positive intranuclear inclusions (**Figure 3**) and evidence for motor and spatial processing deficits [53].

2. The NIH mouse

A second knock-in mouse was developed at NIH with an initial CGG118 tract [54]. The CGG_{nih} KI mice were generated using a different strategy from the CGG_{dut} mice. They were made using a targeting construct in which exon 1 of the mouse gene was retrofitted with two adjacent but incompatible *Sfi* I sites. The repeats were generated *in*

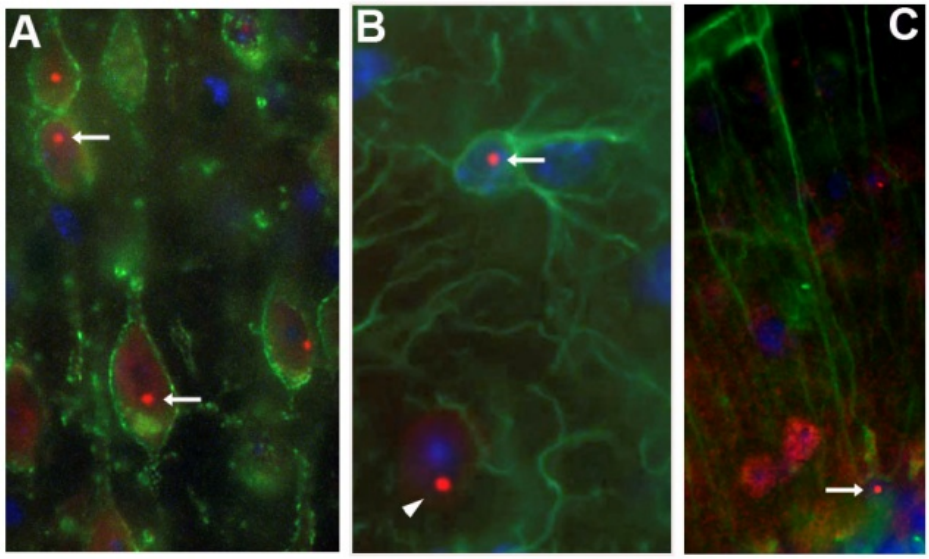

Figure 3. Ubiquitin positive intranuclear inclusions in neurons and astrocytes of CGG_{dut} KI mice. Immunofluorescent photomicrographs of ubiquitin-positive intranuclear inclusions (arrows) immunolabeled red in (**A**) pyramidal neurons in motor cortex, (**B**) astrocytes and (**C**) Bergmann glia of CGG KI mice. Neurons (**A**) were immunolabeled for Kv2.1 potassium channels in the membrane (green), (**B**) lamina I neocortical astrocytes and (**C**) Bergmann glia were immunolabeled with GFAP (green). In (**B**) note an intranuclear inclusion in an adjacent neuron (arrowhead). Nuclei were stained with DAPI.
(Adapted from [36])

vitro in such a way that they were flanked by the appropriate *Sfi* I sites. This allowed the CGG-repeats to be inserted into the mouse locus in the correct orientation and in such a way as to make minimal changes to the mouse flanking sequence. As a result of this strategy, the CGG_{nih} mouse retains the translational TAA stop codon just upstream of the CGG118 repeat that is present in the endogenous murine gene but not the human gene. As with the CGG_{dut} mice, the CGG_{nih} mice showed elevated *Fmr1* mRNA levels, decreased FMRP levels, moderate intergenerational expansions, no methylation, even when repeat numbers were >300, and ubiquitin-positive intranuclear inclusions [55]. Furthermore, the CGG_{nih} mice show high repeat instability with a bias toward expansions. In yeast and *Escherichia coli* it has been reported that the rate of instability is changed in different repair-deficient strains [56-58]. One DNA damage checkpoint protein that may have an effect on CGG repeat instability is the Ataxia-telangiectasia and rad3-related (ATR) kinase. ATR heterozygosity led to an increased frequency of expansion of maternally transmitted alleles. This suggests that expansion of the CGG repeat can occur prior to fertilization of the oocyte [59]. Recently, it was reported that two DNA damage repair pathways are involved in instability of the CGG repeat expansion. Firstly, the transcription

coupled repair protein ERCC6/CSB protects against repeat expansions [60]. Secondly, the base pair excision pathway is involved, since heterozygosity for a hypomorphic Polβ mutation reduces the expansion frequency [61].

3. Similarities and differences between CGG_{dut} and CGG_{nih} KI models

The two CGG KI mouse models show similarities as well as some differences [55, 62]. Both models show several fold increase in levels of *Fmr1* mRNA and a reduction in brain levels of FMRP that is inversely related to CGG repeat length. However, they differ in that the reduction in FMRP in the CGG_{dut} KI mouse (20-30%) is typically much less than that reported in the CGG_{nih} KI (>50%). Ubiquitin positive intranuclear inclusions are found in both models, but are more common in neurons and astrocytes in the CGG_{dut} KI model [41]. Inclusions in CGG_{dut} KI mice are widespread in the brain, including the hippocampus, cortex, cerebellum, olfactory bulb, superior and inferior colliculi and hypothalamus [52]. Purkinje cell loss is seen in postmortem tissue from FXTAS brains, as well as in the CGG_{nih} KI mouse, but has not been reported in the CGG_{dut} KI mouse [55]. Behaviorally, there is evidence for memory impairment in both models [63, 64], but the CGG_{dut} KI mouse shows increased anxiety [65] while the CGG_{nih} KI mouse shows lower anxiety [64]. Both models show modest intergenerational repeat instability. Neither model, however, reliably shows large expansions in the length of the CGG repeat tract seen with maternal transmission in FXS, and no methylation or silencing of *Fmr1* expression has been reported in either model. It has been suggested that this difference between humans and mice in the frequency of large germline expansions may be due to differences in the length of the perigametic interval in males of both species (i.e., weeks), female mice (months) and human females (decades) [59]. The levels of the proteins involved in generating or preventing expansions during the perigametic interval could also contribute to these differences [66].

The reasons for differences between the two models in FMRP reduction, Purkinje cell loss and the frequency of intranuclear inclusions are unclear since both were generated with CGG repeat sequences that differed only by approximately 20 repeats. However, the cloning strategy used to make these mouse lines differed in that the CGG_{nih} KI mouse retains a greater region of the mouse 5' UTR flanking the CGG repeat, including a TAA stop codon that is not present in the CGG_{dut} KI mouse. The absence of this stop codon in the CGG_{dut} KI may allow, and its absence in the CGGnih KI may block CGG repeat-associated non-ATG translation (RAN) and the subsequent translation of a novel polyglycine protein that appears to contribute to CGG repeat toxicity in human cells line and in Drosophila [41]. The ability to compare the pathology between the two mouse models represents an important and powerful tool for understanding the mechanisms of disease in the PM and in FXTAS.

4. Ectopic expression of an expanded CGG90 in transgenic mice

In order to determine whether ectopic expression of an expanded CGG90 repeat would cause neurodegeneration in the cerebellum, transgenic mice (L7-CGG90-Fmr1) were generated in which expression was spatially restricted to cerebellar Purkinje neurons using the L7 promoter [67]. In these mice, the CGG90 repeat was upstream of either Fmr1 or EGFP cDNA (L7-CGG90-Fmr1, L7-EGG90-EGFP), with control mice expressing Fmr1 or EGFP but without a CGG90 repeat expansion (L7-Fmr1, L7-EGFP). Significant Purkinje cell loss was observed in 32-week old L7-CGG90-Fmr1 and L7-CGG90-EGFP mice compared to wildtype (WT) littermates or L7-Fmr1/L7-EGFP mice (**Figure 4**). Ubiquitin-positive intranuclear inclusions were found in Purkinje neurons of both the L7-CGG90-Fmr1 and L7-CGG90-EGFP lines, but were not found in either WT littermates

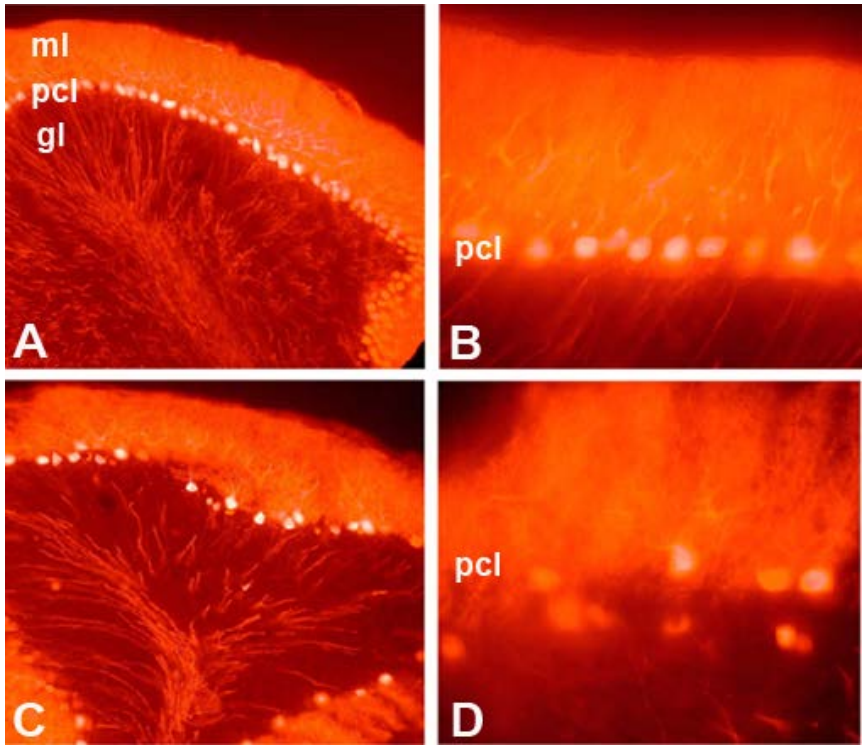

Figure 4. Ectopic expression of a CGG90 repeat results in Purkinje cell loss. (**A**) Cerebellum of control mice without a CGG90 repeat (i.e., L7*Fmr1*) showing normal distribution of Purkinje cells in the Purkinje cell layer (pcl). (**B**) Higher magnification of pcl in control mice. (**C**) Selective Purkinje cell loss in 32 week old mice expressing a CGG90 repeat under the L7 Purkinje cell-specific promotor i.e., L7CGG90*Fmr1*). (**D**) Purkinje cell loss in shown at higher magnification in L7CGG90*Fmr1* mice. ml – molecuar layer; pcl – Purkinje cell layer; gl- granule cell layer. (Adapted from [29])

or the L7-Fmr1 or L7-EGFP control lines. Lack of inclusions in control mice, in addition to their presence in the L7-CGG90-EGFP line, demonstrates an essential role for the CGG repeat expansion in inclusion formation, and that expressed CGG repeat containing RNA is sufficient to induce inclusions. These Purkinje neurons stained positive for the 20S core complex of the protesome, Hsp40, and Rad23B. Interestingly, staining was negative for Purα, hnRNPA2/B1, Tau, and α-synuclein; all proteins that have been reported in human intranuclear inclusions in human FXTAS [43]. Motor performance on the rotarod was also impaired in mice expressing the CGG90 repeat compared to controls, and this impairment was not age-related, as similar impairment was seen in 20 and 40 week old mice. These results provide evidence that CGG repeat mRNA expression is sufficient to cause Purkinje neuron dysfunction and loss similar to that reported in FXTAS [40].

The neuropathological observations to date demonstrate a connection between formation of intranuclear inclusions and cell death. While it is tempting to speculate that the formation of inclusions is the cause of cell loss, such a conclusion is contingent upon understanding what the functional ramifications are when proteins and their interacting partners are sequestered within an inclusion body. A *Drosophila* model ectopically expressing premutation-length CGG repeats showed a neurodegenerative eye phenotype and *Hsp70*/*ubiquitin*-positive inclusions [68]. A subsequent genetic screen showed that CELF1 (CUGBP1), when ectopically expressed, was able to suppress the neurodegenerative eye phenotype [69]. CELF1 was also shown to directly interact with hnRNPA2/B1, known to be present in inclusions of FXTAS patients [43]. CELF1, better known for its involvement in myotonic muscular dystrophy type 1 (DM1) [70-72], is upregulated overall in the presence of CUG repeats >50, contributing to the mis-regulation of mRNA splicing and translation and the muscle atrophy and weakness observed in DM1. CELF1 is therefore predicted to be one potential modifier of CGG repeat-mediated neurodegeneration. Preliminary findings in mice show modulation of neuropathological phenotypes previously reported in the L7CGG90 transgenic mice when the expression of CELF1 is altered (Zalewski, et al. Abstracts of the 1st Premutation Meeting, Perugia, Italy, 2013). Such findings support an RNA toxicity mechanism, specifically that the sequestration of such proteins within an inclusion inhibits their normal function, leading to dysregulation (at least at the level of RNA processing) in the cell and, over time, cell death. Galloway, et al performed translational profiling in L7CGG90 mice and demonstrated a significant change in their translational profile. Over five hundred transcripts were differentially associated with ribosomes. Interestingly, *Tardbp* mRNA (important in many other neurodegenerative disorders) has a reduced association with the ribosomes, resulting in loss of TDP-43 protein expression in Purkinje cells of L7CGG90 mice [73]. In two *Drosophila* models expressing the rCGG repeat, TDP-43 suppresses CGG-mediated toxicity [73, 74]. However, in postmortem brain material from FXTAS patients TDP-43 is

localized within the nucleus without any aggregation, similar as in controls. In fibroblast lines from PM carriers, FXTAS patients and controls no differences in TDP-43 RNA or protein expression could be observed [74].

5. Fmr1 Over-expressing mice

Levels of *FMR1* mRNA bearing an expanded CGG are elevated several fold in premutation carriers and in FXTAS patients, supporting the hypothesis that pathology is the result of *FMR1* mRNA toxicity. However, the possibility exists that toxicity could be due to either the CGG repeat itself, elevated *FMR1* mRNA independent of the repeat expansion, or both. In a *Drosophila* model of FXTAS, high expression levels of a CGG60 repeat causes formation of ubiquitin-positive inclusions and neurodegeneration in the retina in a dosage-and repeat length-dependent manner, while moderate expression of the repeat allele results in little pathology. These findings support the notion that overall abundance of a CGG repeat molecule may be important for generating a pathological phenotype [68]. To investigate the potential deleterious effects produced by over-expression of *FMR1* mRNA with a normal CGG repeat length, transgenic mice that over-express *FMR1* mRNA bearing a normal length CGG29 repeat have been generated [75]. The CGG29 transgenic mouse was obtained by pronuclear injection of a construct containing the human *FMR1* cDNA with 29 CGG repeats under control of a SV40/T7 promoter. This model results in a 20-100 fold increase in *FMR1* mRNA in all tissues studied (e.g., liver, cerebral cortex and cerebellum). However, these animals did not show significant differences from WT mice in general activity or anxiety-related behaviors in open-field tests. These results suggest it is expression of the expanded CGG repeat that is primarily responsible for pathology, and not over-expression of *Fmr1* mRNA *per se*. Other transgenic mice over-expressing *FMR1* mRNA have been made using a yeast artificial chromosome (YAC) containing the full-length human *FMR1* gene. These YAC mice show a 2-3 fold increase in expression of *FMR1* mRNA and a 10-15 fold increase in FMRP compared with control littermates [76, 77]. When crossed with a knock-out (KO) mouse model of FXS that lacks FMRP, some of the pathological features of FXS were reversed. Importantly there were no changes in overall brain morphology at the light microscopic level due to over-expression of mRNA or protein. However, over expression in otherwise WT mice (i.e., not KO mice) also resulted in some abnormal behaviors, including decreased activity, increased anxiety-like behavior and enhanced startle response. Although the authors attributed these behavioral effects to over-expression of FMRP, the high levels of *Fmr1* mRNA could also have contributed to the behavioral effects [77].

6. YAC transgenic mouse models of the PM

Yeast artificial chromosome (YAC) transgenic mouse lines have also been generated in order to study CGG repeat instability [78]. These mice were generated using a CGG92

allele isolated from an adult male premutation carrier, a CGG repeat length that would be expected to show expansion to the full mutation when transmitted through the female germ line in humans. The CGG92 region, including several hundred base pairs of flanking sequence, was cloned into a YAC and purified YAC DNA was injected into FVB/N mouse oocytes and then transplanted into foster mothers. A line of offspring (i.e., line TG296) carrying a CGG90 repeat were then identified. Although not yet well characterized, these YAC mice show modest intergenerational CGG repeat instability, expansion and contraction of 1-3 trinucleotides across generations. There was no influence of parental sex, or age on transmission of the repeat.

7. Inducible mouse models

Continued development of new mouse models to study the PM and FXTAS has resulted in generation of doxycycline (dox)-inducible transgenic mouse lines with overexpression of RNA containing an expanded CGG90 repeat [79, 80]. Ubiquitous overexpression of RNA containing an expanded CGG90 repeat using an hnRNP-rtTA driver resulted in dysfunction of the liver and eventually death of the mice within five days after dox induction. The livers of these mice showed increased steatosis, mitochondrial dysfunction and apoptosis. Due to the early death of these mice no neuropathology could be observed. Subsequent studies were designed using a brain specific prion protein (PrP)-rtTA driver [79]. In these mice the RNA containing an expanded CGG repeat was expressed throughout the brain, with the strongest expression in cerebellum, hippocampus and striatum. Ubiquitin- and FMRpolyG-positive intranuclear inclusions were found after eight weeks of dox-induction and these inclusions increased in number and size over time. After stopping expression of the RNA containing an expanded CGG repeat at an early stage it could be demonstrated that inclusion formation was reversible. Turning off transgene expression at a later time point could only halt disease pathogenesis. Furthermore, deficits in the compensatory eye movements of mice were observed after20 weeks of dox treatment. This functional phenotype could be halted by stopping expression of the RNA containing an expanded CGG repeat after 12 weeks of dox treatment. These results indicate that the functional phenotype can be halted and neuropathology reversed if expression of the expanded CGG repeat is stopped. It also suggests that an early therapeutic intervention might be beneficial for FXTAS patients.

Brain and cellular pathology in mouse models

The description of brain pathology associated with PM and FXTAS is limited by the availability of tissue for analysis. As a result virtually all that is known about such pathology has come from studies of postmortem tissue from PM carriers who developed FXTAS, and from findings in animal models. To date, studies on brain pathology seen in

PM carriers without FXTAS have not been published, including if and when intranuclear inclusions and cell loss (e.g., Purkinje neurons) may be occurring.

1. Intranuclear inclusions

The hallmark histopathology in FXTAS includes the presence of ubiquitin-positive inclusions in neurons and astrocytes that is widespread throughout the brain. As a further parallel between human FXTAS and the CGG KI mice, both show the presence of ubiquitin-positive intranuclear inclusions in many regions of the brain [54, 81, 82]. The CGG_{dut} KI develops intranuclear inclusions in neurons in many brain regions, including cerebral cortex, olfactory nucleus, parafascicular thalamic nucleus, medial mammillary nucleus and colliculus inferior, cerebellum, amygdala and pontine nucleus cortex, hippocampus, hypothalamus and in granule cells of the cerebellum (**Figure 3**) [52, 62]. Inclusions in the dentate gyrus of the hippocampus are evident as early as 12 weeks of age [63]. The number of inclusions in glia, including astrocytes and Bergmann glia, and their distribution in brain are more limited, and not as numerous as found in postmortem FXTAS brain tissue [82, 83]. In addition, the size of the inclusions correlates significantly with the age of CGG_{dut} KI mice, with smaller inclusions found in younger mice. Interestingly, the gradual increase in the size of the inclusions and the percentage of ubiquitin-positive neurons appears to parallel the progressive development of the neurological phenotype of FXTAS in humans [11]. In addition, brain regions showing the presence of intranuclear inclusions correlate with the clinical features in symptomatic FXTAS patients [81]. Importantly, inclusions are not limited to the nervous system, and are found in both human FXTAS and in the CGG_{dut} KI mouse in a variety of other tissues, including pancreas, thyroid, adrenal gland, gastrointestinal, pituitary gland, pineal gland, heart, and mitral valve. Inclusions were also found in the testes, epididymis, and kidney of FXTAS cases, but not in the KI mice [84]. Therefore, FXTAS should be considered a multiorgan disease. Systematic analysis of these inclusions in postmortem FXTAS brain and transfected COS7 cells shows the presence of more than 20 proteins including ubiquitin, molecular chaperone Hsp40, 20S proteasome complex, DNA repair-ubiquitin-associated HR23B factor and SAM-68, DGCR8, and DROSHA [43, 45, 46]. The presence of most these proteins is confirmed in the mouse models for FXTAS [43, 49, 52, 79, 85-87]. The inclusions also contain *FMR1* mRNA, but surprisingly not FMRP [43, 88]. Similar studies on the protein composition of inclusions found in CGG mouse models have not been carried out, but it is already apparent that there are some similarities between the inclusions in FXTAS and mouse models, including the presence of ubiquitin, SAM68, DGCR8, lamin A/C, as well as several differences [43, 49, 52, 55, 85, 89]. Purα has been detected in intranuclear inclusions in a *Drosophila* model of the premutation and overexpression can suppress CGG repeat-mediated neurodegeneration. However,

purα has not yet been detected in inclusions in murine models and evidence for its presence in human inclusions is inconclusive [43, 89]. Similarly, hnRNP-A2/B1 are found in the intranuclear inclusions in FXTAS [43], but little or none has been found in CGG KI mice [67]. Additional research on composition of intranuclear inclusions in FXTAS and mouse models would clearly be of value.

2. Cell loss

An important neuropathological finding in human FXTAS is the presence of Purkinje cell degeneration [40]. This has also been observed in the CGG_{nih} KI mouse, and in mice expressing an ectopic CGG90 repeat expansions limited to cerebellar Purkinje neurons as shown in **Figure 4** [55, 67]. However, the generalized brain atrophy, including enlarged ventricles, that has been reported in some FXTAS patients has not been systematically examined in any of the existing mouse models. Such studies need to be carried out using structural MRI imaging and quantitative stereology of neurons in brain regions known to be affect in FXTAS, to establish whether similar pathology also occurs in mouse models.

3. White matter disease

FXTAS is also characterized by white matter disease, including loss of glial cells, enlarged astrocytes, spongiosis and pallor in subcortical and cerebellar white matter, including in the middle cerebellar peduncle (MCP) [40, 83, 90]. Additional pathology in FXTAS is seen on T2-weight MRI images that show hyperintensities in white matter tracts, including the MCP [91]. Tractography studies using diffusion weighted MRI imaging (DTI) has provided additional evidence for degeneration in major white matter fibers tracts in FXTAS, including the MCP, superior cerebellar peduncle and corpus callosum, that was not found in premutation carriers without FXTAS [90]. As yet, these important findings have not been systematically examined in mouse models of the PM or FXTAS, and there are no published reports of white matter pathology or degeneration of major fiber tracts in animal models.

4. Dendrite and dendritic spine morphology

Studies of Golgi stained neurons have also revealed ultrastructural changes in dendrites and dendritic spines in both CGG_{dut} and CGG_{nih} KI mice [64, 92]. The CGG_{dut} KI mouse shows fewer dendritic branches proximal to the soma, reduced total dendritic length and longer dendritic spines on basilar, but not on apical dendrites in pyramidal neurons in primary visual cortex. Neither total dendritic spine density, nor the density for specific dendritic spine subtypes (i.e., stubby, mushroom, filipodial) differed between WT and KI mice. Dendrite and dendritic spine morphology has also been examined in CGG_{nih} KI mice in several brain regions, including the medial prefrontal cortex, hippocampus and

basal lateral amygdala. In all three brain regions the branching complexity of apical and basilar dendrites was significantly lower and spines were longer in KI mice compared to WT, consistent with findings in the CGG_{dut} KI mouse. However, in the CGG_{nih} KI mouse dendritic spine density was generally increased in all three brain regions in contrast to the CGG_{dut} KI mouse that did not show changes in spine density. It is interesting to note that longer dendritic spines found in the cortex of CGG KI mice have also been reported in Golgi studies of postmortem tissue in FXS [93, 94] and in *Fmr1* KO mice [95, 96], while the reduction in dendritic branching complexity in CGG KI mice was not found in the *Fmr1* KO mouse [95]. To our knowledge dendritic branching and spine morphology have not been examined in postmortem tissues from carriers of the PM or FXTAS patients.

5. Lamin A/C disruption

Expression of expanded CGG-RNA also results in the widespread disruption of lamin A/C proteins with associated abnormalities in nuclear envelope morphology in cellular models [97, 98]. In frontal cortex sections and isolated nuclei from FXTAS brain, lamin A/C is present in intranuclear inclusions [43]. Lamins A/C are intermediate filament proteins that line the inner nuclear membrane where they help maintain the shape and mechanical integrity of the nucleus [99]. They are generated from a single LMNA gene by alternative splicing and mutations have been linked to a variety of neurodegenerative diseases. Cells deficient in lamin A/C show decreased survival and defective response to DNA damage [100].

These observations suggest that FXTAS may result in a functional laminopathy. This is consistent with recent findings that demonstrate that laminopathy diseases, including restrictive dermopathy (RD) and Hutchinson Gilford progeria syndrome (HGPS), result in increased levels of reactive oxygen species and accumulation of DNA damage [101]. Moreover, several proteins involved in telomere maintenance [102-104] are present in the intranuclear inclusions characteristic of FXTAS (e.g. lamin A/C, Ku80, γH2AX) [43] and could account for shorter telomere length demonstrated in patients with FXTAS [105, 106]. Shorter telomere length could also contribute to the reduce life-expectancy associated with longer CGG repeat lengths in FXTAS patients [82, 83]. While disruption of nuclear lamin a/c architecture has been reported in mouse embryonic fibroblasts from CGG_{dut} KI mice, studies in mice examining Ku80 and γH2AX have not been carried out [97].

6. Mitochondrial dysfunction

Several symptoms reported in FXTAS share some commonalities with mitochondrial respiratory chain enzyme deficiencies (MRCDs), including gait ataxia, white matter disease, peripheral neuropathology, muscular weakness and neuropsychiatric disorders [107]. Mitochondrial dysfunction occurs in PM and FXTAS and has been examined in

cultured skin fibroblasts and in frozen frontal cortex from postmortem brain tissue samples from premutation carriers with or without FXTAS [107]. Decreased NAD- and FAD-linked oxygen uptake rates have been found in premutation carriers compared to controls. In addition there is reduced expression of the mitochondrial proteins MnSOD, an antioxidant enzyme, and nitration of ATPB, a putative marker for nitrative/oxidative stress is elevated approximately 2-fold in PM and FXTAS compared to controls, indicating mitochondrial dysfunction. Mitochondrial dysfunction has also been found in cultured hippocampal neurons isolated from CGG_{dut} KI mice as early as 4 days-in-vitro (DIV) [108]. Density and mobility were assessed by time-lapse imaging of mitochondria labeled with Mitotracker Red CMXRos, and oxygen consumption was estimated by measuring the rate of change of dissolved O_2 in the medium surrounding the cultured hippocampal neurons using a Seahorse Bioscience extracellular flux analyzer. CGG_{dut} KI mice showed reduced density of mitochondria in proximal neurites (i.e., within 25 µm of soma), and as well as significantly reduced mobility compared to WT mice. Neurons from CGG_{dut} KI mice also showed high basal oxygen consumption rates and evidence for increased protein leakage and higher ATP production. The authors suggested that these abnormalities in mitochondrial distribution and bioenergetics may contribute to previous reports of lower viability and reduced dendritic branching of cultured hippocampal neurons [109] as well as to reduced dendritic branching and altered spine morphology in CGG KI mouse neocortex [64, 92]. A recent study with the dox inducible mouse model suggests that ubiquitous overexpression of RNA containing an expanded CGG leads to steatosis in liver [80]. Steatosis is an indication for mitochondrial dysfunction. Indeed, in livers from animals with expanded repeat expression, RNA expression levels of GPX1 are downregulated and expression of Cytochrome C is upregulated. GPX1, a glutathione oxidase, inhibits cytochrome C release from mitochondria. Cytochrome C initiates apoptosis through caspase-3 activation [110]. Semi-quantitative immunostainings of liver sections showed elevated levels of activated caspase 3. This suggests that induced expression of RNA containing an expanded CGG repeat leads to toxicity by affecting ROS signaling [80]. It is important to consider the possibility that mitochondrial disease may contribute to the risk for PM carriers to become symptomatic or to develop FXTAS, and this potential link should be explored in future studies in mouse models.

Molecular findings

1. *Fmr1* mRNA and FMRP

Both the CGG_{dut} KI and the CGG_{nih} KI mice have proven to be very useful models to study the molecular aspects of the expanded CGG repeat. The brains of these two mouse lines show small (10-30%) to moderate (i.e., >50%) reductions in FMRP, respectively, despite

the fact that 2-3 fold elevated levels of *Fmr1* mRNA are found [54, 81, 111, 112]. These results parallel to a great extent what is found in some human PM carriers and in FXTAS patients as outlined in **table 1** [53]. However, in contrast to what was reported for the linear correlation between *FMR1* mRNA levels and the repeat size in human FXTAS patients [113], the increase in *Fmr1* mRNA levels in mice was not clearly correlated with the length of the repeat in the CGG_{dut} mouse [114]. It is important to note that data from the human patients were not from brain samples, but from blood samples or lymphoblasts. Entezam, et al. were able to show a direct relationship between CGG-CCG repeat size and *Fmr1* mRNA levels in the brains of the CGG_{nih} KI mice, although the number of mice studied for the different repeat sizes was limited [55]. The cellular mechanism underlying the increase in *Fmr1* mRNA levels is unknown, but could be due to a feedback mechanism resulting from reduced levels of FMRP. Mechanisms underlying reduced FMRP include impeded migration of the 40S ribosomal complex along the expanded CGG tract, as well as the use of an alternative internal ribosome entry site (IRES) for initiation of translation. An IRES has been identified in the 5'-UTR of *FMR1* mRNA [115]

2. *Fmr1* splice variants & FMRP isoforms

The *FMR1* gene has 17 exons with alternative splice sites on exons 12, 14, 15 and 17 that result in the expression of multiple FMRP isoforms [116-118]. The splicing pattern of these isoforms is of interest as, in some isoforms, the truncation or absence of functional domains would suggest a change in FMRP functional properties including its selection of protein partners and mRNA targets and its cellular localization. For instance, the N-terminus of FMRP harbors a nuclear localization signal and *FMR1* mRNA binding activity is driven by two KH domains encoded by exons 8-12 and an RGG box domain in exons 14-15 [119]. Additionally, a nuclear export signal is localized to exon 14 and serine phosphorylation sites shown to be involved in translational regulatory activity of FMRP as well as methylation sites are also localized to exon 15. The transcript levels of these isoforms were found to be developmentally regulated in the brain of the WT C57BL/6 mouse strain [117], the same strain used to construct the CGG_{dut} KI mouse model [52]. Isoform distributions were similar across 11 different brain regions with the exception of the hippocampus and the olfactory bulb. Although to date no information is available on isoform distribution in the CGG_{dut} KI mouse, the polyadenylation state of *Fmr1* transcripts, which can be informative for the stability and the translational efficiency of the mRNA, has been investigated in these mice. The CGG_{dut} KI mouse exhibits an increased population of short poly(A) mRNAs, usually indicative of inefficiently translated transcripts, compared to WT [120]. It would be interesting to know whether particular mRNA isoforms are thus more efficiently translated than others in the CGG_{dut} KI background.

3. Expression profiling

Dysfunction of the GABAergic system has been reported in CGG_{dut} KI mice [121]. Specifically, over-expression of genes for several $GABA_A$ receptor subunits (e.g., α1,3,4; β2; γ2) and proteins involved in GABA metabolism (gad1, gat2, gat 4) has been observed in cerebellum, but not cortex, of CGG_{dut} KI mice, which could be related to the motor phenotype observed in FXTAS [27, 122]. Interestingly, in *Fmr1* KO mice expression was increased for some of these same genes (e.g., gad1, gat1, gat4), but the reasons for this difference are unclear. Microarray analysis in cerebellum of transgenic mice that overexpress human *FMR1* with a normal range CGG29 repeat has also been carried out, but there were no clear changes in the GABAergic system compared to controls. Among GABA related genes, only up-regulation of the $GABA_A$ receptor-associated protein-like 2 (*Gabarapl2*) gene was observed [75]. These results provide additional support that pathology in CGG KI mice, at least in the GABA system, is due to expansion of CGG repeats rather than increased mRNA levels, since in these transgenic mice the *FMR1* mRNA levels were increased 20-100 times compared with those of WT littermates. However, other changes were seen in the transcriptome of these mice that could be a consequence of *FMR1* mRNA over abundance. Interestingly, the two most altered genes in the transcriptome were *transthyretin* (*Trt*), and *serpina3*, putative biomarkers for Alzheimer disease [123, 124]. Serpina3, a serine protease inhibitor that is released during inflammatory responses, was up-regulated and may reflect the increased prevalence of autoimmune disease (e.g., lupus, multiple sclerosis, fibromyalgia, thyroid disease) in females with the *FMR1* PM [125]. Transthyretin, a transport protein for retinol and thyroxine (T4) thought to contribute to thyroid hormone homeostasis, was down-regulated [126], while speculative, reduced transcription could be related to hypothyroidism reported in some FXTAS patients [3]. In addition, two microRNAs, mir-181a-1 and let-7 appeared up-regulated in these mice [127]. Up-regulation of Let-7 miRNA has also been reported in a *Drosophila* model of FXTAS [128]. This is important because several miRNAs have been found up-regulated in human PM carriers [129], although they differed from those observed in mice that overexpress *FMR1* mRNA bearing a normal length CGG29 repeat [75].

Electrophysiological findings

1. GABA/Glutamate imbalance and abnormal synaptic network activity

The origin of pathology in FXS and in some PM carriers, with or without FXTAS mutations is the presence of a CGG repeat expansion on *FMR1*, raising the possibility that some of the same molecular pathways could be affected in both disorders, and those associated with glutamatergic signaling in particular [1, 130-132]. This is in spite of differences in the causal molecular underpinnings in the disorders, and specifically the lack of FMRP

expression in FXS versus the overexpression of *FMR1* mRNA in the PM and FXTAS. In fact, the dysregulation in excitatory and inhibitory neurotransmission in the CNS of FXS KO mice has been the subject of active investigation during the last decade, and evidence has recently surfaced that suggests a similar dysregulation in the CGG KI mice [1, 130, 131].

Hippocampal CGG_{dut} KI neurons *in vitro* show a developmental defect in connectivity and impaired dendritic growth observed at 7 and 21 days DIV. There is also a loss of cell viability, also suggestive of a neurodegenerative component to the PM [109]. Interestingly, in the same neurons, the expression of the vesicular GABA and glutamate transporters VGAT and VGLUR1, respectively, is reduced at 21 DIV, but not at 7 DIV. These alterations are associated with a 4- to 8-fold increase in *Fmr1* mRNA and an approximately 50% decrease in FMRP.

Abnormal patterns of electrical activity are also seen *in vitro* in hippocampal neurons from CGG_{dut} KI mice, including enhanced clustered burst firing. Specifically, hippocampal neurons cultured from CGG_{dut} KI mice display clustered burst (CB) electrical spiking activity and abnormal patterns of spontaneous synchronous Ca^{2+} oscillations under basal culture conditions [133]. The principal mechanisms contributing to these neuronal network defects in basal electrical activity appear to be associated with a gain of function in type I mGluRs and/or a loss of function in $GABA_A$ receptor signaling. This conclusion is supported by data indicating that: (1) type I mGluR receptor agonist DHPG, but neither NMDA and AMPA receptor agonists, increased CB firing patterns in WT neurons with increased spike rate and mean burst duration similar to those observed in PM hippocampal neurons; (2) selective mGluR1/5 antagonists (CPCCOEt and MPEP) abrogated abnormal electrical activity in PM neurons; (3) PM astrocytes have impaired glutamate uptake [108, 134]; (4) WT cultures exposed to the astrocyte Glu transport competitive antagonist TBOA produced electrical firing patterns indistinguishable from those of CGG_{dut} KI neurons; (5) $GABA_A$ receptor block with picrotoxin generated CB firing behavior observed in CGG_{dut} neurons; and (6) the allosteric $GABA_A$ receptor enhancer allopregnanolone essentially restored WT electrical spiking patterns.

These functional deficits are directly pertinent to the altered patterns of neuronal complexity reported earlier using the same *in vitro* CGG_{dut} KI model [109]. Neuronal network activity is essential for normal neuronal migration, dendritic growth, and synaptic plasticity, processes mediated by spatially and temporally orchestrated intracellular Ca^{2+} signals. Therefore, the abnormal CB electrical activity and abnormal patterns of spontaneous Ca^{2+} oscillations observed in hippocampal neurons from CGG_{dut} KI mice are likely to contribute, at least in part, to impaired dendritic growth and synaptic architecture.

2. Hippocampal synaptic plasticity

Deficits in processing spatial and temporal information have been reported in PM carriers and in patients with FXTAS, suggesting hippocampal-associated pathology. In

order to fully characterize the CGG KI mouse and to provide clues to which brain regions that may mediate these cognitive deficits (e.g., hippocampus), *in vitro* studies of synaptic plasticity in acute hippocampal slices isolated from CGG_{dut} KI mice and WT mice have been carried out. Specifically long-term potentiation of synaptic transmission (LTP) and long-term synaptic depression (LTD) in CGG_{dut} and WT mice have been examined. The results demonstrated that the magnitude of LTP was significantly lower in CGG KI mice compared to WT mice, indicating impaired synaptic plasticity. Similarly, LTD, whether induced by low-frequency electrical stimulation (1 Hz) or bath application of the mGluR1/5 agonist DHPG, was also limited in CGG KI mice versus WT mice. These findings implicate loss of neuroplasticity in the hippocampus in the spatial and temporal cognitive deficits associated with CGG repeat expansions and the neurological pathology in FXTAS [135]. In contrast, enhanced LTD has been reported in the CGG_{nih} KI mouse model [136]. LTD at CA3-CA1 hippocampal synapses induced by bath application of the group I mGluR agonist DHPG was enhanced relative to that seen in WT litter mates. *Fmr1* mRNA production was increased, FMRP translational efficiency in response to DHPG was impaired, and basal FMRP levels were moderately reduced. The authors note that *Fmr1* knockout mice completely lacking FMRP also show enhanced LTD, suggesting that the enhanced LTD in the CGG_{nih} KI mouse may be due, at least in part, to lower levels of FMRP. The differing results for LTD between the CGG_{dut} and CGG_{nih} KI mouse models may therefore be the result of small versus moderate reductions in FMRP, respectively, indicating different cellular mechanisms for the differing results.

Developmental aspects in PM and FXTAS

FXTAS was originally described as a late-onset neurodegenerative disorder typically appearing in PM carriers in the 5^{th} or 6^{th} decade of life. However, it is clear from both human [137, 138] and mouse studies [63] that the consequences of the expanded CGG repeat can be seen in PM carriers much earlier in development, indicating that the disease process likely begins much earlier in life, and possibly as early as during gestation [139]. Specifically, some children with the PM have been reported to show cognitive deficits and behavioral problems, including symptoms of autism spectrum disorder (ASD) and attention-deficit hyperactivity disorder (ADHD) [137, 138]. Young (<12 week old) CGG_{dut} and CGG_{nih} KI mice show impaired processing of spatial information [63] and abnormal locomotor activity and anxiety in the elevated Plus-maze [64].

The possibility that the PM may affect early brain development is supported by findings in the CGG_{dut} KI mouse where abnormal migration and differentiation of neuronal precursors during development of the embryonic cortical plate has been found [139]. In this study precursor cells and embryonic neurons were labeled in utero on embryonic day 14 (E14) by intracerebral injections of a retrovirus encoding eGFP. The entire cell body, cytoplasm

and processes of infected cells and their progeny are labeled with the eGFP reporter. The morphology of eGFP-labeled radial glial cells and immature neurons was not different between KI and WT neurons when examined on E17. However, there was evidence for altered differentiation of embryonic neural progenitor cells in the developing neocortex.

Radial glial cells in the ventricular zone (VZ) express the transcription factor Pax6 (i.e., $Pax6^+$), divide at the ventricular surface and give rise to intermediate neuronal progenitor cells that express the transcription factor Tbr2 ($Tbr2^+$) [140, 141]. The CGG_{dut} KI mice had a greater number of $Pax6^+$ cells in the VZ and fewer $Tbr2^+$ cells in the SVZ than in WT mice, suggesting that delayed differentiation of the Pax6 cells in the CGG_{dut} KI mice may have produced a shift towards more $Pax6^+$ and fewer $Tbr2^+$ cells. Importantly, the shift in cell distribution could not be attributed to increased proliferation of $Pax6^+$ cells, decreased proliferation of $Tbr2^+$, or increased cell death among $Tbr2^+$ cells. These data suggest that the *Fmr1* CGG repeat allele impacts the developing brain during gestation, much earlier than previously realized, and point to a neurodevelopmental component in FXTAS.

Neurobehavioral correlates

Key features of FXTAS patients are late-onset ataxia and memory impairments. Similar phenotypes have been found for CGG KI mice. Motor performance on the rotarod declines with age in CGG_{dut} KI mice [65]. In addition, sensory-motor coordination is impaired in adult CGG_{dut} KI animals when they are required to traverse a horizontal ladder (i.e., ladder rung task). Both male and female CGG_{dut} KI mice showed impairments that were positively correlated with CGG repeat size [142]. Poor performance in the rotarod and ladder rung test may reflect the ataxia seen in FXTAS. Adult female CGG KI mice are also impaired in learning a skilled forelimb motor task in which they are trained to reach through a narrow opening in a Plexiglas box order to grasp and obtain a small food reward positioned just outside the box. Again, performance was worse with longer CGG repeat lengths [143]. Similar experiments have not yet been carried out in adult male mice. To date studies in CGG KI mice have not reported intention tremors, a key neurological feature in FXTAS. The reason for this is unclear, but may be related to the quadrapedal organization of the rodent motor system.

Spatial learning and memory in the Morris water maze is impaired in CGG_{dut} KI mice at 52 weeks of age, but not in 20 weeks indicating a progressive nature of the deficit [65]. Additional spatial deficits in CGG_{dut} KI mice are seen in the "metric" spatial processing test that involves processing precise angles and distances that separate objects in space, without regard to the identity of the objects [144]. In this test mice are allowed to explore two identical objects separated in space by a fix distance for 15 min (e.g., study phase), showing very little further exploration at the end of this time. Mice are removed from the apparatus, the distance between the objects changed (e.g., moved closer

together), and the mice are allowed to re-explore the objects for 5 min (e.g., test phase). During the test phase WT mice showed increased object exploration indicating that they detected a change in the distance between objects, while CGG_{dut} KI mice failed to re-explore the objects. Deficits in this task were seen as early as 12 weeks of age when small but easily detectable intranuclear inclusions are present in neurons in the dentate gyrus of the hippocampus but not in parietal cortex [63]. Lesion studies have implicated the dentate gyrus and CA3 hippocampus in processing of metric spatial information, a form of spatial pattern separation [145]. This suggests that histopathology (e.g., presence of intranuclear inclusions, altered dendritic and spine morphology) in the dentate gyrus and CA3 subregion of the hippocampus in CGG KI mice may contribute to this spatial processing deficit. Although the role of intranuclear inclusions to pathology in FXTAS is unclear, the presence of intranuclear inclusions in different brain regions at different ages appears to follow a similar time course as the emergence of behavioral dysfunction in the CGG KI mouse, suggesting there might be a relationship between spatial deficits and inclusion formation [52, 146, 147]. Additional behavioral pathology found in the CGG_{nih} KI mouse model of the PM and FXTAS includes mild hyperactivity, decreased anxiety in elevated plus maze, and impaired shock avoidance learning [64].

Finally, the recently reported inducible mouse model show high RNA expression and neuropathology in lobule X of the cerebellum and two laterally located flocculi, together the vestibulo-cerebellum. In two independent behavioral tests linked to this region, the optokinetic reflex (OKR), and the vestibulo-ocular reflex (VOR), a behavioral deficit was found in mice treated with dox for twenty weeks. After 8 weeks of dox induction and 12 weeks of wash-out this eye movement phenotype could be halted [79].

Evidence for current disease models

1. RNA toxicity

Studies in mouse models have been particularly useful in identifying molecular mechanisms in the PM and FXTAS. An RNA "toxic gain of function" mechanism has been proposed in which elevated *FMR1* mRNA transcripts bearing an expanded CGG repeat are cytotoxic. Toxicity appears to be the result of the expanded CGG repeat *per se*, and not to over-expression of *FMR1* or overexpression of an CGG11 repeat [79, 80]. This is supported by the fact that ectopic expression of a CGG repeat expansion in the PM range is sufficient to induce formation of intranuclear inclusions, reduce cell viability, trigger neuronal death (e.g., Purkinje cell loss) and produce behavioral deficits [67, 98, 148], while over-expression of *Fmr1* mRNA with a CGG repeat expansion does not appear to be toxic [75]. Similar RNA toxicity has been suggested to underlie the pathology in several repeat diseases, including the myotonoic muscular dystrophies. In this model sequestration of important

proteins through their interactions with expanded repeats prevents the proteins from carrying out their normal functions. As shown in **Figure 2A**, a similar protein sequestration mechanism has been proposed to underlie disease processes in the PM and in FXTAS [2, 27, 68, 149]. Based on studies in human and animal (e.g., mouse, fly) tissues, a number of candidate RNA binding proteins have been identified, including DGCR8 and DROSHA [85], SAM68 [49], purα [150, 151], hnRNPA2/B1 and CUGBP1 [69].

2. Sequestration of DROSHA/DGCR8 & miRNAs

While the evidence is strong for the binding of proteins to CGG expansions and sequestration of proteins within ubiquitin-positive inclusions, the consequences of sequestration for cell function remain to be described. However, a recent study has linked sequestration of proteins associated with microRNA (miRNA) processing with the disease process in FXTAS [85]. Specifically, the double stranded RNA-binding protein DGCR8 binds preferentially to CGG repeats of pathogenic length (i.e., >CGG repeat length >60). As depicted in **Figure 2A**, this leads to partial sequestration of DGCR8 and its binding partner DROSHA to expanded CGG repeats within CGG RNA aggregates. DGCR8 and DROSHA are important for processing pre-miRNAs into mature miRNAs by the DICER enzyme. Dgcr8 deficiency in heterozygous Dgcr8+/- mice results in reduced synaptic potentiation in layer 5 pyramidal neurons in the medial prefrontal cortex of mice [152], and large deletions in the 22q11 locus, that include Dgcr8, result in altered dendritic spine morphology, reduced dendritic branching complexity, and impaired working memory [153]. Similarly, loss of DICER in mice results in progressive neuronal degeneration [154], reduced dendritic branching and increased dendritic spine length [155], ataxia and reduced brain size following deletion from striatal neurons [156]. These results suggested a model in which double-stranded CGG RNA forms hairpins [131] that mimic the RNA structure of pri-miRNAs recognized by DGCR8 [85]. DGCR8 and its partner DROSHA bind to the expanded CGG repeat element and are therefore sequestered, reducing the production of mature miRNAs causing neuronal dysfunction and death [85]. This possibility is supported by the observation that the expression of mature miRNAs was decreased in postmortem brain samples from patients with FXTAS. In addition, *in vitro* over-expression of DGCR8 restored normal dendritic growth and branching, and alleviated cell death of cultured neurons expressing a toxic 60 CGG repeat [85].

3. Repeat associated non-AUG (RAN) translation

An additional mechanism of toxicity is shown in **Figure 2B**. In this model toxicity is triggered by CGG repeat associated non-AUG initiated (RAN) translation [41]. This is based on evidence that trinucleotide repeats can be translated into protein even if they do not reside in an AUG-initiated open reading frame (ORF) [157], and such translation

can occur in all three possible ORF's of a transcript generating multiple potentially toxic products from a single repeat [158]. In the case of FXTAS it has been proposed that RAN translation initiated in the 5'-UTR of *FMR1* mRNA results in the production of a cytotoxic polyglycine-containing protein named FMRpolyG [41]. This is supported by results from human FXTAS and animal model studies. Specifically, the presence of the FMRpolyG was confirmed by western blot in cerebellar lysates of postmortem FXTAS brains. FMRpolyG staining was specific for FXTAS, and was not found in control brains, brain sections from spinocerebellar ataxia 3 patients or in Alzheimers brain tissue. FMRpolyG-positive intranuclear inclusions were also found in brain, kidney, adrenal gland, heart, thyroid, and pituitary of postmortem material from a patient with FXTAS [34, 41, 42] and in ovarian stromal cells of a PM carrier with FXPOI [34]. In the inducible mouse model, containing the human 5'UTR, FMRpolyG-positive inclusions were observed after 8 weeks of dox induction [79]. In primary hippocampal neurons derived from this mouse model FMRpolyG-positive intranuclear inclusions were observed after 2 weeks of dox induction (Buijsen, et al. Abstracts of the 2nd Premutation Meeting, Sitges, Spain, 2015 and chapter 6). Interestingly clear differences were observed between the CGG_{dut} KI and CGG_{nih} KI mouse models, with co-localization of FMRpolyG- and ubiquitin-positive intranuclear inclusions in the cortex and hypothalamus of the CGG_{dut} KI mouse, but not in the CGG_{nih} KI mouse. The CGG_{nih} KI mouse has a TAA stop codon 18 base pairs upstream of the polyglycine frame. This stop codon is not present in the CGG_{dut} KI mouse. These data suggest that some of the differing pathology between the two mouse models could be explained by differences in the ability to generate the toxic polyglycine peptide. The mechanisms underlying RAN translation are as yet unknown, but the presence of the polyglycine peptide (i.e., FMRpolyG) in FXTAS and the CGG KI mouse models led to the proposal by Todd, et al that a scanning 43S ribosomal pre-initiation complex stalls at the CGG repeat, resulting in use of alternative non-AUG start sites for translation in the +1 reading frame (i.e., GGC, polyGlycine) and the production of the FMRpolyG protein. Sellier, et al. demonstrated that an ACG sequence embedded in a potential Kozac consensus sequence located upstream of the CGG repeat is responsible for RAN translation even without a CGG repeat (Sellier, et al., manuscript in preparation). Interestingly the data did not show translation product from the +0 (i.e., CGG, polyarginine) reading frame, but some, albeit less efficient, translation in the +2 reading frame was observed (i.e., GCG, polyalanine) [41]. It is has been shown in *Drosophila* and cell models that RAN translation of FMRpolyG underlies the genetic interaction between protein quality control pathways and CGG-repeat-mediated toxicity. Driving expression of FMRpolyG leads to impairment of ubiquitin proteasome system (UPS) function, while prevention of RAN translation attenuated UPS impairment. This study suggest that therapeutic interventions that either block RAN translation or enhance UPS activity are likely to have beneficial effects in

FXTAS [159]. Recently, Yang, et al. developed small chemical compounds that bind to the hairpin structure of the CGG RNA and selectively inhibited RAN translation without affecting translation of the downstream open reading frame [160]. These compounds also prevent the binding of RNA binding proteins to the expanded CGG repeat and rescues FXTAS-related splicing deficits [161, 162]. In primary hippocampal neurons generated from E18 inducible embryos used in [80], formation of intranuclear FMRpolyG- and ubiquitin-positive intranuclear inclusions can be inhibited by using compound 1a (Buijsen, et al. Abstracts of the 2nd Premutation Meeting, Sitges, Spain, 2015 and chapter 6). Studies in mice with these small molecules have not been carried out so far.

CONCLUSIONS

While uniquely human components of disease cannot be fully captured in animal models, mouse models of FXTAS have provided useful research tools to test hypotheses about the molecular underpinnings of the disorder, and to develop effective treatments. Generation of expanded CGG knock-in mice have provided insight into the natural history of the disorder, the molecular correlates, pathology in brain and other organ systems, as well as an understanding of the neurobehavioral deficits caused by expanded CGG repeat expression. These KI mice allow studies for the evaluation of novel therapeutic strategies, either pharmacological or gene-targeted, to halt or reverse disease processes and to improve neurological outcome. Ongoing development of new mouse lines, including conditional and inducible mice, should further increase our knowledge to understand the pathology of repeat disorders such as FXTAS. There are many open questions to be answered that will continue to rely on mouse models, including the mechanism of repeat instability, why mRNA levels are elevated, the role of reduced FMRP in pathology, whether intranuclear inclusions are toxic or protective, and how protein sequestration and repeat associated non-AUG (RAN) translation contribute to the disease process in patients with FXTAS.

REFERENCES

1. Bear, M.F., K.M. Huber, and S.T. Warren, *The mGluR theory of fragile X mental retardation.* Trends Neurosci, 2004. **27**(7): p. 370-7.
2. Renoux, A.J. and P.K. Todd, *Neurodegeneration the RNA way.* Prog Neurobiol, 2012. **97**(2): p. 173-89.
3. Hagerman, R. and P. Hagerman, *Advances in clinical and molecular understanding of the FMR1 premutation and fragile X-associated tremor/ataxia syndrome.* Lancet Neurol, 2013. **12**(8): p. 786-98.
4. Verkerk, A.J., et al., *Identification of a gene (FMR-1) containing a CGG repeat coincident with a breakpoint cluster region exhibiting length variation in fragile X syndrome.* Cell, 1991. **65**(5): p. 905-14.
5. Willemsen, R., J. Levenga, and B. Oostra, *CGG repeat in the FMR1 gene: size matters.* Clin Genet, 2011. **80**(3): p. 214-25.
6. Hantash, F.M., et al., *FMR1 premutation carrier frequency in patients undergoing routine population-based carrier screening: insights into the prevalence of fragile X syndrome, fragile X-associated tremor/ataxia syndrome, and fragile X-associated primary ovarian insufficiency in the United States.* Genet Med, 2011. **13**(1): p. 39-45.
7. Jacquemont, S., et al., *Penetrance of the fragile x-associated tremor/ataxia syndrome in a premutation carrier population.* JAMA, 2004. **291**(4): p. 460-9.
8. Hunter, J., et al., *Epidemiology of fragile X syndrome: A systematic review and meta-analysis.* American Journal of Medical Genetics Part A, 2014. **164**(7): p. 1648-1658.
9. Rodriguez-Revenga, L., et al., *Penetrance of FMR1 premutation associated pathologies in fragile X syndrome families.* Eur J Hum Genet, 2009. **17**(10): p. 1359-62.
10. Chonchaiya, W., et al., *Clinical involvement in daughters of men with fragile X-associated tremor ataxia syndrome.* Clin Genet, 2010. **78**: p. 38-46.
11. Jacquemont, S., et al., *Aging in individuals with the FMR1 mutation.* Am J Ment Retard, 2004. **109**(2): p. 154-64.
12. O'Dwyer, J.P., et al., *Fragile X-associated tremor/ataxia syndrome presenting in a woman after chemotherapy.* Neurology, 2005. **65**(2): p. 331-2.
13. Paul, R., et al., *Early onset of neurological symptoms in fragile X premutation carriers exposed to neurotoxins.* Neurotoxicology, 2010. **31**: p. 399-402.
14. Muzar, Z., et al., *Addictive substances may induce a rapid neurological deterioration in fragile X-associated tremor ataxia syndrome: A report of two cases.* Intractable Rare Dis Res, 2014. **3**(4): p. 162-5.
15. Muzar, Z., et al., *Methadone use in a male with the FMR1 premutation and FXTAS.* American Journal of Medical Genetics Part A, 2015. **167**(6): p. 1354-1359.
16. Saldarriaga, W., et al., *Phenobarbital Use and Neurological Problems in Fmr1 Premutation Carriers.* Neurotoxicology, 2016.
17. Tassone, F., et al., *CGG repeat length correlates with age of onset of motor signs of the fragile X-associated tremor/ataxia syndrome (FXTAS).* Am J Med Genet, 2007. **144B**: p. 566-569.
18. Grigsby, J., et al., *Cognitive profile of fragile X premutation carriers with and without fragile X-associated tremor/ataxia syndrome.* Neuropsychology, 2008. **22**(1): p. 48-60.
19. Kim, S.Y., et al., *Altered neural activity of magnitude estimation processing in adults with the fragile X premutation.* J Psychiatr Res, 2013.
20. Berry-Kravis, E., et al., *Fragile X-associated tremor/ataxia syndrome: clinical features, genetics, and testing guidelines.* Mov Disord, 2007. **22**(14): p. 2018-30, quiz 2140.
21. Hagerman, P.J. and R.J. Hagerman, *Fragile X-associated Tremor/Ataxia Syndrome (FXTAS).* Ment Retard Dev Disabil Res Rev, 2004. **10**(1): p. 25-30.
22. Coffey, S.M., et al., *Expanded clinical phenotype of women with the FMR1 premutation.* American Journal of Medical Genetics Part A, 2008. **146A**(8): p. 1009-1016.
23. Leehey, M.A., et al., *Fibromyalgia in fragile X mental retardation 1 gene premutation carriers.* Rheumatology (Oxford), 2011. **50**: p. 2233-2236.
24. Bailey, D.B., et al., *Co-occurring conditions associated with FMR1 gene variations: Findings from a national parent survey.* American Journal of Medical Genetics Part A, 2008. **146A**(16): p. 2060-2069.

25. Au, J., et al., *Prevalence and risk of migraine headaches in adult fragile X premutation carriers*. Clinical Genetics, 2013. **84**(6): p. 546-551.

26. Greco, C.M., et al., *Testicular and pituitary inclusion formation in fragile X associated tremor/ataxia syndrome*. J Urol, 2007. **177**(4): p. 1434-7.

27. Hagerman, R.J., et al., *Intention tremor, parkinsonism, and generalized brain atrophy in male carriers of fragile X*. Neurology, 2001. **57**(1): p. 127-30.

28. Jacquemont, S., et al., *Fragile X Premutation Tremor/Ataxia Syndrome: Molecular, Clinical, and Neuroimaging Correlates*. Am J Hum Genet, 2003. **72**(4): p. 869-78.

29. Hunsaker, M.R., et al., *Widespread non-central nervous system organ pathology in fragile X premutation carriers with fragile X-associated tremor/ataxia syndrome and CGG knock-in mice*. Acta Neuropathol, 2011. **122**: p. 467-479.

30. Sullivan, S.D., C. Welt, and S. Sherman, *FMR1 and the continuum of primary ovarian insufficiency*. Semin Reprod Med, 2011. **29**(4): p. 299-307.

31. Coulam, C.B., S.C. Adamson, and J.F. Annegers, *Incidence of premature ovarian failure*. Obstet Gynecol, 1986. **67**(4): p. 604-6.

32. Allingham-Hawkins, D.J., et al., *Fragile X premutation is a significant risk factor for premature ovarian failure: the International Collaborative POF in Fragile X study- -preliminary data*. Am J Med Genet, 1999. **83**(4): p. 322-325.

33. Sherman, S.L., *Premature ovarian failure in the fragile X syndrome*. Am J Med Genet, 2000. **97**(3): p. 189-94.

34. Buijsen, R.A., et al., *Presence of inclusions positive for polyglycine containing protein, FMRpolyG, indicates that repeat-associated non-AUG translation plays a role in fragile X-associated primary ovarian insufficiency*. Hum Reprod, 2015.

35. Dioguardi, C.C., et al., *Granulosa Cell and Oocyte Mitochondrial Abnormalities in a Mouse Model of Fragile X Primary Ovarian Insufficiency*. Mol Hum Reprod, 2016.

36. Sherman, S.L., et al., *Use of model systems to understand the etiology of fragile X-associated primary ovarian insufficiency (FXPOI)*. J Neurodev Disord, 2014. **6**(1): p. 26.

37. Berry-Kravis, E., et al., *Fragile X-associated tremor/ataxia syndrome: Clinical features, genetics, and testing guidelines*. Movement Disorders, 2007. **22**(14): p. 2018-2030.

38. Hall, D.A., et al., *Emerging topics in FXTAS*. J Neurodev Disord, 2014. **6**(1): p. 31.

39. Greco, C.M., et al., *Neuropathology of fragile X-associated tremor/ataxia syndrome (FXTAS)*. Brain, 2006. **129**(Pt1): p. 243-255.

40. Greco, C.M., et al., *Neuronal intranuclear inclusions in a new cerebellar tremor/ataxia syndrome among fragile X carriers*. Brain, 2002. **125**(Pt 8): p. 1760-1771.

41. Todd, P.K., et al., *CGG Repeat-Associated Translation Mediates Neurodegeneration in Fragile X Tremor Ataxia Syndrome*. Neuron, 2013. **78**(3): p. 440-455.

42. Buijsen, R.A., et al., *FMRpolyG-positive inclusions in CNS and non-CNS organs of a fragile X premutation carrier with fragile X-associated tremor/ataxia syndrome*. Acta Neuropathol Commun, 2014. **2**(1): p. 162.

43. Iwahashi, C.K., et al., *Protein composition of the intranuclear inclusions of FXTAS*. Brain, 2006. **129**(Pt 1): p. 256-271.

44. Iwahashi, C. and P.J. Hagerman, *Isolation of pathology-associated intranuclear inclusions*. Methods Mol Biol, 2008. **463**: p. 181-90.

45. Sellier, C., et al., *Sequestration of DROSHA and DGCR8 by Expanded CGG RNA Repeats Alters MicroRNA Processing in Fragile X-Associated Tremor/Ataxia Syndrome*. Cell Rep, 2013. **3**(3): p. 869-880.

46. Sellier, C., et al., *Sam68 sequestration and partial loss of function are associated with splicing alterations in FXTAS patients*. Embo J, 2010. **29**: p. 1248-1261.

47. Gokden, M., J.T. Al-Hinti, and S.I. Harik, *Peripheral nervous system pathology in fragile X tremor/ataxia syndrome (FXTAS)*. Neuropathology, 2009. **29**(3): p. 280-4.

48. Louis, E., et al., *Parkinsonism, dysautonomia, and intranuclear inclusions in a fragile X carrier: A clinical-pathological study*. Movement Disorders, 2006. **21**(3): p. 420-425.

49. Sellier, C., et al., *Sam68 sequestration and partial loss of function are associated with splicing alterations in FXTAS patients*. Embo J, 2010. **29**(7): p. 1248-61.

50. Bontekoe, C.J., et al., *Instability of a (CGG)(98) repeat in the Fmr1 promoter*. Hum Mol Genet, 2001. **10**(16): p. 1693-9.

51. Brouwer, J.R., et al., *Elevated Fmr1 mRNA levels and reduced protein expression in a mouse model with an unmethylated Fragile X full mutation.* Exp Cell Res, 2007. **313**(2): p. 244-53.

52. Willemsen, R., et al., *The FMR1 CGG repeat mouse displays ubiquitin-positive intranuclear neuronal inclusions; implications for the cerebellar tremor/ataxia syndrome.* Hum Mol Genet, 2003. **12**(9): p. 949-59.

53. Berman, R.F. and R. Willemsen, *Mouse models of fragile x-associated tremor ataxia.* J Investig Med, 2009. **57**(8): p. 837-41.

54. Entezam, A., et al., *Regional FMRP deficits and large repeat expansions into the full mutation range in a new Fragile X premutation mouse model.* Gene, 2007. **395**: p. 125-134.

55. Entezam, A., et al., *Regional FMRP deficits and large repeat expansions into the full mutation range in a new Fragile X premutation mouse model.* Gene, 2007. **395**(1-2): p. 125-34.

56. Iyer, R.R., et al., *DNA polymerase III proofreading mutants enhance the expansion and deletion of triplet repeat sequences in Escherichia coli.* J Biol Chem, 2000. **275**(3): p. 2174-84.

57. Jakupciak, J.P. and R.D. Wells, *Genetic instabilities in (CTG.CAG) repeats occur by recombination.* J Biol Chem, 1999. **274**(33): p. 23468-79.

58. White, P.J., R.H. Borts, and M.C. Hirst, *Stability of the human fragile X (CGG)(n) triplet repeat array in saccharomyces cerevisiae deficient in aspects of DNA metabolism.* Mol Cell Biol, 1999. **19**(8): p. 5675-5684.

59. Entezam, A. and K. Usdin, *ATR protects the genome against CGG.CCG-repeat expansion in Fragile X premutation mice.* Nucleic Acids Res, 2008. **36**(3): p. 1050-6.

60. Zhao, X.N. and K. Usdin, *The transcription-coupled repair protein ERCC6/CSB also protects against repeat expansion in a mouse model of the fragile X premutation.* Hum Mutat, 2015. **36**(4): p. 482-7.

61. Lokanga, R.A., et al., *Heterozygosity for a Hypomorphic Polbeta Mutation Reduces the Expansion Frequency in a Mouse Model of the Fragile X-Related Disorders.* PLoS Genet, 2015. **11**(4): p. e1005181.

62. Brouwer, J.R., et al., *CGG-repeat length and neuropathological and molecular correlates in a mouse model for fragile X-associated tremor/ataxia syndrome.* J Neurochem, 2008. **107**(6): p. 1671-82.

63. Hunsaker, M.R., et al., *Progressive spatial processing deficits in a mouse model of the fragile X premutation.* Behav Neurosci, 2009. **123**(6): p. 1315-24.

64. Qin, M., et al., *A mouse model of the fragile X premutation: effects on behavior, dendrite morphology, and regional rates of cerebral protein synthesis.* Neurobiol Dis, 2011. **42**(1): p. 85-98.

65. Van Dam, D., et al., *Cognitive decline, neuromotor and behavioural disturbances in a mouse model for fragile-X-associated tremor/ataxia syndrome (FXTAS).* Behav Brain Res, 2005. **162**(2): p. 233-9.

66. Baxter, M.G. and E.A. Murray, *Opposite relationship of hippocampal and rhinal cortex damage to delayed nonmatching-to-sample deficits in monkeys.* Hippocampus, 2001. **11**(1): p. 61-71.

67. Hashem, V., et al., *Ectopic expression of CGG containing mRNA is neurotoxic in mammals.* Hum Mol Genet, 2009. **18**(13): p. 2443-51.

68. Jin, P., et al., *RNA-Mediated Neurodegeneration Caused by the Fragile X Premutation rCGG Repeats in Drosophila.* Neuron, 2003. **39**(5): p. 739-747.

69. Sofola, O.A., et al., *RNA-Binding Proteins hnRNP A2/B1 and CUGBP1 Suppress Fragile X CGG Premutation Repeat-Induced Neurodegeneration in a Drosophila Model of FXTAS.* Neuron, 2007. **55**(4): p. 565-71.

70. Timchenko, L.T., et al., *Identification of a (CUG)n triplet repeat RNA-binding protein and its expression in myotonic dystrophy.* Nucleic Acids Res, 1996. **24**(22): p. 4407-14.

71. Timchenko, N.A., et al., *Molecular basis for impaired muscle differentiation in myotonic dystrophy.* Mol Cell Biol, 2001. **21**(20): p. 6927-38.

72. Zola, S.M. and L.R. Squire, *Relationship between magnitude of damage to the hippocampus and impaired recognition memory in monkeys.* Hippocampus, 2001. **11**(2): p. 92-8.

73. Galloway, J.N., et al., *CGG repeats in RNA modulate expression of TDP-43 in mouse and fly models of fragile X tremor ataxia syndrome.* Hum Mol Genet, 2014. **23**(22): p. 5906-15.

74. He, F., et al., *TDP-43 suppresses CGG repeat-induced neurotoxicity through interactions with HnRNP A2/B1.* Hum Mol Genet, 2014. **23**(19): p. 5036-51.

75. Fernandez, J.J., et al., *Gene expression profiles in the cerebellum of transgenic mice over expressing the human FMR1 gene with CGG repeats in the normal range.* Genet Mol Res, 2012. **11**(1): p. 467-83.

76. Peier,A.M., et al., *(Over)correction of FMR1 deficiency with YAC transgenics: behavioral and physical features.* Hum Mol Genet, 2000. **9**(8): p. 1145-1159.

77. Spencer, C.M., et al., *Social behavior in Fmr1 knockout mice carrying a human FMR1 transgene.* Behav Neurosci, 2008. **122**(3): p. 710-5.

78. Peier, A.M. and D.L. Nelson, *Instability of a premutation-sized CGG repeat in FMR1 YAC transgenic mice.* Genomics, 2002. **80**(4): p. 423-32.

79. Hukema, R.K., et al., *Reversibility of neuropathology and motor deficits in an inducible mouse model for FXTAS.* Human Molecular Genetics, 2015. **24**(17): p. 4948-4957.

80. Hukema, R.K., et al., *Induced expression of expanded CGG RNA causes mitochondrial dysfunction in vivo.* Cell Cycle, 2014. **13**(16): p. 2600-2608.

81. Willemsen, R., et al., *The FMR1 CGG repeat mouse displays ubiquitin-positive intranuclear neuronal inclusions; implications for the cerebellar tremor/ataxia syndrome.* Hum Mol Genet, 2003. **12**(9): p. 949-59.

82. Wenzel, H.J., et al., *Ubiquitin-positive intranuclear inclusions in neuronal and glial cells in a mouse model of the fragile X premutation.* Brain Res, 2010. **1318**: p. 155-166.

83. Greco, C.M., et al., *Neuropathology of fragile X-associated tremor/ataxia syndrome (FXTAS).* Brain, 2006. **129**(Pt 1): p. 243-55.

84. Hunsaker, M.R., et al., *Widespread non-central nervous system organ pathology in fragile X premutation carriers with fragile X-associated tremor/ataxia syndrome and CGG knock-in mice.* Acta Neuropathol, 2011. **122**(4): p. 467-79.

85. Sellier, C., et al., *Sequestration of DROSHA and DGCR8 by Expanded CGG RNA Repeats Alters MicroRNA Processing in Fragile X-Associated Tremor/Ataxia Syndrome.* Cell Rep, 2013.

86. Tassone, F., et al., *Intranuclear inclusions in neural cells with premutation alleles in fragile X associated tremor/ataxia syndrome.* J Med Genet, 2004. **41**(4): p. E43.

87. Bergink, S., et al., *The DNA repair-ubiquitin-associated HR23 proteins are constituents of neuronal inclusions in specific neurodegenerative disorders without hampering DNA repair.* Neurobiol Dis, 2006. **23**(3): p. 708-16.

88. Tassone, F., C. Iwahashi, and P.J. Hagerman, *FMR1 RNA withinthe intranuclear inclusions of fragile X-associated Tremor/Ataxia syndrome (FXTAS).* RNA biology, 2004. **1**: p. 103-105.

89. Galloway, J.N. and D.L. Nelson, *Evidence for RNA-mediated toxicity in the fragile X-associated tremor/ataxia syndrome.* Future Neurol, 2009. **4**(6): p. 785.

90. Wang, J.Y., et al., *Fragile X-associated tremor/ataxia syndrome: influence of the FMR1 gene on motor fiber tracts in males with normal and premutation alleles.* JAMA Neurol, 2013. **70**(8): p. 1022-9.

91. Brunberg, J.A., et al., *Fragile X Premutation Carriers: Characteristic MR Imaging Findings of Adult Male Patients with Progressive Cerebellar and Cognitive Dysfunction.* AJNR Am J Neuroradiol, 2002. **23**(10): p. 1757-1766.

92. Berman, R.F., et al., *Abnormal dendrite and spine morphology in primary visual cortex in the CGG knock-in mouse model of the fragile X premutation.* Epilepsia, 2012. **53 Suppl 1**: p. 150-60.

93. Hinton, V.J., et al., *Analysis of neocortex in three males with the fragile X syndrome.* Am J Med Genet, 1991. **41**(3): p. 289-294.

94. Irwin,S.A., et al.,*Abnormal dendritic spine characteristics in the temporal and visual cortices of patients with fragile-X syndrome: A quantitative examination.* Am J Med Genet, 2001. **98**(2): p. 161-167.

95. Irwin, S.A., et al., *Dendritic spine and dendritic field characteristics of layer V pyramidal neurons in the visual cortex of fragile-X knockout mice.* Am J Med Genet, 2002. **111**(2): p. 140-6.

96. McKinney, B.C., et al., *Dendritic spine abnormalities in the occipital cortex of C57BL/6 Fmr1 knockout mice.* Am J Med Genet B Neuropsychiatr Genet, 2005. **136B**(1): p. 98-102.

97. Garcia-Arocena, D., et al., *Fibroblast phenotype in male carriers of FMR1 premutation alleles.* Hum Mol Genet, 2010. **19**(2): p. 299-312.

98. Arocena, D.G., et al., *Induction of inclusion formation and disruption of lamin A/C structure by premutation CGG-repeat RNA in human cultured neural cells.* Hum Mol Genet, 2005. **14**(23): p. 3661-71.

99. Lammerding, J., et al., *Lamins A and C but not lamin B1 regulate nuclear mechanics.* J Biol Chem, 2006. **281**(35): p. 25768-80.

100. Singh, M., et al., *Lamin A/C depletion enhances DNA damage-induced stalled replication fork arrest.* Mol Cell Biol, 2013. **33**(6): p. 1210-22.

101. Richards, S.A., et al., *The accumulation of un-repairable DNA damage in laminopathy progeria fibroblasts is caused by ROS generation and is prevented by treatment with N-acetyl cysteine.* Hum Mol Genet, 2011. **20**(20): p. 3997-4004.

102. Blasco, M.A., *Telomeres and human disease: ageing, cancer and beyond.* Nat Rev Genet, 2005. **6**(8): p. 611-22.

103. Cao, K., et al., *Progerin and telomere dysfunction collaborate to trigger cellular senescence in normal human fibroblasts.* J Clin Invest, 2011. **121**(7): p. 2833-44.

104. Gonzalez-Suarez, I., et al., *Novel roles for A-type lamins in telomere biology and the DNA damage response pathway.* Embo J, 2009. **28**(16): p. 2414-27.

105. Garcia-Arocena, D. and P.J. Hagerman, *Advances in understanding the molecular basis of FXTAS.* Hum Mol Genet, 2010. **19**(R1): p. R83-9.

106. Jenkins, E.C., et al., *Reduced telomere length in older men with premutation alleles of the fragile X mental retardation 1 gene.* Am J Med Genet A, 2008. **146A**(12): p. 1543-6.

107. Ross-Inta, C., et al., *Evidence of mitochondrial dysfunction in fragile X-associated tremor/ataxia syndrome.* Biochem J, 2010. **429**(3): p. 545-52.

108. Kaplan, E.S., et al., *Early mitochondrial abnormalities in hippocampal neurons cultured from Fmr1 pre-mutation mouse model.* J Neurochem, 2012. **123**(4): p. 613-21.

109. Chen, Y., Tassone, F., Berman, R.F., Hagerman, P.M., Hagerman, R.J., Willemsen, R. & Pessah, I.N., *Murine hippocampal neurons expressing Fmr1 gene premutation show early developmental deficits and late degeneration.* Human Molecular Genetics, 2010. **19**(1): p. 196-208.

110. Lei, X.G., W.H. Cheng, and J.P. McClung, *Metabolic regulation and function of glutathione peroxidase-1.* Annual Review of Nutrition, 2007. **27**: p. 41-61.

111. Brouwer, J.R., et al., *Elevated Fmr1 mRNA levels and reduced protein expression in a mouse model with an unmethylated Fragile X full mutation.* Exp Cell Res, 2007. **313**: p. 244-253.

112. Brouwer, J.R., et al., *CGG-repeat length and neuropathological and molecular correlates in a mouse model for fragile X-associated tremor/ataxia syndrome.* J Neurochem, 2008. **107**: p. 1671-1682.

113. Kenneson, A., et al., *Reduced FMRP and increased FMR1 transcription is proportionally associated with CGG repeat number in intermediate-length and premutation carriers.* Hum Mol Genet, 2001. **10**(14): p. 1449-1454.

114. Brouwer, J.R., et al., *Altered hypothalamus-pituitary-adrenal gland axis regulation in the expanded CGG-repeat mouse model for fragile X-associated tremor/ataxia syndrome.* Psychoneuroendocrinology, 2008. **33**: p. 863-873.

115. Chiang, P.W., L.E. Carpenter, and P.J. Hagerman, *The 5'-untranslated region of the FMR1 message facilitates translation by internal ribosome entry.* J Biol Chem, 2001. **276**(41): p. 37916-21.

116. Ashley, C.T., et al., *Human and murine FMR-1: alternative splicing and translational initiation downstream of the CGG-repeat.* Nat Genet, 1993. **4**(3): p. 244-51.

117. Brackett, D.M., et al., *FMR1 transcript isoforms: association with polyribosomes; regional and developmental expression in mouse brain.* PLoS ONE, 2013. **8**(3): p. e58296.

118. Sittler, A., et al., *Alternative splicing of exon 14 determines nuclear or cytoplasmic localisation of fmr1 protein isoforms.* Hum Mol Genet, 1996. **5**(1): p. 95-102.

119. Bagni, C. and B.A. Oostra, *Fragile X syndrome: From protein function to therapy.* Am J Med Genet A, 2013.

120. Tassone, F., et al., *Differential usage of transcriptional start sites and polyadenylation sites in FMR1 premutation alleles.* Nucleic Acids Res, 2011. **39**(14): p. 6172-6185.

121. D'Hulst, C., et al., *Expression of the GABAergic system in animal models for fragile X syndrome and fragile X associated tremor/ataxia syndrome (FXTAS).* Brain Res, 2009. **1253**: p. 176-183.

122. Hashimoto, R., et al., *Diffusion tensor imaging in male premutation carriers of the fragile X mental retardation gene.* Mov Disord, 2011. **26**(7): p. 1329-36.

123. Porcellini, E., et al., *Elevated plasma levels of alpha-1-anti-chymotrypsin in age-related cognitive decline and Alzheimer's disease: a potential therapeutic target.* Curr Pharm Des, 2008. **14**(26): p. 2659-64.

124. Buxbaum, J.N., et al., *Transthyretin protects Alzheimer's mice from the behavioral and biochemical effects of Abeta toxicity.* Proc Natl Acad Sci U S A, 2008. **105**(7): p. 2681-6.

125. Chonchaiya, W., et al., *Autoimmune disease in mothers with the FMR1 premutation is associated with seizures in their children with fragile X syndrome.* Hum Genet, 2010. **128**(5): p. 539-48.

126. Episkopou, V., et al., *Disruption of the transthyretin gene results in mice with depressed levels of plasma retinol and thyroid hormone.* Proc Natl Acad Sci U S A, 1993. **90**(6): p. 2375-9.

127. Fernandez, J.J., et al., *Gene expression profiles in the cerebellum of transgenic mice over expressing the human FMR1 gene with CGG repeats in the normal range.* Genetics and Molecular Research, 2012. **11**(1): p. 467-483.

128. Tan, H., et al., *MicroRNA-277 Modulates the Neurodegeneration Caused by Fragile X Premutation rCGG Repeats.* PLoS Genet, 2012. **8**(5): p. e1002681.

129. Alvarez-Mora, M.I., et al., *MicroRNA expression profiling in blood from fragile X-associated tremor/ataxia syndrome patients.* Genes Brain Behav, 2013. **12**(6): p. 595-603.

130. Fernandez, E., N. Rajan, and C. Bagni, *The FMRP regulon: from targets to disease convergence.* Front Neurosci, 2013. **7**: p. 191.

131. Kratovac, S. and J.G. Corbin, *Developmental changes in expression of inhibitory neuronal proteins in the Fragile X Syndrome mouse basolateral amygdala.* Brain Res, 2013. **1537**: p. 69-78.

132. Pretto, D.L., et al., *Reduced EAAT1 and mGluR5 expression in the cerebellum of Fmr1 premutation carriers with FXTAS.* Neurobiology of Aging, 2014. **35**(5):p. 1189-97.

133. Cao, Z., et al., *Clustered burst firing in FMR1 premutation hippocampal neurons: amelioration with allopregnanolone.* Hum Mol Genet, 2012.

134. Cao, Z., et al., *Enhanced asynchronous Ca(2+) oscillations associated with impaired glutamate transport in cortical astrocytes expressing Fmr1 gene premutation expansion.* J Biol Chem, 2013. **288**(19): p. 13831-41.

135. Hunsaker, M.R., et al., *CGG trinucleotide repeat length modulates neural plasticity and spatiotemporal processing in a mouse model of the fragile X premutation.* Hippocampus, 2012.

136. Iliff, A.J., et al., *Impaired activity-dependent FMRP translation and enhanced mGluR-dependent LTD in Fragile X premutation mice.* Hum Mol Genet, 2013. **22**(6): p. 1180-92.

137. Farzin, F., et al., *Autism spectrum disorders and attention-deficit/hyperactivity disorder in boys with the fragile X premutation.* J Dev Behav Pediatr, 2006. **27**(2 Suppl): p. S137-44.

138. Aziz, M., et al., *Clinical features of boys with fragile X premutations and intermediate alleles.* Am J Med Genet B Neuropsychiatr Genet, 2003. **121**(1): p. 119-27.

139. Cunningham, C.L., et al., *Premutation CGG-repeat expansion of the Fmr1 gene impairs mouse neocortical development.* Hum Mol Genet, 2011. **20**(1): p. 64-79.

140. Noctor, S.C., et al., *Neurons derived from radial glial cells establish radial units in neocortex.* Nature, 2001. **409**(6821): p. 714-20.

141. Englund, C., et al., *Pax6, Tbr2, and Tbr1 are expressed sequentially by radial glia, intermediate progenitor cells, and postmitotic neurons in developing neocortex.* J Neurosci, 2005. **25**(1): p. 247-51.

142. Hunsaker, M.R., et al., *Motor deficits on a ladder rung task in male and female adolescent and adult CGG knock-in mice.* Behav Brain Res, 2011. **222**(1): p. 117-21.

143. Diep, A.A., et al., *Female CGG knock-in mice modeling the fragile X premutation are impaired on a skilled forelimb reaching task.* Neurobiol Learn Mem, 2012. **97**(2): p. 229-34.

144. Gallistel, C.R., *The organization of learning*. 1993, Cambridge, MA: M.I.T. Press.

145. Hunsaker, M.R., J.S. Rosenberg, and R.P. Kesner, *The role of the dentate gyrus, CA3a,b, and CA3c for detecting spatial and environmental novelty.* Hippocampus, 2008. **18**(10): p. 1064-73.

146. Brouwer, J.R., R.Willemsen, and B.A. Oostra, *The FMR1 gene and fragile X-associated tremor/ataxia syndrome.* Am J Med Genet B Neuropsychiatr Genet, 2009. **150B**(6): p. 782-98.

147. Hunsaker, M.R., et al., *Mouse models of the fragile x premutation and the fragile x associated tremor/ataxia syndrome.* Results Probl Cell Differ, 2012. **54**: p. 255-69.

148. Hoem, G., et al., *CGG-repeat length threshold for FMR1 RNA pathogenesis in a cellular model for FXTAS.* Hum Mol Genet, 2011. **20**(11): p. 2161-70.

149. Handa, V., et al., *Long CGG-repeat tracts are toxic to human cells: Implications for carriers of Fragile X premutation alleles*. FEBS Lett, 2005. **579**(12): p. 2702-8.

150. Aumiller, V., et al., *Drosophila Pur-alpha binds to trinucleotide-repeat containing cellular RNAs and translocates to the early oocyte*. RNA Biol, 2012. **9**(5): p. 633-43.

151. Jin, P., et al., *Pur alpha Binds to rCGG Repeats and Modulates Repeat-Mediated Neurodegeneration in a Drosophila Model of Fragile X Tremor/Ataxia Syndrome*. Neuron, 2007. **55**(4): p. 556-64.

152. Fenelon, K., et al., *Deficiency of Dgcr8, a gene disrupted by the 22q11.2 microdeletion, results in altered short-term plasticity in the prefrontal cortex*. Proc Natl Acad Sci U S A, 2011. **108**(11): p. 4447-52.

153. Stark, K.L., et al., *Altered brain microRNA biogenesis contributes to phenotypic deficits in a 22q11-deletion mouse model*. Nat Genet, 2008. **40**(6): p. 751-60.

154. Schaefer, A., et al., *Cerebellar neurodegeneration in the absence of microRNAs*. J Exp Med, 2007. **204**(7): p. 1553-8.

155. Davis, T.H., et al., *Conditional loss of Dicer disrupts cellular and tissue morphogenesis in the cortex and hippocampus*. J Neurosci, 2008. **28**(17): p. 4322-30.

156. Damiani, D., et al., *Dicer inactivation leads to progressive functional and structural degeneration of the mouse retina*. J Neurosci, 2008. **28**(19): p. 4878-87.

157. Zu, T., et al., *Non-ATG-initiated translation directed by microsatellite expansions*. Proc Natl Acad Sci U S A, 2011. **108**(1): p. 260-5.

158. Pearson, C.E., *Repeat associated non-ATG translation initiation: one DNA, two transcripts, seven reading frames, potentially nine toxic entities!* PLoS Genet, 2011. **7**(3): p. e1002018.

159. Oh, S.Y., et al., *RAN translation at CGG repeats induces ubiquitin proteasome system impairment in models of fragile X-associated tremor ataxia syndrome*. Human Molecular Genetics, 2015. **24**(15): p. 4317-4326.

160. Yang, W.Y., et al., *Inhibition of Non-ATG Translational Events in Cells via Covalent Small Molecules Targeting RNA*. Journal of the American Chemical Society, 2015. **137**(16): p. 5336-5345.

161. Disney, M.D., et al., *A Small Molecule That Targets r(CGG)(exp) and Improves Defects in Fragile X-Associated Tremor Ataxia Syndrome*. Acs Chemical Biology, 2012. **7**(10): p. 1711-1718.

162. Tran, T., et al., *Targeting the r(CGG) Repeats That Cause FXTAS with Modularly Assembled Small Molecules and Oligonucleotides*. Acs Chemical Biology, 2014. **9**(4): p. 904-912.

163. Berman, R.F. and R. Willemsen, *Mouse Models of Fragile X-Associated Tremor Ataxia*. J Investig Med, 2009. **57**: p. 837-841.

FMRPOLYG-POSITIVE INCLUSIONS IN CNS AND NON-CNS ORGANS OF A FRAGILE X PREMUTATION CARRIER WITH FRAGILE X-ASSOCIATED TREMOR/ATAXIA SYNDROME

R.A.M. Buijsen[1], C. Sellier[2], E.A.W.F.M. Severijnen[1], M. Oulad-Abdelghani[1], R.F.M. Verhagen[1], R.F. Berman[3], N. Charlet-Berguerand[2], R. Willemsen[1,#], R.K. Hukema[1,#]

[1] Department of Clinical Genetics, Erasmus MC, Rotterdam, the Netherlands
[2] Department of Neurobiology and Genetics, IGBMC, Illkirch, France
[3] Department of Neurological Surgery, UC Davis, Davis, USA

[#] Both authors contributed equally

Acta Neuropathologica Communications 2014 Nov 26;2:162

FMRpolyG-positive inclusions in CNS and non-CNS organs of a PM carrier with FXTAS

Fragile X-associated Tremor/Ataxia syndrome (FXTAS), a late-onset monogenetic neurodegenerative disorder, is caused by a CGG-repeat expansion (55-200) in the 5' UTR of the *fragile-X mental retardation 1* (*FMR1*) gene on the X-chromosome [1]. The prevalence of the *FMR1* premutation (PM) is about 1:855 in males and 1:291 in females [2]. Approximately 45.5% of male and 16.5% of female PM carriers older than 50 years will develop signs of FXTAS [3]. In addition to the core features of tremor and gait ataxia, unexplained medical co-morbidities have been reported, including thyroid disease, cardiac arrhythmias, hypertension, migraine, impotence, and neuropathy [4]. PM carriers have increased levels of *FMR1* mRNA (2 to 8 fold in leucocytes) and normal to slightly reduced FMR1 protein (FMRP) levels [5]. The current hypothesis is that FXTAS is caused by an RNA gain-of-function mechanism. Ubiquitin-positive intranuclear inclusions, are found in both brain and non-central nervous system (CNS) organs of patients with FXTAS [6, 7]. So far, it is not clear whether these inclusions are protective or toxic. Recently, it has been hypothesized that repeat-associated non-AUG (RAN) translation plays a role in disease process and inclusion formation. Todd, et al. [8] demonstrated that through initiation at a near-ATG codon located in the 5'UTR of the *FMR1* gene a polyGlycine-containing protein, FMRpolyG, is expressed. This protein accumulates in ubiquitin-positive inclusions in *Drosophila*, cell culture, mouse disease models and brain from FXTAS patients.

To investigate the link between FMRpolyG expression and the co-morbid medical problems associated with the PM we have developed two novel mouse monoclonal antibodies against polyGlycine; 8FM and 9FM (for epitopes and specificity see online Additional file 1: **Figure S1**), and performed immunostaining in CNS as well as in non-CNS organs of FXTAS patient J.L. (case 6 in [7]; other cases not available). To establish antibody specificity, we performed immunostaining with both antibodies on brain sections from FXTAS patient J.L., healthy non-demented controls (n = 3) and a patient with Parkinson disease, Alzheimer disease, or C9FTD. In hippocampus and cerebellum from FXTAS patient J.L. we identified FMRpolyG-positive inclusions with both 8FM (1:10) and 9FM (1:10) antibody (**Figure 1a-b**, online Additional file 2: **Figure S2a-b**), as was described previously [8]. None of the controls showed FMRpolyG-positive inclusions (data not shown). Next, we studied the immunolocalization of FMRpolyG protein in heart, kidney, adrenal gland and thyroid in patient J.L. with 8FM (1:10) and 9FM (1:10), compared to post mortem non-CNS somatic organ tissues from 3 healthy controls. We also examined tissues for FMRP (mouse T1A; 1:200) expression and ubiquitin-positive inclusions (DAKO, ZO458; 1:200). Consistent with our previous report [7], ubiquitin-positive intranuclear inclusions were identified along with a normal distribution of FMRP (data not shown). Intranuclear FMRpolyG-positive inclusions could be detected in all organs examined (**Figure 1c-h**, online Additional file 2: **Figure S2c-h**). No control tissues

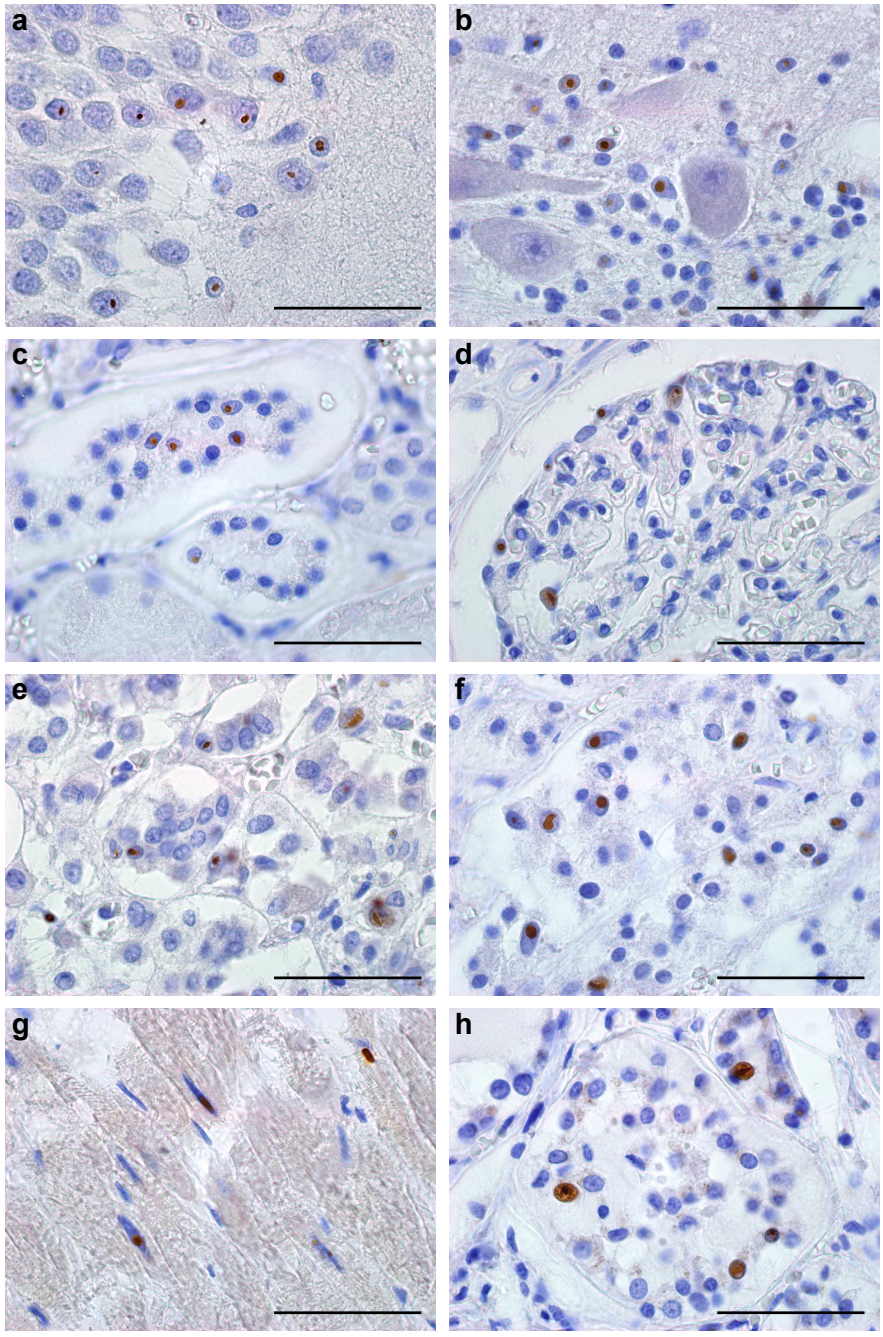

Figure 1. 9FM FMRpolyG-positive intranuclear inclusions in hippocampus, cerebellum and non-CNS tissues of a FXTAS patient. FMRpolyG-positive (9FM) intranuclear inclusions in (**a**) hippocampus, (**b**) cerebellum, (**c**) glomeruli and (**d**) distal tubule of the kidney, (**e**) zona glomerulosa and (**f**) zona reticularis of adrenal gland, (**g**) cardiomyocytes and (**h**) thyroid. All sections were immunostained with 9FM antibody and counterstained with hematoxylin. Scale bars represent 50 µm.

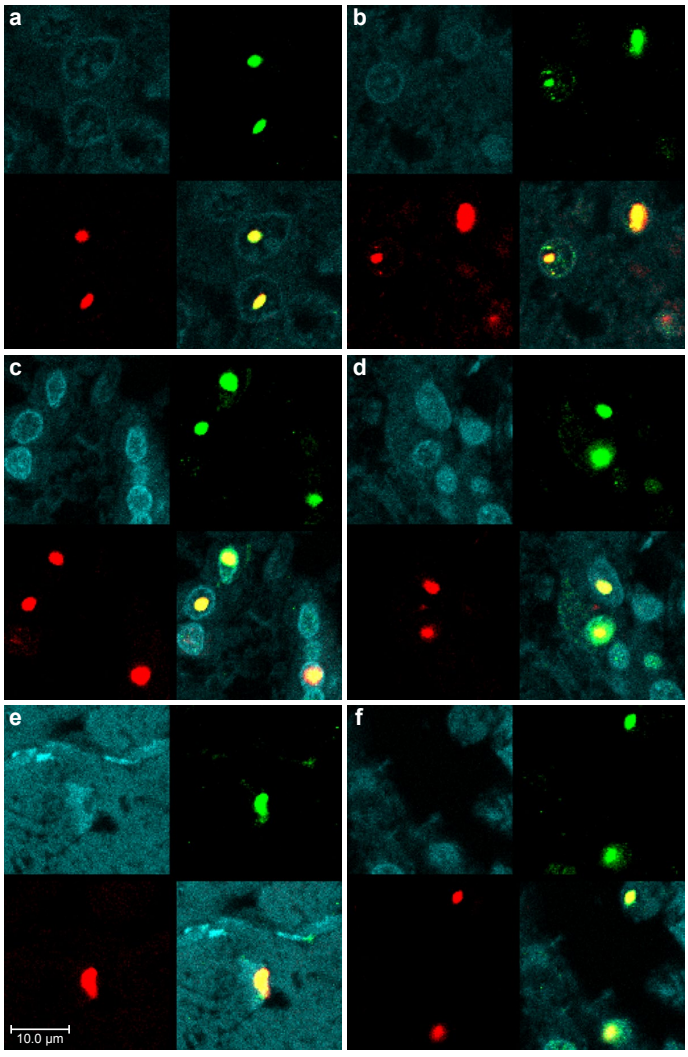

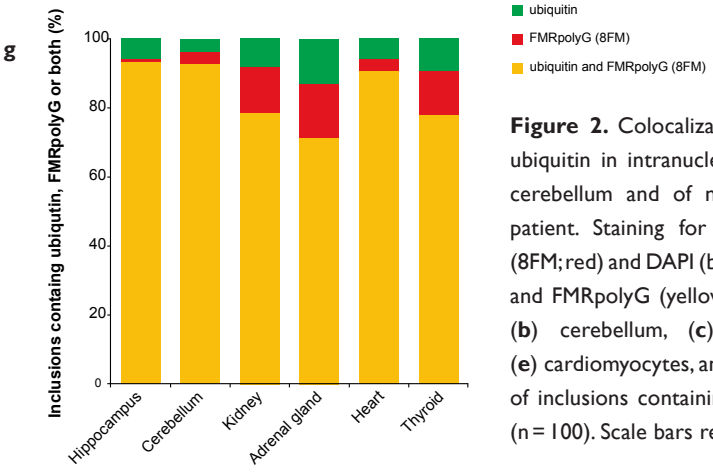

Figure 2. Colocalization of FMRpolyG (8FM) and ubiquitin in intranuclear inclusions in hippocampus, cerebellum and of non-CNS tissues of a FXTAS patient. Staining for ubiquitin (green), FMRpolyG (8FM; red) and DAPI (blue). Colocalization of ubiquitin and FMRpolyG (yellow) is seen in (**a**) hippocampus, (**b**) cerebellum, (**c**) kidney, **d**) adrenal gland, (**e**) cardiomyocytes, and (**f**) thyroid; (**g**) quantification of inclusions containing ubiquitin and/or FMRpolyG (n = 100). Scale bars represent 10 µm.

showed any FMRpolyG-positive inclusions (data not shown). Colocalization of ubiquitin- and FMRpolyG-positive inclusions was visualized and quantified by immunofluorescent double staining using antibodies against ubiquitin and FMRpolyG (8FM) (**Figure 2a-f**). For hippocampus, cerebellum and the non-CNS organs most inclusions are positive for both FMRpolyG and ubiquitin, although some rare inclusions positive for only one of the proteins could also be detected (**Figure 2g**, n = 100 inclusions). In conclusion, using two novel antibodies the present report not only confirms the existence of FMRpolyG-positive aggregates in CNS tissue from a FXTAS individual but also demonstrates for the first time the presence of FMRpolyG-positive intranuclear inclusions in post mortem non-CNS material of a PM carrier with FXTAS. Furthermore, colocalization of FMRpolyG and ubiquitin is found in the vast majority of inclusions. The presence of FMRpolyG-positive intranuclear inclusions in heart, kidney, adrenal gland and thyroid is consistent with the unexplained medical co-morbidities reported in some patients with FXTAS, including thyroid disease, cardiac arrhythmias, hypertension, migraine, impotence, and neuropathy. We hypothesize that the underlying pathological mechanisms of the medical co-morbidities in systemic tissues share common features (protein toxic gain-of-function) with CNS pathology of patients with FXTAS. Our report suggests that in addition to elevated levels of *FMR1* mRNA containing an expanded CGG repeat, and ubiquitin-positive inclusions, FMRpolyG expression might also play a role in a toxic gain-of-function mechanism in medical co-morbidities in FXTAS (RNA versus FMRpolyG toxic gain-of-function). Interestingly, a very recent report suggests that RAN translation products in C9FTD/ALS, toxic dipeptide repeat proteins (poly-(glycine-arginine) and poly-(proline-arginine)), are toxic in *Drosophila* [9]. Further research is needed to understand how FMRpolyG may elicit toxicity in both CNS and non-CNS organs and its precise role in co-morbidities in PM carriers. Importantly, if FMRpolyG production is important for cellular toxicity this will open new avenues for therapeutic intervention studies for FXTAS by developing drugs that block this aberrant translation.

Supplemental data

Supplemental data is available online.

REFERENCES

1. Hagerman, R.J., et al., *Intention tremor, parkinsonism, and generalized brain atrophy in male carriers of fragile X.* Neurology, 2001. **57**(1): p. 127-30.
2. Hunter, J., et al., *Epidemiology of fragile X syndrome: A systematic review and meta-analysis*. American Journal of Medical Genetics Part A, 2014. **164**(7): p. 1648-1658.
3. Rodriguez-Revenga, L., et al., *Penetrance of FMR1 premutation associated pathologies in fragile X syndrome families*. Eur J Hum Genet, 2009. **17**(10): p. 1359-62.
4. Willemsen, R., J. Levenga, and B. Oostra, *CGG repeat in the FMR1 gene: size matters*. Clin Genet, 2011. **80**(3): p. 214-25.
5. Tassone, F., et al., *Elevated levels of FMR1 mRNA in carrier males: A new mechanism of involvement in the Fragile-X syndrome*. Am J Hum Genet, 2000. **66**(1): p. 6-15.
6. Greco, C.M., et al., *Neuronal intranuclear inclusions in a new cerebellar tremor/ataxia syndrome among fragile X carriers*. Brain, 2002. **125**(Pt 8): p. 1760-1771.
7. Hunsaker, M.R., et al., *Widespread non-central nervous system organ pathology in fragile X premutation carriers with fragile X-associated tremor/ataxia syndrome and CGG knock-in mice*. Acta Neuropathol, 2011. **122**: p. 467-479.
8. Todd, P.K., et al., *CGG Repeat-Associated Translation Mediates Neurodegeneration in Fragile X Tremor Ataxia Syndrome*. Neuron, 2013. **78**(3): p. 440-455.
9. Mizielinska, S., et al., *C9orf72 repeat expansions cause neurodegeneration in Drosophila through arginine-rich proteins*. Science, 2014. **345**(6201): p. 1192-4.

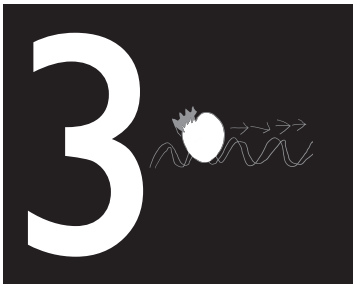

INDUCED EXPRESSION OF EXPANDED CGG RNA CAUSES MITOCHONDRIAL DYSFUNCTION *IN VIVO*

R.A.M. Buijsen[1,*], R.K. Hukema[1,*], C. Raske[2], E.A.W.F.M. Severijnen[1], I. Nieuwenhuizen-Bakker[1], M. Minneboo[1], A. Maas[3], R. de Crom[3], J.M. Kros[4], P.J. Hagerman[2], R.F. Berman[5,#], R. Willemsen[1,#]

[1] Department of Clinical Genetics, Erasmus MC, Rotterdam, the Netherlands
[2] Department of Biochemistry and Molecular Medicine, UC Davis, USA
[3] Department of Cell Biology, Erasmus MC, Rotterdam, the Netherlands
[4] Department of Pathology, Erasmus MC, 3000CA Rotterdam, the Netherlands
[5] Department of Neurological Surgery, UC Davis, Davis, USA

*,# these authors contributed equally

Cell Cycle 2014;13(16):2600-8

ABSTRACT

Fragile X-associated tremor/ataxia syndrome (FXTAS) is a late-onset neurodegenerative disorder affecting carriers of premutation forms of the *FMR1* gene, resulting in a progressive development of tremor, ataxia and neuropsychological problems. The disease is caused by an expanded CGG repeat in the *FMR1* gene, leading to an RNA gain-of-function toxicity mechanism. In order to study the pathogenesis of FXTAS, new inducible transgenic mouse models have been developed that expresses either 11CGGs or 90CGGs at the RNA level under control of a Tet-On promoter. When bred to an hnRNP-rtTA driver line, doxycycline (dox) induced expression of the transgene could be found in almost all tissues. Dox exposure resulted in loss of weight and death within 5 days for the 90CGG RNA expressing mice. Immunohistochemical examination of tissues of these mice revealed steatosis and apoptosis in the liver. Decreased expression of GPX1 and increased expression of cytochrome C is found. These effects were not seen in mice expressing a normal sized 11CGG repeat. In conclusion, we were able to show *in vivo* that expression of an expanded CGG-repeat rather than overexpression of a normal CGG-repeat causes pathology. In addition, we have shown that expanded CGG RNA expression can cause mitochondrial dysfunction by regulating expression levels of several markers. Although FTXAS patients do not display liver abnormalities, our findings contribute to understanding of the molecular mechanisms underlying toxicity of CGG repeat RNA expression in an animal model. In addition, the dox inducible mouse lines offer new opportunities to study therapeutic interventions for FXTAS.

INTRODUCTION

Fragile X-associated tremor/ataxia syndrome (FXTAS) is a late-onset neurodegenerative disorder affecting carriers of the Fragile X premutation forms of the *FMR1* gene located on the X-chromosome [1]. The chances of developing FXTAS increase dramatically with age, with approximately 30% of male and 8-11% of female PM carriers over the age of 50 years [2]. Premutation alleles of the *FMR1* gene contain 55-200 CGG repeats in the 5'UTR compared to less than 54 for most individuals in the general population. FXTAS results in progressive development of tremor, ataxia and neuropsychological problems, including anxiety, memory impairment and dementia. Medical co-morbidities may include thyroid disease, fibromyalgia, gastro-intestinal symptoms, hypertension, migraine, auto-immune disease, impotence and neuropathy [3, 4]. The prevalence of premutation carriers in the general population is approximately 1 in 200 females and 1 in 400 males [5, 6]. Premutation carriers irrespective of showing signs of FXTAS, have been shown to have up to eight-fold elevated *FMR1* mRNA levels in peripheral blood leukocytes, despite close to normal or slightly lowered FMRP protein levels [7]. Neurohistological examination of brains of both male and female premutation carriers who displayed the neurological phenotype revealed the presence of eosinophilic, intranuclear inclusions in neurons and astrocytes, and Purkinje cell dropout [8, 9]. The inclusions were seen in various regions throughout the brain. The intranuclear inclusions stain positively with antibodies against several proteins, including ubiquitin, molecular chaperones, components of the proteasome, Sam68 and Drosha [10-12]. Based on the toxic RNA gain-of-function model proposed for FXTAS, it was predicted that *FMR1* mRNA would be present within the intranuclear inclusions. Indeed, *FMR1* mRNA could be detected in inclusions from post-mortem human FXTAS brain tissue, although FMRP has not been localized in the inclusions [13]. Recently, an additional mechanism of toxicity that is triggered by CGG repeat associated non-AUG initiated (RAN) translation has been proposed to underlie pathology in FXTAS [14]. This is based on evidence that trinucleotide repeats can be translated into protein even if they do not reside in an AUG-initiated open reading frame (ORF), and such translation can occur in all three possible ORF's of a transcript generating multiple potentially toxic products from a single repeat. In the case of FXTAS it has been proposed that RAN translation initiated in the 5'-UTR of *FMR1* mRNA results in the production of a cytotoxic polyglycine- and polyalanine-containing protein named FMRpolyG and FMRpolyA, respectively. Indeed, the presence of FMRpolyG could be demonstrated in brain tissue from patients with FXTAS and the expanded CGG knock-in (KI) mouse models. The mechanisms underlying RAN translation are as yet unknown.

The development of mouse models of FXTAS has facilitated studies on the underlying cellular and molecular bases of this neurodegenerative disease. Knock-in mouse lines have been generated with either an expanded human CGG98 or CGG118 repeat, which

exhibit most of the symptoms observed in humans with FXTAS, including ubiquitin-positive intranuclear neuronal inclusions, elevated levels of *Fmr1* mRNA and reduced Fmrp expression [15-18]. In addition, neuropsychological and cognitive deficits, including poor motor function, impaired memory, progressive spatial processing deficits and evidence of increased anxiety could be demonstrated using various behavioral tests [19-23]. Such studies have provided critical information about the molecular events that occur with the onset and progression of the disorder, including new insights into the role of RNA toxicity in the pathophysiology of FXTAS and the relationship between the number of CGG repeats and disease progression.

However, the pathological consequences of the intranuclear inclusions as well as the exact mechanisms involved in the RNA gain-of-function toxicity model remain to be elucidated. Therefore we developed a new inducible transgenic mouse model with RNA overexpression of a normal length 11CGG repeat or an expanded 90CGG repeat in order to study their effects *in vivo.* Our model is a Tet-On system using the hnRNP-rtTA driver to regulate expression of the CGG repeat RNA (i.e., either 11CGG or 90CGG) in almost all tissues of the bigenic mice by adding doxycycline (dox) to the drinking water or to the food. In this study we show that overexpression of a 90CGG repeat, but not an 11CGG repeat, at the RNA level can induce toxicity *in vivo*. Expression of expanded 90CGG RNA induced dysfunction of the liver and eventually death of the animals. We found increased steatosis, apoptosis and disrupted expression of several enzymes involved in the processing of reactive oxygen species (ROS).

RESULTS

A new dox inducible mouse model to study the role of expanded CGG repeat RNA

Although a leading hypothesis for the cause of FXTAS is a toxic RNA gain-of-function mechanism, it has not been clear whether overexpression of a CGG-repeat containing RNA *per se* is sufficient to cause toxicity *in vivo*, even when the repeat size is within the normal size range, or whether toxicity depends on the presence of an expanded CGG repeat. Therefore, we generated new dox inducible mouse lines in which a normal sized (i.e., for mouse) 11CGG or an expanded 90CGG repeat was over-expressed, and examined the mice for pathology (**Figure 1A**). We never observed any repeat instability when breeding the TRE-nCGG-eGFP mice (data not shown). The repeat size remained equal during all breedings, with an estimated 90CGGs for the expanded transgene, corresponding to a 630 bp band by agarose gel electrophoresis (**Figure 1B**).

We first generated mouse lines bearing a TRE-nCGG-eGFP transgene. We cross-bred this line with an existing hnRNP-rtTA mouse line that expresses a reverse tetracycline-controlled transactivator protein (rtTA) that is activated when mice are

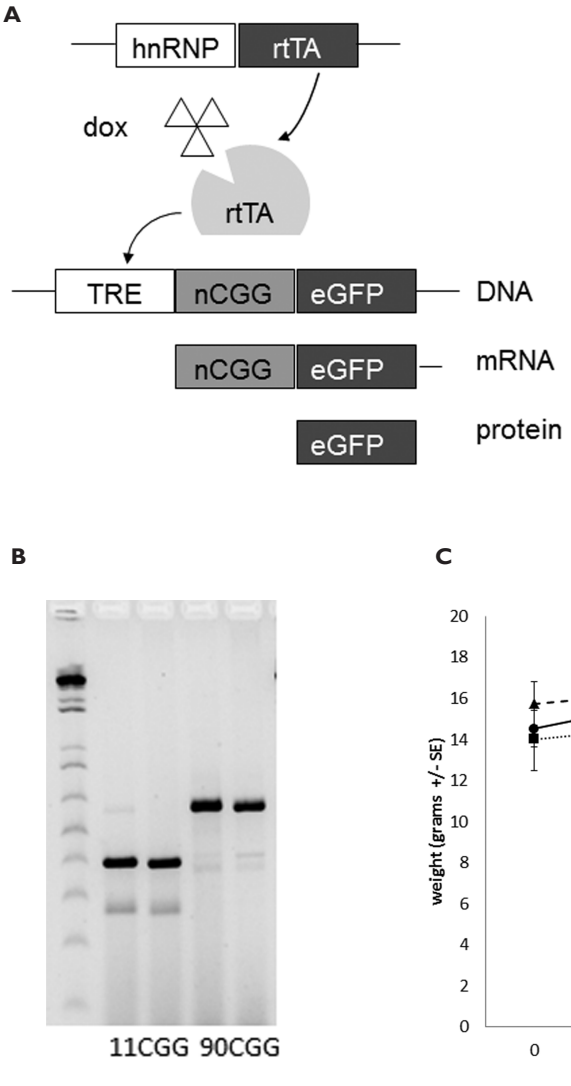

Figure 1. New inducible transgenic mouse model. (**A**) The Tet-On system was used to generate bigenic mice expressing a 11CGG or a 90CGG repeat at the RNA level in all tissues. Expression of rtTA is controlled by the hnRNP promoter on a transgene. Upon dox administration rtTA will be activated and can bind the Tet Responsive Element (TRE) on another transgene, this induces expression of the nCGG repeat at the RNA level and eGFP at the protein level. (**B**) Genotyping PCR showing the repeat size of 2x 11 and 2x 90 CGGs at approximately 390 bp and 630 bp, respectively. (**C**) 90CGG expressing mice lose weight when compared to 11CGG expressing mice or bigenic mice (TRE-90CGG-eGFP/hnRNP-rtTA) without dox treatment. The straight line with circles shows the weight of mice not treated with dox (n=7), the dotted line with squares shows the weight of 11CGG expressing mice after 2 mg/ml dox-water treatment (n=7), and the striped line with triangles show the weight of 90CGG expressing mice after 2 mg/ml dox-water treatment (n=6). Error bars are +/- SE; * = $p < 0.05$

treated with dox in drinking water or food.[24] Bigenic offspring with the expanded CGG RNA (TRE-90CGG-eGFP/hnRNP-rtTA) treated with dox in their drinking water (2mg/ml) or food (1mg/kg) starting at three weeks of age, began to lose weight after 2 days of dox treatment. Therefore we stopped dox treatment after 4 days since the mice died after five days of treatment (**Figure 1C**). In contrast, TRE-11CGG-eGFP/hnRNP-rtTA mice did not show this weight loss, steadily gained weight, and remained viable. In addition, monogenic mice with only the hnRNP-rtTA or only the TRE-90CGG-eGFP transgene treated with dox, and untreated bigenic TRE-90CGG-eGFP/hnRNP-rtTA mice did not show any weight loss or loss of viability (**Figure 1C**; data not shown). These results suggest that the weight loss and subsequent deaths observed in TRE-90CGG-eGFP/hnRNP-rtTA are caused by expression of the 90CGG transgene and are not due to dox treatment or overexpression of mRNA per se (without a CGG repeat expansion). Indeed, we were able to treat TRE-11CGG-eGFP/hnRNP-rtTA mice with a higher dose of dox-water (4mg/ml) or for as long as 25 days without evidence of weight loss (data not shown).

Expression of expanded CGG repeat RNA is toxic *in vivo*

Dox treatment of bigenic TRE-nCGG-eGFP/hnRNP-rtTA mice resulted in eGFP expression in all tissues examined (**Figure 2**). Immunological staining revealed eGFP expression in heart, lung, intestine, liver, kidney, spleen, and brain. The level of transgene expression was compared in different tissues. Quantitative RT-PCR showed that the level of nCGG-eGFP RNA expression was higher in liver when compared to lung, kindey and brain. In liver, the overexpression of 99CGG RNA was 600 ± 80 times higher when compared to endogenous *Fmr1* RNA levels.

No eGFP expression was found after dox treatment of monogenic TRE-nCGG-eGFP mice (data not shown). Also, no eGFP expression was seen in bigenic TRE-nCGG-eGFP/hnRNP-rtTA mice not treated with dox (**Figure 2, 3B and 3C**), indicating that our Tet-On system does not show any leakage of expression.

We compared the expression levels of CGG RNA and eGFP protein of the TRE-11CGG-eGFP/hnRNP-rtTA and TRE-90CGG-eGFP/hnRNP-rtTA mice after 4 days of dox treatment (2 mg/ml in drinking water). No significant differences were found in the expression levels of 11CGG and 90CGG RNA (**Figure 3A**; data not shown). In addition, there were no significant differences in eGFP protein levels between 11CGG and 90CGP expressing mice as determined by Quantitative Western blot (**Figure 3B,C**; data not shown). Because there were no differences in expression of 90CGG RNA in mice treated with doxycycline in water when compared to mice treated with doxycycline in their food (data not shown), the two dox exposed groups were combined into one group.

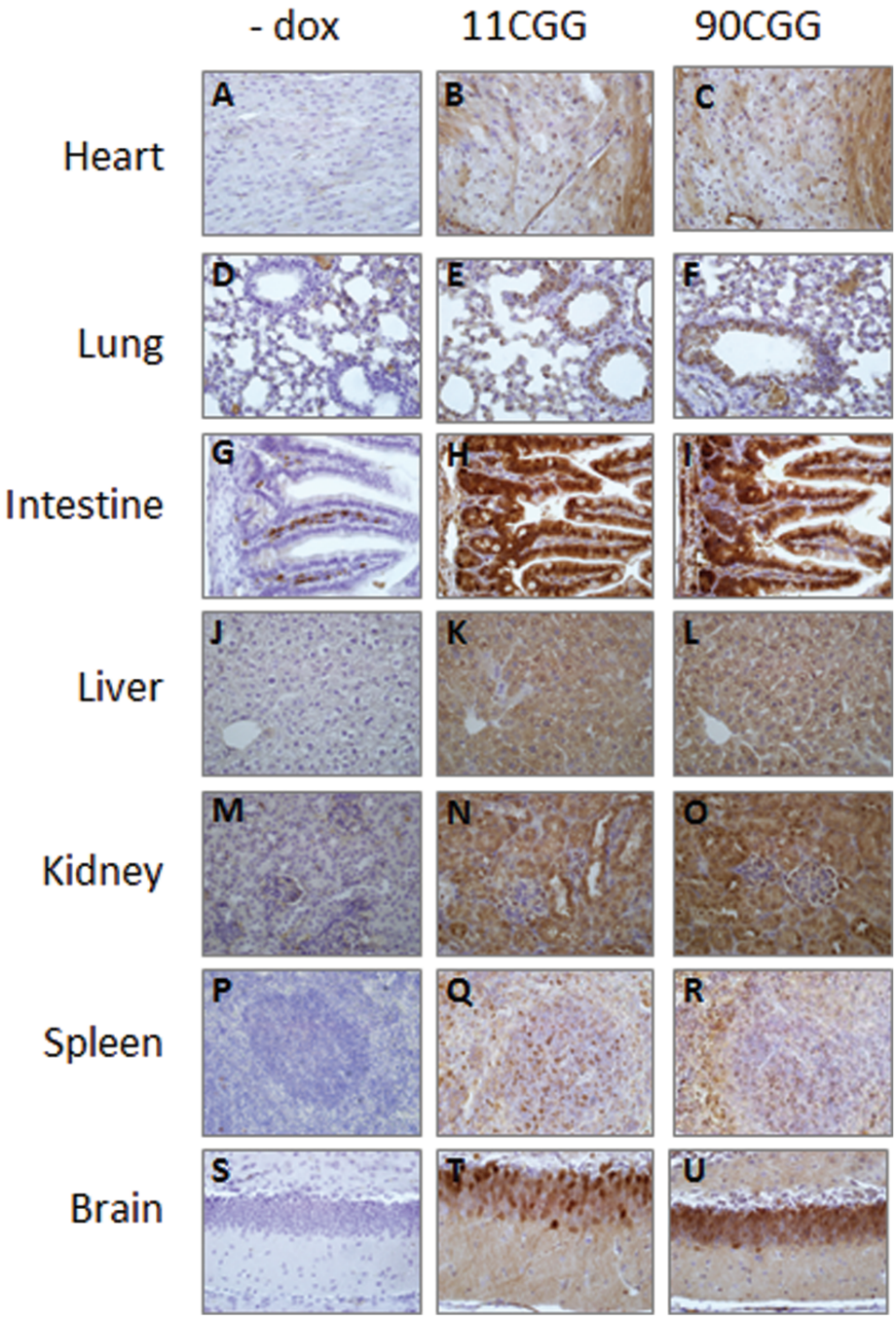

Figure 2. eGFP expression in different tissues. Representative photomicrographs (40x) of immunohistochemical staining with GFP antibody on heart (**A,B,C**), lung (**D,E,F**), intestine (**G,H,I**), liver (**J,K,L**), kidney (**M, N, O**), spleen (**P,Q,R**), and brain (**S,T,U**) from no dox control mice (**A,D,G,J,M,P,S**), TRE-11CCG-eGFP mice (**B,E,H,K,N,Q,T**), and TRE-90CGG-eGFP mice (**C,F,I,L,O,R,U**).

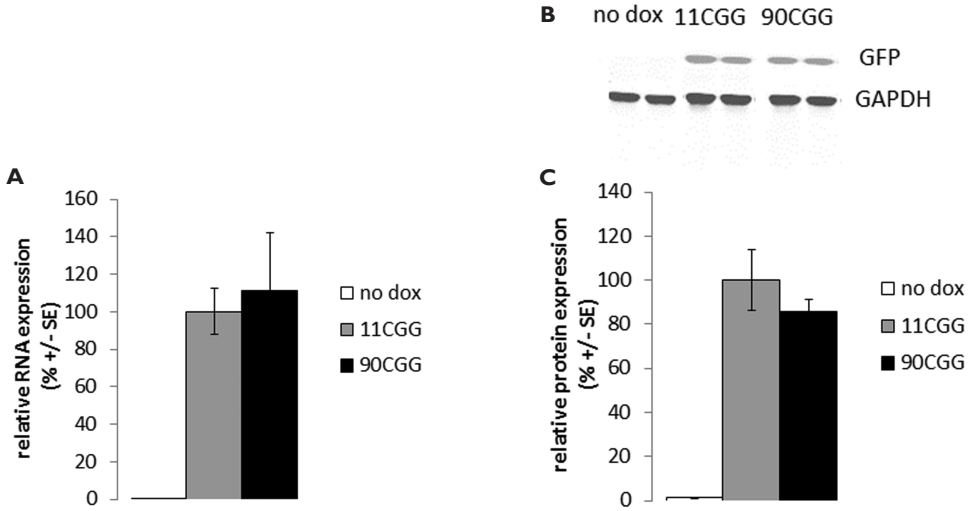

Figure 3. Comparable eGFP RNA and protein expression in the liver of 11CGG and 90CGG mice after 4 days dox treatment. (**A**) Quantitative RT-PCR on RNA isolated from livers of no dox control mice (white bars; n=7), TRE-11CGG-eGFP/hnRNP-rtTA mice treated 4 days with dox (grey bars; n=7), and TRE-90CGG-eGFP/hnRNP-rtTA mice after 4 days dox treatment (black bars; n=6). 90CGG-eGFP levels are not significantly different from 11CGG-eGFP (p=0.7) (**B**) Representative Western blot for eGFP on liver homogenates of no dox control mice and 11CGG or 90CGG expressing mice after 4 days dox treatment with GAPDH as a loading control. (**C**) Quantification of eGFP protein expression after Western blot on liver homogenates from no dox control mice (white bars; n=4), TRE-11CGG-eGFP/hnRNP-rtTA mice treated 4 days with dafter 4 days dox treatment (grey bars; n=8), and TRE-90CGG-eGFP/hnRNP-rtTA mice after 4 days dox treatment (black bars; n=7). 90CGG-eGFP levels do not significantly differ from the 11CGG-eGFP levels (p=0.3). Error bars are +/- SE.

The brains of all mice were evaluated for the presence of ubiquitin positive intranuclear inclusions, the major hallmark of FXTAS. Although the brains of dox treated bigenic TRE-90CGG-eGFP/hnRNP-rtTA mice did show expression of eGFP and thus the expanded CGG RNA (**Figure 2C**), we did not find any ubiquitin positive inclusions. Also all the other organs that did (over)express the expanded CGG RNA did not form any ubiquitin positive inclusions (data not shown). Apparently, the dox treatment of only four days was not long enough to induce the formation of the inclusions.

Expression of expanded repeat RNA causes mitochondrial dysfunction in the liver

When sacrificing the mice it was evident that the liver was affected by the dox induced expression of the 90CGG RNA. The livers in the TRE-90CGG-eGFP/hnRNP-rtTA mice treated with dox were pale and pink in color, compared to the dark reddish-

brown color of a normal, healthy liver (**Figure 4A,B**). All control mice, including TRE-11CGG-eGFP/hnRNP-rtTA or monogenic mice treated with dox, showed livers with normal appearance. We performed routine histological examination of a large number of tissues, including the brain, liver, kidney, spleen, heart, lung and the intestinal tract. The only pathology found was in the liver, with all other tissues appearing normal. Closer examination of the liver using various histological stainings revealed mild steatosis limited to the livers of the TRE-90CGG-eGFP/hnRNP-rtTA mice treated with dox (**Figure 4D,E,F**).

The presence of steatosis of the liver is suggestive of mitochondrial dysfunction, which can in turn lead to apoptosis [25]. Furthermore, evidence has been found for mitochondrial dysfunction and abnormalities in several neurodegenerative diseases, including FXTAS, and in cultured primary neurons from the exCGG-KI mouse model [26, 27]. Thus, we hypothesized that mitochondrial dysfunction might underlie the abnormalities we found in the livers of mice that expressed the 90CGG RNA and consequent early demice of these mice.

RNA expression levels of several markers for mitochondrial stress were tested using qRT-PCR. Expression of SOD2, NPUFS4, and ATPB1 was normal (supplemental data). We did find altered RNA expression levels in the livers for CYP2E1, SOD1, and Catalase, both in TRE-11CGG-GFP/hnRNP-rtTA and TRE-90CGG-GFP/hnRNP-rtTA mice treated with dox when compared with untreated control mice (supplemental data). Since these effects were found in mice expressing both 11CGG RNA and 90CGG RNA, these changes are likely to be caused by the doxycycline treatment and not to expression of the transgene.

However, two other markers, cytochrome C and GPX1, only showed significant effects in the dox treated TRE-90CGG-EGFP/hnRNP-rtTA mice, but not in the dox treated TRE-11CGG-GFP/hnRNP-rtTA mice and also not in dox treated monogenic TRE-99CGG-eGFP mice. GPX1 is a glutathione oxidase, functions in the detoxification of hydrogen peroxide, and is one of the most important antioxidant enzymes. It prevents apoptosis by caspase 3 through inhibition of cytochrome C.[28] We found that expression of GPX1 is significantly downregulated to 45 ± 8 % ($p<0.05$) in liver of mice expressing 90CGG RNA compared with untreated mice (**Figure 4C**). GPX1 RNA levels in the liver of 11CGG RNA expressing mice was normal at 98 ± 16 % of untreated mouse livers ($p=0.9$). In addition, we found that cytochrome C, which is part of the same pathway, is significantly upregulated in the same 90CGG expressing livers to 155 ± 17 % ($p<0.05$) when compared with untreated mouse livers. The 11CGG expressing livers showed normal levels 81.1 ± 8% of cytochrome C ($p=0.3$)(**Figure 4C**).

Since the pathway with GPX1 and cytochrome C can affect apoptosis through caspase 3 activation, we performed an immunostaining for cleaved caspase 3 in the liver.

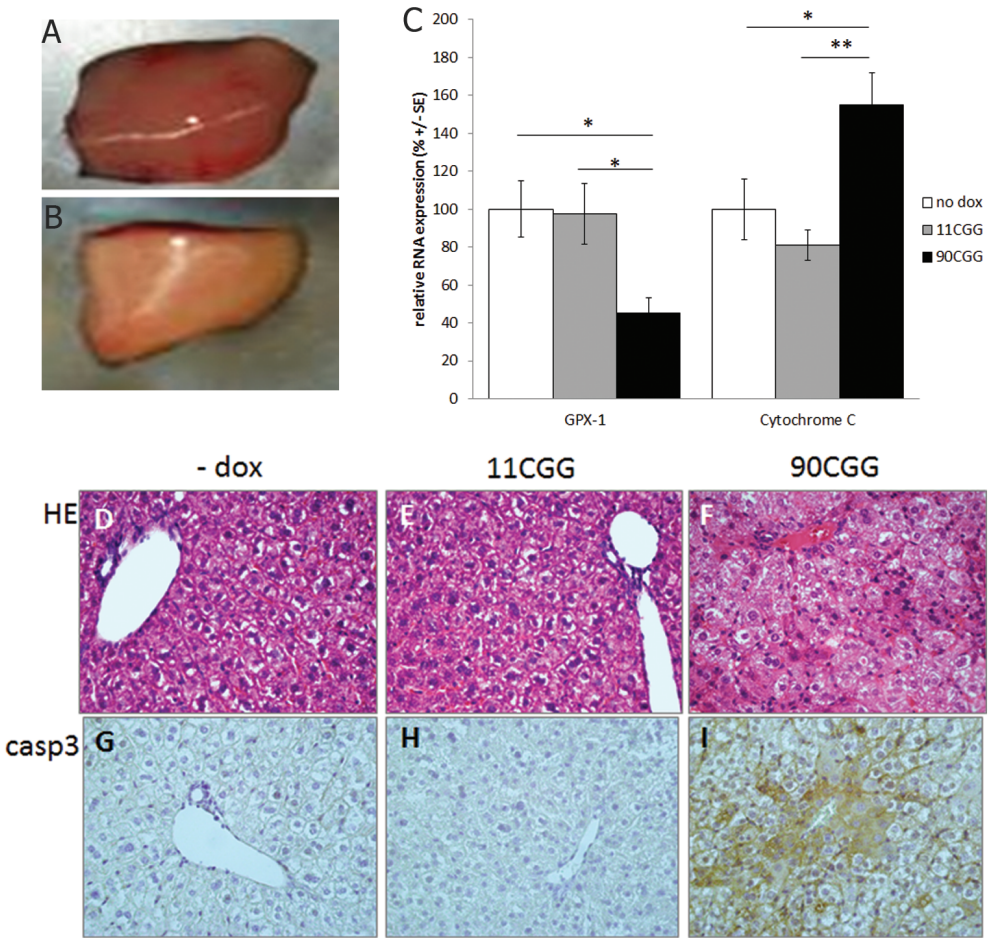

Figure 4. Mitochondrial dysfunction in the liver of 90CGG expressing mice. The color of 90CGG expressing livers is pink and pale (**A**) compared to the dark reddish-brown color of the liver of control mice (**B**). Quantitative RT-PCR on RNA isolated from liver of no dox control mice (white bars; n=7), TRE-11CGG-eGFP/hnRNP-rttA mice treated 4 days with dox (grey bars; n=7), and TRE-90CGGeGFP/hnRNP-rtTA mice treated 4 days with dox (black bars; n=6) for oxidative stress markers GPX1 and cytochrome C (**C**); Error bars are +/- SE; * = p<0.05; ** = p< 0.01. Representative photomicrographs (40x) of haematoxylin and eosin (HE) staining (**D,E,F**) and cleaved caspase 3 (casp3) immunostaining (**G,H,I**) on the livers of no dox controls mice and 11 or 90CGG expressing mice.

Indeed, we could demonstrate semi-quantitatively elevated levels of activated caspase 3 in the livers of 90CGG expressing mice, when compared with 11CGG expressing or untreated mice (**Figure 4 G,H,I**). Both control groups of TRE-11CGG-GFP/hnRNP-rtTA mice with dox and untreated mice show the same, low levels of cleaved caspase 3. Taken together, the data indicate that *in vivo* expression of expanded CGG RNA leads to toxicity in the liver by affecting ROS signaling and thus inducing steatosis and apoptosis.

DISCUSSION

We have successfully generated a new inducible mouse model for FXTAS expressing CGG RNA under control of the Tet-On promoter. Our transgenic mice combined with the hnRNP-rtTA driver mouse show expression upon doxycycline administration in all tissues examined. The system shows no evidence of leaky transcription and allows for the study of the effects of expanded CGG RNA expression compared with similar levels of control size CGG RNA expression. It has been shown before that over-expression of an expanded CGG repeat is toxic in Drosophila[29, 30], but using this murine model we showed*in vivo* in a vertebrate model that toxicity depends on over-expression of an expanded CGG repeat and is not seen with over-expression of RNA with a normal sized CGG repeat. Findings in this new mouse model also show that expression of 90CGG RNA leads to mitochondrial dysfunction in the liver, ultimately resulting in liver pathology and death.

Previously, it has been shown *in vitro* by Hoem, et al. [31] that there is a threshold for CGG repeat length to induce pathology in neuroblastoma-derived SK cells that is not due simply to the amount of RNA transcribed. In the present study we confirm that pathology and toxicity is not caused by a molarity effect from over-expression of large amounts of CGG-containing RNA in the absence of a large CGG repeat expansion. Because pathology was only found with 90CGG RNA and not 11CGG RNA *in vivo*, there must be an *in vivo* threshold for CGG repeat toxicity between 11 and 90 CGG repeats, although the size of this threshold remains to be determined. These findings are also consistent with the *in vitro* cell culture studies by others [11, 12, 31] that show effects of CGG repeat expansions on viability and inclusion formation that are dependent on the size of the repeat. This suggests that the pathological processes involved in FXTAS differ from other repeat associated disease such as myotonic dystrophy where overexpression of a normal-sized repeat RNA can induce pathology as well [32]. The use of the Tet-On system allows us not only to control the expression of the nCGG RNA by adding dox, but it also gives us good controls to check for side-effects of transgene integration sites. Since no abnormalities were found in bigenic TRE-90CGG-eGFP/hnRNP-rtTA mice not treated with dox, we can rule out that the effects found in the mice that were exposed to dox, are caused by the transgene integration site. Since it is expected that if the site of transgene insertion would affect mitochondrial function in the liver, we would also see the effects in mice not treated with dox. Since we do not observe any pathology in mice not treated with dox, this allows us to specifically study the effects of the transgene and not its site of integration. Furthermore, since also the monogenic mice treated with dox and the bigenic TRE-11CGG-eGFP/hnRNP-rtTA control mice treated with dox, do not show an aberrant expression of gpx1, cytochrome C, or activated caspase 3 in the liver, we can also rule out the effects of dox on these markers. Therefore, we can rule out several side effects and pinpoint the effects to the expression of expanded CGG RNA, making our model very valid for studying the *Fmr1* premutation and FXTAS.

The deleterious effects of expanded CGG RNA expression on the normal functioning of the liver was not expected, since human FXTAS patients are not known to display liver damage or dysfunction. Also no inclusions have been observed in the livers of FXTAS patients or mouse models [3]. This observation can be explained by the fact that in this artificial system the CGG repeat RNA is overexpressed 600 times in liver when compared with endogenous *Fmr1* mRNA levels. And also since CGG RNA expression levels are highest in liver compared to other tissues, this can explain the unexpected deleterious effect on this organ. In addition, the fact that the liver was selectively affected rather than other organs may be explained by the fact that the liver is the first organ to clear dox from the body and the liver is one of the organs with the highest content of gpx1, and alterations in its regulation can contribute to several pathologies related to oxidative stress [33]. Hepatic mitochondria are recognized as a major source of oxidative stress, which in turn can regulate vital liver functions and disease pathogenesis. Both in alcoholic and in non-alcoholic steatosis of the liver there is a major role for the depletion of glutathion in mitochondrial dysfunction. Thus, although FXTAS patients do not display liver dysfunction, the bigenic TRE-90CGG-eGFP/hnRNP-rtTA mouse model enables *in vivo* studies to investigate the toxic effect of RNA containing an expanded CGG repeat outside the *Fmr1* message.

Due to the liver problems bigenic TRE-90CGG-eGFP/hnRNP-rtTA mice we were not able to treat the mice long enough with dox in order to induce the formation of ubiquitin positive inclusions and pathology in the brain. Still, inclusion formation and brain pathology would be interesting to study using this inducible model (i.e., TRE-90CGG-eGFP) combined with different rtTA driver lines that specifically expresses in the brain. Currently, these studies are ongoing in our lab using PrP, pcpL7, and CamKIIα drivers. On the other hand, many inclusions have also been observed outside the CNS both in FXTAS patients and in the exCGG-KI mouse model [3]. Therefore, inclusions formation in other tissues besides the brain will be interesting to study. Nevertheless, in this model the study of inclusion formation seems not to be possible since the expression of the expanded CGG RNA can never be long enough and other pathogenic triggers result in such dramatic cellular dysfunctioning that the mice die. This dysfunctioning seems to be caused by the free RNA with the expanded CGG repeat, rather than RNA that is accumulated in inclusions.

Recently, RAN translation was identified as a potential pathogenic trigger for FXTAS. In case of RAN translation. The exact mechanisms underlying RAN translation and its contribution to the pathogenesis of FXTAS are still unkown, but it would be very interesting to determine if RAN tranlation would play a role in the mitochondrial dysfunction described in this study. Unfortunately, no (commercial) antibodies are available to us yet, to perform these experiments. Evidence for mitochondrial dysfunction has been

described in studies using cultured neurons from the exCGG-KI mouse [27], and also in studies in fibroblasts and post-mortem brain materials from premutation carriers with and without FXTAS [26, 34]. Therefore we reasoned that the steatosis we observed in the mice expressing 90CGG RNA might also be related to defective mitochondrial signaling. After testing a range of markers for mitochondrial function, we found that several were affected by dox treatment in both 11CGG RNA expressing mice as well as in the 90CGG RNA expressing mice. This was not entirely unexpected because the antibiotic dox is processed and metabolized by the liver and it is known that tetracyclines affect mitochondrial function [35]. Nevertheless, we did find the mitochondrial enzymes GPX1 and cytochrome C to be differently expressed, specifically in the liver of the 90CGG expressing mice, without any effect in the 11CGG RNA expressing mice. Unfortunately, we were not able to show if this is also the case in the brain, since we are not able to treat the mice long enough with doxycycline to induce inclusion formation in the brain. Future experiments with other rtTA driver lines should shed a light on the question of whether these same mitochondrial markers are also affected in brains expressing expanded CGG RNA for a longer period, as might be expected from the present results. In fact, considerable evidence links GPX1 to neurodegenerative disease including Alzheimer, Parkinson and Huntington. GPX1 is localized in glial cells and its expression regulates vulnerability for neurotoxins. Increased vulnerability to toxins may be important because of the possibility that exposure to environmental toxins, general anesthetics and chemotherapeutic agents, may contribute to the risk for premutation carriers to develop FXTAS [36, 37]. This suggests that mitochondrial dysfunction, and possibly GPX1, may be a common pathological process in neurodegenerative diseases, including FXTAS. Further studies on altered GPX1 and cytochrome C expression related to CGG repeats could offer a new perspective on the development of new biomarkers for FXTAS and future therapeutic intervention studies.

MATERIAL AND METHODS

Constructs and mice

The pCMV-RL plasmid (Promega) was modified to express eGFP (enhanced green fluorescent protein) with an *FMR1* 5' UTR under the control of the tetracycline responsive promoter element (TRE). Utilizing oligonucleotide poly-linkers the CMV promoter in pRL-CMV was replaced with the TRE promoter from the pTRE2 vector (Clontech). Immediately downstream of the TRE promoter, *FMR1* 5'UTRs containing 11, and 90 CGG repeats were cloned upstream of the chimeric intron in pRL-CMV. The eGFP reporter from the eGFPn-1 vector (Clontech) was cloned downstream of the chimeric intron followed by a SV40 poly A signal. The resulting plasmids are TRE-11CGG-eGFP, and TRE-90CGG-eGFP. The *FMR1* 5' UTR containing 90 CGG repeats was cloned from

the parent plasmid CMV-*FMR1*-FL between *Blp*I and *Nhe*I restriction sites (all restriction enzymes from New England Biolabs Inc.). The *FMR1* 5' UTR containing 11 CGG repeats was amplified by PCR from mouse genomic DNA, followed by a *Blp*I-*Xho*I restriction enzyme digestion, and cloned into TRE-90CGG-eGFP. Transgenic mice were generated by injecting linearized contstruct into oocytes of Janvier .c57bl6 mice. For each construct we had several founders. We used the founders that gave optimal expression, combined with good breeding results. For the TRE-90CGG-eGFP construct we had two different founders, that both die when bred with hnRNP-rtTA driver mice and treated with dox.

TRE-nCGG-eGFP mice were crossed with the hnRNP-rtTA driver line [24] and bigenic mice were treated with dox directly after weaning at an age of 3 weeks. In the initial experiments we treated mice with dox either in food or drinking water, we have not observed any differences between mice treated with dox water or dox food (Bio Services). Dox was stable in food pellets and had a concentration of 1 g/kg. Dox drinking water contained 2 mg/ml doxycycline hyclate (Sigma) in 5% sucrose (Sigma) and was refreshed every 2-3 days. All animal experiments were conducted with the permission of the local animal welfare committee (DEC).

Genotyping

For genotyping toe clips were incubated overnight at 55°C in TDB (50 mM KCl, 10 mM Tris-HCl pH9, 0.1% Triton X-100 and 0.15 µg proteinase K). After heat inactivation samples were spun down and 1 µl was used for a PCR. The TRE transgene was amplified using forward primer 5'-GCTTAGATCTCTCGAGTTTAC-3' and reverse primer 5'-ATGGAGGTCAAAACAGCGTG-3' . The rtTA transgene was amplified using forward primer 5'-CAGCAGGCAGCATATCAAGGT-3' and reverse primer 5'-GCCGTGGGCCACTTTACAC-3'.

RNA and protein isolation

Livers were homogenized in 500 µl HEPES buffer (10 mM HEPES, 300 mM KCl, 3 mMMgCl2, 0.1mM CaCl2, 0.45 % Triton, 0.05% Tween-20; pH 7.6) containing Complete protease inhibitor (Roche), 3 mM DTT and 40 units RNAse OUT (Invitrogen). RNA was isolated from 100 µl of homogenate using RNA Bee according to the manufacturer's instructions. For protein isolation, the remaining homogenate was spun down 15000g at 4°C for 15 minutes. The supernatant was collected and the protein concentration was measured using the BCA kit (Pierce).

Quantitative RT PCR

Reverse transcriptase was performed in 1 µg of RNA using iScript cDNA synthesis kit (Biorad) according to manufacturer's instructions. RNA was treated with DNase before

cDNA synthesis. Q-PCR using SYBR Green (KAPA Biosystems) was performed on 0.1 µl RT product. Cycling conditions were an initial denaturation of 3 minutes at 95°C, followed 40 cycles of 5 seconds 95°C and 30 seconds 60°C. As a reference gene actin was used and statistical analysis was performed with a t-test. See supplemental data for primer sequences.

Western blotting

30 µg of total protein homogenate was loaded to Criterion XT precast gels (4-12% bis-tris) (Biorad) and run in MOPS buffer (0.05M Mops, 0.05M Tris, 3.5 mM SDS, 1mM EDTA, pH 7.7). The gel was electroblotted to a nitrocellulose membrane in TG buffer (0.192M glycine, 0.025M Tris, 20% methanol). After blocking in PBS-Tween, the membrane was incubated overnight with rabbit anti-GFP (1:100.000 Abcam) and mouse anti-GAPDH (1:200.000 (Chemicon) antibodies. The secondary antibodies were goat-anti-rabbit IRDye 800cW and donkey-anti-mouse IRDye 680LT (both 1:10.000; Li-cor). The membrane was scanned with an Odyssey Infrared Imager.

Immunohistochemistry

Tissues were fixed overnight in 4% paraformaldehyde and embedded in paraffin according to standard protocols. Sections (7µm) were deparaffinised followed by antigen retrieval using microwave treatment in 0.01M sodium citrate. Endogenous peroxidase activity was blocked and immunostaining was performed overnight at 4°C using mouse anti-GFP (1:2000 Roche) or rabbit anti-cleaved Caspase 3 (1:100 Cell Signaling Technology) antibodies. Antigen-antibody complexes were visualized by incubation with DAB substrate (DAKO) after incubation with Brightvision poly-HRP-linker (Immunologic). Slides were counterstained with haematoxylin and mounted with Entellan (Merck Milipore International).

SUPPLEMENTAL DATA

Supplemental data is available online.

REFERENCES

1. Willemsen, R., J. Levenga, and B. Oostra, *CGG repeat in the FMR1 gene: size matters.* Clin Genet, 2011. **80**(3): p. 214-25.
2. Jacquemont, S., et al., *Penetrance of the fragile x-associated tremor/ataxia syndrome in a premutation carrier population.* JAMA, 2004. **291**(4): p. 460-9.
3. Hunsaker, M.R., et al., *Widespread non-central nervous system organ pathology in fragile X premutation carriers with fragile X-associated tremor/ataxia syndrome and CGG knock-in mice.* Acta Neuropathol, 2011. **122**: p. 467-479.
4. Hagerman, R. and P. Hagerman, *Advances in clinical and molecular understanding of the FMR1 premutation and fragile X-associated tremor/ataxia syndrome.* Lancet Neurol, 2013. **12**(8): p. 786-98.
5. Tassone, F., et al., *FMR1 CGG allele size and prevalence ascertained through newborn screening in the United States.* Genome Med, 2012. **4**(12): p. 100.
6. Hantash, F.M., et al., *FMR1 premutation carrier frequency in patients undergoing routine population-based carrier screening: Insights into the prevalence of fragile X syndrome, fragile X-associated tremor/ataxia syndrome, and fragile X-associated primary ovarian insufficiency in the United States.* Genet Med, 2011. **13**: p. 39-45.
7. Tassone, F., et al., *Elevated levels of FMR1 mRNA in carrier males:A new mechanism of involvement in the Fragile-X syndrome.* Am J Hum Genet, 2000. **66**(1): p. 6-15.
8. Greco, C.M., et al., *Neuronal intranuclear inclusions in a new cerebellar tremor/ataxia syndrome among fragile X carriers.* Brain, 2002. **125**(Pt 8): p. 1760-1771.
9. Greco, C.M., et al., *Neuropathology of fragile X-associated tremor/ataxia syndrome (FXTAS).* Brain, 2006. **129**(Pt1): p. 243-255.
10. 10. Greco, C.M., et al., *Clinical and neuropathologic findings in a woman with the FMR1 premutation and multiple sclerosis.* Arch Neurol, 2008. **65**(8): p. 1114-6.
11. Sellier, C., et al., *Sam68 sequestration and partial loss of function are associated with splicing alterations in FXTAS patients.* Embo J, 2010. **29**: p. 1248-1261.
12. Sellier, C., et al., *Sequestration of DROSHA and DGCR8 by Expanded CGG RNA Repeats Alters MicroRNA Processing in Fragile X-Associated Tremor/Ataxia Syndrome.* Cell Rep, 2013. **3**(3): p. 869-880.
13. Tassone, F., C. Iwahashi, and P.J. Hagerman, *FMR1 RNA withinthe intranuclear inclusions of fragile X-associated Tremor/Ataxia syndrome (FXTAS).* RNA biology, 2004. **1**: p. 103-105.
14. Todd, P.K., et al., *CGG Repeat-Associated Translation Mediates Neurodegeneration in Fragile X Tremor Ataxia Syndrome.* Neuron, 2013. **78**(3): p. 440-455.
15. Willemsen, R., et al., *The FMR1 CGG repeat mouse displays ubiquitin-positive intranuclear neuronal inclusions; implications for the cerebellar tremor/ataxia syndrome.* Hum Mol Genet, 2003. **12**(9): p. 949-59.
16. Entezam, A. and K. Usdin, *ATR protects the genome against CGG*CGG-repeat expansion in Fragile X premutation mice.* Nucleic Acids Res, 2007. **36**: p. 1050-1056.
17. Entezam, A., et al., *Regional FMRP deficits and large repeat expansions into the full mutation range in a new Fragile X premutation mouse model.* Gene, 2007. **395**: p. 125-134.
18. Brouwer, J.R., et al., *Elevated Fmr1 mRNA levels and reduced protein expression in a mouse model with an unmethylated Fragile X full mutation.* Exp Cell Res, 2007. **313**: p. 244-253.
19. Van Dam, D., et al., *Cognitive decline, neuromotor and behavioural disturbances in a mouse model for Fragile-X-associated tremor/ataxia syndrome (FXTAS).* Behavioural Brain Research, 2005. **162**: p. 233-239.
20. Hunsaker, M.R., et al., *Progressive spatial processing deficits in a mouse model of the fragile X premutation.* Behav Neurosci, 2009. **123**(6): p. 1315-24.
21. Hunsaker, M.R., et al., *Motor Deficits on a Ladder Rung Task in Male and Female Adolescent and Adult CGG Knock-in Mice.* Behav Brain Res, 2011. **222**: p. 117-121.
22. Hunsaker, M.R., et al., *Temporal Ordering Deficits in Female CGG KI Mice Heterozygous for the Fragile X Premutation.* Behav Brain Res, 2010. **213**: p. 263-268.

23. Hunsaker, M.R., et al., *Mouse models of the fragile x premutation and the fragile x associated tremor/ ataxia syndrome*. Results Probl Cell Differ, 2012. **54**: p. 255-69.

24. Katsantoni, E.Z., et al., *Ubiquitous expression of the rtTA2S-M2 inducible system in transgenic mice driven by the human hnRNPA2B1/CBX3 CpG island.* BMC Dev Biol, 2007. **7**: p. 108.

25. Tamimi, T.I., et al., *An apoptosis panel for nonalcoholic steatohepatitis diagnosis*. J Hepatol, 2011. **54**(6): p. 1224-9.

26. Ross-Inta, C., et al., *Evidence of mitochondrial dysfunction in fragile X-associated tremor/ataxia syndrome*. Biochem J, 2010. **429**: p. 545-552.

27. Kaplan, E.S., et al., *Early mitochondrial abnormalities in hippocampal neurons cultured from Fmr1 premutation mouse model.* J Neurochem, 2012.

28. Lei, X.G., W.H. Cheng, and J.P. McClung, *Metabolic regulation and function of glutathione peroxidase-1*. Annual Review of Nutrition, 2007. **27**: p. 41-61.

29. Jin, P., et al., *Pur alpha Binds to rCGG Repeats and Modulates Repeat-Mediated Neurodegeneration in a Drosophila Model of Fragile X Tremor/Ataxia Syndrome*. Neuron, 2007. **55**(4): p. 556-64.

30. Sofola, O.A., et al., *RNA-Binding Proteins hnRNP A2/B1 and CUGBP1 Suppress Fragile X CGG Premutation Repeat-Induced Neurodegeneration in a Drosophila Model of FXTAS*. Neuron, 2007. **55**(4): p. 565-71.

31. Hoem, G., et al., *CGG-repeat length threshold for FMR1 RNA pathogenesis in a cellular model for FXTAS*. Hum Mol Genet, 2011. **20**: p. 2161-2170.

32. Mahadevan, M., et al., *Myotonic dystrophy mutation: an unstable CTG repeat in the 3' untranslated region of the gene*. Science, 1992. **255**: p. 1253-1255.

33. Mari, M., et al., *Mitochondrial glutathione, a key survival antioxidant.* Antioxid Redox Signal, 2009. **11**(11): p. 2685-700.

34. Napoli, E., et al., *Altered Zinc Transport Disrupts Mitochondrial Protein Processing/Import in Fragile X-Associated Tremor/Ataxia Syndrome*. Hum Mol Genet, 2011. **20**: p. 3079-3092.

35. Neustadt, J. and S.R. Pieczenik, *Medication-induced mitochondrial damage and disease*. Mol Nutr Food Res, 2008. **52**(7): p. 780-8.

36. Paul, R., et al., *Early onset of neurological symptoms in fragile X premutation carriers exposed to neurotoxins*. Neurotoxicology, 2010. **31**: p. 399-402.

37. O'Dwyer, J.P., et al., *Fragile X-associated tremor/ ataxia syndrome presenting in a woman after chemotherapy.* Neurology, 2005. **65**(2): p. 331-2.

REVERSIBILITY OF NEUROPATHOLOGY AND MOTOR DEFICITS IN AN INDUCIBLE MOUSE MODEL FOR FXTAS

R.A.M. Buijsen[1,*], R.K. Hukema[1,*], M. Schonewille[2,*], C. Raske[3], E.A.W.F.M. Severijnen[1], I. Nieuwenhuizen-Bakker[1], R.F.M. Verhagen[1], L. van Dessel[1], A. Maas[4], N. Charlet-Berguerand[5], C.I. De Zeeuw[2,6], P.J. Hagerman[3], R.F. Berman[7,#], R. Willemsen[1,#]

[1] Department of Clinical Genetics, Erasmus MC, Rotterdam, the Netherlands
[2] Department of Neuroscience, Erasmus MC, Rotterdam, the Netherlands
[3] Department of Biochemistry and Molecular Medicine, University of California, Davis, USA
[4] Department of Cell Biology, Erasmus MC, Rotterdam, the Netherlands
[5] IGBMC, Illkirch, France
[6] Netherlands Institute for Neuroscience, Amsterdam, the Netherlands
[7] Department of Neurological Surgery, University of California, Davis, USA.

*,# these authors contributed equally

Human Molecular Genetics 2015 Sep 1;24(17):4948-57

ABSTRACT

Fragile X-associated tremor/ataxia Syndrome (FXTAS) is a late-onset neurodegenerative disorder affecting carriers of the fragile X-premutation who have an expanded CGG repeat in the 5'-UTR of the FMR1 gene. FXTAS is characterized by progressive development of intention tremor, ataxia, parkinsonism and neuropsychological problems. The disease is thought to be caused by a toxic RNA gain-of-function mechanism and the major hallmark of the disease is ubiquitin positive intranuclear inclusions in neurons and astrocytes. We have developed a new transgenic mouse model in which we can induce expression of an expanded repeat in the brain upon doxycycline (dox) exposure (i.e., Tet-On mice). This Tet-On model makes use of the PrP-rtTA driver and allows us to study disease progression and possibilities of reversibility. In these mice, 8 weeks of dox exposure was sufficient to induce the formation of ubiquitin-positive intranuclear inclusions, which also stain positive for the RAN translation product FMRpolyG. Formation of these inclusions is reversible after stopping expression of the expanded CGG RNA at an early developmental stage. Furthermore, we observed a deficit in the compensatory eye movements of mice with inclusions, a functional phenotype that could be reduced by stopping expression of the expanded CGG RNA early in the disease development. Taken together, this study shows for the first time the potential of disease reversibility and suggests that early intervention might be beneficial for FXTAS patients.

INTRODUCTION

Fragile X-associated tremor/ataxia Syndrome (FXTAS) is a late onset neurodegenerative disorder causing tremor, ataxia, brain atrophy, cognitive loss, dementia, and in some individuals, early death. The disorder develops in individuals, referred to as fragile X-premutation carriers, who have an expansion of 55-200 CGG repeats in the 5'-UTR of the *FMR1* gene [1]. The prevalence of premutation carriers in the general population is high, and is estimated 1:291 for females and 1:855 for males [2]. The chances of developing FXTAS increase dramatically with age, with approximately 45.5% of male and 16.5% of female premutation carriers over the age of 50 developing FXTAS [3]. The major hallmark of FXTAS neuropathology is the presence of intranuclear inclusions that stain for ubiquitin in neurons and astrocytes throughout the brain [4]. Premutation carriers with or without FXTAS show elevated levels of *FMR1* mRNA and normal to slightly reduced levels of FMRP protein [5]. This finding has led to the proposal that FXTAS is caused by a toxic RNA gain-of-function mechanism, in which mutant RNA containing the expanded CGG repeat would be pathogenic [6]. An additional mechanism of toxicity that is triggered by (expanded) CGG repeats involves repeat associated non-AUG (RAN) translation of the CGG repeat and has been proposed to play a role in FXTAS [7]. Mutant RNA bearing a CGG repeat expansion can be translated into protein without using a traditional AUG start codon, and such translation may occur in all three reading frames (i.e., CGG, GGC or GCG) leading to multiple toxic entities from a single repeat expansion. For the CGG repeat in FXTAS it has been proposed [8] that RAN translation initiates in the 5'-UTR of the FMR1 gene and results in the production of a polyglycine (FMRpolyG) and also a polyalanine (FMRpolyA) protein. The presence of FMRpolyG was demonstrated in cell culture, *Drosophila* and mouse models, and brain and other tissues from FXTAS patients while FMRpolyA could only be detected in transfected cells [8, 9].

Previously, we and others have generated knock-in mouse models with expanded CGG repeats that have greatly facilitated the study of FXTAS disease progression [10, 11]. In our knock-in mouse model the murine 8CGG repeat has been replaced repeat by homologous recombination in ES cells with a human expanded 98CGG [12]. This model recapitulates many of the features seen in human FXTAS: not only increased expression of *Fmr1* mRNA, decreased levels of FMRP, and intranuclear aggregates in neurons and astrocytes, but also poor motor function, impaired memory, and progressive spatial processing deficits [13]. Recently, we reported initial findings in our new Tet-On doxycycline-inducible mouse model for FXTAS [14]. In this model expression of either a control size CGG repeat (11CGGs) or a pathogenic expanded repeat (90CGGs) can be activated using the Tet-On system. In this initial study we reported toxic effects of expression of the expanded repeat under control of the ubiquitous hnRNP-rtTA driver. We showed that RNA containing an expanded CGG repeat is pathogenic in the liver,

whereas RNA containing a control sized repeat is not. After 5 days of doxycycline (dox) exposure, the expression of expanded repeat RNA resulted in mitochondrial dysfunction in the liver and early death, hampering the possibility to study the long-term effects of expanded CGG repeat expression in brain. Importantly, the observed effects were due to the ectopically expressed expanded repeat, out of the context of the *Fmr1* gene.

RESULTS

Inducible expression of expanded CGG RNA in the brain

Recently, we have shown that induced expression of an expanded 90CGG RNA produces mitochondrial stress and apoptosis in the liver in a Tet-On mouse model for FXTAS [14]. Here, we used the same strategy to create bigenic transgenic mice in which exposure to dox induces expression of either a control size 11CGG or an expanded 90CGG repeat RNA fused to an enhanced GFP (eGFP) reporter in brain. These mice were created by crossing our new PrP-rtTA "driver" mouse line with "target" mouse lines carrying a tetracycline response element (TRE) linked to either a 11CGG (TRE-11CGG-eGFP) or 90CGG (TRE-90CGG-eGFP) repeat expansion and an eGFP reporter (**Figure 1A**). We opted for the prion protein or PrP promoter, since it drives expression confined to the central nervous system (both neurons and glia cells). We expected that the use of this driver line would avert the liver failure we observed when using the more ubiquitous driver line hnRNP-rtTA[14]. Indeed, the double transgenic TRE-nCGG-eGFP/PrP-rtTA mice could be treated with dox in their drinking water for as long as 28 weeks without signs of overt toxicity. Dox treatment resulted in eGFP expression throughout the brain as expected, but with the strongest expression in cerebellum, hippocampus and striatum (**Figure 2**). We could detect eGFP expression in the brain within two days after the start of dox treatment. Thus dox can quickly and efficiently cross the blood-brain-barrier to activate transgene expression in brain tissue. Lack of eGFP expression in single transgenic TRE-nCGG-eGFP mice treated with dox and double transgenic TRE-nCGG-eGFP/PrP-rtTA mice without dox provides clear evidence that the Tet-On system did not show leaky expression (**Supplemental Figure 1**). We also found that 90CGG RNA levels were slightly lower than 11CGG RNA levels (**Figure 1B**), which could be explained by the different integration site of the transgenes, since an untargeted approach was used to generate the mouse lines 90CGG RNA in brain homogenates was about two times overexpressed when compared with endogenous *Fmr1* levels (**Supplemental Material**, **Figure S2**). Since these RNA levels were in whole brain homogenates and the expression pattern is a mosaic of expressing and non-expressing cells present, the effect of overexpression per expressing cell would be much more dramatic.

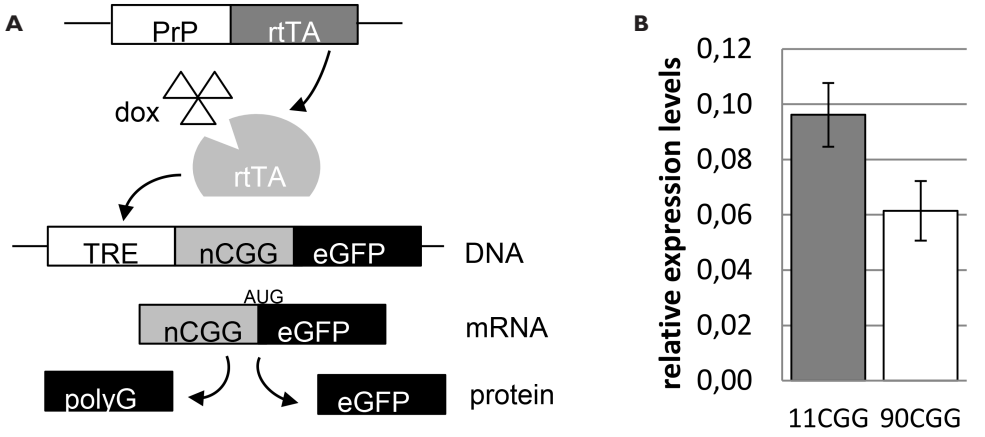

Figure 1. Dox induced expression of nCGG-eGFP in brain. (**A**) The Tet-On system was used to generate bigenic mice expressing an 11CGG or 90CGG repeat at the RNA level. Expression of rtTA is controlled by the PrP promoter on a separate transgene. Upon dox administration rtTA will be activated and can bind the Tet Response Element (TRE) on another transgene, which induces expression of the nCGG repeat at the RNA level and eGFP at the protein level. Since the transgene contains the 5'UTR of the *FMR1 gene, in* addition a polypeptide formed from the repeat by RAN translation. (**B**) Quantitative RT-PCR on RNA isolated from brain of dox treated (16-28 weeks) bigenic TRE-nCGG-eGFP/PrP-rtTA mice. 90CGG RNA levels are lower than 11CGG RNA levels in whole brain homogenates (*N*=8). Error bars represent SEM.

Expanded CGG RNA expression leads to inclusion formation

The major hallmark of FXTAS is the presence of ubiquitin-positive intranuclear inclusions throughout the brain. Thus, after inducing transgene expression in the brains of bigenic mice by dox exposure through drinking water (4mg/ml), we studied the distribution and morphology of ubiquitin-positive inclusions. Initially, we started our histological analysis after 8 weeks dox treatment. In all areas of the brains of TRE-90CGG-eGFP/PrP-rtTA mice that showed eGFP expression, and thus the expanded 90CGG RNA, we detected ubiquitin-positive intranuclear inclusions (**Figure 3**). As expected most intranuclear inclusions were found in those brain regions expressing high levels of eGFP, including lobule X of the cerebellum, hippocampus, and striatum. In hippocampus, round/spherical inclusions were found, with the largest in CA3 area (**Figure 3A**). In contrast, in the granular layer of lobule X of the cerebellum inclusions showed a cat-eye shape (**Figure 3E-H**). Despite differences in shape the inclusions were always intranuclear and only one per nucleus was observed. Ubiquitin-positive inclusions were never observed in mice expressing 11CGG RNA, not even after as long as 28 weeks of dox induction, nor in bigenic mice not treated with dox (**Supplemental Material**, **Figure 3A**). The level of

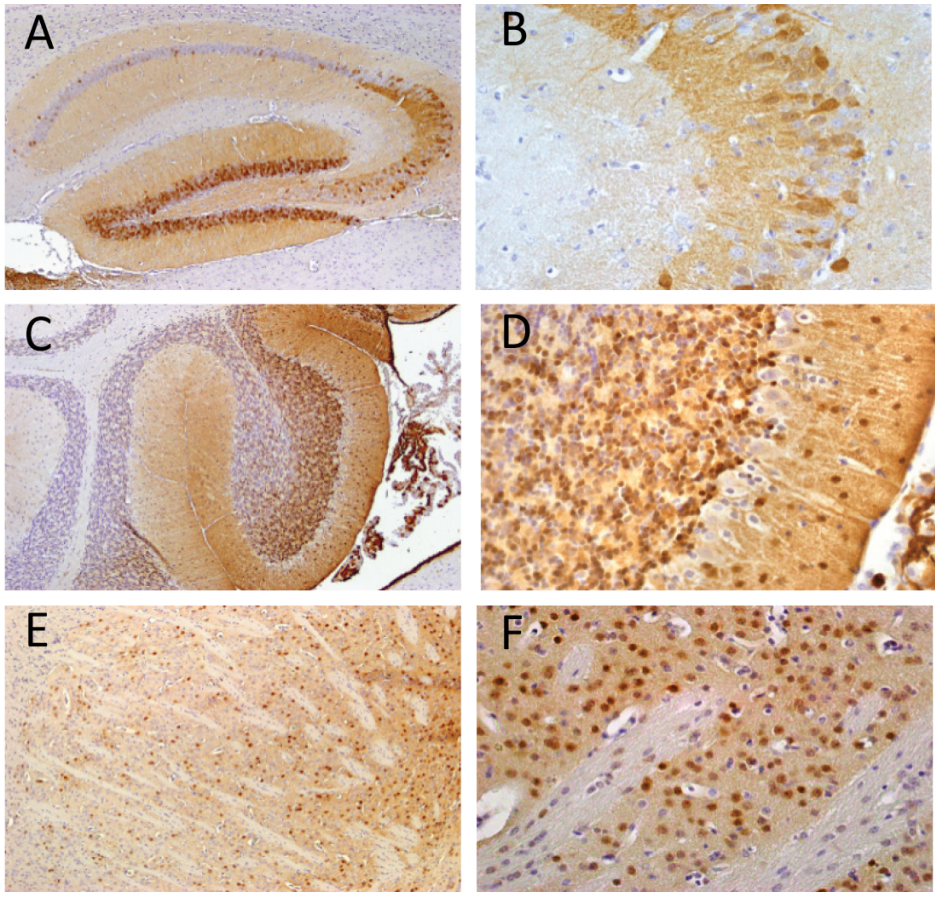

Figure 2. eGFP expression in brain after dox induction of bigenic TRE-nCGG-eGFP/PrP-rtTA mice. Immunohistochemical staining of paraffin section of brain from dox induced nCGG-eGFP-expressing mice in (**A**) hippocampus (10x), (**B**) mainly in CA3 area (40x); (**C**) cerebellum (40x), (**D**) mainly in lobule X (100x); and (**E**) striatum (10x), (**F**) striatum (40x).

RNA expression was lower for 90CGG RNA than for 11CGG RNA, suggesting that the formation of inclusions is dependent on the presence of expanded CGG RNA and is not caused by overexpression of CGG RNA per se.

The formation of inclusions was followed over time by treating the bigenic TRE-90CGG-eGFP/PrP-rtTA mice for different time periods with dox. The percentage of neurons with an inclusion was quantified by analysis of 500 nuclei in the granular cell layer of cerebellar lobule X. In this area of the brain the expression of eGFP was most pronounced and showed the least variation. Also the first ubiquitin positive inclusions were observed in this part of the brain after 6 weeks of dox exposure. After 8 weeks of dox treatment 27% (with a S.E.M. of 7 %) of the nuclei showed an ubiquitin-positive

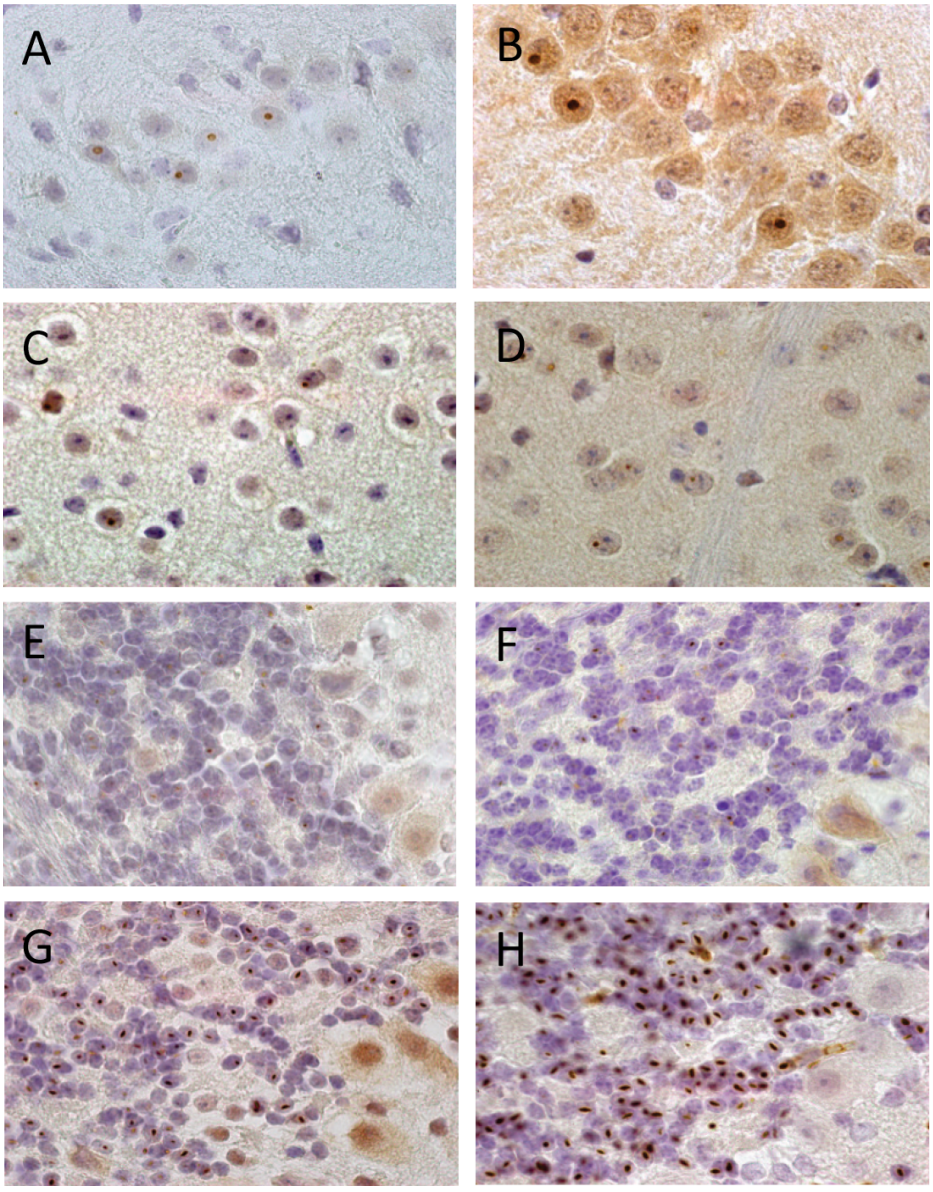

Figure 3. Ubiquitin and FMRpolyG positive intranuclear inclusions in different brain areas after dox induction of bigenic TRE-90CGG-egFP/PrP-rtTA mice. (**A**) Ubiquitin positive intranuclear inclusions in CA3 of hippocampus. (**B**) FMRpolyG positive intranuclear inclusions in CA3 of hippocampus. (**C**) Ubiquitin positive intranuclear inclusions in striatum. (**D**) FMRpolyG positive intranuclear inclusions in striatum. (**E**) Ubiquitin positive intranuclear inclusions in the granular cell layer of lobule X after 8 weeks of dox induction. (**F**) FMRpolG positive intranuclear inclusions in the granular cell layer of lobule X after 8 weeks of dox induction. (**G**) Ubiquitin positive intranuclear inclusions in the granular cell layer of lobule X after 20 weeks of dox induction. (**H**) FMRpolyG positive intranuclear inclusions in the granular cell layer of lobule X after 20 weeks of dox induction. All images 100x magnification.

inclusion, with a significant increase over time to 70% (with a S.E.M. of 3 %) after 28 weeks of dox treatment (**Figure 4A**). In addition, not only the number of inclusions increased, but also the size increased with longer dox exposure times. Specifically, size increased from 0.79 (with a S.E.M. of 0.07) µm at 8 weeks treatment to 1.91 (with a S.E.M. of 0.21) µm at 28 weeks of dox induction (**Figure 4B**). Thus, prolonged expression of expanded CGG RNA results in higher number of and larger-sized inclusions.

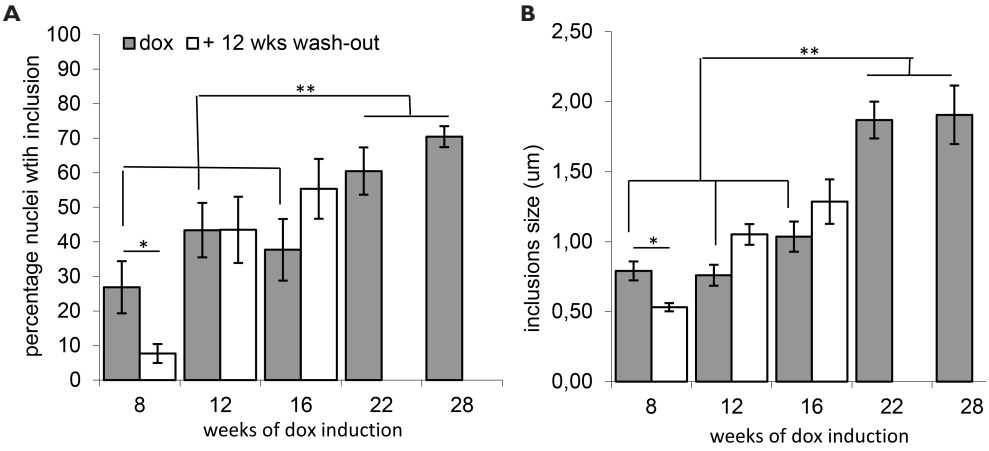

Figure 4. Quantification of ubiquitin positive intranuclear inclusions in cerebellar lobule X of TRE-90CGG-eGFP/PrP-rtTA mice. (**A**) The percentage of nuclei containing a ubiquitin positive inclusions after different dox treatment periods. (**B**) The size of the ubiquitin positive inclusions after different dox treatment periods. Purple bars represent results from dox treated mice, orange bars represent results obtained from mice with an additional wash-out after dox induction. N = 5-7 mice per group. Significance was determined using a 2-tailed t test with 95% confidence interval, with * = $p < 0.05$; ** = $p < 0.01$; *** = $P < 0.001$; *N* = 5-7 mice per group. Error bars represent SEM.

Poly-Glycin and other components of the inclusions

Recently, a new type of translation has been described for several repeat associated diseases, including FXTAS [8]. This repeat associated non-AUG (RAN) translation is thought to be induced by the presence of an expanded repeat in some RNAs. The repeat expansion is thought to stall scanning of the mRNA by the 40S ribosomal subunit, resulting in the use of an alternate downstream non-AUG start site. This in turn could cause a frameshift and translation of polypeptides associated with the CGG repeat expansion. As a result, different polypeptides could theoretically be produced from RAN translation of the CGG repeat (polyArg, polyGly and polyAla), depending on the reading frame (i.e., CGG, GGC or GGC). For FXTAS such translation has been reported to result in production of poly-glycine (FMRpolyG) and poly-alanine (FMRpolyA) peptides [8]. We have used two different

antibodies to detect FMRpolyG, 8FM and 9FM. The 8FM is specific for the sequence directly upstream of the polyG tract, and 9FM is specific for the sequence directly downstream of the polyG tract [9]. Thus both antibodies are specific for polyG translated from the GGC tract in *Fmr1* mRNA. Both the 90CGG and 11CGG repeat transgenes in our dox-inducible mice are of human origin and they also contain some human flanking sequence that include the sequence used as the epitope for these antibodies. Therefore, we explored the presence of FMRpolyG in the brain of the inducible mice. FMRpolyG-positive inclusions were present in those brain regions of 90CGG mice that express high levels of eGFP, whereas 11CGG mice were totally devoid of FMRpolyG-positive inclusions (**Figure 3**; **Supplemental Material**, **Figure S3B**). The FMRpolyG-positive inclusions could be detected with both 8FM and 9FM antibodies. Since both antibodies achieved similar results we continued our studies using only the 8FM (**Supplemental Material**, **Figure S4**). All brains that were studied for the presence of ubiquitin-positive inclusions were also analyzed for the presence of FMRpolyG. The distribution of the FMRpolyG inclusions was similar to the ubiquitin inclusions. Co-localization studies of ubiquitin and FMRpolyG using double immunofluorescence staining demonstrated a complete colocalization in all inclusions at all time points examined (**Figure 5**). We never observed inclusions that stained positive only for ubiquitin or only for FMRpolyG. In addition, to further characterize the nature of the intranuclear inclusions we studied the localization of proteins previously shown to be components of these inclusions [12, 15]. We confirmed the presence of the 20S core complex of the proteasome, Hsp40, and Rad23B (**Figure 5**). Like FMRpolyG, these components almost always show colocalization with ubiquitin.

Reversibility of inclusion formation

The main advantage of the Tet-On system is the ability to shut down transgene expression by removing dox from the drinking water, thus allowing us to study the possibilities of halting and/or reversing disease progression. Since we have demonstrated that these inducible mice are a good model to study FXTAS disease progression, we next studied the effect of a wash-out period with normal drinking water after initial dox induction. Importantly, within 48 hours of removing dox from the drinking water we found a rapid decrease of CGG repeat RNA expression, and no significant levels of eGFP in brain tissue could be detected (**Supplemental Material**, **Fig S5**).

Wash-out periods of 12 weeks were combined with different dox induction periods of 8, 12, and 16 weeks. For quantification of the number of ubiquitin-positive inclusions before and after washout we again choose the granular cell layer of cerebellar lobule X. As illustrated in **Figure 4**, 12 weeks of washout after both 12 and 16 weeks of dox treatment did not result in a significant reduction of the number (**Figure 4A**) or size (**Figure 4B**) of ubiquitin-positive inclusions in cerebellar lobule X. Nevertheless, we also did not observe

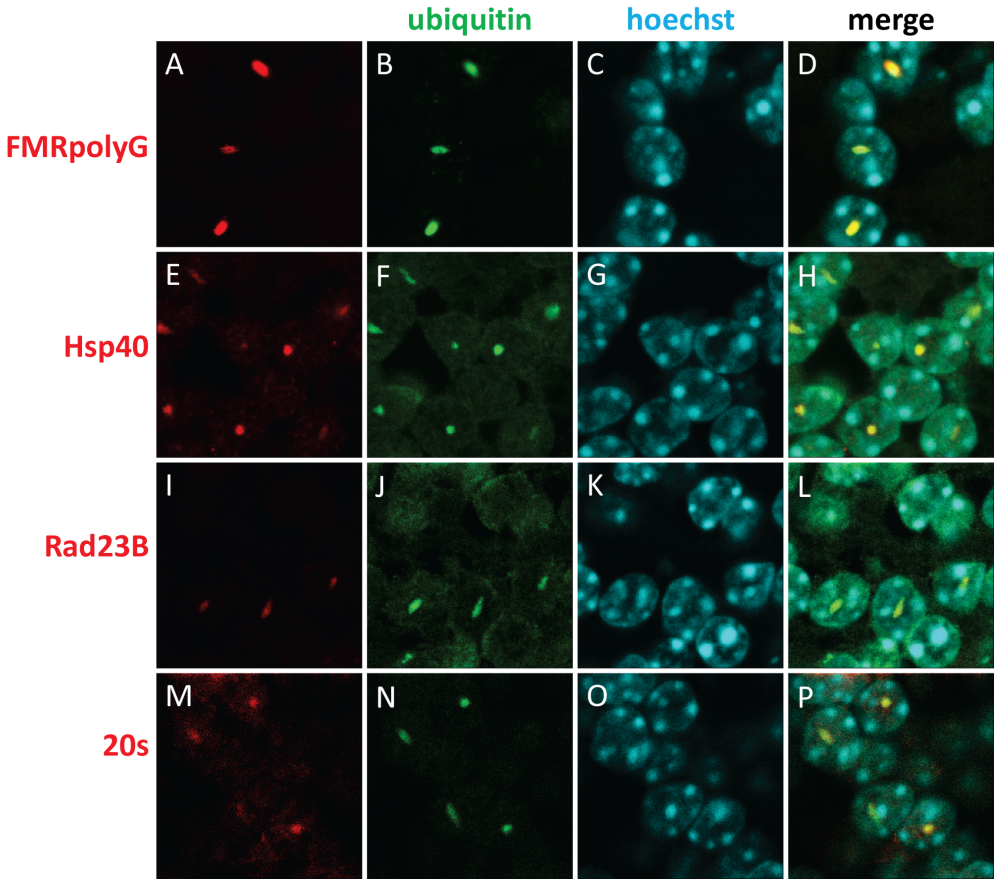

Figure 5. Colocalization of ubiquitin (green) with other components (red) in intranuclear inclusions in the granular cell layer of lobule X of the cerebellum after dox induced 90CGG RNA expression. Ubiquitin (**B**, **F**, **J**, **N**) colocalizes (**D**, **H**, **L**, **P**) in intranuclear inclusions with FMRpolyG (**A**), Hsp40 (**E**), Rad23B (**I**), and 20S subunit of the proteasome (**M**). All images 630x magnification.

an increase in number or size. Thus, upon stopping expanded CGG repeat RNA expression at these time points appears to prevent further progression of neuropathology. However, 12 weeks washout after 8 weeks of dox induction resulted in a significant reduction in the number ($P < 0.05$) and size ($P < 0.05$) of inclusions that were still present. Also, after wash-out the co-localization of ubiquitin and FMRpolyG in the remaining inclusions remained at 100% and no single ubiquitin- or FMRpolyG-positive inclusions were observed. Not only the colocalization of FMRpolyG and ubiquitin didn't change after wash-out, but also the colocalization of ubiquitin with the 20S proteasome, Hsp40, and Radb23B remained unchanged (data not shown). Thus, we were able to demonstrate reversibility of neuropathology using antibodies against different markers for inclusions.

Development of deficits in compensatory eye movements is halted by dox wash-out

Based on the high expression of mutant RNA in the granular cell layer of lobule X after dox treatment one could predict functional deficits and potential functional reversibility in a behavioral test related to this brain region. Lobule X constitutes, together with the two laterally located flocculi, the vestibulo-cerebellum. Although we quantified the inclusions in lobule X, we also found eGFP expression and inclusions in each flocculus. A well-established behavioral test known to be dependent on the flocculus is the optokinetic reflex (OKR). The OKR is a motor reflex driven by full-field visual stimulation that, together with the vestibulo-ocular reflex (VOR), aims to reduce retinal slip, (i.e., the movement of visual input across the retina), to ensure clear vision. We tested the effect of the inclusions on this motor behavior in head-fixed mice by presenting a sinusoidally rotating visual stimulus (amplitude 5°, frequency range 0.1-1.0 Hz) while recording their eye movements (**Figure 6B**,**C**). Behavioral effects were analyzed by determining the gain of eye movements, which represents the size of the eye movements relative to the stimulation. Eight weeks of dox induction did not result in a behavioral deficit, as OKR gain was not affected in 90CGG mice (90CGG vs. 11CGG, $P = 0.286$, repeated measures ANOVA with Tukey's posthoc test) (**Figure 6B**). However, prolonged exposure to dox for 20 weeks did result in a behavioral deficit, in that the gain of the OKR in 90CGG mice was lower, compared to that of control mice ($P < 0.001$) and that of mice exposure to dox for only 8 weeks ($P = 0.001$). As the presence of the inclusions is at least partially reversible in lobule X after 8 weeks of dox induction and 12 weeks of washout, (**Figure 4**, **6A**), one could hypothesize that progression of the behavioral deficits in the OKR, could be attenuated too. This was indeed true, because discontinuing the dox induction after 8 weeks of exposure resulted in a better performance at 20 weeks (vs. 20 weeks dox of induction, $P < 0.001$), which was no longer significantly different from that of control mice (vs. 11CGG with 20 weeks of dox induction, $p = 0.993$). When we tested OKR gains evoked by visual stimulation with fixed velocity (8°/s, frequencies 0.05 – 1.6 Hz), instead of fixed amplitude, the same differences were found (**Supplemental Material**, **Figure S6**), strengthening our conclusion that dox exposure correlates with cerebellum-dependent functional deficits.

As described above, the OKR is used in conjunction with the VOR, a reflex based on vestibular input from the semi-circular canals to generate the visually-enhanced reflex, or VVOR. The VVOR functions to stabilize an image on the retina when moving through an environment. To verify if the deficits in OKR are compensated by changes in the processing of vestibular input, we also tested the VOR and VVOR in the same mice (**Fig 6B**, **Supplemental Material**, **Figure S6B**). The VOR, evoked by head rotation in the dark, can be influenced by, but does not require, the cerebellum. In line with that the differences in VOR gain were, compared to those in OKR gain, in the same general

direction but less pronounced (**Supplemental Material**, **Figure S6B**). In VVOR gain, similar to OKR, we observed a significantly lower gain in mice with irreversible inclusions after prolonged, 20 week dox exposure (90CGG vs. 11CGG, P = 0.002; 20 weeks vs. 8 weeks of dox in 90CGG, P = 0.020). Here too, this deficit could be prevented by stopping dox exposure after 8 weeks (20 weeks dox vs. wash-out in 90CGG, P = 0.004).

To conclude, the presence of irreversible inclusions in the vestibulo-cerebellum correlates with deficits in compensatory eye movements, which depends on its proper functioning. Reversing inclusion number and size by ceasing dox induction after 8 weeks of exposure minimized disease progress in that the compensatory eye movements did not further deteriorate.

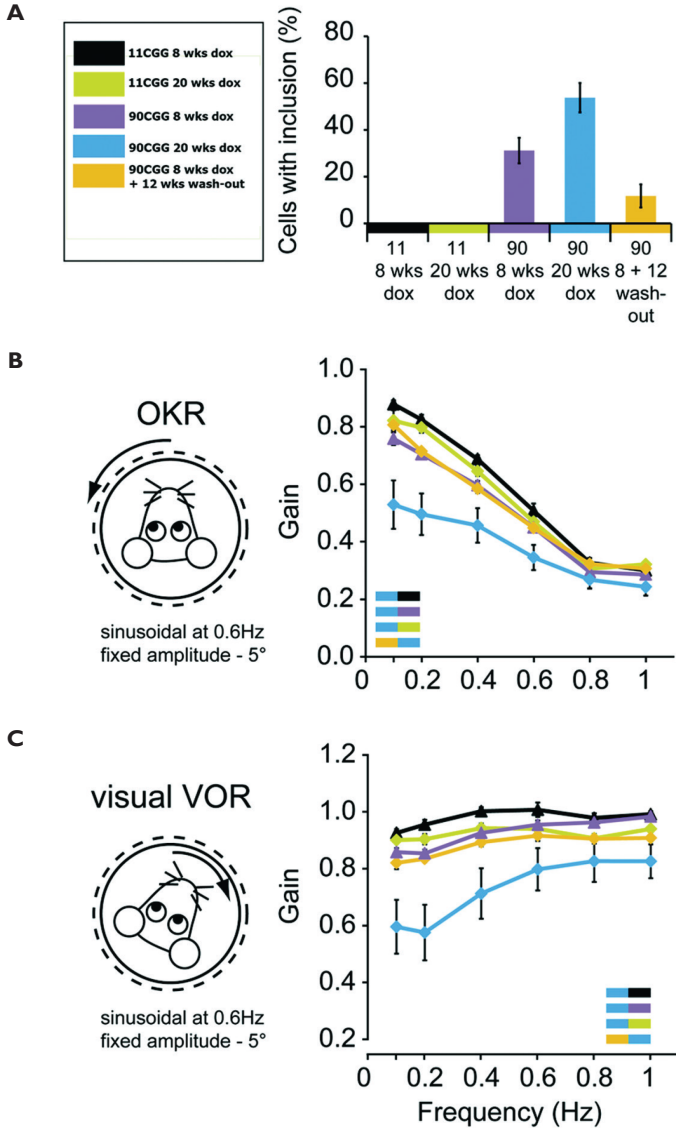

DISCUSSION

Several animal models have contributed to understanding of the molecular mechanisms underlying FXTAS and have characterized the disease process. However, previous mouse models did not make it possible to address questions concerning the possible reversibility of FXTAS or to elucidate critical periods in the natural history of the disease [13]. In order to address such questions, we describe the successful development and initial characterization of an inducible mouse model for the fragile X-premutation and FXTAS. In this model, an expanded CGG RNA is expressed under control of a Tet-On promoter activated by the addition of dox to drinking water [14]. This inducible model shows no evidence of expression in the absence of dox (i.e., no leakage of expression) and allows us to control the timing of CGG RNA expression during development. Consequently, we were able not only to examine disease progression in these mice, but also provide evidence for the potential for halting disease progression and reversal of neuropathology and specific functional deficits. Specifically, the number and size of inclusions formed in these mice by induced expression of expanded CGG RNA was reversible when mice were exposed to dox starting from 3 weeks of age and taken off dox after 8 weeks of exposure. However, reversibility could only be demonstrated after 8 weeks of dox treatment and not after longer treatment periods of 12 and 16 weeks. The present study shows that the *in vivo* formation of the inclusions is dependent on expression of an RNA bearing an expanded CGG repeat rather than on overexpression of CGG RNA per se. Finally, the aberrant behavior of these mice in an eye-reflex test did not deteriorate

← **Figure 6.** Deficits in the compensatory eye movements correlate with the presence of inclusions. To determine the functional consequences of expanded CGG repeat-induced inclusions, we tested, in head-fixed awake mice, the compensatory eye movements that are known to depend on an intact vestibulo-cerebellum. (**A**) The percentage of nuclei in the granular cell layer of cerebellar lobule X containing an inclusion for mice used in the analysis of compensatory eye movements. (**B**) Sinusoidal rotation of the visual field evoked the optokinetic reflex (OKR), a cerebellum-dependent reflex that minimizes retinal slip. OKR gain, the ratio of eye to stimulus velocity, over a range of frequencies was compared between mice with and without (ir)reversible inclusions. Whereas gains 90CCG mice after 8 weeks of dox induction (purple) were not significantly lower than those in controls (black), irreversible inclusions as a result of 20 weeks of exposure to dox (blue) did cause deficits in eye movement performance compared to controls (yellow). In contrast, reversing the presence of inclusions by wash-out (8 weeks dox induction followed by 12 weeks wash-out, orange) prevented the development of performance deficits. (**C**) In everyday life, the OKR works in conjunction with the vestibulo-ocular reflex (VOR), to maintain a stable image on the retina. To test if the deficits in the OKR could also affect more natural behaviors, mice were subjected to sinusoidal rotation of the turntable in the light, to evoke the visually-enhanced vestibulo-ocular reflex (VVOR). All the differences present in OKR were reproduced, confirming the link of inclusions with behavioral deficits. Insets, colors indicate comparisons with $p<0.05$ (repeated measures ANOVA followed by Tukey's posthoc).

further when expression of the expanded CGG RNA was stopped by withdrawal of dox exposure. Our results therefore, suggest that only an early intervention may be beneficial for FXTAS patients and premutation carriers.

The major histopathological hallmark of FXTAS is the presence of ubiquitin-positive intranuclear inclusions in neurons and astrocytes seen in the postmortem brain. We therefore focused on their presence in the quantitative analyses of this new inducible mouse model. In the cerebellum, where we focused our quantitative analyses, we found clear evidence that the number and size of the inclusions increased with longer exposure to dox. It remains to be seen whether these inclusions are pathological or protective in the brain. However, we recently reported that dox-induced expression of expanded CGG RNA can cause mitochondrial damage in the liver, followed by early death of mice within one week of exposure. These experiments were carried out in bigenic mice (TRE-90CGG-eGFP/hnRNP-rtTA) in which expression of the expanded CGG RNA utilized an hnRNP-promoter to drive rtTA expression [14]. Importantly, these bigenic mice express elevated levels of mutant expanded CGG RNA in liver, but show a total absence of ubiquitin-positive inclusions. Based on these results, free expanded CGG RNA appears to be toxic even in the absence of inclusions. This finding does not, however, exclude the possibility that, in human brain, the formation of intranuclear inclusions and subsequent sequestration of specific RNA-binding proteins can also interfere with normal cell functioning, which could then ultimately lead to cell death [4].

The main hypothesis for the cause of FXTAS has been an RNA toxic gain-of-function mechanism, in which high levels of expression of RNA bearing an expanded CGG repeat are the primary mechanism of pathology. This hypothesis is consistent with the fact that the expanded CGG repeat is present in the 5'-UTR of the *FMR1* gene and is therefore not translated into protein. However, for different repeat-associated disorders, including FXTAS, frontotemporal dementia (FTD), and amyotrophic lateral sclerosis (ALS), a new alternative translational mechanism has been described (reviewed in [16]), reopening the discussion about the mechanism of pathology. Specifically, repeat-associated non-AUG (RAN) translation of the trinucleotide repeat has been reported, resulting in the presence of FMRpolyG and FMRpolyA [8].

In this study, we have shown the presence of the RAN translation product FMRpolyG in the ubiquitin-positive inclusions. The observation that inclusions are pathogenic and contain the FMRpolyG peptide is consistent with a role for the polypeptide in disease pathology. Of course, this finding does not rule out a role for *Fmr1* RNA toxicity in the inclusion formation. While the gain-of-function mechanism of pathology therefore remains possible in FXTAS, it might involve both RNA and protein. For the expanded hexanucleotide repeat (GGGGCC) involved in ALS and FTD, it has now been shown in *Drosophila* that toxicity seems to be caused by certain dipeptide repeats rather than

by the repeat RNA [17]. Such models are not yet available for FXTAS, but research is ongoing to establish the roles of the different entities in FXTAS pathology.

The presence of Hsp40, Rad23B and the 20S subunit of the proteasome in the inclusions again suggests a role for the proteasomal degradation pathway in inclusion formation, as was found for other FXTAS mouse models [12, 15, 18]. The involvement of the proteasome is two-fold. First, the proteasome is overloaded with the ubiquitinated proteins present in the inclusions that it should degrade. Second, components of the proteasome itself is sequestered in the inclusions and therefore cannot optimally perform its function. The involvement of the proteasome in pathology is not unique for FXTAS, but is a general process involved in several neurodegenerative diseases with which FXTAS may share common disease mechanisms

To evaluate the functional consequences of the inclusions in the cerebellum of the dox-treated bigenic inducible mice, we quantified reflexive eye movements associated with cerebellar lobule X which showed high levels of expanded CGG RNA expression. The compensatory eye movements evoked by full-field visual stimulation or head rotation are known as the OKR and VVOR, respectively. These eye movements are controlled by the vestibulo-cerebellum, the region of the brain in which most inclusions were observed. The prominent presence of irreversible inclusions after 20 weeks of dox-exposure could be linked to motor performance deficits, in that the gain of the OKR and VVOR was lower in these mice. In fact, the compensatory eye movements in mice treated for 8 weeks with dox already appear to be affected. Although this difference was not statistically significant in the overall group comparison, the differences were statistically significant when individual groups were compared for each reflex (OKR: $P = 0.0013$; VVOR: $P = 0.0002$). This suggests that the phenotype worsens over time in these inducible mice, with an accompanying increase in the number and size of inclusions, whereas transgene RNA expression levels remain the same over time. These ocular reflexes nicely models the progressive character of FXTAS disease development and suggests that the inclusions coincide with disease symptoms in specific brain regions. Ending the exposure to dox after 8 weeks effectively reversed the disease progress in terms of inclusions, and prevented the progressive deterioration of the OKR and VVOR gains. The finding that the development of more severe motor performance deficits could be prevented by halting the expression of the expanded repeat, emphasizes the potential benefit of early intervention.

Regardless of whether FXTAS is caused by RNA directly or by translation of a toxic protein, the results of this study demonstrate that it is possible to halt or even reverse disease progression if expression of the RNA carrying the expanded CGG repeat is stopped. Translating the time course of disease from a transgenic mouse to the human situation is difficult, but what becomes clear from present research is that therapeutic intervention in FXTAS patients and premutation carriers is possible. After longer intervals

we observed that stopping expanded CGG RNA expression stops further disease progression, earlier in the process even reversibility of pathology is possible.

The early time point at which we found reversibility suggests that it might be needed to treat asymptomatic premutation carriers, which raises the ethical question of whom to treat and when to start. Therefore research will also need to focus on identifying biomarkers to predict which premutation carriers are most likely to develop FXTAS. However, later intervention might also be promising to prevent further disease progression. Therefore, for all FXTAS patients it is important to investigate if interfering with the expanded CGG RNA expression is possible. Although it may be a long time before effective therapeutic interventions for FXTAS are available for clinical use, the results of these experiments – reversibility of disease pathogenesis - represent a "proof of principle" that effective treatments are possible. This is a very important step in recognizing the options, and opens new avenues for further research for other repeat related diseases involving gain-of-function mechanisms caused by RAN translation or RNA.

MATERIAL AND METHODS

Mouse lines, dox treatment, and genotyping

TRE-11CGG-eGFP and TRE-90CGG-eGFP mouse strains and genotyping were as described previously [14] in C57BL/6JRj (from Janvier labs) background. The TRE-90CGG-eGFP mouse strain has been bred for several generations and never any instability of the repeat size was observed. In this study, PrP-rtTA was used as the driver to induce expression. The PrP-rtTA transgene were cloned by inserting rtTA2S-MS (kind gift from H.Bujard) into the MoPrP.Xho vector using the XhoI restriction sites. Transgenic mice were generated by injecting linearized constructs into oocytes of C57BL/6JRj (from Janvier labs)mice. We had six founders and used the one with highest expression level and broadest expression pattern. PrP-rtTA mice were cross bred with TRE-nCGG-eGFP mice to obtain bigenic mice. Genotyping of the mice was done as described previously [14]. Dox treatment of bigenic mice started directly after weaning at an age of 3-4 weeks. Dox (Sigma) was added to the drinking water in a concentration of 4 mg/ml supplemented with 5% sucrose. Drinking water was kept from the light and refreshed every 2-3 days. Mice were treated with dox for 8, 12, 16, 22, or 28 weeks. If a wash-out period was added after dox induction, mice received standard drinking water during the 12 weeks after their dox-treatment. All experiments were conducted with the permission of the local animal welfare committee (DEC).

RNA isolation and quantitative RT-PCR

RNA isolation was done as described previously [14]. Briefly, brains were homogenized in HEPES buffer pH 7.6 containing 0.45% Triton-X100, 0.05% Tween-20 and protease inhibitors. RNA was isolated using RNA Bee according to manufacturer's instructions.

Quantitative RT-PCR was performed on cDNA synthesized with iScript (Biorad) according to the manufacturer's instructions, using KAPA SYBR Green (KAPA Biosystems) on a Biorad CFX machine.

Immunohistochemistry and immunofluorescence

Tissues were fixed overnight in 4% paraformaldehyde and embedded in paraffin according to standard protocols. Sections (6µm) were deparaffinized followed by antigen retrieval using microwave treatment in 0.01M sodium citrate. Endogenous peroxidase activity was blocked and immunostaining was performed overnight at 4°C using mouse anti-GFP (Roche 1814460; 1:1000), rabbit anti-ubiquitin (Dako Z0458; 1:250), or mouse-anti FMRpolyG (8FM[9]; 1:10) antibodies. Antigen-antibody complexes were visualized by incubation with DAB substrate (Dako) after incubation with Brightvision poly-HRP-linker (Immunologic). Slides were counterstained with haematoxylin and mounted with Entellan.

Inclusions were quantified by counting 500 nuclei of the granular cell layer of lobule X of the cerebellum and by counting the number of ubiquitin positive inclusions at a 100x magnification. The size of the inclusions was determined using an Olympus BX40 microscope at a 100x magnification and cellSens Dimension software. Researchers were blinded for genotype and treatment. If lobule X was not present in paraffin sections, mice were excluded resulting in the use of 5-7 mice for each group. This number was were used based on previous research[12, 19], both male and female, littermates were randomly distributed over the different groups.

For (double) immunofluorescence, slides were blocked for autofluorescence with Sudan Black in 70% ethanol. Primary antibodies include rabbit-anti ubiquitin (DAKO Z0458; 1:50), mouse-anti ubiquitin (Cytoskeleton AUB01-S; 1:200), mouse-anti FMRpolyG (1:10) [9], rabbit-anti Hsp40 (Stressgen SPA-400; 1:100), rabbit-anti Rad23B (1:100) [15], or rabbit-anti 20S subunit of the proteasome (1:100) [12]. Secondary antibodies include anti-rabbit Fab Alexa 488 (Life technologies A11070; 1:100) and anti-mouse Cy3 (Jackson Immuno research 715-165-150; 1:100). Nuclei were visualized with Hoechst. Analysis was done with a Leica confocal microscope and LAS AF software.

Compensatory eye movements

Male mice, aged 7 or 19 weeks, were surgically prepared for chronic, head-restrained recordings of compensatory eye movements as described previously [20, 21]. Based on this previous research 9-13 mice per group were used, littermates were randomly divided over the different groups. In short, under isoflurane anesthesia (initiation at 4%, maintenance at ~1.5%,with O2) a construct was attached to the skul in parallel to the intracranial midline using Optibond primer and adhesive (Kerr) and Charisma (Haeraeus Kulzer). The construct consisted of a brass holder with magnet (Neodymium,

4x4x2 mm, MTG Europe) inside. After a recovery period (≤ 3 days) mice were head-fixed to a metal bar using the magnet embedded in the pedestal, a complementary magnet in the bar and a securing screw. The body of the mouse was placed in a custom-made cylindrical restrainer and the head centered in the middle of a turntable. A cylindrical screen (diameter 63 cm) with a random-dotted pattern (each element 2°) surrounded the turntable (diameter 60 cm) on which the mouse was placed. The optokinetic reflex (OKR) and vestibulo-ocular reflex in the dark (VOR) and in the light (VVOR) were elicited by sinusoidal rotation of either the drum (OKR) or the table (VOR and VVOR), respectively. Eye movement performance was tested by rotating the drum or table at 0.1-1.0 Hz with 5° amplitude (fixed), or the drum at 0.05-1.6 Hz at 8°/s peak velocity (fixed). Each frequency – amplitude combination was tested twice with 8-20 repeated cycles and results were averaged. To illuminate the eye during the recordings we used two table-fixed infrared emitters (maximum output 600mW, dispersion angle 7°, peak wavelength 880 nm), and a third emitter mounted to the camera aligned horizontally with the camera's optical axis. This third emitter produced the tracked corneal reflection (CR). The pupil position, after subtraction of the corneal reflecting position, was recorded using eye-tracking software (ETL-200, ISCAN systems, Burlington, NA, USA). Calibrations were performed as described previously [22]. Gain and phase values of the eye movements were calculated using a custom-made Matlab routine (Matlab, MathWorks Inc).

Statistics

Statistical significance of the Q-RT-PCR results was analyzed using a student's T test. The quantification and size determination of the inclusions, results were statistically analyzed with a univariate analysis of variance and a subsequent Tukey posthoc. For the analysis of the compensatory eye-movements gain and phase results plotted against frequency or time were statistically analyzed using repeated-measures ANOVA followed by Tukey's posthoc test.

REFERENCES

1. Hagerman, R.J., et al., *Intention tremor, parkinsonism, and generalized brain atrophy in male carriers of fragile X.* Neurology, 2001. **57**(1): p. 127-30.
2. Hunter, J., et al., *Epidemiology of fragile X syndrome: A systematic review and meta-analysis*. American Journal of Medical Genetics Part A, 2014. **164**(7): p. 1648-1658.
3. Rodriguez-Revenga, L., et al., *Penetrance of FMR1 premutation associated pathologies in fragile X syndrome families*. Eur J Hum Genet, 2009. **17**(10): p. 1359-62.
4. Greco, C.M., et al., *Neuropathology of fragile X-associated tremor/ataxia syndrome (FXTAS)*. Brain, 2006. **129**(Pt1): p. 243-255.
5. Tassone, F., et al., *Elevated levels of FMR1 mRNA in carrier males: A new mechanism of involvement in the Fragile-X syndrome*. Am J Hum Genet, 2000. **66**(1): p. 6-15.
6. Hagerman, P., *Fragile X-associated tremor/ataxia syndrome (FXTAS): pathology and mechanisms*. Acta Neuropathol, 2013. **126**(1): p. 1-19.
7. Zu, T., et al., *Non-ATG-initiated translation directed by microsatellite expansions*. Proc Natl Acad Sci U S A, 2011. **108**(1): p. 260-5.
8. Todd, P.K., et al., *CGG Repeat-Associated Translation Mediates Neurodegeneration in Fragile X Tremor Ataxia Syndrome*. Neuron, 2013. **78**(3): p. 440-455.
9. Buijsen, R.A., et al., *FMRpolyG-positive inclusions in CNS and non-CNS organs of a fragile X premutation carrier with fragile X-associated tremor/ataxia syndrome*. Acta Neuropathol Commun, 2014. **2**(1): p. 162.
10. Bontekoe, C.J., et al., *Instability of a (CGG)(98) repeat in the Fmr1 promoter*. Hum Mol Genet, 2001. **10**(16): p. 1693-9.
11. Entezam, A., et al., *Regional FMRP deficits and large repeat expansions into the full mutation range in a new Fragile X premutation mouse model.* Gene, 2007. **395**: p. 125-134.
12. Willemsen, R., et al., *The FMR1 CGG repeat mouse displays ubiquitin-positive intranuclear neuronal inclusions; implications for the cerebellar tremor/ataxia syndrome*. Hum Mol Genet, 2003. **12**(9): p. 949-59.
13. Berman, R.F., et al., *Mouse models of the fragile X premutation and fragile X-associated tremor/ataxia syndrome*. J Neurodev Disord, 2014. **6**(1): p. 25.
14. Hukema, R.K., et al., *Induced expression of expanded CGG RNA causes mitochondrial dysfunction in vivo.* Cell Cycle, 2014. **13**(16): p. 2600-2608.
15. Bergink, S., et al., *The DNA repair-ubiquitin-associated HR23 proteins are constituents of neuronal inclusions in specific neurodegenerative disorders without hampering DNA repair.* Neurobiol Dis, 2006. **23**: p. 708-716.
16. Wojciechowska, M., et al., *RAN translation and frameshifting as translational challenges at simple repeats of human neurodegenerative disorders*. Nucleic Acids Research, 2014. **42**(19): p. 11849-11864.
17. Mizielinska, S., et al., *C9orf72 repeat expansions cause neurodegeneration in Drosophila through arginine-rich proteins*. Science, 2014. **345**(6201): p. 1192-4.
18. Hashem, V., et al., *Ectopic expression of CGG containing mRNA is neurotoxic in mammals*. Hum Mol Genet, 2009. **18**: p. 2443-2451.
19. Brouwer, J.R., et al., *CGG-repeat length and neuropathological and molecular correlates in a mouse model for fragile X-associated tremor/ataxia syndrome.* J Neurochem, 2008. **107**: p. 1671-1682.
20. Schonewille, M., et al., *Reevaluating the role of LTD in cerebellar motor learning.* Neuron, 2011. **70**(1): p. 43-50.
21. Galliano, E., et al., *Silencing the majority of cerebellar granule cells uncovers their essential role in motor learning and consolidation.* Cell Rep, 2013. **3**(4): p. 1239-51.
22. Stahl, J.S., A.M. van Alphen, and C.I. De Zeeuw, *A comparison of video and magnetic search coil recordings of mouse eye movements*. J Neurosci Methods, 2000. **99**(1-2): p. 101-10.

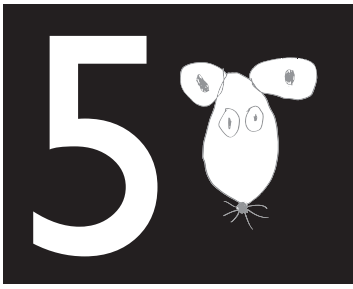

RAN TRANSLATION OF EXPANDED CGG REPEATS IS PATHOGENIC IN FRAGILE X-ASSOCIATED TREMOR/ATAXIA SYNDROME

C. Sellier[1], **R.A.M. Buijsen**[2], F. He[3,4], L. Jung[1], P. Tropel[1], A. Gaucherot[1], H. Jacobs[1,5], H. Meziane[1,5], A. Vincent[1], M. Champy[1,5], T. Sorg[1,5], G. Pavlovic[1,5], M. Wattenhofer-Donze[1,5], M. Birling[1,5], P. Eberling[1], F. Ruffenach[1], A. Page[1], M. Anheim[6], V. Martinez-Cerdeno[7], P.J. Hagerman[7], F. Tassone[8], R. Willemsen[2], R.K. Hukema[2], S. Viville[1,9,10], C. Martinat[11], P.K. Todd[3,4], N. Charlet-Berguerand[1]

[1] IGBMC, Illkirch, France
[2] Department of Clinical Genetics, Erasmus MC, Rotterdam, the Netherlands
[3] Department of Neurology, University of Michigan, Michigan, USA
[4] Veteran Association Health System, Ann Arbor, Michigan, USA
[5] PHENOMIN, Institut Clinique de la Souris (ICS), University of Strasbourg, Illkirch, France
[6] CHU de Strasbourg - Hôpital de Hautepierre, Strasbourg, France
[7] Department of Biochemistry and Molecular Medicine, University of California, Davis, USA
[8] M.I.N.D. Institute, University of California, Davis, USA
[9] Laboratoire de diagnostic génétique, Nouvel Hôpital Civil, Strasbourg, France
[10] IPPTS, Strasbourg, France
[11] INSERM, Evry, France

In revision for **Neuron**, 2016

ABSTRACT

Fragile X-associated Tremor/Ataxia Syndrome (FXTAS) is a neurodegenerative disorder caused by expanded CGG repeats in the 5'UTR of *FMR1*. Two mechanisms are proposed to cause FXTAS: RNA gain-of-function where CGG RNA sequesters specific proteins, and Repeat Associated Non-AUG (RAN) translation of CGG repeats into a polyglycine-containing protein, FMRpolyG. Here, we developed transgenic mice expressing CGG repeats RNA with or without FMRpolyG. Importantly, expression of FMRpolyG is pathogenic, while the sole expression of CGG RNA is not. Toxicity of FMRpolyG is mediated by its carboxy-terminus in primary neuronal cultures and *Drosophila* models. FMRpolyG interacts with the nuclear lamina protein, LAP2ß and disorganizes the nuclear lamina architecture in neurons differentiated from FXTAS iPS cells. Finally, expression of LAP2ß rescues neuronal death induced by FMRpolyG. Overall, novel mouse, fly and human IPS cell models of FXTAS demonstrate that RAN translation of FMRpolyG disrupts the neuronal nuclear lamina architecture and drives pathogenesis in FXTAS.

INTRODUCTION

Fragile X-associated Tremor/Ataxia Syndrome (FXTAS) is a neurodegenerative disorder caused by an expansion, called premutation, of 55 to 200 CGG repeats in the 5'untranslated region of the *Fragile X Mental Retardation 1* (*FMR1*) gene located on the X chromosome [1]. The prevalence carrier of the CGG premutation is approximately 1 of ~200 females and ~450 males, but due to incomplete penetrance, it is estimated that 1 in 3,000 men older than 50 years will develop FXTAS [2-4]. The clinical features of FXTAS include progressive intention tremor and gait ataxia, frequently accompanied by progressive cognitive decline, parkinsonism, peripheral neuropathy and autonomic dysfunctions [5]. Principal neuropathologies of FXTAS include mild brain atrophy and white matter lesions with the presence of ubiquitin-positive nuclear neuronal and astrocytic inclusions [6, 7]. In contrast to Fragile X syndrome, where expanded full mutation alleles (>200 CGG repeats) result in hypermethylation and silencing of the *FMR1* gene, FXTAS carriers of premutation expanded alleles (55–200 CGG repeats) present increased levels of *FMR1* mRNA and near normal expression of the protein encoded by *FMR1*, FMRP [8-10].

Because FXTAS is not observed in Fragile X patients with completely hypermethylated and consequentely fully silenced *FMR1* alleles, a pathogenic mechanism based on expression of mutant *FMR1* mRNAs containing expanded CGG repeats have been proposed [11]. In support of this hypothesis, multiple studies have demonstrated adverse consequences of expressing RNA containing expanded CGG repeats in cell, fly and mouse models [12-18]. However, how *FMR1* mRNA containing expanded CGG repeats is pathogenic is unclear. A first proposed model is that FXTAS results from a toxic RNA gain-of-function mechanism, in which mutant RNA containing expanded CGG repeats would be pathogenic by sequestrating specific RNA binding proteins, ultimately resulting in neuronal cell dysfunctions [19-23]. A second and more recent proposed mechanism is that FXTAS is caused by Repeat-Associated Non-AUG (RAN) translation of the expanded CGG repeats into polyalanine and polyglycine containing proteins, named FMRpolyA and FMRpolyG [24]. Laura Ranum and colleagues originally demonstrated that expanded CAG repeats can be translated in all three frames in the absence of any AUG initiation codon) [25]. Subsequently, RAN translation was described and proposed as a causative mechanism in various inherited microsatellite neurodegenerative disorders (reviewed in [26], including FXTAS [24]. However, the mechanism and pathological consequences of translating expanded CGG repeats are not fully understood. Specifically, which pathological mechanism (RNA gain-of-function or RAN translation) drives FXTAS pathogenesis is a crucial question.

Here we find that RAN translation of expanded CGG repeats occurs predominantly in the glycine frame through initiation at a non-canonical ACG codon located upstream of the expanded CGG repeats. Translation occurs mostly with CGG expansion over 70

CGG repeats, resulting in accumulation of FMRpolyG. To define which mechanism drives pathogenicity in FXTAS we developed two novel mouse models, one that expresses both CGG RNA and FMRpolyG and a second one expressing CGG RNA in isolation. Importantly, transgenic mice expressing both CGG RNA repeats and the polyglycine protein (FMRpolyG mouse), but not mice expressing only the mutant RNA containing expanded CGG repeats (CGG RNA mouse) exhibit inclusion formation, motor phenotypes, and reduced lifespan. Next, we determined that the C-terminal region of the protein contributes to cell death in mammalian neuronal cultures and decreased viability in *Drosophila*, while the polyglycine stretch promotes protein aggregation. The C-terminus of FMRpolyG protein interacts with LAP2ß, a protein essential to anchoring lamin proteins to the inner nuclear membrane. Expression of FMRpolyG alters LAP2ß localization, resulting in disorganization of the nuclear lamina architecture, a finding that is also observed in iPS-cell derived neurons from FXTAS patients. Importantly, over-expression of LAP2ß rescues neuronal cell death induced by expression of FMRpolyG. Overall, these results suggest that expression of FMRpolyG, which disrupts nuclear lamina, is a key pathogenic event in FXTAS.

RESULTS

Translation of expanded CGG repeats initiates at an upstream near-cognate codon

To confirm a previous observation of translation of expanded CGG repeats in absence of a canonical AUG start codon in *Drosophila* [24], we cloned hundred CGG repeats embedded within the natural human 5'UTR of *FMR1* fused to GFP in absence of any ATG and in all three possible frames. These frames were named according to the polypeptide potentially encoded by the expanded CGG repeats, namely glycine, alanine and arginine. Cell transfection and immunoblotting against GFP confirm previous data [24], and demonstrates that the 5'UTR of *FMR1* with expanded CGG repeats allows translation of a GFP protein with a ~12 kDa N-terminal extension corresponding to the expanded CGG repeats translated into the glycine frame. In contrast, we observed little translation in the alanine or arginine frames (**Figure 1A**). Interestingly, we also observed no translation when the 5'UTR of *FMR1* was deleted and the expanded CGG repeats were directly fused to the GFP (**Figure 1A**). Identical results were observed by imaging GFP fluorescence (**Supplemental figure 1A**). As a further control, treatment with Lysostaphin, a polyglycine endopeptidase, confirmed that expanded CGG repeats are translated into a polyglycine-containing protein with no detectable frame shifting (**Supplemental figure 1B**).

Next, we immunoprecipitated this polyglycine-containing protein and determined its sequence by proteomic analysis. LC-MS/MS spectra revealed initiation to an ACG near-

cognate codon located 32 nucleotides upstream of the CGG expansion (**Figure 1B**). Of interest, proteomic analysis also revealed that the initial amino acid of FMRpolyG is a methionine suggesting that ACG is decoded by an initiator Met-tRNA despite imperfect match. Presence of an initiation codon located within the 5'UTR of *FMR1* and upstream of the CGG repeats is consistent with absence of expression of FMRpolyG upon deletion of the 5'UTR of *FMR1* (**Figure 1A**). Also, this ACG near-cognate codon is embedded in a potential Kozac consensus sequence with a purine and a guanine in -3 and +4 positions, and is conserved among multiple species (**Supplemental figure 1C**). To confirm that translation of endogenous FMRpolyG initiates upstream of the expanded CGG repeats in individuals with FXTAS, we developed monoclonal mouse antibodies against the ten amino acids encoded by the sequence upstream of the repeats and that constitute the putative N-terminal part of FMRpolyG (**Supplemental figure1D**). Immunofluorescence assays revealed presence of FMRpolyG, which was detected as single nuclear inclusions that co-localize with ubiquitin in brain sections of FXTAS patients (**Figure 1C** and **Supplemental figure 1E**). As control, immunofluorescence labeling was negative in brain sections of age-matched control individuals (**Supplemental figure 1E**). We confirmed these results by immunoblotting and found that according to the size of the CGG expansion, the FMRpolyG protein was detected as a 10 to 14 kDa protein in the insoluble fraction of brain lysate of FXTAS individuals (**Figure 1D**). As a control, FMRpolyG protein was absent from the insoluble fraction of brain samples of age-matched control individuals (**Figure 1D**). The poor quality of the immunoblotting is probably due to the aggregation of this glycine-rich protein. We also developed monoclonal mouse antibodies against the C-terminal part of the FMRpolyG protein (**Supplemental figure 1D**), and confirmed expression of FMRpolyG in brain sections of FXTAS patients but not in age-matched control individuals (**Supplemental figure 1F**). These results are consistent with previous immunohistochemistry analyses [24, 27].

To confirm a specific role for the sequence located upstream to the CGG repeats in FMRpolyG translation, we performed various deletions of the 5'UTR of *FMR1* and tested expression of FMRpolyG-GFP by immunoblotting. Two deletions reduced translation of the 5'UTR of *FMR1* (**Figure 1E**). As these deletions include the ACG near-cognate codon, we suspected presence of an upstream ORF (uORF) in the 5'UTR of *FMR1*. Upstream ORFs are short open reading frames initiating at AUG or near cognate codons (GUG, CUG, UUG, ACG, etc.) in poor Kozac consensus sequence contexts. Translation of uORFs can regulate, generally negatively, the translation of downstream ORFs (review in [28]). To test this hypothesis, we cloned various lengths of expanded CGG repeats within the human 5'UTR of *FMR1* fused in the glycine frame with GFP and confirmed that translation occurred with expanded CGG repeats as well as with short stretches of CGG repeats (20 to 30) found in control individuals, or even without any CGG repeats (**Figure 1F**). In

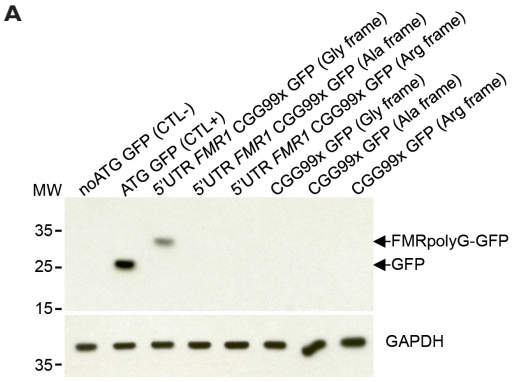

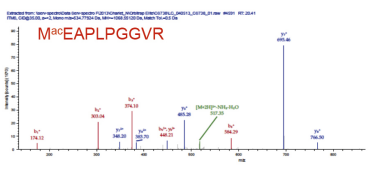

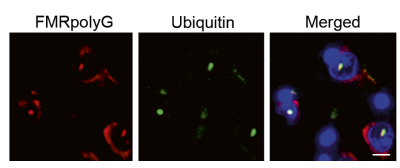

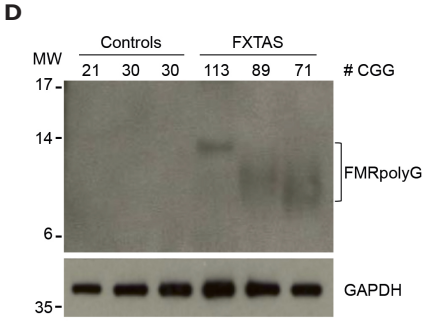

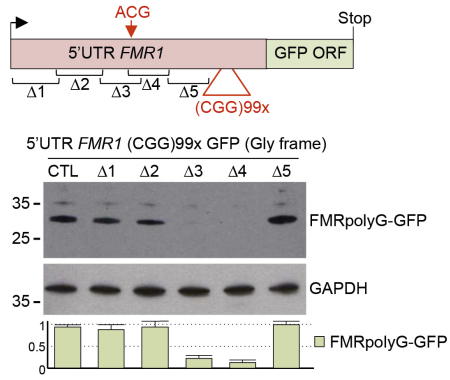

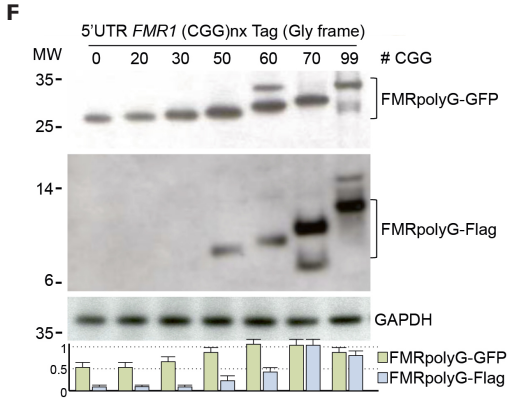

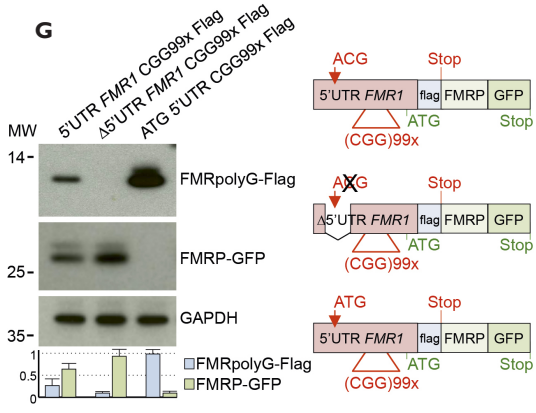

H

```
5'-UTR hsa FMR1
TCCGGTGGAGGGCCGCCTCTGAGCGGGCGGCGGGCCGACGGCGAGCGCGGGCGGCGGCGGTGACGGAGGCGCCGCTGCCAGGGGGCGTGCGGCAGCGCGGCGG
                                                  M  E  A  P  L  P  G  G  V  R  Q  R  G  G
CGGCGGCGGCGGCGGCGGCGGCGGAGGCGGCGGCGGCGGCGGCGGCGGCGGCTGGGCCTCGAGCGCCCGCAGCCCACCTCTCGGGGGCGGGCTCCCGGCG
  G  G  G  G  G  G  G  G  G  G  G  G  G  G  G  G  G  G  W  A  S  S  A  R  S  P  P  L  G  G  G  L  P  A
CTAGCAGGGCTGAAGAGAAGATGGAGGAGCTGGTGGTGGAAGTGCGGGGCTCCAATGGCGCTTTCTACAAGGCATTTGTAAAGGATGTTCATGAAGATTC...
 L  A  G  L  K  R  R  W  R  S  W  W  W  K  C  G  A  P  M  A  L  S  T  R  H  L  *                FMRpolyG
                M  E  E  L  V  V  E  V  R  G  S  N  G  A  F  Y  K  A  F  V  K  D  V  H...  FMRP
```

contrast, fusion in the glycine frame with a smaller flag tag (8 amino acids, ~1 kDa), resulted in detectable expression of flag-tagged FMRpolyG only when expanded repeats where above 50 CGG repeats (**Figure 1F**). This is characteristic of short upstream ORFs that are generally translated into small and most often undetectable peptides (<5 kDa), but which are detected when fused with large tags, resulting in stable and detectable proteins [29]. Of technical interest, due to instability of the expanded CGG repeats during the cloning process some plasmids present minor products with expanded or contracted number of repeats that appear as higher or lower bands of minor intensity in **Figure 1F**.

To test the presence of a putative upstream ORF in *FMR1*, we then fused its 5'UTR with a flag tag in the glycine frame, but also fused a GFP tag in the native frame of the downstream FMRP ORF (**Figure 1G**). This construct would potentially expresses either the FMRpolyG flag-tagged uORF or the downstream GFP-tagged FMRP ORF. FMRpolyG and FMRP ORFs are in different frames with the last 20 amino acids of FMRpolyG naturally overlapping the N-terminal part of FMRP. Thus, translation of the FMRpolyG uORF may potentially impair ribosomal re-initiation to the downstream FMRP ORF. Consistent

← **Figure 1.** Expanded CGG repeats are translated into polyglycine through initiation at a non-canonical ACG codon

(A) Western blotting analysis with anti GFP antibody of HeLa cells transfected with expanded CGG repeats embedded or not in the 5'UTR of *FMR1* and fused in all three possible frames with the GFP. (**B**) LC-MS/MS spectra of the N-terminal part of immunoprecipitated protein translated from expanded CGG embedded in the 5'UTR of *FMR1*. (**C**) Immunofluorescence using antibodies against the N-terminal part of FMRpolyG (red, 8FM antibody) and ubiquitin (green) on brain section (hippocampal area) of a FXTAS patient. Scale bars, 10 μm. Nuclei were counterstained with DAPI. (**D**) Western blotting analysis with anti FMRpolyG N-terminus antibody (8FM) of insoluble fraction of brain lysate of FXTAS and age-matched individuals. Number of expanded CGG is indicated as # CGG. (**E**) Upper panel, schemes of the serial deletion constructs of the 5'UTR of *FMR1*. Middle panel, western blotting analysis with anti GFP antibody of HeLa cells transfected with mutants of the 5'UTR of *FMR1* with expanded CGG repeats fused to the GFP in the glycine frame. Lower panel, quantification of FMRpolyG-GFP expression reported to GAPDH. (**F**) Upper panel, western blotting analyzes with either anti GFP or anti flag antibody of HeLa cells transfected with various length of expanded CGG repeats embedded in the 5'UTR of *FMR1* and fused in the glycine frame with either GFP or flag tag. Lower panel, quantification of FMRpolyG-GFP and FMRpolyG-Flag levels reported to control GAPDH. (**G**) Left upper panel, western blotting analyzes with anti GFP and anti flag antibodies of HeLa cells transfected with mutants of the 5'UTR of *FMR1* containing expanded CGG repeats fused to the flag tag in the glycine frame, while the downstream FMRP ORF is fused to the GFP. Left lower panel, quantification of FMRpolyG-flag and FMRP-GFP levels reported to GAPDH. Right panel, schemes of the 5'UTR of FMR1 constructs with ACG mutations. FMRpolyG uORF is flag-tagged, while FMRP ORF is GFP-tagged. (**H**) Nucleotide sequence of the human 5'UTR of *FMR1* with 20 CGG repeats. Amino acid sequence of *FMR1* uORF translated into FMRpolyG is indicated in red with a red arrow highlighting the ACG translation start. Amino acid sequence of the beginning of the downstream FMRP ORF is indicated in green.

with this hypothesis, deletion of the 5'UTR sequence containing the ACG near-cognate initiation codon abolished expression of the flag-tagged FMRpolyG uORF, but enhanced translation of the downstream GFP-tagged FMRP ORF in mammalian cells (**Figure 1G**). In contrast, mutation of the ACG near-cognate codon into a cognate AUG initiation codon enhanced translation of the flag-tagged FMRpolyG uORF, but abolished expression of the downstream GFP-tagged FMRP ORF (**Figure 1G**). Overall, these results suggest that the 5'UTR of human *FMR1* may contain an upstream ORF initiating to a near-cognate ACG codon that overlaps with the downstream FMRP ORF and inhibits its translation. This uORF is predicted to encode for a small 6 to 7 kDa polypeptide in control individuals with 20 to 30 CGG repeats, while in FXTAS individuals, expansion of CGG repeats extends this upstream ORF into a detectable small protein ranging from ~10 kDa with 70 CGG repeats to ~15 kDa with 150 CGG repeats (sequence presented in **Figure 1H**).

Translation of expanded CGG repeats into FMRpolyG is pathogenic in mice

The presence of both CGG RNA aggregates, which can titrate out RNA binding proteins, and FMRpolyG–positive inclusions in individuals with FXTAS questions which pathogenic mechanism is required for neuronal degeneration in this disease. To differentiate between these two hypotheses, we developed two transgenic mouse models. The first one contains the full human 5'UTR of *FMR1* with expanded 99 CGG repeats that shall express both CGG RNA and FMRpolyG protein, while the second mouse model also expresses 99 CGG repeats but the non-canonical ACG initiation codon and surrounding 5'UTR sequence is deleted, such that it only expresses the CGG RNA (**Figure 2A**). Both constructs are driven by the strong chimeric ubiquitous CAG promoter, and inserted by homologous recombination within the neutral *Rosa26* mouse locus to avoid any bias due to random insertion of the transgenes. We controlled by southern blot and PCR the correct insertion of the transgenes into the *Rosa26* locus, the absence of concatamerization at the locus and the presence of 99 CGG repeats, which were stably transmitted with no obvious contraction or expansion, at least in the few generations (~8) of this study. To control expression of the transgenes, three upstream SV40-polyadeneylation sites bordered by loxP sites limit transcription of the expanded CGG repeats. Hence, expression and potential pathogenicity of the expanded CGG repeats is permitted only in offspring of the transgenic CGG mice crossed with mice expressing Cre recombinase.

Deletion of the loxP cassette using a ubiquitously and embryonically expressed Cre recombinase [30] led to high expression of RNA with expanded CGG repeats throughout the brain, heart and liver, with lower expression in skeletal muscle, kidneys and other organs (**Figure 2B**). Transgene RNA expression was similar between mice with the full or mutant *FMR1* 5'UTR (**Figure 2B**). However, we found only rare CGG RNA foci in brain

sections of full or mutant *FMR1* 5'UTR transgenic mice at any age analyzed (**Supplemental figures 2A** and **2B**). This is consistent with the rare occurrence of CGG RNA aggregates in other transgenic mice model expressing expanded CGG repeats [23].

Concerning the FMRpolyG protein, imunohistochemistry assays using an antibody directed against the N-terminus of FMRpolyG demonstrated expression and accumulation of nuclear aggregates of FMRpolyG in brain sections from the full 5'UTR *FMR1* transgenic mice, but not in the mutant 5'UTR mice (**Figure 2C**). Similar results were obtained with an antibody targeting the C-terminus of FMRpolyG (**Supplemental figure 2C**). As observed in brain samples of individuals with FXTAS, aggregates of FMRpolyG co-localized with ubiquitinated inclusions (**Figure 2D**). Nuclear aggregates of FMRpolyG accumulated over time, with the largest burden of inclusions occurring within the hypothalamus, mirroring transgene mRNA expression (**Supplemental figures 2C** and **2D**). These results suggest that accumulation of FMRpolyG into nuclear inclusions precedes formation of CGG RNA foci in mice over the time frame of our study (**Supplemental figure 2B**). These results also confirm that translation of FMRpolyG requires the *FMR1* 5'UTR sequence containing the ACG-near cognate codon located upstream of the CGG repeat.

To determine the consequences of FMRpolyG production *in vivo* in mice, we conducted a series of behavioral and locomotor assays on both mouse lines. Mice with the full 5'UTR of *FMR1* develop obesity at 6 months of age. Therefore, behavioral tests were performed at 3 months of age when weight is identical between full and mutant *FMR1* 5'UTR transgenic mice. Importantly, we observed that only mice with the full 5'UTR sequence of *FMR1* and expressing the FMRpolyG protein present locomotor deficiency (**Supplemental video 1 and 2**), with increased falling from rotarod (**Figure 2E**), decreased ability of traction from the hind limbs (**Figure 2F**), decreased grip strength (**Figure 2G**) and decreased number of rears in open field observation (**Figure 2H**). At six months of age, mice with the full 5'UTR of *FMR1* loss mobility and develop obesity, while mice with the mutant 5'UTR that express only the CGG RNA remain normal (**Figure 2I**). At 9 months of age, we found a mild but significant loss of Purkinje cells in mice with the full 5'UTR of *FMR1* compared to control or mutant *FMR1* 5'UTR mice (**Figure 2J**). Finally, the survival curve indicates that expression of FMRpolyG is deleterious since none of the mice with the full 5'UTR of *FMR1* survive past 10 months, while mutant *FMR1* 5'UTR mice exhibit normal longevity and are indistinguishable from control mice (**Figure 2K**).

These phenotypes are likely of neuronal origin as offspring of full 5'UTR transgenic mice crossed with Nestin-cre mice, which express the Cre recombinase in precursors of neurons and glia cells around E10.5 [31] (**Supplemental figure 2E**), show neuronal restricted expression of the expanded CGG RNA (**Supplemental figure 2F**), nuclear inclusions of FMRpolyG (**Supplemental figure 2G**), but also develop motor alterations (**Supplemental figure 2H**), obesity (**Supplemental figure 2I**) and reduced longevity

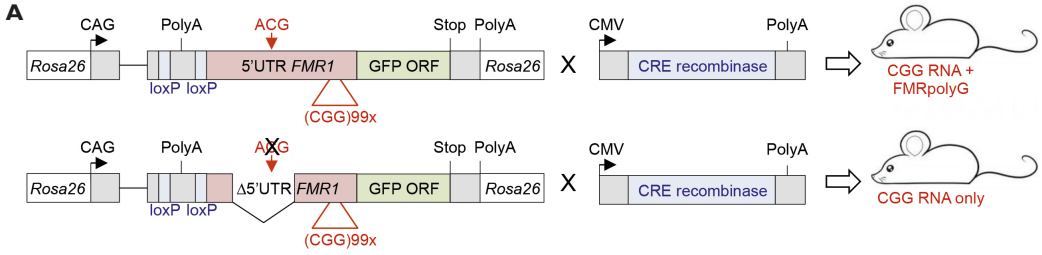
A
CAG
PolyA
ACG
Stop
PolyA
Rosa26
5'UTR FMR1
GFP ORF
Rosa26
loxP loxP
(CGG)99x
X
CMV
PolyA
CRE recombinase
CGG RNA + FMRpolyG
CAG
PolyA
ACG
Stop
PolyA
Rosa26
Δ5'UTR FMR1
GFP ORF
Rosa26
loxP loxP
(CGG)99x
X
CMV
PolyA
CRE recombinase
CGG RNA only

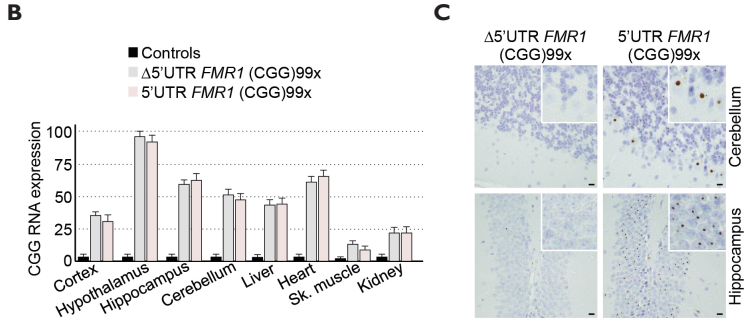
B
Controls
Δ5'UTR FMR1 (CGG)99x
5'UTR FMR1 (CGG)99x
CGG RNA expression
100
75
50
25
0
Cortex
Hypothalamus
Hippocampus
Cerebellum
Liver
Heart
Sk. muscle
Kidney
C
Δ5'UTR FMR1 (CGG)99x
5'UTR FMR1 (CGG)99x
Cerebellum
Hippocampus
D
5'UTR FMR1 (CGG)99x
Ubiquitin
FMRpolyG
Merged
Magnification

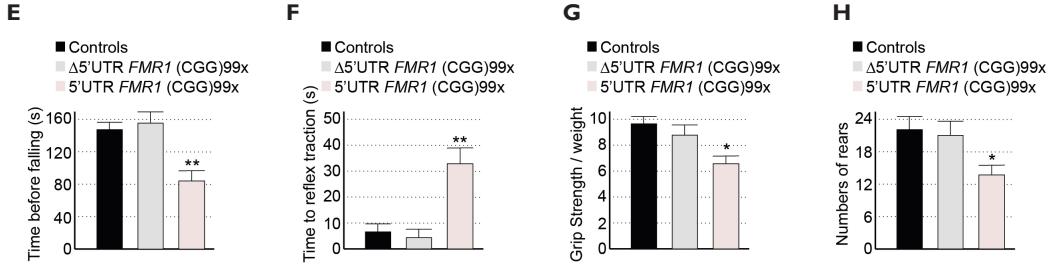
E
Controls
Δ5'UTR FMR1 (CGG)99x
5'UTR FMR1 (CGG)99x
Time before falling (s)
160
120
80
40
0
**
F
Controls
Δ5'UTR FMR1 (CGG)99x
5'UTR FMR1 (CGG)99x
Time to reflex traction (s)
50
40
30
20
10
0
**
G
Controls
Δ5'UTR FMR1 (CGG)99x
5'UTR FMR1 (CGG)99x
Grip Strength / weight
10
8
6
4
2
0
*
H
Controls
Δ5'UTR FMR1 (CGG)99x
5'UTR FMR1 (CGG)99x
Numbers of rears
24
18
12
6
0
*

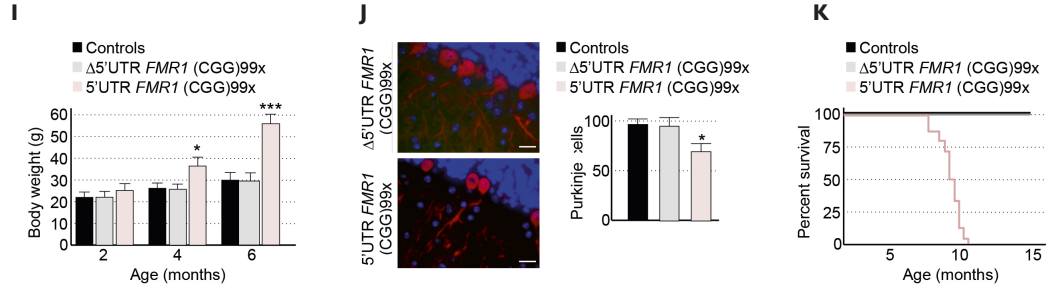
I
Controls
Δ5'UTR FMR1 (CGG)99x
5'UTR FMR1 (CGG)99x
Body weight (g)
60
50
40
30
20
10
0
*
***
2
4
6
Age (months)
J
Δ5'UTR FMR1 (CGG)99x
5'UTR FMR1 (CGG)99x
Controls
Δ5'UTR FMR1 (CGG)99x
5'UTR FMR1 (CGG)99x
Purkinje cells
100
50
0
*
K
Controls
Δ5'UTR FMR1 (CGG)99x
5'UTR FMR1 (CGG)99x
Percent survival
100
75
50
25
0
5
10
15
Age (months)

(**Supplemental figure 2J**). Overall, these results indicate that translation of expanded CGG repeats into FMRpolyG is pathogenic, while expression of mutant RNA with expanded CGG repeats in isolation is insufficient to elicit phenotypes in mice over the time course (15 months) of this study.

The C-terminal region of FMRpolyG drives toxicity

Since expression of the FMRpolyG protein correlates with pathogenicity in mouse, we next investigated the timing of FMRpolyG aggregates and CGG RNA foci formation in primary cultures of embryonic cortical mouse neurons transfected with 99 CGG repeats embedded within the natural human 5'UTR of *FMR1* fused to GFP in the glycine frame. Confocal imaging of the GFP at different time point indicated that FMRpolyG first accumulates in the cytoplasm where it quickly forms aggregates that migrated within the cell nucleus (**Figure 3A**). RNA FISH assays indicated formation of nuclear RNA foci containing the expanded CGG repeats RNA 48 hours post-transfection (**Supplemental**

← **Figure 2.** Expression of FMRpolyG is pathogenic to mice

(A) Schemes of the mouse transgene constructs. The human full-length or deleted 5'UTR of *FMR1* are represented as red boxes, GFP ORF as green boxes, loxP sites as blue boxes, while promoters, polyadenylation sequences and start and stop of translation are indicated by arrow or black lines. (**B**) Quantitative RT-PCR analysis of transgenes expression relative to the *Rplp0* mRNA in different brain areas and tissues of 6 months old control (n=3) or bigenic CMV-cre / full-length (n=3) or deleted (n=3) *FMR1* 5'UTR transgenic mice. (**C**) Immunohistochemistry using an antibody directed against FMRpolyG N-terminus (8FM) of cerebellum and hippocampus areas of 6 months old bigenic CMV-cre / full-length or deleted *FMR1* 5'UTR transgenic mice. Scale bars, 10 µm. Sections were counterstained with Nissl staining. (**D**) Immunofluorescence using antibodies against FMRpolyG N-terminus (green, 8FM antibody) and ubiquitin (red) on cerebellum areas of 6 months old bigenic CMV-cre / full-length or deleted *FMR1* 5'UTR transgenic mice. Scale bars, 10 µm. Nuclei were counterstained with DAPI. (**E**) Rotarod test. Time before falling from a rotating rod of 3 months old control (n=8) or bigenic CMV-cre / full-length (n=9) or deleted (n=9) *FMR1* 5'UTR transgenic male mice. (**F**) String test. Time to gain hindlimb traction for forelimb-hanging 3 months old control (n=8) or bigenic CMV-cre / full-length (n=9) or deleted (n=9) *FMR1* 5'UTR transgenic male mice. (**G**) Grip test. Maximal force relative to mouse body weight exerted to releases 3 months old control (n=8) or bigenic CMV-cre / full-length (n=9) or deleted (n=9) *FMR1* 5'UTR transgenic male mice holding a grid with their forepaws. (**H**) Open field. Numbers of rears during 5 minutes observation in open field of 3 months old control (n=8) or bigenic CMV-cre / full-length (n=9) or deleted (n=9) *FMR1* 5'UTR transgenic male mice. (**I**) Body weight of 2, 4 and 6 months old control (n=6) or bigenic CMV-cre / full-length (n=6) or deleted (n=6) *FMR1* 5'UTR transgenic male mice. (**J**) Left panel, immunofluorescence labeling of calbinding (red) of cerebellum sections of 9 months old bigenic CMV-cre / full-length or deleted *FMR1* 5'UTR transgenic mice. Scale bars, 10 µm. Nuclei were counterstained with DAPI. Right panel, quantification of purkinje cells (n=100) in cerebellum sections of 9 months old bigenic CMV-cre / full-length (n=3) or deleted *FMR1* 5'UTR (n=3) transgenic mice. (**K**) Kaplan-Meier survival curve of control male and female mice (n=15) or bigenic CMV-cre / full-length (n=15) or deleted (n=15) *FMR1* 5'UTR male and female transgenic mice. Error bars indicate s.e.m. Student T-test , ** indicates $p<0.01$ and * indicates $p<0.05$.

figure 3A). However, we noted that transfection of expanded CGG repeats embedded in the 5'UTR of *FMR1* resulted in formation of only rare RNA foci compared to previous reports [22, 23]. We hypothesized that these differences may originate from differences in the backbones containing the expanded CGG repeats and, indeed, transfection of a construct expressing expanded CGG repeats in absence of any *FMR1* natural sequence resulted in formation of a higher number of RNA foci (**Supplemental figure 3A**). Furthermore, RT-PCR performed on nuclear and cytoplasmic fractions indicated that most of RNAs containing expanded CGG repeats embedded within the 5'UTR of *FMR1*

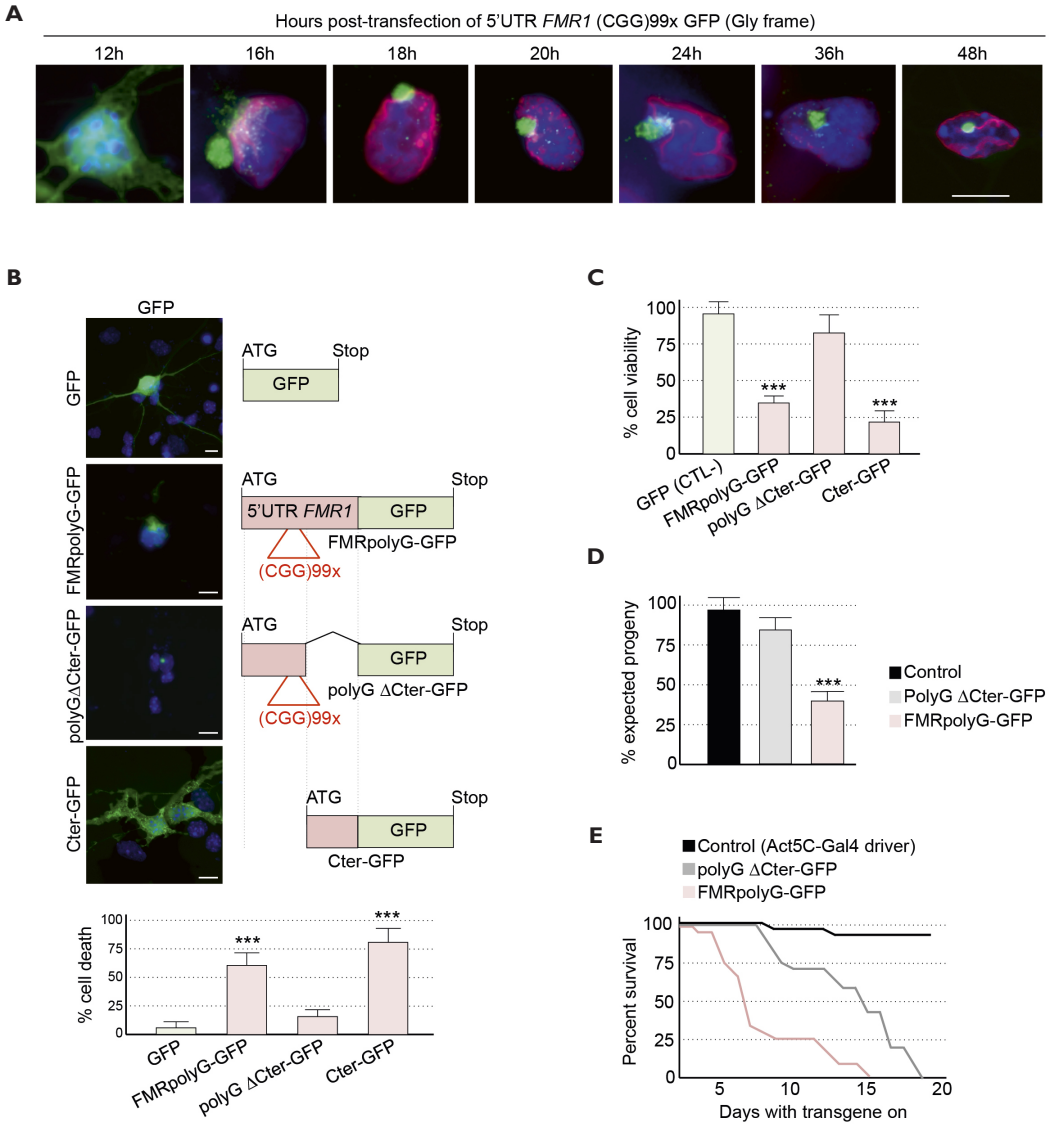

were exported from the nucleus to the cytoplasm (**Supplemental figure 3B**). In contrast, expanded CGG repeats RNA without any *FMR1* sequence is mainly retained within cell nuclei (**Supplemental figure 3B**). These results highlight the bias induced by chimeric constructs artificially enhancing nuclear retention of RNA, but also indicate that, in their natural *FMR1* sequence context, most of the CGG-containing RNAs are exported and available for translation into the FMRpolyG protein. These results are consistent with a previous study demonstrating cytoplasmic localization of endogenous *FMR1* mRNAs with expanded CGG repeats in blood cells of individuals with FXTAS [10].

To investigate the mechanisms by which FMRpolyG protein elicits neuronal cell dysfunction and death, we first isolated soluble and insoluble fractions from neuronal cells transfected with FMRpolyG-GFP. FMRpolyG progressively accumulates in the insoluble fraction, which is consistent with its propensity to form aggregates (**Supplemental figure 3C**). Next, we searched the sequence driving aggregation of FMRpolyG. FMRpolyG is composed of a short N-terminus, a central glycine stretch which length corresponds to the number of expanded CGG repeats and a C-terminus of 42 amino acids with no predicted structure or homology. We cloned mutants of FMRpolyG expressing either its N-terminus with the glycine repeats or its C-terminus in isolation. As a control, expression of the full FMRpolyG protein in primary cultures of E18 mouse cortical neurons leads to nuclear aggregates associated with cell death (**Figure 3B**). Expression of the polyglycine stretch in isolation, separate from FMRpolyG C-terminus, was sufficient to elicit aggregation. However, these aggregates were not associated with an increase in neuronal cell death above control non-transfected or

← **Figure 3.** The C-terminal part of FMRpolyG is toxic

(A) Immunofluorescence using antibodies against FMRpolyG N-terminal part (8FM antibody, green) and nuclear lamina (Lmnb1, red) in primary cultures of E18 mouse cortical neurons transfected for the indicated time period with expanded CGG repeats embedded within the 5'UTR of *FMR1* and fused to the GFP in the glycine frame. Scale bars, 10 µm. Nuclei were counterstained with DAPI. (**B**) Left panel, representative images of primary cultures of E18 mouse cortical neurons transfected with deletion mutants of the 5'UTR of *FMR1* with expanded CGG repeats and fused to the GFP in the glycine frame. Scale bars, 10 µm. Nuclei were counterstained with DAPI. Right panel, schemes of the mutant constructs of the 5'UTR of *FMR1* fused to the GFP in the glycine frame. Lower panel, quantification of neuronal cell death (trypan blue) of GFP-positive (n=100 cells, 3 independent transfections) E18 mouse cortical neurons. (**C**) Cell viability (TO-PRO-3 assay) of N2A mouse neuronal cultures (n=3) transfected with deletion mutants of the 5'UTR of *FMR1* containing expanded CGG repeats and fused to the GFP in the glycine frame. Error bars indicate s.e.m. Student T-test, *** indicates p<0.001. (**D**) Progeny eclosion ratio of *Drosophila* expressing FMRpolyG full-length or deleted of its C-terminus compared to control driver line (*Actin5C-GaL4*/+). Error bars indicate s.e.m. Student T-test, *** indicates p< 0.001. (**E**) Kaplan-Meier survival curve of *Drosophila* expressing FMRpolyG full-length or deleted of its C-terminus compared to control driver line (*Tub5-GAL4*/+).

GFP-expressing neurons. In contrast, expression of GFP fused to the last 42 amino acids constituting the C-terminus of FMRpolyG caused neuronal cell death without forming nuclear aggregates (**Figure 3B)**. We confirmed these results in a second cell model. Transfection of neuronal Neuro2A cells demonstrated that expression of polyglycine in isolation was not toxic, while expression of the C-terminal part of FMRpolyG induced cell death (**Figure 3C**).

To overcome potential bias due to cell transfection, we further investigated the contribution of its C-terminus to FMRpolyG toxicity in a model organism. We developed two *Drosophila* transgenic lines expressing either the full FMRpolyG protein or polyglycine in isolation under a *UAS* promoter. Toxicity was assessed by two separate assays. First, *UAS* FMRpolyG-GFP and *UAS* polyG-GFP flies, both expressed under an ATG initiator codon, were crossed with an *Act5c-Gal4* driver line, which leads to ubiquitous expression of the transgene during development. Total progeny carrying either the transgenes or a balancer chromosome were then quantified over 3 independent crosses. In flies expressing the full FMRpolyG including the C terminus, there was significant reduction in progeny eclosion. However, in flies expressing only polyglycine, progeny eclosion rates were not significantly different from control flies expressing the balancer chromosome alone (**Figure 3D**). As a second measure, we crossed these same transgenic fly lines to a *Tubulin-Gal4* Geneswitch driver, which allowed us to activate expression after flies had matured into adults. Adult transgenic flies reared off of drug exhibited no differences in viability compared to control flies. In contrast, when transgenic flies were moved to food containing RU-486, activating ubiquitous transgene expression, there was a decrease in viability over time for both polyglycine and FMRpolyG expressing flies (**Figure 3E**). Interestingly, flies expressing the full FMRpolyG transgene had a reduced viability compared to *Drosophila* expressing the polyglycine stretch alone (**Figure 3E**). Both transgenes exhibited similar induced CGG repeats RNA expression by RT-qPCR (**Supplemental figure 3D**). Overall, these results confirm that expression of FMRpolyG is pathogenic, with the polyglycine stretch driving aggregation and its C-terminus enhancing toxicity in neurons and in model organisms.

FMRpolyG recruits LAP2 and alters the nuclear lamina

Next, we reasoned that if the C-terminal region of FMRpolyG was contributing to toxicity this might be through interaction with other proteins. To identify FMRpolyG binding proteins, we performed a tandem tag purification of HA-flag-tagged FMRpolyG transfected into Neuro2A cells followed by nano-LC-MS/MS analysis of associated proteins. This approach identified various FMRpolyG-associated proteins (**Supplemental table 1**), among which two of the most prominent were Lap2α and Lap2ß (**Figure 4A**). Lamina associated polypeptide 2 (LAP) alpha and beta are two isoforms of the LAP2 protein that

differ in their C-termini, which originate from alternative splicing of the *TMPO* pre-mRNA. LAP2α is diffusely localized in the nucleus, while LAP2ß carries a transmembrane domain in its C-terminus that anchors it to the inner nuclear membrane with the Lamin B1 and B2 proteins [32, 33]. Consequently, alteration of LAP2ß results in disorganization of the nuclear lamina architecture [34, 35]. Since alteration of the nuclear lamina has been observed in FXTAS [14, 19, 36], we pursued the study of LAP2 further.

Co-immunoprecipitation studies confirmed the association of the LAP2 proteins with HA-Flag-tagged FMRpolyG (**Figure 4B**). The interaction with LAP2ß required the C-terminus of FMRpolyG as the polyglycine stretch alone did not co-immunprecipitate LAP2ß (**Figure 4C**). Conversely, a construct expressing only the C-terminal part of FMRpolyG did interact with LAP2ß (**Figure 4C**). Transfection in primary cultures of cortical neurons from mouse embryo indicated that FMRpolyG recruited endogenous Lap2ß in nuclear aggregates, while constructs containing only the polyglycine stretch of FMRpolyG did not alter Lap2ß localization (**Figure 4D**). This alteration in Lap2ß localization was associated with disorganization of the nuclear lamina as evidenced by Lamin B1 labeling (**Supplemental figure 4A**). As a control, expression of the polyglycine in isolation did not affect nuclear lamina organization (**Supplemental figure 4A**).

Since these results were obtained in transfected cells, we next investigated the nuclear lamina in neuronal cells expressing endogenous levels of FMRpolyG. To accomplish this, we developed human induced pluripotent stem cells (iPS) derived from fibroblasts from two age-matched controls and three different FXTAS patients with expansion of 84, 90 and 99 CGG repeats. Fibroblasts were successfully reprogrammed using retroviruses expressing Oct4, Sox2, Nanog and Lin28 [37]. In addition to karyotype analyses, which were normal for all cell lines, retroviral silencing as well as stemness and pluripotency were confirmed by classic RT-qPCR and teratoma assays (data not shown). Of interest, expanded CGG repeats were stable with no contraction or expansion in iPS clones compared to fibroblasts. Since FXTAS affect various brain regions, including the cortex, iPS from control and FXTAS individuals were differentiated into homogenous populations of telencephalic neurons using a protocol based, first, on the production of neural precursors by treatment with SMAD inhibitors and, next, by differentiation of these precursors by removal of growth factors (FGF2 and EGF) and treatment with survival factors (BDNF and GDNF) for 45 days [38, 39]. Number of CGG repeats was stable during differentiation, and we observed no gross alterations or delay in neuronal differentiation of FXTAS iPS compared to control iPS cells (**Supplemental figure 4B**). As observed previously [40], expression of *FMR1* mRNA was two to three fold increased in neurons derived from FXTAS iPS compared to controls (**Supplemental figure 4C**). This is consistent with the increased levels of *FMR1* mRNA observed in carriers of a CGG premutation [8-10].

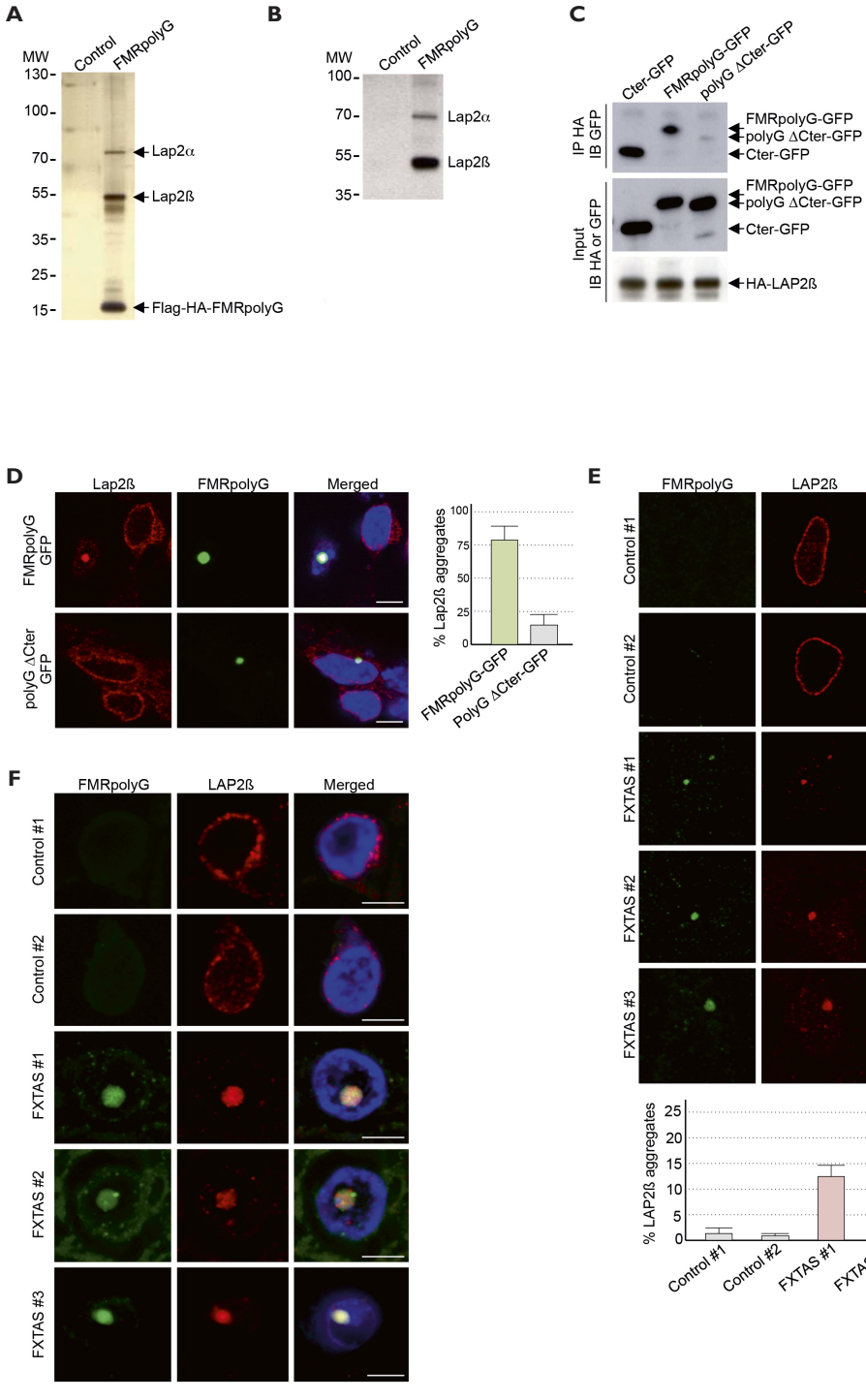
A
MW
Control
FMRpolyG
130
100
70
55
35
25
15
Lap2α
Lap2ß
Flag-HA-FMRpolyG
B
MW
Control
FMRpolyG
100
70
55
35
Lap2α
Lap2ß
C
Cter-GFP
FMRpolyG-GFP
polyG ΔCter-GFP
IP HA
IB GFP
FMRpolyG-GFP
polyG ΔCter-GFP
Cter-GFP
Input
IB HA or GFP
FMRpolyG-GFP
polyG ΔCter-GFP
Cter-GFP
HA-LAP2ß
D
Lap2ß
FMRpolyG
Merged
FMRpolyG GFP
polyG ΔCter GFP
% Lap2ß aggregates
100
75
50
25
0
FMRpolyG-GFP
PolyG ΔCter-GFP
E
FMRpolyG
LAP2ß
Merged
Control #1
Control #2
FXTAS #1
FXTAS #2
FXTAS #3
% LAP2ß aggregates
25
20
15
10
5
0
Control #1
Control #2
FXTAS #1
FXTAS #2
FXTAS #3
F
FMRpolyG
LAP2ß
Merged
Control #1
Control #2
FXTAS #1
FXTAS #2
FXTAS #3

Immunofluorescence using antibodies against either the N- or the C-terminal part of the FMRpolyG protein detected accumulation of nuclear aggregates of FMRpolyG in FXTAS neurons after differentiation, but not in control differentiated neurons (**Figure 4E**). FMRpolyG aggregates accumulated over time post-differentiation, with 5 to 10% of neurons exhibiting small FMRpolyG aggregates at 20 days of differentiation, while 20 to 30% of neurons present FMRpolyG nuclear aggregates after 40 days of differentiation (**Figure 4E**). In contrast, RNA foci of expanded CGG repeats were rare and observed in less than 5% of FXTAS neurons at 40 days of differentiation (**Supplemental figure 4D**), suggesting that like in transgenic mice, formation of FMRpolyG aggregates precedes the accumulation of CGG RNA foci.

Importantly, nuclear aggregates of endogenous FMRpolyG recruited endogenous LAP2ß (**Figure 4E**). Aggregation of FMRpolyG correlated with disruption of the nuclear lamina structure as shown by alteration of the Lamin B1 labeling (**Supplemental figures 4E** and **4F**). In contrast, control iPS derived neurons exhibited normal LAP2ß and Lamin B1 localization (**Figure 4E** and **Supplemental figure 4E**). We next confirmed these results in brain sections of FXTAS patients. Immunofluorescence assays demonstrated that LAP2ß co-localized with FMRpolyG in FXTAS but not in age-matched control individuals (**Figure 4F**). Furthermore and as reported previously with Lamin A [19], the localization of Lamin B1 was altered in brain sections of FXTAS compared to control age-matched individuals (**Supplemental figure 4G**). These results indicate that LAP2ß localization is altered in FXTAS cell models and individuals.

← **Figure 4.** FMRpolyG interacts with LAP2ß and alters nuclear lamina architecture
(A) Silver staining of proteins captured through consecutive anti-Flag and anti-HA affinity purification steps from N2A neuronal cells transfected with Flag-HA-tagged FMRpolyG. (**B**) Western blotting analysis with anti LAP2 proteins of tandem-tag purified proteins from N2A cells expressing Flag-HA-tagged FMRpolyG. (**C**) Western blotting analysis with anti HA or anti GFP antibody of HA-tagged immunoprecipitated proteins from N2A cells transfected with HA-LAP2ß and deletion mutants of the 5'UTR of *FMR1* with expanded CGG repeats fused to the GFP in the glycine frame. (**D**) Left panel, immunofluorescence using antibodies against FMRpolyG N-terminal part (8FM antibody, green) and Lap2 (red) in primary cultures of E18 mouse cortical neurons transfected with expanded CGG repeats embedded within the full-length or C-terminus deleted 5'UTR of *FMR1* fused to the GFP in the glycine frame. Right panel, quantification of nuclear aggregates of Lap2ß in FMRpolyG-positive E18 mouse cortical neurons (n=100 neurons, 3 independent transfections). (**E**) Upper panel, immunofluorescence using antibodies against the N-terminal part of FMRpolyG (green, 8FM antibody) and Lap2 (red) on neuronal cultures differentiated 40 days from iPS cells of FXTAs patients or control individuals. Lower panel, quantification of LAP2ß nuclear aggregates in neurons from IPSC of FXTAS and control individuals (n=100 neurons, 3 independent cultures). (**F**) Immunofluorescence using antibodies against the N-terminal part of FMRpolyG (green, 8FM antibody) and Lap2 (red) on brain sections (hippocampal area) of FXTAS patients or age-matched controls. For all images, scale bars, 10 µm. Nuclei were counterstained with DAPI

Overexpression of LAP2 rescues neuronal cell death caused by FMRpolyG

If binding of FMRpolyG to Lap2ß is a key pathogenic event in FXTAS, then resupplying excess Lap2ß should suppress FMRpolyG-induced toxicity. To address this question, we co-expressed LAP2ß or an empty vector control with FMRpolyG in mouse neuronal cultures. LAP2ß co-expression was sufficient to rescue the cell death induced by FMRpolyG co-expression (**Figure 5A**). Consistent with LAP2ß binding to the C-terminal part of the FMRpolyG protein, expression of LAP2ß also rescued cell death caused by expression of the FMRpolyG C-terminus in isolation (**Figure 5A**). As controls, LAP2ß had no effect on neuronal survival in control GFP-transfected cells or neurons expressing the polyglycine fragment in isolation. These results indicate that the interaction FMRpolyG with LAP2ß is a key pathogenic event in FXTAS. Furthermore, these data also provide a mechanism by which FMRpolyG can elicit toxicity (**Figure 5B**), and an explanation for the previously observed nuclear lamina disorganization in FXTAS [14, 19, 36].

DISCUSSION

Previous pioneering studies have demonstrated that FXTAS is caused by expression of mutant RNAs containing expanded CGG repeats [12-18]. However, whether expanded CGG repeats are pathogenic through an RNA gain-of-function mechanism or through RNA translation into a toxic protein was unclear. Using novel mouse models expressing or not FMRpolyG, our study now demonstrates a direct role for FMRpolyG in CGG repeat associated toxicity. In contrast, expression of expanded CGG repeats as RNA in isolation is not sufficient to induce pathogenicity. This study confirms into a mammalian system previous results obtained in *Drosophila* [24] and establishes that FMRpolyG synthesis is required for formation of ubiquitin-positive inclusions in mouse. Moreover, we found that FMRpolyG disrupts nuclear lamina architecture through binding to the LAP2ß protein. In some aspect this is strikingly reminiscent to Amyotrophic Lateral Sclerosis and FrontoTemporal Dementia (ALS-FTD) in which expanded GGGGCC repeats in the C9ORF72 gene [41, 42] are RAN translated into pathogenic di-peptide containing proteins [43-45] that disrupt nucleocytoplasmic transport proteins [46-49].

This work also extends a prior study indicating that translation of FMRpolyG initiates upstream to the CGG repeats in the 5'UTR of *FMR1* [24] by identifying a non-canonical ACG codon as the predominant site of translation initiation. Moreover, we provide mass-spectroscopy data that the N-terminal amino acid of FMRpolyG is a methionine in mammalian cells. Finally, our data suggest that expanded CGG repeats belong to a potential small ORF translated upstream to the main FMRP ORF. Ribosome profiling and bioinformatics analyses reveal that upstream ORF (uORF) are commons in mammalian mRNAs and can initiate at non-canonical codons [50-53]. Mutations in uORF are known to cause human

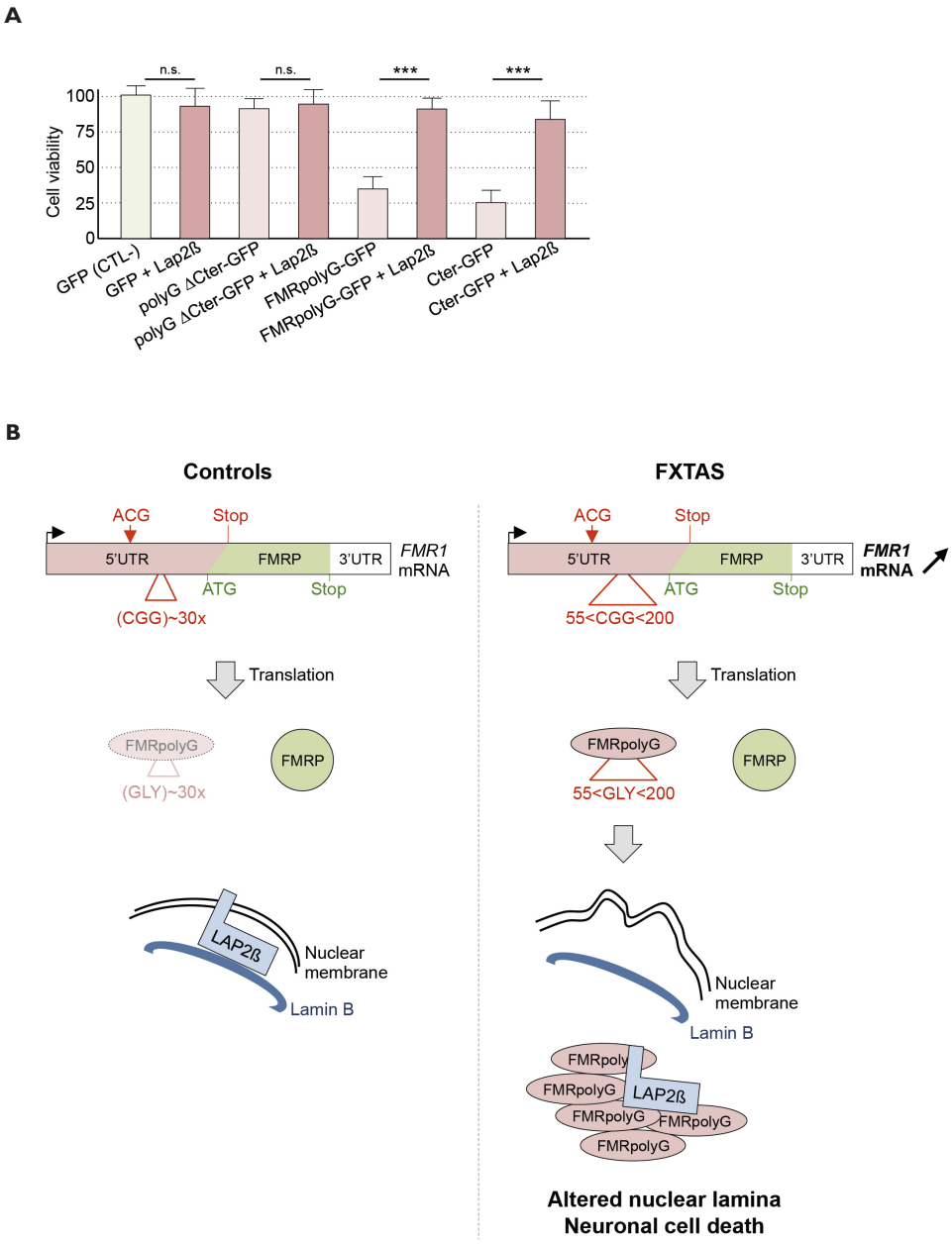

Figure 5. LAP2ß rescues neuronal cell death induced by FMRpolyG

(A) Cell viability (TO-PRO-3 assay) of neuronal N2A cells transfected (n=5) with deletion mutants of FMRpolyG and with or without a plasmid expressing LAP2ß. Error bars indicate s.e.m. Student T-test, *** indicates $p<0.001$. (**B**) Tentative model of pathogenicity in FXTAS. Expanded CGG repeats are translated into a polyglycine containing protein through initiation to a non-canonical ACG codon located upstream to the CGG repeats. In FXTAS, higher expression of *FMR1* mRNA as well as increased translation of the expanded CGG repeats result in accumulation of FMRpolyG in nuclear aggregates that sequester the LAP2ß protein and alter the nuclear lamina architecture.

diseases, but mostly if not exclusively, by altering the expression of their downstream ORF (reviewed in [54]). In contrast, we propose here that FXTAS is characterized by a mutation extending the length of a uORF resulting in expression of a toxic polyglycine-containing protein, FMRpolyG. This model is reminiscent of expansion of tri-nucleotides repeats in ORF resulting in expression of pathogenic polyglutamine or polyalanine-containing proteins.

This model may provide some molecular basis to the threshold of severity and incomplete penetrance observed in FXTAS. Indeed, while the prevalence of carriers of a premutation, which is defined as an expansion between 55 and 200 CGG repeats, ranges from 1:130 and 1:256 for females and 1:250 and 1:813 for males according to ethnic groups and countries (review in [4], it is estimated that only 1 in 3,000 men older than 50 years will develop FXTAS. This less than expected frequency is explained by an incomplete penetrance but also by most of FXTAS cases occurring in the range of ~70 to ~150 CGG repeats, with rare FXTAS cases below 70 CGG repeats where most (80%) of premutation alleles are found [4, 55]. This pathogenic range (70-150) of CGG repeats correlates with percent of nuclear ubiquitin-positive aggregates both in brain of FXTAS patients [7], as well as in brain of mouse model of FXTAS [56]. Importantly, our experiments demonstrate that expression of small-tagged FMRpolyG is hardly detectable below 70 CGG repeats. This is consistent with the difficulties to detect small proteins below 10 kDa, but also with the increase expression of mutant CGG RNA in carriers of premutation above 70 CGG repeats [8-10], as well as with the proposed increase stalling of the ribosome to the CGG hairpin structure, which would promote translation initiation to near-cognate codons located upstream to the CGG repeats [24]. Furthermore, previous work demonstrated that translation is impaired by expansion of CGG above 150 CGG repeats [57, 58]. Thus, we propose that most of FXTAS cases may be restricted to a more limited premutation range (70 – 150) of CGG expansion since expression of the toxic FMRpolyG protein is reduced below ~70 and above ~150 CGG repeats. This model may explain the lesser incidence of FXTAS cases observed, compared to the relatively high frequency of CGG premutation.

One of the main conclusions of this work is that mice expressing FMRpolyG develop a severe phenotype with reduced longevity, while mice expressing only the expanded CGG repeats RNA are indistinguishable from control mice. While informative on the pathogenicity of FMRpolyG, these mouse models present also some limitations. First, we observed only mild neurodegeneration in the full 5'UTR transgenic mice. However, our behavioural and locomotor investigations were limited to 3 months aged mice since animals expressing FMRpolyG widely in the brain develop severe obesity and grew immobile around 6 months of age. Furthermore, no FMRpolyG-expressing mice survived past 10 months of age, impairing any chance to observe potential neurodegeneration at later age. Thus and as reported previously [15], analysis of potential Purkinje cell dropout and ataxia will require specific expression of FMRpolyG in mouse cerebellum.

Comparison of these novel mice with previous models of FXTAS expressing either mRNA with 90 CGG repeats and FMRpolyG protein [12, 15, 18] or only mRNA with ~118 CGG repeats [16, 59] is difficult as these pioneering mice express either endogenous level of transgene due to knock-in of the expanded CGG repeats within the endogenous *Fmr1* gene [12, 16], or express the expanded repeats in more restricted regions of the brain [15, 18] compared to the mouse models developed in the present study. It is noteworthy that knock-in mice with expanded CGG repeats, but that do not express FMRpolyG due to presence of a stop codon located upstream of the CGG repeats [16, 24], present some Purkinje cell dropout at 2 years of age but with no ataxia or rotarod deficiency, and a mild behaviour phenotype with hyperactivity, reduced anxiety and some subtle deficits in social interaction [16, 59]. These behaviour alterations are similar to the one observed in *Fmr1* knock-out mouse model, which suggest that they might be caused by the reduced expression of Fmrp observed in this CGG knock-in mouse model [59]. In contrast, the mild Purkinje cell dropout could be caused by expression of the mutant RNA containing expanded CGG repeats [16]. Similarly, we cannot exclude that the alterations observed in the full *FMR1* 5'UTR transgenic mice is caused by expression of both mutant RNA with expanded CGG repeats and FMRpolyG protein. In that aspect, it remains to formally demonstrate that FMRpolyG expressed in isolation is pathogenic. However, an important distinction not addressed previously is the timing of the pathogenic events in FXTAS models. Indeed, we observed that at time where FMRpolyG readily accumulates in nuclear inclusions, RNA foci of expanded CGG repeats are rare or undetectable both in mouse models and in neurons from human iPS cells derived from individuals with FXTAS. These data strongly suggest that expression of FMRpolyG precedes accumulation of mutant RNA into nuclear foci and establish a hierarchy of the pathogenic events in FXTAS. Thus, CGG RNA foci may be characteristic of an end stage of the disease, while FMRpolyG may potentially represent a relevant biomarker to follow disease progression, as well as a most promising therapeutic target [60].

We found that toxicity of FMRpolyG is mediated at least in part through sequestration of LAP2ß protein into nuclear aggregates, leading to disruption of the nuclear lamina architecture and neuronal cell death. These data provide a molecular mechanism to the previously reported nuclear lamina disorganization in FXTAS [14, 19, 36]. However, it is likely that the FMRpolyG protein mediates its toxic effect through more than one mechanism and/or protein partners. Notably, LAP2ß regulates gene expression through association with various transcription factors as well as to DNA and with the DNA-binding protein BAF1 (Barrier To Autointegration Factor 1) protein [61-66]. Thus, it remains to be determined whether FMRpolyG alters the transcriptional regulatory activity of LAP2. Also, proteomic analysis indicates that FMRpolyG pulls down various other proteins, including mitochondrial and proteasome proteins as well as actinin and

actin related proteins. Some of these proteins are good candidates to contribute to the mitochondrial and proteasome alterations that have been observed in FXTAS [17, 67-69]. Further investigations are required to test the potential pathological effect of FMRpolyG on mitochondria, protein degradation mechanisms and cell cytoskeleton in FXTAS.

Finally, this novel pathogenic mechanism where expansion of nucleotide repeats into a uORF results in expression of a toxic protein may apply to other diseases, such as Fragile X-associated Primary Ovarian Insufficiency (FXPOI) caused alike FXTAS by expanded CGG repeats in the *FMR1* gene [70]. Similarly, it is striking to note that expanded GGGGCC repeats, which are located upstream to the C9ORF72 ORF and are the main genetic cause of ALS-FTD, are in frame with an upstream CTG near-cognate codon in a good Kozac sequence (gctCTGg) to encode a Glycine Alanine-polypeptide, which is the most common dipeptide-repeats protein detected in individuals with ALS-FTD [71].

MATERIAL AND METHODS

Human samples

All brain samples were obtained from the FXTAS brain repository at the UC Davis School of Medicine with the informed consent of individuals and approved by the Institutional Review Board of the University of California, Davis. Patients have been described previously (Cases LR, 58-02-WD and 1007-05-HP from [7] and [72]. Fibroblasts of three FXTAS male individuals with confirmed premutation of 84, 90 and 99 CGG repeats were obtained with the informed consent of individuals and approved by the Institutional Review Board of the Hospital La Pitié Salpêtrière.

Constructs

PCMV6 containing C-terminally flag-tagged human cDNAs of LAP2ß was purchased from OriGene. Plasmids containing the 5'UTR of human FMR1 fused to Flag or GFP tags are available on Addgene. Mutations of the ACG into ATG or deletions of the 5'UTR of *FMR1* were achieved by oligonucleotide ligations. To insure stability of the expanded CGG repeats, all CGG plasmids were transformed into STBL3 bacterial strain (Invitrogen) and growth at room temperature (22°C).

Cell cultures, viability assays, and transfections

Neuro2A or HeLa cells were plated in 6 well tissue culture plates in DMEM 1 g/l glucose with 5% FCS and gentamycin. After 24 hours, cells were transfected with plasmid DNA using Lipofectamine 2000 (Invitrogen) according to manufacturer instructions. Primary cortical neurons were prepared from C57Bl/6 mice embryos of day E18 and grown on polylysine coated 24-well plates in Neurobasal Medium (NBM) supplemented with 1xB27, 0.5 mM L-glutamine and 100 IU/ml penicillin/streptomycin at 37° C with 5% CO2.

Neurons were transfected at day 3 with Lipofectamine 2000 (Invitrogen) in 400 µl NBM. Medium was replaced after 3h with a 1:1 (v:v) mixture of conditioned and fresh NBM. For cell viability, cells were detached by scraping and resuspended in PBS. TO-PRO-3 iodide (Fisher scientific, T-3605) was added at 20 nM to each sample and gently mix just prior to analysis on the FACS and 30 000 cells were counted.

Generation and differentiation of iPSC into neurons

Primary dermal fibroblasts were maintained on gelatin-coated dishes in DMEM 1 g/l glucose with antibiotic, antimycotic and 0.1 mM non-essential amino acids (Invitrogen) and 10% FBS for 5 passages. On day 1, 1x10exp5 fibroblasts were transduced by lentivirus carrying cDNAs of Oct4, Sox2, Nanog and Lin28 with 8 mg/ml of polybrene (Sigma). On day 2, medium was replaced with fresh medium and on day 3, infected cells were transferred onto a 100-mm dish containing 1x10exp6 feeder cells (passage 3 mitomycin-C treated mouse embryonic fibroblasts). From day 6 to 9, fibroblast medium was progressively switched to human induced pluripotent stem cell medium (KO-DMEM, 20% KOSR, 2 mM L-glutamine, 0.1 mM non-essential amino acids, Penicillin-Streptomycin, 0.1 mMb-mercaptoethanol supplemented with 10 ng/ml of bFGF (R&D Systems). Human iPSC clones were picked at week 4 and expanded on matrigel coated 35 mm dishes (BD Biosciences) in mTeSR1 medium (Stemcell Technologies). For embryoid body formation, hiPSC were dissociated with dispase solution (1 mg/ml, Stemcell Technologies), resuspended in 1 ml of Aggrewell medium (Stemcell Technologies) containing 2 mM Y27632 (Stemgent), centrifuged in Aggrewell plates for 3 min at 80g and further incubated at 37°C for 24 h. The next day, embryoid bodies were transferred in 3 ml of Aggrewell medium. The following days, medium was progressively switched to KO-DMEM, 20% FBS, 2 mM L-glutamine, 0.1 mM Non-Essential Amino Acids, penicillin–streptomycin and after 30 days, embryoid bodies were collected. For karyotype analysis, hiPSC cells were treated with colchicine (Sigma) for 4 h and cells were shocked with hypotonic KCl 0.075 M solution for 20 min at 37°C. Cells were fixed in methanol:acetic acid solution (3:1) and conventional cytogenetic was performed applying RHG banding on metaphase chromosomes. Expression of pluripotent surface markers of hIPSC was analyzed by FACS using anti-Tra-I-60, anti-Tra-I-81 and anti-SSEA4 antibodies (Millipore). Expression of 90 validated genes associated with stem cell pluripotency and differentiation to all three germ layers of hiPSC and corresponding embryoid bodies were analyzed using the Human Stem Cell Pluripotency Array (Applied Biosystems) according to manufacturer instructions. For in vivo teratoma formation, cells from one Matrigel coated 60 mm-dish were collected by dispase treatment and resuspended in 75 ml of KO-DMEM, mixed with 75 ml of Matrigel (BD Biosciences) and the hiPSC-Matrigel mixture was injected subcutaneously in 8-week-old NOD/SCID female mice (Charles River Laboratory, 2 mices injected for each hiPSC clone). After two

to three months, teratomas were dissected and fixed in formalin, embedded in paraffin and processed with hematoxylin and eosin staining at the histology laboratory of the Institute Clinique de la Souris (ICS). For differentiation of human pluripotent cells in Neuronal Stem cell (NSC), one B6 dish of IPS (60-80 % confluence) was washed with NFS medium (N2B27 supplemented with FGF2 5 ng/ml (Peprotech, AF-100-18B), hNoggin 260 ng/ml (R&D120-10C), SB431542 8,7 µg/ml (Tocris, 1614) containing ROCK inhibitor 3,5 µg/ml (Y-27632, Calbiochem, 688000) before to cut clumps. Clumps were collected and incubated overnight at 37°C in B3 UltraLow Attachment Dish (Corning). The next day, the clumps were transferred to a dish pre-coated with poly-ornithine 0,1% (Sigma, p4957) and laminine at 1 mg/ml (Sigma, L2020) and maintained with medium. After 24 hours, the medium was changed to NFS medium without rock inhibitor and medium was changed every two days during 8-10 days. After the appearance of neural rosette, the medium was replaced with NSC (N2B27 supplemented with FGF2 10 ng/ml, EGF 10 ng/ml (R&D, 263-EG-200RD), hBDNF 20 ng/ml (R&D, 248-BD-025CF). At confluence, cells were passaged 1:3 in NSC medium. For differentiation of NSC in neurons, confluent cells were dissociated with trypsin and plated on pre-coated with polyornithine (Sigma) and laminin (Sigma) in 24-well plate (50000 cells/well) in neuron medium (N2B27 supplemented with hBDNF 20 ng/ml and laminine 2 µg/ml). Media change was performed every 2 days and cells were differentiated during 55 days.

Monoclonal antibody production

To generate anti-FMRpolyG monoclonal antibodies, 8 week old female BALB/c mice were injected intraperitoneally with KLH conjugated peptides (8FM: MEAPLPGGVRQRG or 9FM: GGWASSARSPPLGGGLPALA) with 200ug of poly(I/C) as adjuvant. Three injections were performed at 2 weeks intervals and four days prior to hybridoma fusion, mice with positively reacting sera were re-injected. Spleen cells were fused with Sp2/0.Agl4 myeloma cells. Supernatants of hybridoma culture were tested at day 10 by ELISA for cross-reaction with either 8FM or 9FM peptides. Positive supernatants were then tested by Immunofluorescence and western blot on FMRpolyG transfected HeLa cells. Specific cultures were cloned twice on soft agar. Specific hybridomas were established and ascites fluid was prepared by injection of 2x106 hybridoma cells into Freund adjuvant-primed BALB/c mice. All animal experimental procedures were performed according to the French and European authority guidelines.

Western blotting

Concerning FMRpolyG-GFP tagged (>30kDa) analysis, 20 µg of proteins from transfected cells were homogenized in 1x laemmli sample loading buffer, denatured 3 min at 95°C, separated on 4-12% bis-Tris Gel (NuPAGE), transferred on nitrocellulose membranes

(Whatman Protan), blocked with 5% non-fat dry milk in TBS-Tween 1% (Tris Buffer Saline buffer), incubated with anti-FMRpolyG (8FM or 9 FM, 1/100), Lap2b (BD Biosciences 611000), GFP (abcam ab290), GAPDH (ab125247, Abcam), Flag (rabbit PA1-984B) or HA (ThermoFisher Scientific 26183) in TBS-Tween 1%, washed 3 times and incubated with anti-rabbit or mouse Peroxidase antibody (1:3000, Cell Signaling) 1 hour in TBS-Tween 1%, followed by washing and ECL chemoluminescence revelation (Amersham ECL Prime). Concerning human brain tissue preparation, small pieces of lyophilized frozen brain tissue were homogenized in 100 µl of Tris-SDS buffer (100 mM Tris pH 9, 5 % SDS 20%, 5 % b-mercaptoethanol), boiled at 100°C during 5 min then centrifuged at 13 000 rpm for 20 min at 4 °C. The supernatant was removed. The pellet was washed twice with water and homogenized in 20 µl of formic acid and incubated at 37°C during 30 min. Next, the homogenate was dried in speed-vac and resuspended in 40 µl Laemmli loading buffer prior to western blot analysis. Importantly, for western analysis of the small FMRpolyG-Flag tagged or endogenous FMRpolyG (<15kDa), 20 to 50 µg of proteins were resolved by 12% bis-Tris Gel (NuPAGE) and transferred onto PVDF 0,2 µm membrane. The membrane was blocked with 5% non-fat dry milk in TBS-Tween 1% and incubated with 8FM or 9FM antibody (1:100) overnight at 4°C. Membrane was washed 3 times and incubated with anti-mouse peroxidase antibody (1:3000, Cell Signaling) 1 hour in TBS-Tween 1%, followed by washing and ECL chemoluminescence revelation (Amersham ECL Prime).

Lysostaphin treatment

3x10exp5 HeLa cells transfected with FMRpolYG-GFP were scrapped in PBS 1X and centrifuged during 10 min at 3000 rpm at 4°C. The pellet was resuspended in 800 µl of RIPA. 16 µl of cell extract was incubated with 1 µg of lysostaphin (Prospec, ENZ-269) during 10 to 30 minutes at 37°C. Laemmli buffer was add to the mix and proteins were analyze by western blot.

HA-Flag tandem affinity purification and determination of FMRpolyG N-terminus

5x10exp6 HeLa cell were transfected with 18 µg of 5'UTR *FMR1* Flag-Ha double tagged plasmid using Fugen HD (Promega) for 24h hours. Proteins were purified by Ha-Flag tandem purification kit according to the manufacturer's instruction (Sigma-Aldrich). The bound proteins were visualized by silver staining (SilverQuest, Invitrogen) after separation of 4-12% bis-Tris Gel (NuPAGE) and interacting proteins were identified using NanoESI_Ion Trap (Thermo Fisher). For determination of the peptide sequence of FMRpolyG, identical procedure was performed and the band corresponding to FMRpolyG-HA-Flag tagged was gel extracted and peptides were identified using NanoESI_Ion Trap (Thermo Fisher).

Immunofluorescence and immunohistochemistry

Mouse or human brain sections were deparaffinized two times for 20 min in Histosol Plus (Shandon) and dehydrated as follows: twice in ethanol 100% (5 min), twice in ethanol 95% (5 min), once in ethanol 80% (5 min), once in ethanol 70% (5 min) and rinsed in PBS. Glass coverslips containing plated cells or brain sections treated as described above were fixed in PFA during 10 min and washed three times with PBS. The coverslips or slides were incubated for 10 min in PBS plus 0.5% Triton X-100 and washed three times with PBS before incubation during 1 hours with primary antibody against FMRpolyG (8FM or 9FM, 1/50), ubiquitin (DAKO, Z0458), GFP (abcam ab1218), Lap2b (Millipore, 06-1002), LaminB1 (abcam ab16048). Slides or coverslips were washed twice with PBS before incubation with a goat anti-rabbit or goat anti-mouse secondary antibody conjugated with Cyanine 3 (1/500 dilution; Fisher) for 60 min; incubated for 2 min in PBS 1X-DAPI (1/10 000 dilution) and rinsed twice with PBS 1X before mounting in Pro-Long media (Molecular Probes). Slides were examined using a fluorescence microscope (Leica). For immunochemistry, brain sections were deparaffinized followed by antigen retrieval using microwave treatment in 0.01 m sodium citrate and treatment with 10 µg/ml protein kinase for 20 min at 37°c. Endogenous peroxidase activity was blocked, and immunostaining was performed overnight at 4°C using rabbit anti-ubiquitin (Dako Z0458; 1:250) or mouse anti-FMRpolyG (8FM or 9FM, 1:10 to 1/50) antibodies. Antigen–antibody complexes were visualized by incubation with DAB substrate (Dako) and slides were counterstained with hematoxylin and eosin.

RNA FISH coupled to immunofluorescence

Mouse brain sections were deparaffinized and rehydrated. Coverslips containing primary culture of E18 mouse cortical neurons cells or brain sections were fixed in PFA during 10 min and washed three times with PBS. The coverslips or slides were incubated for 10 min in PBS plus 0.5% Triton X-100 and washed three times with PBS before pre-hybridization in 40% DMSO, 40% formamide, 10% BSA (10 mg/ml), 2 × SCC for 30 min. The coverslips or slides were hybridized for 2 h in 40% formamide, 10% DMSO, 2 × SCC, 2 mM vanadyl ribonucleoside, 60 µg/ml tRNA, 30 µg/ml BSA plus 0.75 µg (CCG)8x-Cy3 DNA oligonucleotide probe (Sigma). The coverslips or slides were washed twice in 2 × SCC/50% formamide and twice in 2 × SCC. The coverslips were incubated for 2 min in 2 × SCC/DAPI (1/10 000 dilution) and rinsed twice in 2 × SSC before mounting in Pro-Long media (Molecular Probes). Coverslips were examined using a fluorescence microscope (Leica). For FISH followed by immunofluorescence, after 2 × SCC wash, the slide were washed twice in PBS 1X. The slides were incubated 1 hour with primary antibody against FMRpolyGly antibody (8FM, 1/50). Slides were washed twice with PBS before incubation with a goat anti-mouse secondary antibody conjugated with cyanine-3 (1/500 dilution; Fisher) for 60 min; incubated for 2 min in PBS 1X-DAPI (1/10 000 dilution) and rinsed twice in PBS 1X before mounting in Pro-Long media (Molecular Probes). Slides were examined using a fluorescence microscope (Leica).

Drosophila models of FMRpolyG

All Drosophila lines were maintained on standard culture and food conditions at 25°C, while all crosses and experiments were performed at 29°C. Control and driver lines used in this study are *w1118* (control) from Bloomington, *Actin5C-GAL4*/*CyO* driver (ubiquitous driver line) as a gift from Zhe Han's lab, and RU486-inducible Geneswitch tubulin driver line *Tub5-GAL4* (ubiquitous expression) as a gift from Scott Pletcher's lab. DNA fragments containing FMRpolyG-GFP or polyG-GFP without the C-terminal sequence were PCR amplified from counterpart of mammalian transfection vectors described elsewhere and inserted to a pUAST vector between EcoRI and XbaI sites. All constructs were sequence verified by Sanger sequencing and transgenic flies with these constructs were made via standard p-element insertion (BestGene, CA). Transgene expression levels of GFP gene were analyzed 3 days after induction with RU486 in flies from the individual lines crossed to the *Tub5-GAL4* driver, and those with comparable RNA expression levels were used for this study. The fly eclosion assay has been described elsewhere (Todd et al, 2013). Briefly, homozygous UAS transgenic lines or control lines were crossed to a *Actin5C-GAL4* ubiquitous driver line balanced over a marker chromosome (CyO), on standard food at 29°C, if the transgene elicited no toxicity, then the number of progeny bearing the GAL4 driver would be expected to be equivalent to those bearing the CyO marker. Over 100 flies of each genotype were scored from multiple crosses. The ratio of expected progeny carrying the transgene compared to those carrying the CyO marker was expressed as a percentage of the expected ratio of one. These percentages were then compared using a Fischer exact test to determine statistical significance. For the fly survival assay, The UAS transgenic lines or control lines were crossed to *Tub5-Gal4* geneswitch driver flies on standard food absent of RU486 at 29°C. Adult offspring of the desired genotypes were collected 2-3 days after eclosion and transferred to standard fly food containing 200 μM RU486 without yeast granules. The flies were transferred to fresh food with drug every 2-3 days. Each genotype started with at least 4 vials of 25 flies/vial and the survival was determined daily or every other day for 3 weeks.

Mouse models, genotyping, and phenotyping

All mouse procedures were done according protocols approved by the Committee on Animal Resources of the ICS animal facility and under the French and European authority guidelines.

For transgene construction, human 5'UTR FMR1 fused in the glycine frame to the GFP (Addgene) was cloned between the FseI and SmaI sites of the Rosa26 5' arm – CAG promoter – LOXP - SV40 polyA 3x - LOXP – Rosa26 3' arm vector Ai2 (Addgene). Deleted transgene for the ACG near-cognate codon was constructed by deleting 100 nucleotides from FseI to KasI sites within the *FMR1* 5'UTR plasmid. Both mutant mouse lines were established at the ICS (Mouse Clinical Institute; http://www-mci.u-strasbg.fr). Both linearized constructs were electroporated separately in C57Bl/l6N mouse

embryonic stem (ES) cells. After G418 selection, targeted clones were identified by long-range PCR using external primers and further confirmed by Southern blot with an internal probe against Neomycin and 5' external probe against Rosa26. Two positive ES clones for each future transgenic mice were injected into Balb/cN blastocysts. Resulting male chimeras were bred with wild type C57Bl/6N females to obtain germline transmission. Deletion of the floxed STOP cassette were performed by breeding F1 males with CMV-cre deleter females [30] or Nestin-cre delete mice (Isaka et al., 1999). Genotyping across the expanded CGG repeats was performed using the Expand High Fidelity PCR System (Roche, 11-732 -650 001) according manufacturer instructions and supplemented with 2,5 M Betaine (B0300 Sigma, 12,5 µl of 5 M Betaine for a final PCR volume of 25 µl) with one denaturation step at 94 °C for 2 min, 30 cycles of amplification 94 °C for 1 min, 60 °C for 1 min, 72 °C for 2 min and a final step at 72 °C for 5 min using the forward primer 5'-TCGACCTGCAGCCCAAGCTAGATCG and the reverse primer 5'-TCCTTGAAGAAGATGGTGCGCTCC. Rotarod test (Bioseb, Chaville, France) was performed with three testing trials during which the rotation speed accelerated from 4 to 40 rpm in 5 min. Trials were separated by 5-10 min interval. The average latency was used as index of motor coordination performance. Grip test: this test measures the maximal muscle strength (g) using an isometric dynamometer connected to a grid (Bioseb). Mice were allowed to grip the grid with all its paws then they were pulled backwards until they released it. Each mouse was submitted to 3 consecutive trials immediately after the modified SHIRPA procedure. The maximal strength developed by the mouse before releasing the grid was recorded and the average value of the three trials adjusted to body weight. The string test consisted of 3 trials separated by 5-10 min interval. On each trial the forepaws of the animal were placed on the thread that is a wire stretched horizontally 40 cm above the bench. The latency the animal took to catch the wire with its hindpaws was recorded. Open field test: mice were tested in automated open fields (Panlab, Barcelona, Spain), each virtually divided into central and peripheral regions. The open fields were placed in a room homogeneously illuminated at 150 Lux. Each mouse was placed in the periphery of the open field and allowed to explore freely the apparatus for 30 min, with the experimenter out of the animal's sight. The distance traveled, the number of rears, and time spent in the central and peripheral regions were recorded over the test session. The number of entries and the percent time spent in center area are used as index of emotionality/anxiety

Quantitative real time RT-PCR

Total RNAs from mouse tissues or cells were isolated by TriReagent (Molecular Research Center). cDNAs were generated using the Transcriptor High Fidelity cDNA synthesis kit (Roche Diagnostics) for quantification of mRNAs. qPCR of mRNAs were realized using

the LightCycler 480 SYBR Green I Master (Roche) in a Lightcycler 480 (Roche) with 15 min at 94°C followed by 50 cycles of 15 sec at 94°C, 20 sec at 58°C and 20 sec at 72°C. RPLPO mRNA was used as standard and data were analyzed using the Lightcycler 480 analysis software (2ΔCt method).

Subcellular fractionation and PCR

Cells were scraped in PBS, cells were pelleted by centrifugation at 3000 rpm for 10 min minutes. The pellet was resuspended in Dautry Buffer (Tris HCl pH 7,8, 10 mM; NaCl 140 mM, MgCl2 1,5 mM; EDTA 10 mM, NP40 0,5%) and kept on ice 5 minutes. The homogenate was centrifuged at 3000 rpm for 15 minutes during 5 min at 4°C, pellet corresponding to nuclear fraction and supernatant to cytosolic fraction. Cytosolic fraction was centrifuged at 13000 rpm for 15 minutes to remove potential nucleus and 1 ml TriReagent (Molecular Research Center) was added. The pellet was washed with 400 µl of Dautry Buffer, centrifuged at 3000 rpm for 5 minutes at 4°C. Supernatant was removed and the pellet was homogenized in 400 µl of Dautry Buffer and 1 ml TriReagent (Molecular Research Center) was added. Total RNA from nuclear or cytosolic fraction was isolated as described in the manufacturer's protocol of TriReagent (Molecular Research Center). cDNAs were generated using the Transcriptor High Fidelity cDNA synthesis kit (Roche Diagnostics) for quantification of mRNAs. PCR was performed with Taq polymerase (Roche), one denaturation step at 94 °C for 2 min, 25 cycles of amplification 94 °C for 1 min, 60 °C for 1 min, 72 °C for 2 min and a final step at 72 °C for 5 min using the primer described below. The PCR products were precipitated, analyzed by electrophoresis on a 6.5% polyacrylamide gel, stained with ethidium bromide and quantified with a Typhoon scanner.

Oligonucleotides

RPLO_FW	GAAGTCACTGTGCCAGCCCA
RPLO_REV	GAAGGTGTAATCCGTCTCCA
U6_FW	CTCGCTTCGGCAGCACATATA
U6_REV	GGAACGCTTCACGAATTTGCG
FMR1_FW	GAAAACAACTGGCAGCCTGA
FMR1_REV	AGCTAACCACCAACAGCAAG
GFP_FW	ACGTAAACGGCCACAAGTTC
GFP_REV	AAGTCGTGCTGCTTCATGTG
(CGG)60x_FW	GAACCCACTGCTTACTGGCTTA
(CGG)60x_REV	AACGCTAGCCAGTTGGGTC
Transgene mouse FMRpolyG_FW	GCAAGCTGACCCTGAAGTTC
Transgene mouse FMRpolyG_REV	GTCTTGTAGTTGCCGTCGTC

REFERENCES

1. Hagerman, R.J., et al., *Intention tremor, parkinsonism, and generalized brain atrophy in male carriers of fragile X.* Neurology, 2001. **57**(1): p. 127-30.
2. Jacquemont, S., et al., *Penetrance of the fragile x-associated tremor/ataxia syndrome in a premutation carrier population.* JAMA, 2004. **291**(4): p. 460-9.
3. Seltzer, M.M., et al., *Prevalence of CGG expansions of the FMR1 gene in a US population-based sample.* American Journal of Medical Genetics Part B-Neuropsychiatric Genetics, 2012. **159B**(5): p. 589-597.
4. Tassone, F., et al., *FMR1 CGG allele size and prevalence ascertained through newborn screening in the United States.* Genome Med, 2012. **4**(12): p. 100.
5. Jacquemont, S., et al., *Fragile X Premutation Tremor/Ataxia Syndrome: Molecular, Clinical, and Neuroimaging Correlates.* Am J Hum Genet, 2003. **72**(4): p. 869-78.
6. Greco, C.M., et al., *Neuronal intranuclear inclusions in a new cerebellar tremor/ataxia syndrome among fragile X carriers.* Brain, 2002. **125**(Pt 8): p. 1760-1771.
7. Greco, C.M., et al., *Neuropathology of fragile X-associated tremor/ataxia syndrome (FXTAS).* Brain, 2006. **129**(Pt1): p. 243-255.
8. Tassone, F., et al., *Fragile X males with unmethylated, full mutation trinucleotide repeat expansions have elevated levels of FMR1 messenger RNA.* Am J Med Genet, 2000. **94**(3): p. 232-6.
9. Kenneson, A., et al., *Reduced FMRP and increased FMR1 transcription is proportionally associated with CGG repeat number in intermediate-length and premutation carriers.* Hum Mol Genet, 2001. **10**(14): p. 1449-1454.
10. Tassone, F., et al., *Elevated FMR1 mRNA in premutation carriers is due to increased transcription.* RNA, 2007. **13**: p. 555-562.
11. Hagerman, P.J. and R.J. Hagerman, *The Fragile-X Premutation: A Maturing Perspective.* Am J Hum Genet, 2004. **74**(5): p. 805-816.
12. Willemsen, R., et al., *The FMR1 CGG repeat mouse displays ubiquitin-positive intranuclear neuronal inclusions; implications for the cerebellar tremor/ataxia syndrome.* Hum Mol Genet, 2003. **12**(9): p. 949-59.
13. Jin, P., et al., *RNA-Mediated Neurodegeneration Caused by the Fragile X Premutation rCGG Repeats in Drosophila.* Neuron, 2003. **39**(5): p. 739-747.
14. Arocena, D.G., et al., *Induction of inclusion formation and disruption of lamin A/C structure by premutation CGG-repeat RNA in human cultured neural cells.* Hum Mol Genet, 2005. **14**: p. 3661-3671.
15. Hashem, V., et al., *Ectopic expression of CGG containing mRNA is neurotoxic in mammals.* Hum Mol Genet, 2009. **18**: p. 2443-2451.
16. Entezam, A., et al., *Regional FMRP deficits and large repeat expansions into the full mutation range in a new Fragile X premutation mouse model.* Gene, 2007. **395**: p. 125-134.
17. Hukema, R.K., et al., *Induced expression of expanded CGG RNA causes mitochondrial dysfunction in vivo.* Cell Cycle, 2014. **13**(16): p. 2600-2608.
18. Hukema, R.K., et al., *Reversibility of neuropathology and motor deficits in an inducible mouse model for FXTAS.* Human Molecular Genetics, 2015. **24**(17): p. 4948-4957.
19. Iwahashi, C.K., et al., *Protein composition of the intranuclear inclusions of FXTAS.* Brain, 2006. **129**(Pt 1): p. 256-271.
20. Sofola, O.A., et al., *RNA-Binding Proteins hnRNP A2/B1 and CUGBP1 Suppress Fragile X CGG Premutation Repeat-Induced Neurodegeneration in a Drosophila Model of FXTAS.* Neuron, 2007. **55**(4): p. 565-71.
21. Jin, P., et al., *Pur alpha Binds to rCGG Repeats and Modulates Repeat-Mediated Neurodegeneration in a Drosophila Model of Fragile X Tremor/Ataxia Syndrome.* Neuron, 2007. **55**(4): p. 556-64.
22. Sellier, C., et al., *Sequestration of DROSHA and DGCR8 by Expanded CGG RNA Repeats Alters MicroRNA Processing in Fragile X-Associated Tremor/Ataxia Syndrome.* Cell Rep, 2013. **3**(3): p. 869-880.
23. Sellier, C., et al., *Sam68 sequestration and partial loss of function are associated with splicing alterations in FXTAS patients.* Embo J, 2010. **29**: p. 1248-1261.
24. Todd, P.K., et al., *CGG Repeat-Associated Translation Mediates Neurodegeneration in Fragile X Tremor Ataxia Syndrome.* Neuron, 2013. **78**(3): p. 440-455.

25. Zu, T., et al., *Non-ATG-initiated translation directed by microsatellite expansions*. Proc Natl Acad Sci U S A, 2011. **108**(1): p. 260-5.

26. Cleary, J.D. and L.P.W. Ranum, *Repeat associated non-ATG (RAN) translation: new starts in microsatellite expansion disorders*. Current Opinion in Genetics & Development, 2014. **26**: p. 6-15.

27. Buijsen, R.A., et al., *FMRpolyG-positive inclusions in CNS and non-CNS organs of a fragile X premutation carrier with fragile X-associated tremor/ataxia syndrome*. Acta Neuropathol Commun, 2014. **2**(1): p. 162.

28. Sonenberg, N. and A.G. Hinnebusch, *Regulation of translation initiation in eukaryotes: mechanisms and biological targets*. Cell, 2009. **136**(4): p. 731-45.

29. Aspden, J.L., et al., *Extensive translation of small Open Reading Frames revealed by Poly-Ribo-Seq*. Elife, 2014. **3**: p. e03528.

30. Birling, M.C., et al., *Highly-efficient, fluorescent, locus directed cre and FlpO deleter mice on a pure C57BL/6N genetic background*. Genesis, 2012. **50**(6): p. 482-9.

31. Isaka, F., et al., *Ectopic expression of the bHLH gene Math1 disturbs neural development*. Eur J Neurosci, 1999. **11**(7): p. 2582-8.

32. Foisner, R. and L. Gerace, *Integral membrane proteins of the nuclear envelope interact with lamins and chromosomes, and binding is modulated by mitotic phosphorylation*. Cell, 1993. **73**(7): p. 1267-79.

33. Furukawa, K., et al., *Cloning of a cDNA for lamina-associated polypeptide 2 (LAP2) and identification of regions that specify targeting to the nuclear envelope*. Embo J, 1995. **14**(8): p. 1626-36.

34. Gant, T.M., C.A. Harris, and K.L. Wilson, *Roles of LAP2 proteins in nuclear assembly and DNA replication: truncated LAP2beta proteins alter lamina assembly, envelope formation, nuclear size, and DNA replication efficiency in Xenopus laevis extracts*. J Cell Biol, 1999. **144**(6): p. 1083-96.

35. Dubinska-Magiera, M., et al., *Xenopus LAP2beta protein knockdown affects location of lamin B and nucleoporins and has effect on assembly of cell nucleus and cell viability*. Protoplasma, 2016. **253**(3): p. 943-56.

36. Hoem, G., et al., *CGG-repeat length threshold for FMR1 RNA pathogenesis in a cellular model for FXTAS*. Hum Mol Genet, 2011. **20**: p. 2161-2170.

37. Jung, L., et al., *ONSL and OSKM cocktails act synergistically in reprogramming human somatic cells into induced pluripotent stem cells*. Mol Hum Reprod, 2014. **20**(6): p. 538-49.

38. Marteyn, A., et al., *Mutant human embryonic stem cells reveal neurite and synapse formation defects in type 1 myotonic dystrophy*. Cell Stem Cell, 2011. **8**(4): p. 434-44.

39. Boissart, C., et al., *Differentiation from human pluripotent stem cells of cortical neurons of the superficial layers amenable to psychiatric disease modeling and high-throughput drug screening*. Transl Psychiatry, 2013. **3**: p. e294.

40. Liu, J., et al., *Signaling defects in iPSC-derived fragile X premutation neurons*. Human Molecular Genetics, 2012. **21**(17): p. 3795-3805.

41. Renton, A.E., et al., *A hexanucleotide repeat expansion in C9ORF72 is the cause of chromosome 9p21-linked ALS-FTD*. Neuron, 2011. **72**(2): p. 257-68.

42. DeJesus-Hernandez, M., et al., *Expanded GGGGCC hexanucleotide repeat in noncoding region of C9ORF72 causes chromosome 9p-linked FTD and ALS*. Neuron, 2011. **72**(2): p. 245-56.

43. Ash, P.E., et al., *Unconventional translation of C9ORF72 GGGGCC expansion generates insoluble polypeptides specific to c9FTD/ALS*. Neuron, 2013. **77**(4): p. 639-46.

44. Mori, K., et al., *The C9orf72 GGGGCC repeat is translated into aggregating dipeptide-repeat proteins in FTLD/ALS*. Science, 2013. **339**(6125): p. 1335-8.

45. Zu, T., et al., *RAN proteins and RNA foci from antisense transcripts in C9ORF72 ALS and frontotemporal dementia*. Proc Natl Acad Sci U S A, 2013. **110**(51): p. E4968-77.

46. Zhang, Y.J., et al., *C9ORF72 poly(GA) aggregates sequester and impair HR23 and nucleocytoplasmic transport proteins*. Nat Neurosci, 2016.

47. Zhang, Y.J., et al., *Aggregation-prone c9FTD/ALS poly(GA) RAN-translated proteins cause neurotoxicity by inducing ER stress*. Acta Neuropathol, 2014. **128**(4): p. 505-24.

48. Freibaum, B.D., et al., *GGGGCC repeat expansion in C9orf72 compromises nucleocytoplasmic transport*. Nature, 2015. **525**(7567): p. 129-33.

49. Jovicic, A., et al., *Modifiers of C9orf72 dipeptide repeat toxicity connect nucleocytoplasmic transport defects to FTD/ALS*. Nat Neurosci, 2015. **18**(9): p. 1226-9.

50. Calvo, S.E., D.J. Pagliarini, and V.K. Mootha, *Upstream open reading frames cause widespread reduction of protein expression and are polymorphic among humans.* Proc Natl Acad Sci U S A, 2009. **106**(18): p. 7507-12.

51. Ingolia, N.T., L.F. Lareau, and J.S. Weissman, *Ribosome profiling of mouse embryonic stem cells reveals the complexity and dynamics of mammalian proteomes.* Cell, 2011. **147**(4): p. 789-802.

52. Fritsch, C., et al., *Genome-wide search for novel human uORFs and N-terminal protein extensions using ribosomal footprinting.* Genome Res, 2012. **22**(11): p. 2208-18.

53. Ji, M.H., et al., *Physiological Expression and Accumulation of the Products of Two Upstream Open Reading Frames mrtl and MycHex1 Along With p64 and p67 Myc From the Human c-myc Locus*. J Cell Biochem, 2016. **117**(6): p. 1407-18.

54. Barbosa, C., I. Peixeiro, and L. Romao, *Gene expression regulation by upstream open reading frames and human disease.* PLoS Genet, 2013. **9**(8): p. e1003529.

55. Jacquemont, S., et al., *Size bias of fragile X premutation alleles in late-onset movement disorders.* J Med Genet, 2006. **43**: p. 804-809.

56. Brouwer, J.R., et al., *CGG-repeat length and neuropathological and molecular correlates in a mouse model for fragile X-associated tremor/ataxia syndrome.* J Neurochem, 2008. **107**: p. 1671-1682.

57. Feng, Y., D. Lakkis, and S.T. Warren, *Quantitative comparison of FMR1 gene expression in normal and premutation alleles.* Am J Hum Genet, 1995. **56**: p. 106-113.

58. Primerano, B., et al., *Reduced FMR1 mRNA translation efficiency in Fragile X patients with premutations.* Rna-a Publication of the Rna Society, 2002. **8**(12): p. 1482-1488.

59. Qin, M., et al., *A mouse model of the fragile X premutation: Effects on behavior, dendrite morphology, and regional rates of cerebral protein synthesis.* Neurobiol Dis, 2011. **42**: p. 85-98.

60. Yang, W.Y., et al., *Inhibition of Non-ATG Translational Events in Cells via Covalent Small Molecules Targeting RNA.* Journal of the American Chemical Society, 2015. **137**(16): p. 5336-5345.

61. Zullo, J.M., et al., *DNA sequence-dependent compartmentalization and silencing of chromatin at the nuclear lamina.* Cell, 2012. **149**(7): p. 1474-87.

62. Nili, E., et al., *Nuclear membrane protein LAP2beta mediates transcriptional repression alone and together with its binding partner GCL (germ-cell-less).* J Cell Sci, 2001. **114**(Pt 18): p. 3297-307.

63. Shumaker, D.K., et al., *LAP2 binds to BAF.DNA complexes: requirement for the LEM domain and modulation by variable regions.* Embo J, 2001. **20**(7): p. 1754-64.

64. Cai, M., et al., *Solution structure of the constant region of nuclear envelope protein LAP2 reveals two LEM-domain structures: one binds BAF and the other binds DNA.* Embo J, 2001. **20**(16): p. 4399-407.

65. Somech, R., et al., *The nuclear-envelope protein and transcriptional repressor LAP2beta interacts with HDAC3 at the nuclear periphery, and induces histone H4 deacetylation.* J Cell Sci, 2005. **118**(Pt 17): p. 4017-25.

66. Naetar, N., et al., *Loss of nucleoplasmic LAP2alpha-lamin A complexes causes erythroid and epidermal progenitor hyperproliferation.* Nat Cell Biol, 2008. **10**(11): p. 1341-8.

67. Ross-Inta, C., et al., *Evidence of mitochondrial dysfunction in fragile X-associated tremor/ataxia syndrome.* Biochem J, 2010. **429**: p. 545-552.

68. Kaplan, E.S., et al., *Early mitochondrial abnormalities in hippocampal neurons cultured from Fmr1 pre-mutation mouse model.* Journal of Neurochemistry, 2012. **123**(4): p. 613-21.

69. Oh, S.Y., et al., *RAN translation at CGG repeats induces ubiquitin proteasome system impairment in models of fragile X-associated tremor ataxia syndrome.* Human Molecular Genetics, 2015. **24**(15): p. 4317-4326.

70. Buijsen, R.A., et al., *Presence of inclusions positive for polyglycine containing protein, FMRpolyG, indicates that repeat-associated non-AUG translation plays a role in fragile X-associated primary ovarian insufficiency.* Hum Reprod, 2015.

71. Mackenzie, I.R., et al., *Quantitative analysis and clinico-pathological correlations of different dipeptide repeat protein pathologies in C9ORF72 mutation carriers.* Acta Neuropathol, 2015. **130**(6): p. 845-61.

72. Pretto, D., et al., *Clinical and molecular implications of mosaicism in FMR1 full mutations.* Front Genet, 2014. **5**: p. 318.

SUPPLEMENTAL DATA

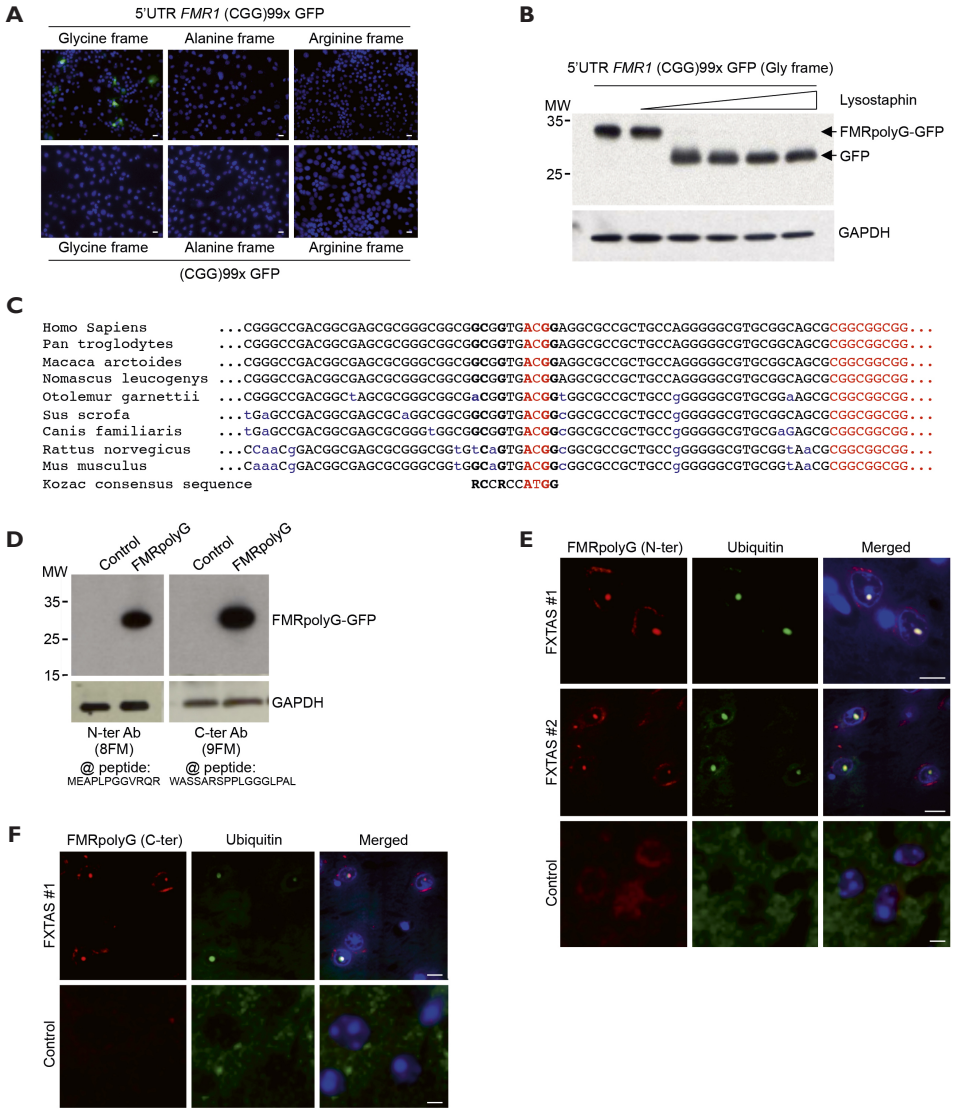

Supplemental Figure 1. Expanded CGG repeats are translated into FMRpolyG.

(A) GFP fluorescence of HeLa cells transfected with expanded CGG repeats embedded or not in the 5'UTR of *FMR1* and fused in all three possible frames with the GFP. (**B**) Western blotting analysis with anti GFP antibody of FMRpolyG expressing HeLa cell lysate treated with increasing quantity of lysostaphin, a glycine endopeptidase. (**C**) Sequence alignment of the 5'UTR of *FMR1* from human, chimpanzee, macaque, gibbon, galago, wild boar, dog, rat and mouse with Kozac consensus sequence. ACG translation start of FMRpolyG is indicated in red. (**D**) Western blotting validation of 8FM and 9FM antibodies directed against the N- or C-terminal part of FMRpolyG, respectively. (**E**) Immunofluorescence using antibodies against the N-terminal part of FMRpolyG (red, 8FM antibody) and ubiquitin (green) on brain sections (hippocampal area) of FXTAS patients compared to a age-matched control individual. (**F**) Immunofluorescence using antibodies against the C-terminal part of FMRpolyG (red, 9FM antibody) and ubiquitin (green) on brain sections (hippocampal area) of a FXTAS patient compared to a age-matched control individual. Scale bars, 10 µm. Nuclei were counterstained with DAPI.

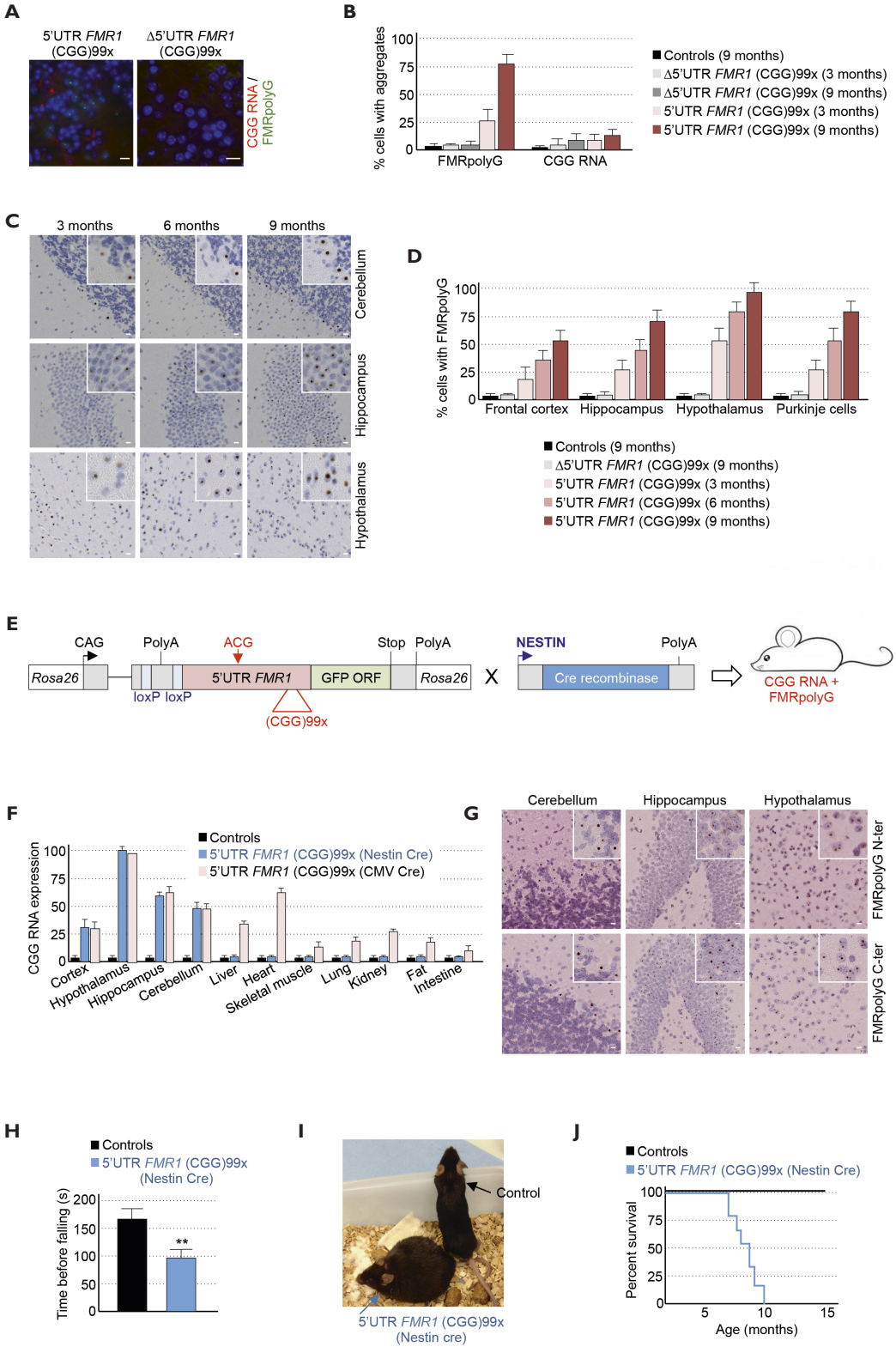
A
5'UTR FMR1 (CGG)99x
Δ5'UTR FMR1 (CGG)99x
CGG RNA / FMRpolyG
B
% cells with aggregates
FMRpolyG
CGG RNA
Controls (9 months)
Δ5'UTR FMR1 (CGG)99x (3 months)
Δ5'UTR FMR1 (CGG)99x (9 months)
5'UTR FMR1 (CGG)99x (3 months)
5'UTR FMR1 (CGG)99x (9 months)
C
3 months
6 months
9 months
Cerebellum
Hippocampus
Hypothalamus
D
% cells with FMRpolyG
Frontal cortex
Hippocampus
Hypothalamus
Purkinje cells
Controls (9 months)
Δ5'UTR FMR1 (CGG)99x (9 months)
5'UTR FMR1 (CGG)99x (3 months)
5'UTR FMR1 (CGG)99x (6 months)
5'UTR FMR1 (CGG)99x (9 months)
E
CAG
PolyA
ACG
Stop
PolyA
Rosa26
5'UTR FMR1
GFP ORF
Rosa26
loxP loxP
(CGG)99x
X
NESTIN
PolyA
Cre recombinase
CGG RNA + FMRpolyG
F
CGG RNA expression
Controls
5'UTR FMR1 (CGG)99x (Nestin Cre)
5'UTR FMR1 (CGG)99x (CMV Cre)
Cortex
Hypothalamus
Hippocampus
Cerebellum
Liver
Heart
Skeletal muscle
Lung
Kidney
Fat
Intestine
G
Cerebellum
Hippocampus
Hypothalamus
FMRpolyG N-ter
FMRpolyG C-ter
H
Controls
5'UTR FMR1 (CGG)99x (Nestin Cre)
Time before falling (s)
**
I
Control
5'UTR FMR1 (CGG)99x (Nestin cre)
J
Controls
5'UTR FMR1 (CGG)99x (Nestin Cre)
Percent survival
Age (months)

← **Supplemental Figure 2.** Expression of FMRpolyG is pathogenic to mice

(A) RNA FISH against CGG RNA foci (red) coupled to immunofluorescence against FMRpolyG (green) in brain of 6 months old bigenic CMV-cre / full-length or deleted *FMR1* 5'UTR transgenic mice. (**B**) Quantification of FMRpolyG protein aggregates and CGG RNA foci in 3 or 9 months old control (n=3) or bigenic CMV-cre / full-length (n=3) or deleted (n=3) *FMR1* 5'UTR transgenic mice (n=100 cells). (**C**) Immunohistochemistry using an antibody directed against FMRpolyG C-terminal part (9FM) of cerebellum, hippocampal and hypothalamic areas of 3, 6 or 9 months old bigenic CMV-cre / full-length *FMR1* 5'UTR transgenic mice. Scale bars, 10 µm. Sections were counterstained with Nissl staining. (**D**) Quantification of FMRpolyG protein aggregates in control (n=3) or bigenic CMV-cre / full-length (n=3) or deleted (n=3) *FMR1* 5'UTR transgenic mice. (**E**) Schemes of the mouse transgene constructs. The human full-length 5'UTR of *FMR1* is represented as a red box, GFP ORF as a green box, loxP sites as blue boxes, while promoters, polyadenylation sequences and start and stop of translation are indicated by arrow or black lines. (**F**) Quantitative RT-PCR analysis of transgenes expression relative to the *RplpO* mRNA in different tissues of 6 months old control (n=3) or bigenic CMV-cre / full-length *FMR1* 5'UTR (n=3) or bigenic Nestin-cre / full-length *FMR1* 5'UTR (n=3) mice. (**G**) Immunohistochemistry using an antibody directed against the N-terminal part (8FM) of FMRpolyG in the cerebellum, hippocampus and hypothalamus of 6 months old bigenic Nestin-cre / full-length *FMR1* 5'UTR mice. Scale bars, 10 µm. Sections were counterstained with HE staining. (**H**) Time before falling of 3 months old control (n=6) or bigenic Nestin-cre / full-length *FMR1* 5'UTR (n=6) male mice. (**I**) Representative image of 8 months old control or bigenic Nestin-cre / full-length *FMR1* 5'UTR mice. (**I**) Kaplan-Meier survival curves of control (n=10) or bigenic Nestin-cre / full-length *FMR1* 5'UTR (n=10) male and female mice. Error bars indicate s.e.m. Student T-test, ** indicates $p<0.01$.

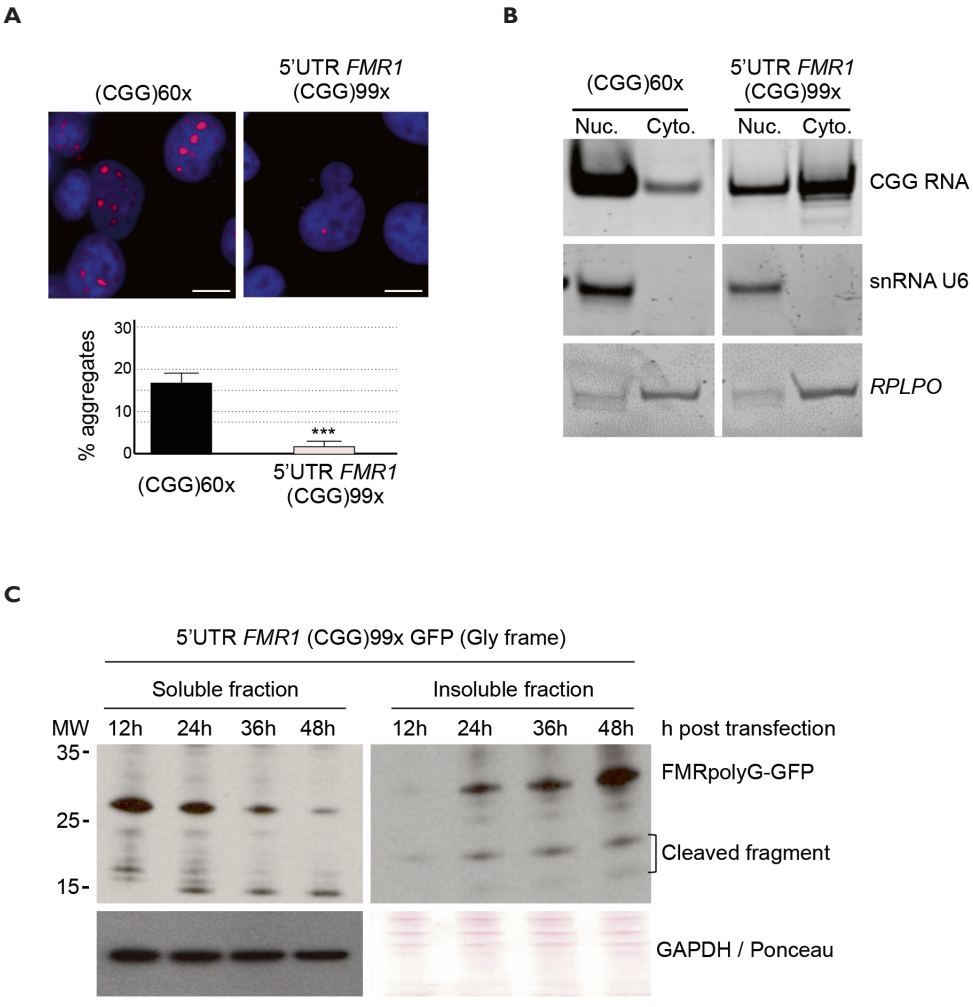

Supplemental Figure 3. The C-terminal part of FMRpolyG is toxic (**A**) Upper panel, RNA FISH against CGG RNA foci in cells transfected with expanded CGG repeats embedded or not in the 5'UTR of *FMR1*. Scale bars, 10 µm. Nuclei were counterstained with DAPI. Lower panel, quantification of cells (n=50) with CGG RNA foci (n=3 transfection). (**B**) RT-PCR analysis of nuclear and cytoplasmic fractions of neuronal cells transfected with expanded CGG repeats embedded or not in the 5'UTR of *FMR1*. Correct nuclear and cytoplasmic fractionation was controlled by RT-PCR for nuclear U6 snRNA and for cytoplasmic *RPLP0* mRNA. (**C**) Western blotting analysis using anti GFP antibody of soluble and insoluble fractions of neuronal cells transfected with expanded CGG repeats embedded within the 5'UTR of *FMR1* and fused to the GFP in the glycine frame. (**D**) Transgene mRNA expression of *Drosophila* expressing FMRpolyG full-length or deleted of its C-terminus.

Supplemental table 1. Proteins interacting with FMRpolyG

Proteins associated with HA-flag-tagged FMRpolyG expressed in mouse N2A neuronal cells were captured through consecutive anti-Flag and anti-HA affinity purification steps and identified by orbitrap ion trap mass analyzer.

Accession	Description	Score	Coverage	# Peptides	# PSM	# AAs	MW [kDa]
Q61029-3	**Lamina-associated polypeptide 2, isoforms beta/delta/epsilon/ gamma OS=Mus musculus GN=Tmpo - [LAP2B_MOUSE]**	**48**	**16**	**13**	**15**	**412**	**46**
P57780	Alpha-actinin-4 OS=Mus musculus GN=Actn4 PE=1 SV=1 - [ACTN4_MOUSE]	23	7	5	7	912	105
Q9CPW4	Actin-related protein 2/3 complex subunit 5 OS=Mus musculus GN=Arpc5 PE=2 SV=3 - [ARPC5_MOUSE]	20	31	3	4	151	16
Q5SW19-2	Isoform 2 of Clustered mitochondria protein homolog OS=Mus musculus GN=Cluh - [CLU_MOUSE]	17	8	5	5	818	92
Q61033	**Lamina-associated polypeptide 2, isoforms alpha/zeta OS=Mus musculus GN=Tmpo PE=1 SV=4 - [LAP2A_MOUSE]**	**15**	**7**	**4**	**5**	**693**	**75**
Q9WUI1	Mitogen-activated protein kinase 11 OS=Mus musculus GN=Mapk11 PE=1 SV=2 - [MK11_MOUSE]	15	10	3	5	364	41
Q9QUR6	Prolyl endopeptidase OS=Mus musculus GN=Prep PE=2 SV=1 - [PPCE_MOUSE]	7	4	2	2	710	81
P61290	Proteasome activator complex subunit 3 OS=Mus musculus GN=Psme3 PE=1 SV=1 - [PSME3_MOUSE]	7	4	1	2	254	29
Q08189	Protein-glutamine gamma-glutamyltransferase E OS=Mus musculus GN=Tgm3 PE=1 SV=2 - [TGM3_MOUSE]	7	2	1	2	693	77
O70250	Phosphoglycerate mutase 2 OS=Mus musculus GN=Pgam2 PE=2 SV=3 - [PGAM2_MOUSE]	6	10	2	2	253	29
P08032	Spectrin alpha chain, erythrocytic 1 OS=Mus musculus GN=Spta1 PE=2 SV=3 - [SPTA1_MOUSE]	6	1	2	2	2415	280
P08752	Guanine nucleotide-binding protein G(i) subunit alpha-2 OS=Mus musculus GN=Gnai2 PE=1 SV=5 - [GNAI2_MOUSE]	6	7	2	2	355	40

Supplemental table 1. (continuded)

Accession	Description	Score	Coverage	# Peptides	# PSM	# AAs	MW [kDa]
Q9R0Q6	Actin-related protein 2/3 complex subunit 1A OS=Mus musculus GN=Arpc1a PE=1 SV=1 - [ARC1A_MOUSE]	6	7	2	2	370	42
Q922D4-2	Serine/threonine-protein phosphatase 6 regulatory subunit 3 OS=Mus musculus GN=Ppp6r3 - [PP6R3_MOUSE]	6	2	1	2	827	93
Q8C6G8	WD repeat-containing protein 26 OS=Mus musculus GN=Wdr26 PE=2 SV=3 - [WDR26_MOUSE]	6	4	2	2	641	70
Q4KML4	Costars family protein ABRACL OS=Mus musculus GN=Abracl PE=3 SV=1 - [ABRAL_MOUSE]	6	16	1	2	81	9
P10853	Histone H2B type 1-F/J/L OS=Mus musculus GN=Hist1h2bf PE=1 SV=2 - [H2B1F_MOUSE]	5	7	1	2	126	14
Q8C0D7-4	Isoform 4 of Inhibitor of growth protein 4 OS=Mus musculus GN=Ing4 - [ING4_MOUSE]	5	8	1	2	166	19
P0C0S6	Histone H2A.Z OS=Mus musculus GN=H2afz PE=1 SV=2 - [H2AZ_MOUSE]	5	7	1	2	128	14
Q9D7X8	Gamma-glutamylcyclotransferase OS=Mus musculus GN=Ggct PE=1 SV=1 - [GGCT_MOUSE]	5	6	1	2	188	21
P04117	Fatty acid-binding protein, adipocyte OS=Mus musculus GN=Fabp4 PE=1 SV=3 - [FABP4_MOUSE]	4	9	1	1	132	15
Q8VBT0	Thioredoxin-related transmembrane protein 1 OS=Mus musculus GN=Tmx1 PE=1 SV=1 - [TMX1_MOUSE]	4	4	1	1	278	31
P15532	Nucleoside diphosphate kinase A OS=Mus musculus GN=Nme1 PE=1 SV=1 - [NDKA_MOUSE]	3	11	1	1	152	17
Q8BQP8	Rab11 family-interacting protein 4 OS=Mus musculus GN=Rab11fip4 PE=1 SV=1 - [RFIP4_MOUSE]	3	2	1	1	635	72
Q8BH74	Nuclear pore complex protein Nup107 OS=Mus musculus GN=Nup107 PE=2 SV=1 - [NU107_MOUSE]	3	1	1	1	926	107

Supplemental table 1. (continued)

Accession	Description	Score	Coverage	# Peptides	# PSM	# AAs	MW [kDa]
O70456	14-3-3 protein sigma OS=Mus musculus GN=Sfn PE=1 SV=2 - [1433S_MOUSE]	3	4	1	1	248	28
O70435	Proteasome subunit alpha type-3 OS=Mus musculus GN=Psma3 PE=1 SV=3 - [PSA3_MOUSE]	3	5	1	1	255	28
O70166	Stathmin-3 OS=Mus musculus GN=Stmn3 PE=1 SV=1 - [STMN3_MOUSE]	3	9	1	1	180	21
Q9JM76	Actin-related protein 2/3 complex subunit 3 OS=Mus musculus GN=Arpc3 PE=1 SV=3 - [ARPC3_MOUSE]	3	6	1	1	178	21
P41969	ETS domain-containing protein Elk-1 OS=Mus musculus GN=Elk1 PE=2 SV=3 - [ELK1_MOUSE]	3	4	1	1	429	45
Q07643	Collagen alpha-2(IX) chain OS=Mus musculus GN=Col9a2 PE=2 SV=1 - [CO9A2_MOUSE]	3	2	1	1	688	65
P68510	14-3-3 protein eta OS=Mus musculus GN=Ywhah PE=1 SV=2 - [1433F_MOUSE]	3	6	1	1	246	28
O89094-2	Isoform 2 of Caspase-14 OS=Mus musculus GN=Casp14 - [CASPE_MOUSE]	3	5	1	1	159	18
Q61176	Arginase-1 OS=Mus musculus GN=Arg1 PE=1 SV=1 - [ARG11_MOUSE]	3	3	1	1	323	35
Q91UZ4	Egl nine homolog 3 OS=Mus musculus GN=Egln3 PE=2 SV=1 - [EGLN3_MOUSE]	3	5	1	1	239	27
P97372	Proteasome activator complex subunit 2 OS=Mus musculus GN=Psme2 PE=2 SV=4 - [PSME2_MOUSE]	3	4	1	1	239	27
Q61941	NAD(P) transhydrogenase, mitochondrial OS=Mus musculus GN=Nnt PE=1 SV=2 - [NNTM_MOUSE]	3	1	1	1	1086	114
P50580-2	Isoform 2 of Proliferation-associated protein 2G4 OS=Mus musculus GN=Pa2g4 - [PA2G4_MOUSE]	3	3	1	1	340	38
Q64331	Unconventional myosin-VI OS=Mus musculus GN=Myo6 PE=1 SV=1 - [MYO6_MOUSE]	3	1	1	1	1265	146

Supplemental table 1. (continued)

Accession	Description	Score	Coverage	# Peptides	# PSM	# AAs	MW [kDa]
Q91WD9	Secretagogin OS=Mus musculus GN=Scgn PE=2 SV=1 - [SEGN_MOUSE]	3	7	1	1	276	32
P31695	Neurogenic locus notch homolog protein 4 OS=Mus musculus GN=Notch4 PE=1 SV=2 - [NOTC4_MOUSE]	3	1	1	1	1964	207
O54818	Tumor protein D53 OS=Mus musculus GN=Tpd52l1 PE=2 SV=1 - [TPD53_MOUSE]	3	7	1	1	204	23
O35685	Nuclear migration protein nudC OS=Mus musculus GN=Nudc PE=1 SV=1 - [NUDC_MOUSE]	3	4	1	1	332	38
Q9CWP6-2	Isoform 2 of Motile sperm domain-containing protein 2 OS=Mus musculus GN=Mospd2 - [MSPD2_MOUSE]	3	3	1	1	481	55
Q7TSH3	Zinc finger protein 516 OS=Mus musculus GN=Znf516 PE=1 SV=1 - [ZN516_MOUSE]	3	2	1	1	1157	125
P30658	Chromobox protein homolog 2 OS=Mus musculus GN=Cbx2 PE=1 SV=2 - [CBX2_MOUSE]	3	3	1	1	519	55
P62305	Small nuclear ribonucleoprotein E OS=Mus musculus GN=Snrpe PE=3 SV=1 - [RUXE_MOUSE]	3	13	1	1	92	11
Q9WTX8	Mitotic spindle assembly checkpoint protein MAD1 OS=Mus musculus GN=Mad1l1 PE=2 SV=1 - [MD1L1_MOUSE]	3	2	1	1	717	83
Q791T5-2	Isoform 2 of Mitochondrial carrier homolog 1 OS=Mus musculus GN=Mtch1 - [MTCH1_MOUSE]	3	5	1	1	372	40
Q9CXF0	Kynureninase OS=Mus musculus GN=Kynu PE=2 SV=3 - [KYNU_MOUSE]	3	3	1	1	464	52
Q60770	Syntaxin-binding protein 3 OS=Mus musculus GN=Stxbp3 PE=1 SV=1 - [STXB3_MOUSE]	3	2	1	1	592	68
Q61687	Transcriptional regulator ATRX OS=Mus musculus GN=Atrx PE=1 SV=3 - [ATRX_MOUSE]	3	1	1	1	2476	278

Supplemental table 1. (continued)

Accession	Description	Score	Coverage	# Peptides	# PSM	# AAs	MW [kDa]
Q8BKT8-2	Isoform 2 of HAUS augmin-like complex subunit 7 OS=Mus musculus GN=Haus7 - [HAUS7_MOUSE]	3	4	1	1	248	28
Q62407-2	Isoform 2 of Striated muscle-specific serine/threonine-protein kinase OS=Mus musculus GN=Speg - [SPEG_MOUSE]	3	2	1	1	861	94
O88508	DNA (cytosine-5)-methyltransferase 3A OS=Mus musculus GN=Dnmt3a PE=1 SV=2 - [DNM3A_MOUSE]	3	1	1	1	908	102
O54774	AP-3 complex subunit delta-1 OS=Mus musculus GN=Ap3d1 PE=1 SV=1 - [AP3D1_MOUSE]	3	1	1	1	1199	135
Q9WUM3	Coronin-1B OS=Mus musculus GN=Coro1b PE=1 SV=1 - [COR1B_MOUSE]	3	2	1	1	484	54
Q8BQM8	Echinoderm microtubule-associated protein-like 5 OS=Mus musculus GN=Eml5 PE=2 SV=2 - [EMAL5_MOUSE]	3	1	1	1	1977	220
Q9JIT1	RING finger protein 32 OS=Mus musculus GN=Rnf32 PE=2 SV=1 - [RNF32_MOUSE]	3	4	1	1	368	42
Q925I7-2	Isoform 2 of Platelet-derived growth factor D OS=Mus musculus GN=Pdgfd - [PDGFD_MOUSE]	3	3	1	1	364	42
Q5DU28-3	Isoform 3 of Pecanex-like protein 2 OS=Mus musculus GN=Pcnxl2 - [PCX2_MOUSE]	3	1	1	1	1121	121
P28741	Kinesin-like protein KIF3A OS=Mus musculus GN=Kif3a PE=1 SV=2 - [KIF3A_MOUSE]	3	1	1	1	701	80
Q99PL5-5	Isoform RRp16.8 of Ribosome-binding protein 1 OS=Mus musculus GN=Rrbp1 - [RRBP1_MOUSE]	3	3	1	1	398	42
Q6NZL8-3	Signal peptide, CUB and EGF-like domain-containing protein 1 OS=Mus musculus GN=Scube1 - [SCUB1_MOUSE]	3	1	1	1	961	104
A2AM05-2	Isoform 2 of Centlein OS=Mus musculus GN=Cntln - [CNTLN_MOUSE]	3	3	1	1	318	36
Q9D952	Envoplakin OS=Mus musculus GN=Evpl PE=2 SV=3 - [EVPL_MOUSE]	3	0	1	1	2035	232

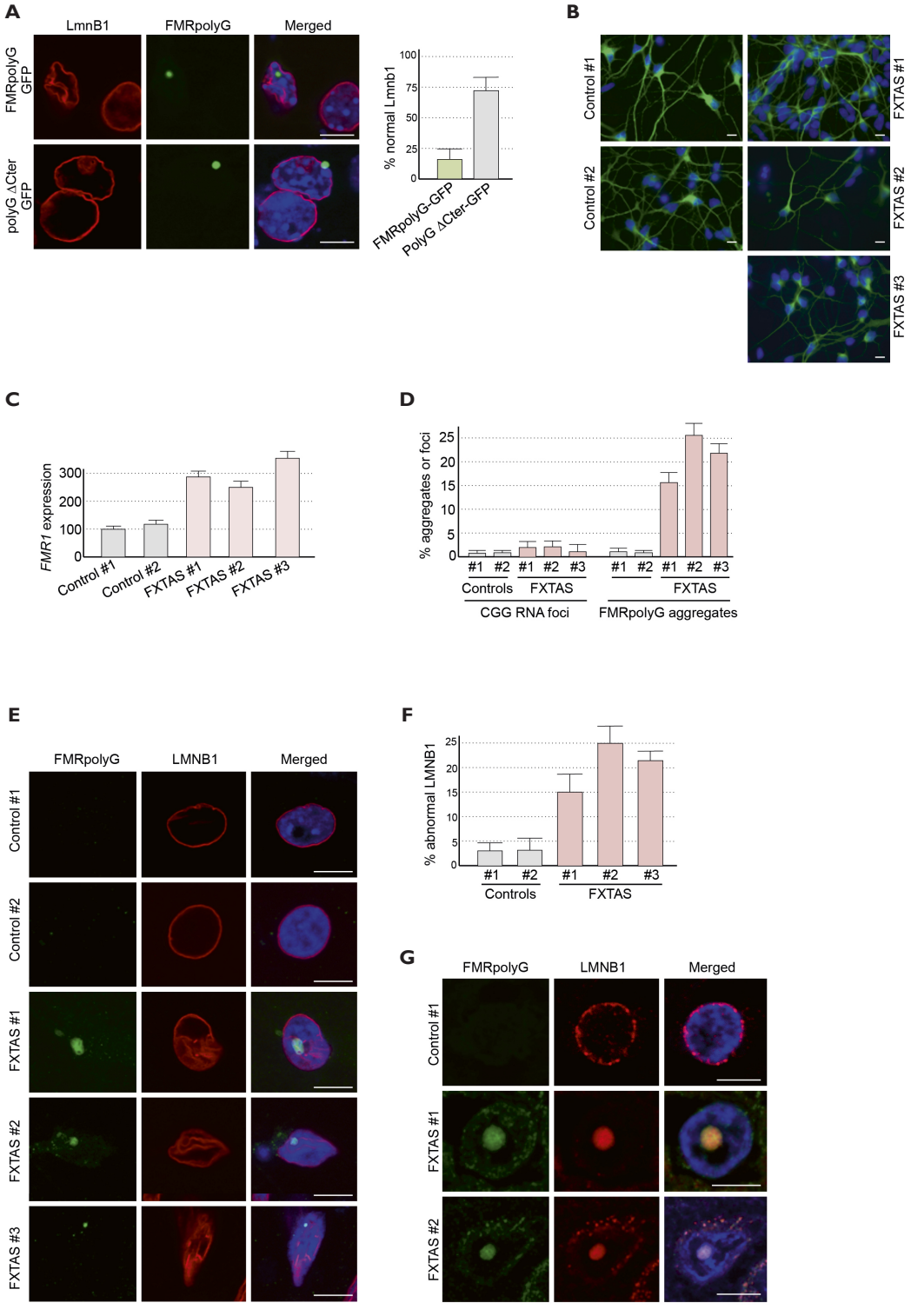
A
LmnB1
FMRpolyG
Merged
FMRpolyG GFP
polyG ΔCter GFP
% normal Lmnb1
100
75
50
25
0
FMRpolyG-GFP
PolyG ΔCter-GFP
B
Control #1
Control #2
FXTAS #1
FXTAS #2
FXTAS #3
C
FMR1 expression
300
200
100
0
Control #1
Control #2
FXTAS #1
FXTAS #2
FXTAS #3
D
% aggregates or foci
25
20
15
10
5
0
#1 #2 #1 #2 #3 #1 #2 #1 #2 #3
Controls
FXTAS
FXTAS
CGG RNA foci
FMRpolyG aggregates
E
FMRpolyG
LMNB1
Merged
Control #1
Control #2
FXTAS #1
FXTAS #2
FXTAS #3
F
% abnormal LMNB1
25
20
15
10
5
0
#1 #2 #1 #2 #3
Controls
FXTAS
G
FMRpolyG
LMNB1
Merged
Control #1
FXTAS #1
FXTAS #2

Supplemental Video 1 and 2

Ledge test of 3 months old bigenic CMV-cre / full-length or deleted *FMR1* 5'UTR transgenic mice indicates that FMRpolyG-expressing mice present some gait instability and increase foot slippage compared to CGG RNA only-expressing mice.

Supplemental video's are available online

← **Supplemental Figure 4.** FMRpolyG interacts with LAP2ß and alters nuclear lamina
(**A**) Left panel, immunofluorescence using antibodies against FMRpolyG N-terminal part (8FM antibody, green) and Lamin B1 (red) in primary cultures of E18 mouse cortical neurons transfected with expanded CGG repeats embedded within the full-length or C-terminus deleted 5'UTR of *FMR1*. Right panel, quantification of normal lamin B1 nuclear round architecture in GFP-positive transfected neurons (n=100 neurons, 3 independent transfections). (**B**) Immunofluorescence using anti-MAP2 antibody on neuronal cultures differentiated 40 days from iPS cells of FXTAs patients or control individuals. (**C**) *FMR1* mRNA expression relative to *RPLP0* in neuronal cultures (n=3) differentiated 40 days from iPS cells of FXTAs patients or control individuals. Error bars indicate s.e.m. (**D**) Quantification of CGG nuclear RNA foci and FMRpolyG nuclear aggregates in neurons differentiated 40 days from iPS cells originating from FXTAS or control individuals (n=100 neurons, 3 independent cell cultures). (**E**) Immunofluorescence using antibodies against the N-terminal part of FMRpolyG (green, 8FM antibody) and Lamin B1 (red) on neuronal cultures differentiated 40 days from iPS cells of FXTAs patients or control individuals. (**F**) Quantification of abnormal intranuclear lamin B1 labeling in neurons differentiated 40 days from iPSC of FXTAS or control individuals (n=100 neurons, 3 independent cultures). (**G**) Immunofluorescence using antibodies against the N-terminal part of FMRpolyG (green, 8FM antibody) and Lamin B1 (red) on brain sections (hippocampal area) of FXTAS patients or age-matched control individual. For all images, scale bars, 10 µm. Nuclei were counterstained with DAPI.

INHIBITION OF THE FORMATION OF INTRANUCLEAR INCLUSIONS BY SMALL CHEMICAL COMPOUNDS IN AN INDUCIBLE NEURONAL CELLULAR MODEL FOR FXTAS

R.A.M. Buijsen[1], H. de Boer[1], E.A.W.F.M. Severijnen[1], M. Minneboo[1], R.F.M. Verhagen[1], M. Schoof[1], V. de Korte[1], R.F. Berman[2], N. Charlet-Berguerand[3], D.G. Wansink[4], M.D. Disney[5], R. Willemsen[1], R.K. Hukema[1]

[1] Department of Clinical Genetics, Erasmus MC, Rotterdam, the Netherlands
[2] Department of Neurological Surgery, UC Davis, Davis, USA
[3] Department of Neurobiology and Genetics, IGBMC, Illkirch, France
[4] Department of Cell Biology, Radboud Institute for Molecular Life Sciences, Nijmegen, the Netherlands
[5] Department of Chemistry and Translational Research Institute, The Scripps Research Institute, Scripps Florida, USA

Manuscript in preparation

INTRODUCTION

Fragile X-associated Tremor/Ataxia syndrome (FXTAS) is a late-onset neurodegenerative disorder caused by an expansion of an CGG repeat (55-200) in the 5'untranslated region (UTR) of the Fragile X Mental Retardation 1 (FMR1) gene [1]. In a meta-analysis, the prevalence of the FMR1 premutation (PM) is estimated to be 1:855 in males and 1:291 in females [2]. The two main clinical features of FXTAS are intention tremor and cerebellar gait ataxia, often accompanied by several comorbidities including short-term memory loss, executive function deficits, cognitive decline, parkinsonism, peripheral neuropathy, lower limb proximal muscle weakness, and autonomic dysfunction [3]. FXTAS neuropathology includes mild brain atrophy, hyper intensity of the middle cerebellar peduncle (MCP) and splenium of the corpus callosum (SCC), loss of Purkinje cells and Bergman gliosis [1, 3-5]. In post-mortem brain tissue from patients with FXTAS the major pathological hallmark is the presence of ubiquitin-positive intranuclear inclusions throughout the brain, in both neurons and astrocytes [6, 7]. Pathology is not only limited to the central nervous system, but intranuclear inclusions are also found in non-central nervous system organs [8-13]. Molecular findings include elevated FMR1 mRNA levels (2 to 8 fold in leucocytes) and slightly reduced fragile X mental retardation protein (FMRP) levels [14-16]. FMR1 mRNA is found in intranuclear inclusions in isolated nuclei and post-mortem brain tissue of FXTAS patients [17, 18]. Furthermore, Todd, et al. demonstrated that via repeat-associated non-AUG (RAN) translation, a polyglycine-containing protein (FMRpolyG) is expressed in cell culture, animal models, and post-mortem brain tissue from FXTAS patients [19]. Altogether, two disease mechanisms for FXTAS have been proposed (reviewed in [20]). The first hypothesis is an RNA gain-of-function mechanism in which the FMR1 RNA containing an expanded CGG repeat sequesters RNA-binding proteins. In turn these proteins can bind other proteins. Depletion of these proteins disturbs critical processes and leads to aberrant miRNA processing, altered RNA splicing, stress and immune effects [18, 21-23]. A second, recently proposed mechanism is a RAN protein gain-of-function mechanism. The exact pathological mechanism is not clear yet, but is has been reported that the polyglycine stretch of FMRpolyG promotes aggregation and the C-terminal part of FMRpolyG drives toxicity (Sellier, et al., manuscript in preparation). Indeed, it has been shown that FMRpolyG protein accumulates in intranuclear inclusions [9, 19] and thus FMRpolyG could contribute to the sequestration of proteins preventing their normal cellular function as well. In addition, a role of free toxic FMRpolyG to the underlying disease mechanism cannot be excluded. To understand the contribution of repeat bearing RNA molecules and FMRpolyG protein in FXTAS, we have generated different mouse models for FXTAS ([24, 25] and Sellier, et al., manuscript in preparation). In an inducible, brain specific mouse model, both ubiquitin- and FMRpolyG-positive intranuclear inclusions were found and their number increases over time and correlates with deficits in functional

tests. Furthermore it has been shown that, by stopping mutant RNA expression, we can halt further disease progression. Strikingly, stopping mutant RNA expression early in the disease process results in reversibility of neuropathology [24]. These results suggest that an early intervention might be beneficial for patients with FXTAS and PM carriers and opens the quest for targeted therapeutic interventions.

Here, we report new inducible cellular models to study FXTAS. Mouse embryonic fibroblasts (MEFs) were derived from dox-inducible mice. In these MEFs RNA levels (expanded CGG fused with GFP) can be reduced by using RNase H-mediated cleavage of the target mRNA. However, no obvious pathology is found in these cells, therefore we also setup a primary neuronal cell culture from the inducible mice. In this new inducible neuronal cell model, induced expression of RNA containing an expanded CGG repeat leads to the formation of ubiquitin- and FMRpolyG-positive inclusions in both neurons and astrocytes. The number of these inclusions increase over time. Next, we studied the effect of small molecules that bind to the internal GG-loop of FMR1 RNA containing the expanded CGG repeat. These compounds prevent both the binding of RNA-binding proteins to the hairpin structure and RAN translation. Our results suggest that it is possible to partially prevent inclusion formation by these small chemical compounds and opens new avenues for a targeted therapeutic intervention.

RESULTS

Reduction of CGG GFP RNA levels by using an antisense oligonucleotide approach

Previously, we reported that it is possible to reverse neuropathology in an inducible mouse model of FXTAS by stopping expression of RNA containing the expanded CGG repeat [24]. After this proof-of-principle for reversibility, the next challenge is to develop a targeted therapeutic intervention. Since the pathogenic trigger for FXTAS, the FMR1 RNA containing an expanded CGG repeat, is well known, the most straightforward approach to develop such an intervention is to target this pathogenic trigger. To test potential therapeutic interventions we setup a mouse embryonic fibroblast (MEF) culture derived from the inducible bigenic TRE-nCGG-eGFP/hnRNP-rtTA mice [25]. In these cells, either RNA containing the 5'UTR of the FMR1 gene with a control size of 11 CGG repeats or RNA containing the 5'UTR of the FMR1 gene with a PM size of 90 CGG repeats was coupled to eGFP. Addition of doxycycline (dox) to the culture medium resulted in expression of CGG RNA and eGFP protein. No GFP-positive cells were observed in cultures without dox and control cultures containing only one of the two transgenes. (**Figure. 1A** and data not shown). The levels of CGG RNA and GFP protein expression showed a dox dosage-dependent effect (data not shown). We started an initial characterization of these MEFs using several FXTAS pathology hallmarks, including RNA

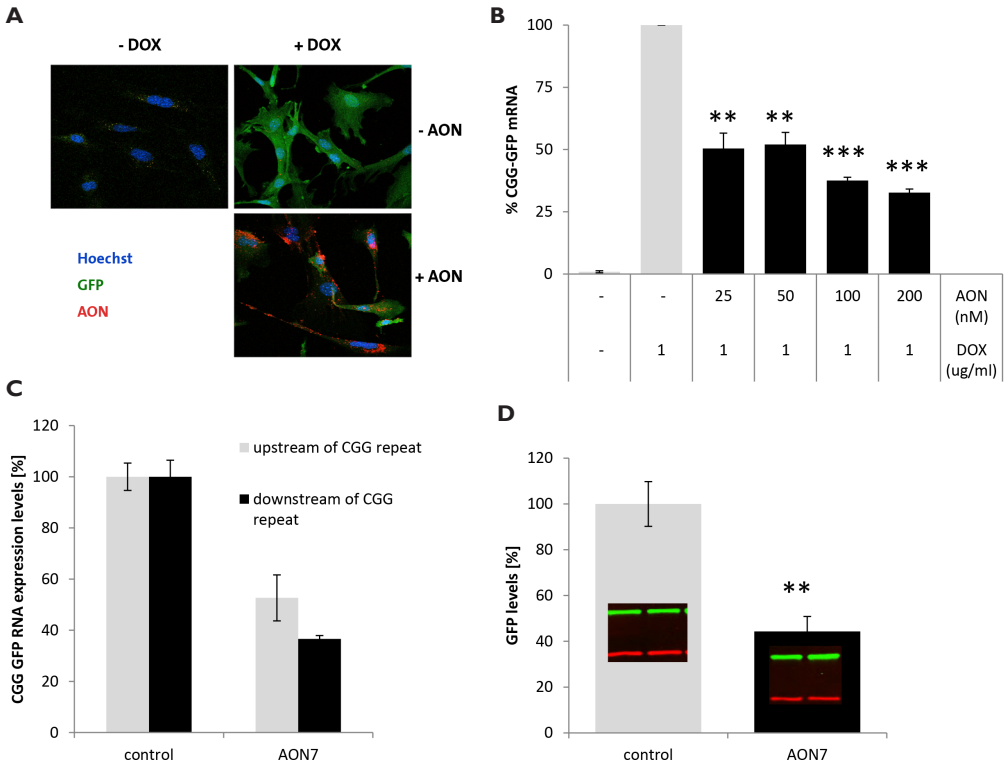

Figure 1. (**A**) eGFP expression and AON transfection eGFP expression (green) after dox-induction of bigenic TRE-nCGG-eGFP/hnRNP-rtTA MEFs. No eGFP expression is observed in bigenic cultures without dox. MEFs were successfully transfected using a Cy5 labelled AON (red) directed to the GFP sequence in the RNA. (**B**) CGG-GFP RNA expression levels. Quantitative RT-PCR showed that different concentrations of GFP-AON can significantly reduce CGG-GFP RNA levels. (**C**) RNA expression levels after transfection of 100 nM GFP-AON. Quantitative RT-PCR showed that 100 nM of GFP-AON can significantly reduce CGG-GFP RNA levels. Using primer sets located up- and downstream of the CGG repeat, no difference in reduction of RNA expression levels is found. (**D**) eGFP protein levels after transfection of 100 nM GFP-AON. A quantitative Western blot showed that 100 nM of GFP-AON can significantly reduce eGFP protein levels.

foci, ubiquitin-positive intranuclear inclusions and nuclear lamin A/C disorganisation. None of these hallmarks could be observed in the inducible MEFs (data not shown). Even the use of culture medium with low fetal calf serum (FCS) levels preventing the cells to divide and allowing the CGG RNA to accumulate did not result in any obvious pathology.

Despite the fact that no pathology was observed in MEFs, these cells could be used for targeting the mutant RNA for degradation. Reduced expression of (toxic) RNA molecules can be established by antisense oligonucleotides (AONs) using the gapmer technology. These AONs contain a phosphorothioate-modified, nuclease-resistant DNA segment

activating RNase H cleavage of target mRNAs (reviewed in [26]). These gapmers are flanked with 2′-O-methyl RNA designed to confer increased nuclease stability and affinity of the AONs to the target mRNA [27]. To explore the possibilities of targeting FMR1 RNA for RNase H-mediated breakdown, we transfected different concentrations of an AON (Cy5 labelled) directed to the GFP sequence in the RNA, using our inducible MEFs (**Figure 1A**). Quantitative RT-PCR showed that the GFP-AON can significantly reduce CGG-GFP RNA levels down to approximately 30% when compared with untransfected dox-treated cells (**Figure 1B**). The reduction in CGG-GFP RNA levels were shown with primer sets both upstream and downstream of the CGG repeat. For both primer sets, similar effects on RNA levels were found, suggesting the CGG-GFP RNA is degraded efficiently (**Figure 1C**). A quantitative Western blot for GFP protein levels confirmed effectiveness of the GFP-AON, since the use of 100 nM of GFP-AON resulted in a similar reduction of GFP protein level as was found for CGG-GFP RNA (**Figure 1D**).

Intranuclear inclusions in an inducible neuronal cell model for FXTAS

To further determine the effectiveness of a therapeutic intervention approach other read-outs are needed besides the levels of CGG-GFP RNA and eGFP protein levels. Thus, we setup primary hippocampal neuronal cell cultures derived from the inducible TRE-nCGG-eGFP/hnRNP-rtTA mice [25]. These cultures were derived from E18 embryos from timed-breedings with heterozygous transgenic mice. This will result in a mixture of CGG-GFP RNA positive and negative cells. Indeed, addition of dox to the culture medium resulted in GFP-positive and GFP-negative cells in cultures from both 11CGG and 90CGG target mice. No GFP-positive cells were observed in bigenic cultures without the addition of doxycycline to the culture medium and control cultures containing only one of the two transgenes (**Figure 2A** and data not shown).

To test if intranuclear inclusions could be formed in the primary hippocampal neuronal cell cultures, we performed immunofluorescence (IF) staining for ubiquitin. The first ubiquitin-positive inclusions were observed in GFP-positive cells in TRE-90CGG-eGFP/hnRNP-rtTA cultures after 10 days of dox-induction. The number of ubiquitin-positive intranuclear inclusions significantly increases in time to 37% of the GFP positive cells at 24 days of dox-induction (**Figures 2B-C**). Previously, co-localisation of ubiquitin and FMRpolyG has been demonstrated in the vast majority of inclusions in transfected cells, brain tissue of mouse models and post-mortem brain tissue from patients with FXTAS [9, 19, 24]. In IF double stainings on inducible hippocampal mouse neurons it has been shown that most of the intranuclear inclusions stain positive for both ubiquitin and FMRpolyG (Fig. 2D). To study which cell types contain an intranuclear inclusion, we performed IF double stainings in the primary neuronal cell cultures. We found that FMRpolyG- and ubiquitin-

positive intranuclear inclusions can be found in both neurons and astrocytes by staining for the neuronal marker microtubule-associated protein 2 (MAP2), or the astrocytic marker glial fibrillary acidic protein (GFAP) (**Figures 3A-B**). More specifically, with antibodies against gamma-aminobutyric acid (GABA) and Ca2+/calmodulin-dependent protein kinase II (CamKII) we could demonstrate that intranuclear inclusions can be found in both inhibitory and excitatory neurons, respectively (**Figures 3C-D**).

Therapeutic interventions: small chemical RNA-binding compounds

Next to degrading the mutant CGG RNA molecules, another approach to develop a therapeutic intervention is to shield the expanded CGG repeat in the RNA and thus prevent it from causing damage. For several repeat associated disorders such compounds have been described (reviewed by [28]). In case of FXTAS, the laboratory of Matthew Disney developed several small chemical compounds, which can bind to the internal GG-loop of the expanded CGG repeat in the RNA [29].

First, compound 1a and 2HE-5NMe were tested for toxicity. Titration experiments showed that using concentrations of 1 and 10 nM of either compound, the cells were viable up to 24 days after compound administration, whereas higher concentrations of both compounds were toxic to the cells (data not shown).

Next, we performed IF stainings and the number of FMRpolyG-positive intranuclear inclusions were quantified. First the compounds were added 1 day prior to the start of dox induction followed by 17 and 24 days of dox treatment. Significantly less intranuclear inclusions were observed with a concentration of both 1 and 10 nM of either compound 1a or 2HE-5NMe (**Figures 4A-B**).The addition of the compounds one week after start of dox-induction resulted also in a significant reduction of the number of intranuclear inclusions compared with untreated cultures. No significant difference was observed compared with cultures that received the compound prior to the dox-induction (**Figure 4B**).

DISCUSSION

Cellular and animal models have significantly contributed to our understanding of the underlying disease mechanisms of FXTAS. Recently, reversibility of both neuropathology and functional deficits were demonstrated in an inducible FXTAS mouse model. The formation of intranuclear inclusions is reversible if expression of the expanded CGG repeat is stopped at an early stage (8 weeks). Stopping expression at a later time point (12 weeks) showed that the formation of inclusions can be halted, however, reversibility could not be demonstrated. Moreover, a functional deficit in the compensatory eye movements of mice could be halted as well by stopping RNA expression [24]. This study demonstrated a proof-of-principle that effective treatments

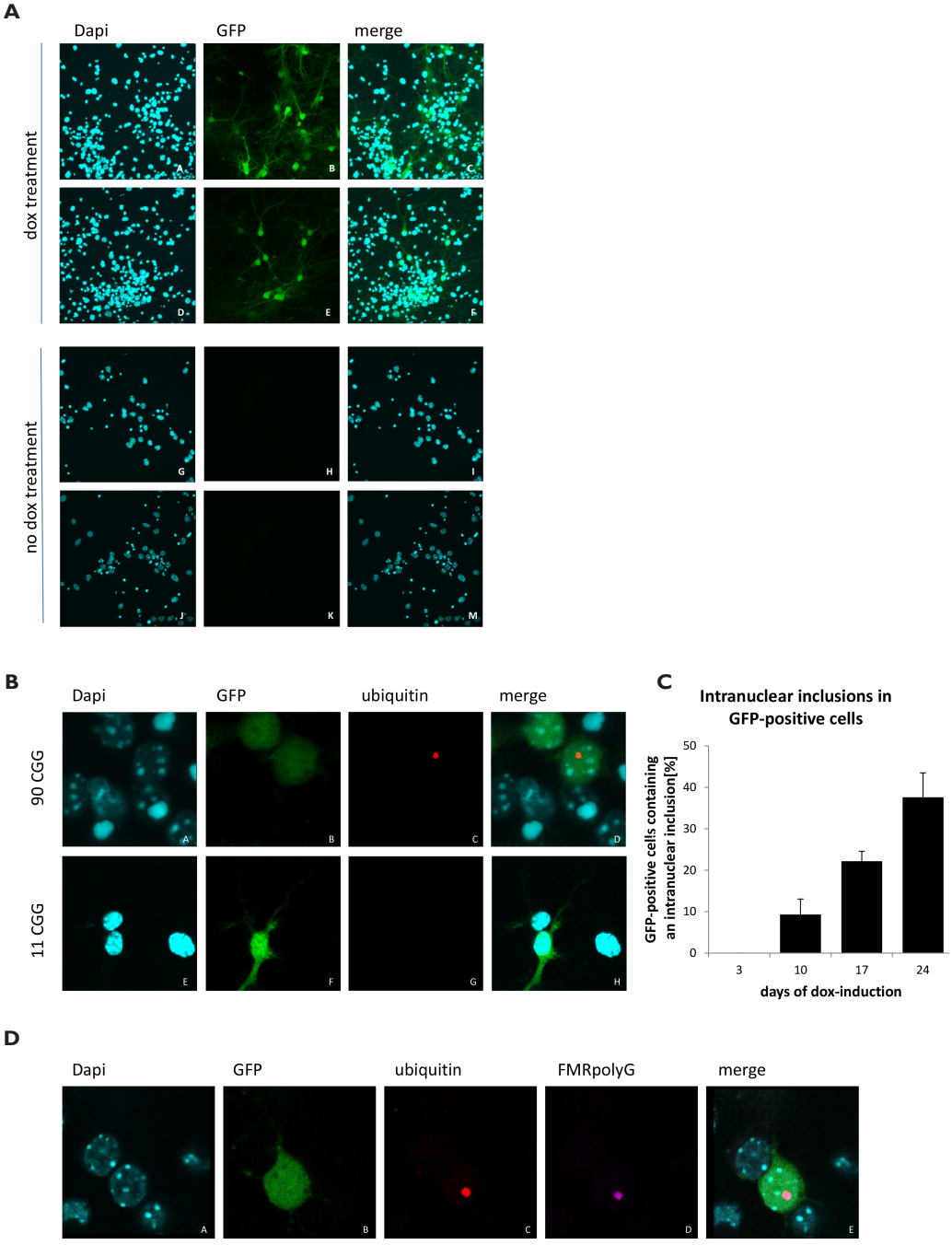

Figure 2. (**A**) eGFP expression (green) after dox-induction of bigenic TRE-nCGG-eGFP/hnRNP-rtTA primary hippocampal neurons. No eGFP expression is observed in bigenic cultures without dox. (**B**) Ubiquitin-positive intranuclear inclusions (red) are found in GFP-positive TRE-90CGG-eGFP/hnRNP-rtTA cells, but not in GFP-positive TRE-11CGG-eGFP/hnRNP cells or GFP-negative cells. (**C**) Quantification of intranuclear inclusions in GFP-positive cells. The percentage of GFP-positive nuclei containing GFP-positive inclusions after different dox-treatment periods. (**D**) Co-localisation of ubiquitin (red) with FMRpolyG (purple) in intranuclear inclusions.

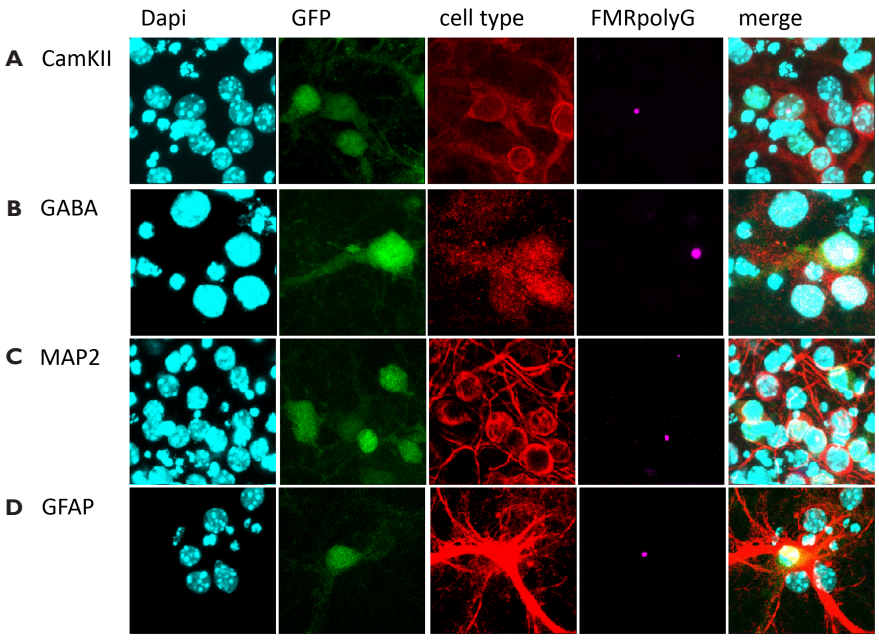

Figure 3. FMRpolyG and ubiquitin-positive intranuclear inclusions can be found in both neurons (inhibitory and excitatory) and astrocytes in primary hippocampal cultures. IF double stainings show that intranuclear inclusions can be found in (**A**) CamKII-, (**B**) GABA-, (**C**) MAP2-, and (**D**) GFAP-positive cells.

for patients with FXTAS might be possible. In the search for therapeutic interventions a first step would be to test these interventions in a cellular model, using disease specific outcome measures. It has been shown that both the FMR1 RNA and ubiquitin accumulate in intranuclear inclusions in post-mortem FXTAS brain and in transfected cells [6, 17, 18]. Furthermore, abnormal cellular distribution of lamin A/C has been shown in human FXTAS fibroblasts and MEFs generated from a knock-in (KI) mouse model [30]. To establish such an in vitro model we isolated MEFs from the inducible mouse model for FXTAS [25]. Although we used a variety of different culturing conditions (e.g. inducing stress by serum starvation) none of the characteristics seen in post-mortem FXTAS brain tissue or FXTAS mouse brain tissue, including RNA foci, ubiquitin- and FMRpolyG-positive intranuclear inclusions or abnormal nuclear distribution of lamin A/C [6, 9, 17-19, 31, 32], could be detected in MEFs generated from the inducible mouse model. This suggests that MEFs are not the most appropriate cell type to study disease pathology. Nevertheless, as a proof-of-principle the CGG-GFP RNA molecules can be targeted for RNase H-mediated degradation by using an AON against GFP. Our results suggest that it is possible to reduce CGG-GFP RNA levels using an AON approach. QPCR primer sets both upstream and downstream of the CGG repeat showed a similar reduction of CGG-GFP RNA, suggesting that the CGG-GFP RNA was degraded efficiently. In addition

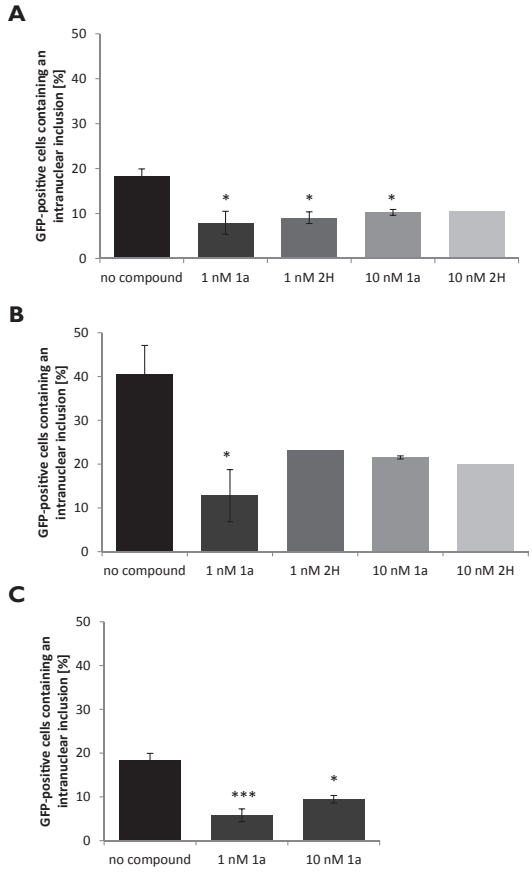

Figure 4. Quantification of intranuclear inclusions. FMRpolyG-positive intranuclear inclusions were quantified. Significantly less intranuclear inclusions were observed with a concentration of both 1 and 10 nM of either compound 1a or 2HE-5NMe. Compounds were added 1 day prior to the start of dox induction followed by (**A**) 17 and (**B**) 24 days of dox treatment. No significant difference was found between compound 1a and 2HE-5NMe or the concentrations used. (**C**) Addition of the compounds one week after start of dox-induction resulted also in a reduction of the number of intranuclear inclusions compared with untreated cultures. No significant difference was observed compared with cultures that received the compound prior to the dox-induction.

a similar reduction of GFP protein was seen. Since both the 5' and 3' flanking sequences of the CGG repeat are degraded, it is assumed that the CGG repeat is degraded as well. However, this will need to be verified with an in situ hybridisation experiment. As proof-of-principle we used an AON directed to a sequence of GFP. Next the optimal specific sequence for efficient degradation of FMR1 RNA molecules has to be determined for AONs. After establishing an efficient degradation of FMR1 RNA containing an expanded CGG repeat by AONs in vitro, effectiveness will need to be confirmed in vivo. Initially the inducible mice ubiquitously expressing RNA containing the expanded CGG repeat seem most valuable. We have shown that these mice die within 5 days of expression [25]. These mice show mitochondrial dysfunction in the liver that might be rescued by the AON, preventing the death of these mice as outcome measure. As the AON does not need to cross the blood-brain-barrier we can easily test its effectiveness in vivo with a reliable read-out. Next, we can test the compounds in mouse lines with brain specific expression of the RNA containing the expanded CGG repeat, which we used for the reversibility study [24].

On the other hand it might prove difficult to rescue a phenotype that is caused by such massive overexpression as in the inducible mice. Liver cells express the 90CGG-GFP RNA approximately 600 times more than endogenous Fmr1 RNA levels [25]. The effect of the AON might appear only small, while in fact the impact of mutant RNA degradation will appear much greater in for example KI mice or in fibroblasts from patients with FXTAS, both having only 2 to 3 fold elevated FMR1 mRNA levels. For several microsatellite disorders AON-related therapies have been very successful in both cellular and animal models. In fibroblasts derived from patients suffering from frontotemporal degeneration (FTD)/amyotrophic lateral sclerosis (ALS) (C9FTD/ALS) both RNA levels and intranuclear RNA-positive foci can be reduced by several c9orf72 RNA specific AONs [33]. In addition, a single intracerebroventricular (ICV) stereotactic injection of a mouse specific c9orf72 AON into the right lateral ventricle of control animals resulted in a 60-70% reduction of c9orf72 RNA levels in spinal cord and brain [33]. Reduced RNA levels can be found up to 18 weeks post injection. Similar observations have been made in a mouse model for Huntington's disease (HD) [34].

A drawback of this strategy is that degradation of FMR1 mutant mRNA will ultimately result in lower levels of functional fragile X mental retardation protein (FMRP). Lack of FMRP causes fragile X syndrome, the most common inherited form of intellectual disability [35]. To date, it is unknown whether depletion of FMRP later in life may cause a fragile X syndrome phenotype. To prevent such effects proper titration of AONs and residual FMRP levels is required.

Another, more disease related in vitro model are the primary hippocampal neurons derived from the inducible mice. We were able to show that dox induces expression of GFP and thus CGG RNA in these cells, without any leakage of the tet-On system. The formation of inclusions staining positive for both ubiquitin and FMRpolyG, together with the presence of these inclusions in both neurons and astrocytes, like in post-mortem brain material from patients with FXTAS, points to a good in vitro model to further test possible therapeutic interventions for FXTAS. After supplementation of dox to the culture medium approximately 25% of the cells show GFP expression, as expected by mendelian inheritance. In contrast to the inducible mouse model or cultured MEFs, it is not possible to study reversibility in these cells. Culture medium cannot be replaced, because neurons need factors secreted by astrocytes for neuronal survival, synapse formation, and plasticity [36]. One way to overcome this problem is to use culture medium from cells cultured at the same day.

Our primary neuronal cell culture model shows the presence of characteristic intranuclear inclusions in both neurons (excitatory and inhibitory) and astrocytes illustrating similarities between this model and post-mortem brain tissue from patients with FXTAS [6]. To date, the role of inclusions in both neurons and astrocytes in

the pathogenesis of FXTAS is unknown. To dissect the contribution of these different cell types in the pathogenesis of FXTAS we started to generate new, cell type specific, rtTA driver lines.

The use of small chemical compounds that shield the CGG repeat (reviewed in [28]) has great potential to ameliorate FXTAS. It has been shown that RNA containing an expanded CGG repeat forms hairpin structures with periodically repeating internal GG-loops. The laboratory of Matthew Disney developed several RNA binding small molecule compounds targeting the internal GG-loop of the expanded CGG repeat [29, 37-39]. In transfected COS7 cells that transiently expressed RNA containing an expanded CGG repeat they showed that 2 of these compounds, called 1a and 2HE-5NMe, can improve FXTAS-associated pre-mRNA splicing defects and reduce the size and number of nuclear RNA foci. Furthermore, the binding of these compounds does not affect translation of the downstream open reading frame (ORF) [29, 40, 41]. The advantage of this approach is that it prevents RNA-binding proteins from binding to the hairpin structure and additionally the small molecules will block RAN translation, without having an effect on the translation of FMR1 mRNA. In the inducible neuronal cultures the number of intranuclear inclusions is significantly reduced by adding compound 1a and 2HE-5NMe to the culture medium. This suggests that the use of compounds is a promising intervention strategy and it is crucial to test these compounds in both the ubiquitous expressing and the brain specific inducible mouse models using survival, liver pathology, neuropathology and animal behaviour as outcome measures. A similar approach has been used for c9FTD/ALS. Small chemical compounds targeting RNA containing the expanded GGGGCC repeat were designed and found to significantly inhibit RAN translation and foci formation in cultured cells expressing mutant RNA in neurons transdifferentiated from fibroblasts of repeat expansion carriers. To date, there are no publications about the use of small chemical compounds in animal models.

Furthermore, it has been shown that iPSC-derived fragile X premutation neurons have reduced postsynaptic density protein 95 (PSD95) expression, reduced synaptic puncta density, and reduced neurite length [42]. More recently it has been shown that FMRpolyG and LAP2β can be detected in intranuclear inclusions in iPSC-derived neurons (Sellier, et al., manuscript in preparation). It would be interesting to study the effect of small chemical compounds on patient-derived neuronal cell culture, using relevant outcome measures. In addition, with the recent introduction of automated, large-scale iPSC-cell culture methods it would be interesting to perform an unbiased drug screen or to determine effectiveness of therapeutic interventions in iPSC-derived neurons from patients with FXTAS.

MATERIALS AND METHODS

Isolation of mouse embryonic fibroblasts

E12,5 TRE-nCGG-GFP/hnRNP-rtTA embryos were decapitated after which limbs, tail and inner organs were removed. Embryos were pulled three times through a 19G and 23G needle, respectively. Minced embryos were cultured in DMEM medium (Lonza) containing 10% fetal calf serum (FCS), penicillin/streptomycin (Gibco), and MEM non-essential amino acids (Gibco).

AON treatment

A Cy5 labelled phosphorothioate-modified AON flanked with 2′-O-methyl RNA was dissolved in RNase free water. The AON was directed at a sequence in GFP: 5'-/5Cy5/mC*mU*mC*mG*mC*C*G*G*A*C*A*C*G*C*T*mG*mA*mA*mC*mU-3' (IDT). MEFs were transfected using 3 µl GeneJuice transfection reagent (Novagen) according to manufacturer's instructions.

RNA isolation and quantitative PCR

RNA was isolated using the RNeasy Mini Kit (Qiagen) according to manufacturer's instructions. Then, reverse transcriptase was performed on 1 µg of RNA using iScript cDNA synthesis kit (Biorad) according to manufacturer's instructions. Q-PCR using SYBR Green (KAPA Biosystems) was performed on 0.1 µl RT product. Cycling conditions were an initial denaturation of 3 minutes at 95°C, followed 40 cycles of 5 seconds 95°C and 30 seconds 60°C. Actin was used as a reference gene.

Western blotting

Thirty µg of total protein cell lysate was loaded to Criterion XT precast gels (4-12% bis-tris) (Biorad) and run in MOPS buffer (0.05M Mops, 0.05M Tris, 3.5 mM SDS, 1mM EDTA, pH 7.7). The gel was blotted to a nitrocellulose membrane in TG buffer (0.192M glycine, 0.025M Tris, 20% methanol). After blocking in PBS-Tween, the membrane was incubated overnight with rabbit anti-GFP (1:100.000 Abcam) and mouse anti-GAPDH (1:200.000 Chemicon) antibodies. The secondary antibodies were goat-anti-rabbit IRDye 800cW and donkey-anti-mouse IRDye 680LT (both 1:10.000; Li-Cor). The membrane was scanned with an Odyssey Infrared Imager and analysed with Odyssey software.

Primary hippocampal neuron culture

Primary hippocampal neurons were cultured as described before [43]. In summary, up to 8 E17-E18 TRE-nCGG-GFP/hnRNP-rtTA embryos from time point pregnancies using heterozygous hnRNP-rtTA fathers and heterozygous TRE-nCGG-eGFP mothers were decapitated after which hippocampi were removed and dissociated with trypsin/EDTA.

Cells were plated on poly-D-lysine (100 µg/ml, Sigma) and laminin (50 µg/ml, Sigma) coated 30 mm glass coverslips and attached to the substrate in a drop of neurobasal medium (Gibco), containing penicillin/streptomycin (Gibco), glutamax (Gibco) and B-27(Gibco) supplements (NBM+++). After 90 minutes, medium volume was adjusted to 2 ml per coverslip in a 6-well plate. Doxycycline treatment started after 4 days (+/- 1 day).

Compound treatment

Compound 1a and 2HE-5NMe were dissolved in DMSO at final concentrations of 2 and 20 µM, respectively. One µl was added to 2ml of NBM+++ culture medium.

Immunofluorescence

Cells were fixed in 4% paraformaldehyde (PFA) in phosphate-buffered saline (PBS) for 15 minutes and permeabilised with 0.5% Triton X-100 in PBS for 10 minutes. IF (double) stainings were performed overnight at 4°C using rabbit anti-ubiquitin (Dako Z0458; 1:250), mouse anti-ubiquitin (Cytoskeleton AUB01-S; 1:200), rabbit anti-GFAP (Sigma G9269; 1:200), mouse anti-Map2 (Roche #1284959; 1:400), rabbit anti-GABA (Sigma A2052; 1:100), mouse anti-CaMKII (Chemicon Mab3119; 1:100) or mouse anti-FMRpolyG (8FM and 9FM [9]; 1:10) antibodies. Secondary antibodies include anti-mouse Cy3 (JacksonImmunoResearch 715-165-150; 1:200) and anti-rabbit Cy5 (JacksonImmunoResearch 711-175-152 1100; 1:200). Nuclei were visualised using Hoechst and slides were mounted with ProLong® Gold antifade reagent. Analysis was performed with a Leica confocal microscope and LAS AF software.

REFERENCES

1. Hagerman, R.J., et al., *Intention tremor, parkinsonism, and generalized brain atrophy in male carriers of fragile X.* Neurology, 2001. **57**(1): p. 127-30.
2. Hunter, J., et al., *Epidemiology of fragile X syndrome: A systematic review and meta-analysis*. American Journal of Medical Genetics Part A, 2014. **164**(7): p. 1648-1658.
3. Jacquemont, S., et al., *Fragile X Premutation Tremor/Ataxia Syndrome: Molecular, Clinical, and Neuroimaging Correlates*. Am J Hum Genet, 2003. **72**(4): p. 869-78.
4. Hall, D.A., et al., *Emerging topics in FXTAS*. J Neurodev Disord, 2014. **6**(1): p. 31.
5. Brunberg, J.A., et al., *Fragile X Premutation Carriers: Characteristic MR Imaging Findings of Adult Male Patients with Progressive Cerebellar and Cognitive Dysfunction.* AJNR Am J Neuroradiol, 2002. **23**(10): p. 1757-1766.
6. Greco, C.M., et al., *Neuronal intranuclear inclusions in a new cerebellar tremor/ataxia syndrome among fragile X carriers.* Brain, 2002. **125**(Pt 8): p. 1760-1771.
7. Greco, C.M., et al., *Neuropathology of fragile X-associated tremor/ataxia syndrome (FXTAS).* Brain, 2006. **129**(Pt1): p. 243-255.
8. Hunsaker, M.R., et al., *Widespread non-central nervous system organ pathology in fragile X premutation carriers with fragile X-associated tremor/ataxia syndrome and CGG knock-in mice.* Acta Neuropathol, 2011. **122**: p. 467-479.
9. Buijsen, R.A., et al., *FMRpolyG-positive inclusions in CNS and non-CNS organs of a fragile X premutation carrier with fragile X-associated tremor/ataxia syndrome.* Acta Neuropathol Commun, 2014. **2**(1): p. 162.
10. Greco, C.M., et al., *Testicular and pituitary inclusion formation in fragile X associated tremor/ataxia syndrome.* J Urol, 2007. **177**(4): p. 1434-7.
11. Gokden, M., J.T. Al-Hinti, and S.I. Harik, *Peripheral nervous system pathology in fragile X tremor/ataxia syndrome (FXTAS).* Neuropathology, 2009. **29**(3): p. 280-4.
12. Louis, E., et al., *Parkinsonism, dysautonomia, and intranuclear inclusions in a fragile X carrier: A clinical-pathological study.* Movement Disorders, 2006. **21**(3): p. 420-425.
13. Tassone, F., et al., *Intranuclear inclusions in neural cells with premutation alleles in fragile X associated tremor/ataxia syndrome.* J Med Genet, 2004. **41**(4): p. E43.
14. Peprah, E., et al., *Examination of FMR1 transcript and protein levels among 74 premutation carriers*. J Hum Genet, 2010. **55**: p. 66-68.
15. Kenneson, A., et al., *Reduced FMRP and increased FMR1 transcription is proportionally associated with CGG repeat number in intermediate-length and premutation carriers*. Hum Mol Genet, 2001. **10**(14): p. 1449-1454.
16. Tassone, F., et al., *Elevated levels of FMR1 mRNA in carrier males: A new mechanism of involvement in the Fragile-X syndrome*. Am J Hum Genet, 2000. **66**(1): p. 6-15.
17. Tassone, F., C. Iwahashi, and P.J. Hagerman, *FMR1 RNA withinthe intranuclear inclusions of fragile X-associated Tremor/Ataxia syndrome (FXTAS).* RNA biology, 2004. **1**: p. 103-105.
18. Sellier, C., et al., *Sam68 sequestration and partial loss of function are associated with splicing alterations in FXTAS patients.* Embo J, 2010. **29**: p. 1248-1261.
19. Todd, P.K., et al., *CGG Repeat-Associated Translation Mediates Neurodegeneration in Fragile X Tremor Ataxia Syndrome*. Neuron, 2013. **78**(3): p. 440-455.
20. Sellier, C., et al., *The multiple molecular facets of fragile X-associated tremor/ataxia syndrome*. J Neurodev Disord, 2014. **6**(1): p. 23.
21. Sellier, C., et al., *Sequestration of DROSHA and DGCR8 by Expanded CGG RNA Repeats Alters MicroRNA Processing in Fragile X-Associated Tremor/Ataxia Syndrome.* Cell Rep, 2013. **3**(3): p. 869-880.
22. Jin, P., et al., *Pur alpha Binds to rCGG Repeats and Modulates Repeat-Mediated Neurodegeneration in a Drosophila Model of Fragile X Tremor/Ataxia Syndrome*. Neuron, 2007. **55**(4): p. 556-64.
23. Sofola, O.A., et al., *RNA-Binding Proteins hnRNP A2/B1 and CUGBP1 Suppress Fragile X CGG Premutation Repeat-Induced Neurodegeneration in a Drosophila Model of FXTAS.* Neuron, 2007. **55**(4): p. 565-71.
24. Hukema, R.K., et al., *Reversibility of neuropathology and motor deficits in an inducible mouse model for FXTAS.* Human Molecular Genetics, 2015. **24**(17): p. 4948-4957.

25. Hukema, R.K., et al., *Induced expression of expanded CGG RNA causes mitochondrial dysfunction in vivo.* Cell Cycle, 2014. **13**(16): p. 2600-2608.

26. Evers, M.M., L.J. Toonen, and W.M. van Roon-Mom, *Antisense oligonucleotides in therapy for neurodegenerative disorders*. Adv Drug Deliv Rev, 2015. **87**: p. 90-103.

27. Monia, B.P., et al., *Evaluation of 2'-modified oligonucleotides containing 2'-deoxy gaps as antisense inhibitors of gene expression.* J Biol Chem, 1993. **268**(19): p. 14514-22.

28. Childs-Disney, J.L. and M.D. Disney, *Approaches to Validate and Manipulate RNA Targets with Small Molecules in Cells*. Annu Rev Pharmacol Toxicol, 2016. **56**: p. 123-40.

29. Disney, M.D., et al., *A Small Molecule That Targets r(CGG)(exp) and Improves Defects in Fragile X-Associated Tremor Ataxia Syndrome*. Acs Chemical Biology, 2012. **7**(10): p. 1711-1718.

30. Garcia-Arocena, D., et al., *Fibroblast phenotype in male carriers of FMR1 premutation alleles*. Hum Mol Genet, 2009. **19**: p. 299-312.

31. Willemsen, R., et al., *The FMR1 CGG repeat mouse displays ubiquitin-positive intranuclear neuronal inclusions; implications for the cerebellar tremor/ataxia syndrome.* Hum Mol Genet, 2003. **12**(9): p. 949-59.

32. Iwahashi, C.K., et al., *Protein composition of the intranuclear inclusions of FXTAS*. Brain, 2006. **129**(Pt 1): p. 256-271.

33. Lagier-Tourenne, C., et al., *Targeted degradation of sense and antisense C9orf72 RNA foci as therapy for ALS and frontotemporal degeneration.* Proceedings of the National Academy of Sciences of the United States of America, 2013. **110**(47): p. E4530-E4539.

34. Kordasiewicz, H.B., et al., *Sustained therapeutic reversal of Huntington's disease by transient repression of huntingtin synthesis*. Neuron, 2012. **74**(6): p. 1031-44.

35. Willemsen, R., et al., *Timing of the absence of FMR1 expression in full mutation chorionic villi.* Human Genetics, 2002. **110**(6): p. 601-605.

36. Jones, E.V., D. Cook, and K.K. Murai, *A neuron-astrocyte co-culture system to investigate astrocyte-secreted factors in mouse neuronal development.* Methods Mol Biol, 2012. **814**: p. 341-52.

37. Parkesh, R., et al., *Design of a bioactive small molecule that targets the myotonic dystrophy type 1 RNA via an RNA motif-ligand database and chemical similarity searching.* J Am Chem Soc, 2012. **134**(10): p. 4731-42.

38. Lee, M.M., A. Pushechnikov, and M.D. Disney, *Rational and modular design of potent ligands targeting the RNA that causes myotonic dystrophy 2.* ACS Chem Biol, 2009. **4**(5): p. 345-55.

39. Su, Z., et al., *Discovery of a biomarker and lead small molecules to target r(GGGGCC)-associated defects in c9FTD/ALS*. Neuron, 2014. **83**(5): p. 1043-50.

40. Tran, T., et al., *Targeting the r(CGG) Repeats That Cause FXTAS with Modularly Assembled Small Molecules and Oligonucleotides*. Acs Chemical Biology, 2014. **9**(4): p. 904-912.

41. Yang, W.Y., et al., *Inhibition of Non-ATG Translational Events in Cells via Covalent Small Molecules Targeting RNA.* Journal of the American Chemical Society, 2015. **137**(16): p. 5336-5345.

42. Liu, J., et al., *Signaling defects in iPSC-derived fragile X premutation neurons*. Human Molecular Genetics, 2012. **21**(17): p. 3795-3805.

43. DeVrij, F.M.S., et al., *Rescue of behavioral phenotype and neuronal protrusion morphology in FMR1 KO mice.* Neurobiol Dis, 2008. **31**: p. 127-132.

GENERAL DISCUSSION

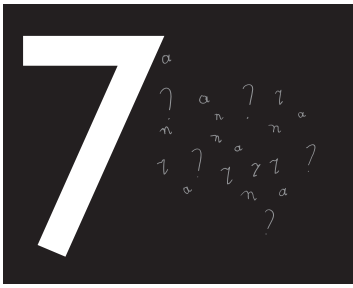

Disease mechanisms: RNA or RAN?

Fragile X-associated Tremor/Ataxia Syndrome (FXTAS) is one of the many microsatellite-expansion diseases caused by an expansion of short sequences of repetitive DNA (3-6 base pairs) in the human genome [1-4]. In addition to FXTAS examples of other, repeat containing, mostly neurodegenerative, disorders are: spinocerebellar ataxia type 8 (SCA8), myotonic dystrophy type1 (DM1), frontotemporal dementia (FTD) and amyotrophic lateral sclerosis (ALS) (both C9FTD/ALS), and Huntington disease (HD) [5-8]. In the last fifteen years a large number of studies have been performed in order to identify the underlying disease mechanism(s) of FXTAS (reviewed in [9]). Advances in molecular understanding of FXTAS is crucial to identify new biomarkers and to find potential targets for therapeutic intervention.

Over the last decade traditional biological rules have changed. The idea that a gene is transcribed in one direction and encodes for an AUG-initiated protein is no longer applicable. Genes can be transcribed bidirectionally, including many genes involved in microsatellite-expansion related diseases. The emerging role of antisense transcripts in the pathogenesis of microsatellite-expansion diseases also includes a potential role in modifying RNA stability of the toxic mRNA products [10]. In addition, genes can be transcribed without the use of a traditional start codon. This way of transcription is called "repeat associated non-AUG (RAN) translation", which can occur in all six possible reading frames (of both the sense and antisense transcripts) [11-14]. Here, I will discuss what we have learned about the molecular mechanisms underlying FXTAS and these other, mechanistically related, microsatellite-expansion disorders.

Until recently, when a gene involved in a micro-satellite expansion disorder was discovered, it was thought that the genomic location of the repeat could have the following effects: 1) repeat expansions located in the coding sequence of a gene can result in the generation of a toxic or malfunctioning protein; 2) non-coding repeats can have an effect on chromosome fragility, gene silencing, and sequestration of proteins involved in cellular processes such as splicing and cell architecture (reviewed in [15]). FXTAS is caused by an CGG repeat expansion in the 5' untranslated region (UTR) of the *FMR1* gene. Carriers of the premutation produce elevated *FMR1* mRNA levels (2 to 8 fold in leucocytes of FXTAS patients) and RNA levels positively correlate with the CGG repeat length [16, 17]. Additionally, *FMR1* mRNA was found in intranuclear inclusions in isolated nuclei and post-mortem brain tissue of FXTAS patients [18, 19]. Both of these observations led to the toxic RNA gain-of-function model for FXTAS [20]. Importantly, at that time, no evidence was present that the CGG repeat could be translated in FMRpolyG (see below). The transcript containing an expanded repeat changes the secondary structure of the RNA molecule, forms intranuclear RNA foci, and sequesters RNA-binding proteins, which ultimately leads to cellular dysfunction. [18, 19, 21-26]. Thus far, in FXTAS several

RNA-binding proteins that directly bind to the expanded CGG repeat have been identified [19, 21, 27, 28]. First, two RNA-binding proteins, hnRNP A2/B1 and Purα, were discovered using mass spectrometric analyses of the protein composition of isolated human inclusions and later also in a *Drosophila* screen [19, 27-29]. In the *fly* model binding of Purα to the expanded CGG repeat ultimately leads to sequestration of Rm62, which results in nuclear accumulation of specific mRNAs involved in stress and immune responses [30]. Notably, in the initial *fly* model, inclusions were present in both nuclei and the cytoplasm of cells from the retina. Another discrepancy with the human neuropathological studies is the presence of more than one aggregate per nucleus [31]. Purα-positive inclusions could be demonstrated in FXTAS post-mortem brain [28]. However, we, and others, could not confirm Purα-positive inclusions in FXTAS post-mortem brain or brain tissue of one of the available mouse models (unpublished data). A possible explanation for the discrepancy between the *fly* model and FXTAS brain tissue versus mouse brain tissues might be that there is a different composition of the intranuclear inclusions in patients with FXTAS and in *Drosophila* than in the vertebrate model organisms. Strikingly, in a mouse model lacking Purα, histopathological findings include axonal swellings and hyperphosphorylation of neurofilaments [32]. Further research is needed to determine the precise role of Purα in the pathogenesis of FXTAS. It has been shown that the second RNA-binding protein found in these screens, hnRNP A2/B1, directly interacts with the CGG repeat in the *fly* model for FXTAS [27]. Furthermore hnRNP A2/B1 is found in intranuclear inclusions in post-mortem brain tissue of FXTAS patients [29]. The CUGBP1 protein interacts with hnRNP A2/B1 resulting in neurodegeneration due to loss of RNA chaperone function and mislocalisation of BC1 RNA in the *fly* model for FXTAS [27]. Later, Sellier, et al., showed that the double-stranded RNA-binding protein DGCR8 binds to expanded CGG repeats, resulting in the partial sequestration of DGCR8 and its partner DROSHA, within CGG RNA aggregates [21]. Consequently, the processing of micro-RNAs (miRNAs) in both transfected cells and post-mortem brain tissue of FXTAS patients is reduced, resulting in decreased levels of mature miRNAs [21]. Other studies suggested that both in the *fly* model for FXTAS and blood of FXTAS patients only specific miRNAs were misregulated [33, 34]. Altogether these studies suggest that an RNA gain-of-function model for FXTAS is very likely. However, there are some additional arguments to consider. Not only the presence of intranuclear inclusions with *FMR1* mRNA, containing an expanded CGG repeat, may cause toxicity, but other factors (discussed below) may also play a role.

First, although expanded *FMR1* mRNA is found within the intranuclear inclusions in post-mortem brain tissue from FXTAS patients [18, 19], in the CGG_{dut} knock-in (KI) mouse model and the newly developed transgenic conditional mouse model (**chapter 5**) only relatively few *Fmr1* RNA-positive inclusions were found compared with the high number of ubiquitin-positive inclusions. Although our mouse models show limited number of

Fmr1 RNA-positive inclusions, these mouse models mimic many of the features (elevated levels of *Fmr1* mRNA, neuropathology, and behavioural deficits) seen in FXTAS patients, suggesting that these features may be caused, at least partially, by a different mechanism (reviewed in **chapter 1** [35]). Moreover, it cannot be excluded that free *Fmr1* mRNA, containing an expanded CGG repeat is toxic. We have demonstrated that increased active caspase-3, a marker for apoptosis, is observed in livers from the inducible mouse model that ubiquitously expresses RNA containing the expanded CGG repeat (**chapter 3** [36]). Since these livers do not show ubiquitin-positive inclusions, free *Fmr1* RNA containing an expanded CGG repeat, may play a role in the early demise of these mice.

Second, if the expanded CGG repeat without any flanking sequences is placed at the 3'UTR position of a GFP expression construct it is less toxic compared with an GFP expression construct with an expanded CGG repeat at the 5' UTR [12]. This suggests that the secondary structure of the expanded CGG repeat may not cause toxicity. Furthermore it has been shown in transfected primary mouse neurons that most of the RNA containing an expanded CGG repeat embedded within the 5'UTR of the *FMR1* gene without the ORF of *FMR1* was present in the cytoplasm, while RNA containing an expanded CGG repeat out of the context of the 5'UTR of the *FMR1* gene is mainly retained in the nucleus. This suggests that there is bias towards nuclear retention for studies conducted with artificially generated constructs without any 5'UTR sequences of the *FMR1* gene (**chapter 5**).

Third, in 2011 a new phenomenon called repeat associated non-AUG (RAN) translation was discovered for SCA8 and DM1 in the laboratory of Laura Ranum [11]. Similarly for FXTAS, Todd, et al., found that *FMR1* RNA containing an expanded CGG repeat initiates RAN translation of a cryptic polyglycine-containing protein, FMRpolyG [12]. We, and others, have demonstrated that FMRpolyG accumulates in intranuclear inclusions in transfected cells, animal models (*fly* and mouse) and post-mortem brain material from FXTAS patients (**chapter 2 and 4**, [12, 37, 38]). Intriguingly, we have demonstrated that the presence of FMRpolyG-positive intranuclear inclusions were not limited to the central nervous system (CNS), but FMRpolyG-positive intranuclear inclusions were also present in heart, kidney, adrenal gland, thyroid and ovarian stromal cells (**chapter 2** [37, 39]). In all examined cell types, colocalisation of FMRpolyG and ubiquitin was found in the vast majority of inclusions. We hypothesized that the presence of FMRpolyG-positive intranuclear inclusions in systemic organs is consistent with the unexplained medical co-morbidities reported in some patients with FXTAS. In addition to FMRpolyG, a polyalanine-containing protein, FMRpolyA, was reported to be expressed in transfected COS7 cells using an expression construct with GFP in the FMRpolyA frame. In contrast to FMRpolyG, FMRpolyA could not be detected in intranuclear inclusions, but shows a diffuse expression pattern in both nucleus and cytoplasm of these transfected cells. FMRpolyA-

positive intranuclear inclusions could also not be detected in post-mortem brain tissue from FXTAS patients or in brain tissue from the mouse models ([12] and **chapter 5**). An explanation for the difference in the ability to form an RAN translation products and/or intranuclear inclusions between the *in vitro* experiments and human and mouse tissues could be that the different RAN translation proteins require another repeat length for RAN translation and/or accumulation to occur. In addition, all *in vitro* experiments were based on constructs that were overexpressed, making it more easy to visualise the RAN proteins. Moreover, these constructs contain an extra tag for visualisation, which may influence RAN protein stability. As shown in **chapter 5**, expression constructs that have a relatively big GFP tag are more stable than similar constructs with a much smaller Flag tag. Interestingly, we were able to demonstrate that an ACG sequence embedded in a potential Kozac consensus sequence located upstream of the CGG repeat is responsible for RAN translation even without a CGG repeat. In **chapter 5**, we could demonstrate that expression of the RNA containing an expanded CGG repeat without the proximal C-terminal part does not cause cell death in transfected primary mouse neurons, while expression of RNA containing an expanded CGG repeat including the proximal C-terminal part does result in cell death. This suggests that the context of the proximal C-terminus sequence is relevant for disease pathogenesis and expression of RNA containing an expanded CGG repeat only, is not sufficient to cause FXTAS. In addition, we showed that LAP2ß interacts with the C-terminal part of FMRpolyG protein. LAP2ß colocalises with both FMRpolyG and ubiquitin in intranuclear inclusions found in transfected primary mouse neurons, induced pluripotent stem cells (iPSCs) derived from patients with FXTAS, and post-mortem FXTAS brain tissue. Moreover, overexpression of LAP2ß was sufficient to rescue neuronal cell death that was induced by expression of FMRpolyG in primary neuronal cultures (**chapter 5**). RAN translation in cells from FXTAS patients shows many similarities with SCA8. Zu, et al., tried to separate the RNA and protein gain-of-function hypotheses by mutating the AUG start codon of SCA8 [11]. By doing this the RNA gain-of-function can be studied without any influences of the toxic AUG-initiated protein. Unexpectedly, they discovered that CAG expansion constructs in the absence of an AUG start codon, were not only translated into a polyglutamine-containing protein, but also in polyalanine- and polyserine-containing proteins. In the same *in vitro* assay, the antisense CUG transcript is translated into polyleucine-, polyalanine-, and polycysteine-containing proteins. Additionally, they showed that RAN translation across human SCA8 CAG expansion transcripts results in the accumulation of SCA8-related polyalanine containing protein in post-mortem brain tissue [11]. The other SCA8 RAN proteins were not found in intranuclear inclusions. Altogether, our studies suggest that RAN translation is a second, potential mechanism of toxicity in FXTAS that is shared with several other microsatellite-expansion diseases [11, 13, 14, 40].

We have started to implement a strategy to discriminate between the RNA and RAN protein gain-of-function mechanisms in FXTAS (**chapter 5**). Transgenic conditional mouse models were generated expressing either RNA containing an expanded CGG repeat including the 5'UTR, or RNA containing an expanded CGG repeat without the 5'UTR. In the first mouse model RNA is produced and translated into FMRpolyG, whereas in the second model RNA is produced, but not translated into FMRpolyG (RNA-only). We found that expression of both FMRpolyG and RNA containing an expanded CGG repeat induces neuropathology and behavioural deficits, while mice that only express the RNA containing an expanded CGG repeat (RNA-only) did not display any neuropathology or behavioural deficits. Thus, the fundamental question remains: is sole FMRpolyG expression sufficient to develop FXTAS. To answer the question whether toxicity is driven by FMRpolyG alone or by the combined expression of *FMR1* RNA containing an expanded CGG repeat and FMRpolyG, it is crucial to generate a new transgenic mouse model that solely expresses FMRpolyG. This is not only important to advance our understanding of the underlying molecular mechanisms of FXTAS, but also for a proof-of-principle whether we need to target FMRpolyG only, or also the *FMR1* RNA molecules containing an expanded CGG repeat for future therapeutic intervention studies. A similar strategy has already been used successfully in C9FTD/ALS. In 2011, a GGGGCC repeat expansion in intron 1 of the *C9ORF72* gene has been found to cause C9FTD/ALS [8]. As described for the other microsatellite expansion diseases, the *C9ORF72* gene is bidirectionally transcribed, forms sense and antisense RNA foci, and RAN translated dipeptides accumulate in both cytoplasmic and intranuclear inclusions [13, 14, 41]. A lot of effort has been made to investigate the role of loss-of-function [42-44], RNA [45-48] and RAN [13, 14, 48, 49] gain-of-function mechanisms in C9FTD/ALS. The fact that a patient with a homozygous *C9ORF72* repeat expansion mutation does not have a more severe, or even completely different clinical phenotype [42], no *C9ORF72* coding mutations have been reported [43], and no motor neuron degeneration, defects in motor function, or altered survival has been observed in a C9orf72 knockout mouse model [44] suggest that C9FTD/ALS is not caused by a loss-of-function mechanism. Interestingly, in a study that resembles the study of Zu, et al. [11], Mizielinska, et al., tried to study in both a cell model and a fly model for *C9ORF72*, whether toxicity is driven by either the RNA with an expanded repeat or by dipeptides generated via RAN translation [50]. Using eye phenotype and survival curves as primary outcome measures, they concluded that the major toxic species are the RAN dipeptides. However, they also conclude that they cannot rule out an additional contribution of RNA toxicity [50].

Finally, one additional mechanism, that has not yet been highlighted, which may contribute to the pathogenesis in microsatellite-expansion disorders is antisense transcription. In the last decade it was discovered that next to the regular sense transcription of *DM1*,

FMR1, and *ATXN8,* antisense transcription can occur as well [51-54]. It has been shown that in addition to the sense *FMR1* transcripts, also antisense *FMR1* transcripts (*ASFMR1*, *FMR4*, and *FMR6*) are produced [53-55]. The *ASFMR1* transcript is transported to the cytoplasm, contains a polyproline-containing open reading frame (ORF), and comparable with *FMR1* RNA, *ASFMR1* RNA is upregulated in carriers of the premutation [53]. Hypothetically, this polyproline-containing protein may also play a role in the pathogenesis of FXTAS. A similar, dual mechanism is true for SCA8. The SCA8-causing ATXN8 gene is bidirectionally transcribed and expresses both CUG- and CAG-containing transcripts. Via regular AUG translation the CUG-containing transcript is translated into a polyglutamine-containing protein. This polyglutamine-containing protein is found in intranuclear inclusions in cerebellar Purkinje neurons and brainstem neurons from both SCA8 expansion mice and in human SCA8 post-mortem brain tissue. These inclusions also stain positive for ubiquitin [52]. This suggests that, at least for SCA8, alongside an RNA gain-of-function mechanism, also an antisense transcript driven protein gain-of-function mechanism could be involved in disease pathogenesis. It might be useful to develop an antibody against the *ASFMR1* polyproline to investigate if a similar mechanism is also involved in FXTAS.

Therapeutic interventions

Currently, treatment of patients with FXTAS is symptomatic (reviewed in [56, 57]). Several case studies suggest that patients with FXTAS show improvement from treatment for some of their symptoms [58]. For tremor, some patients benefit from the use of primidone, β-blockers, or deep brain stimulation (DBS) [58, 59]. For treatment of ataxia it has been reported that patients may benefit from amantadine [58, 60]. Various other drugs have shown beneficial effects for the minor clinical symptoms of FXTAS [56, 57, 61]. Altogether, anecdotal information and case reports regarding various treatments suggest that treatment of some of the symptoms displayed by patients with FXTAS is possible. In the first, randomized, double-blind, placebo controlled trial for FXTAS, memantine was given to thirty-four patients [62]. Memantine is a non-competitive N-methyl-D-aspartate (NMDA) receptor antagonist approved for dementias, particularly moderate to severe AD. Memantine is believed to attenuate glutamate toxicity and serves as a neuroprotective drug that may slow neurodegeneration [63]. In this clinical trial no significant effect was found on primary outcome measures, including behavioural dyscontrol scale (BDS) and intention tremor severity and secondary outcome measures, including postural and writing tremor severity, hand and finger tapping maximum frequency, tests of declarative learning, working memory, and executive function [62, 64]. However, an effect on cued memory retrieval in these patients has been reported later [65]. So far, therapy has focused on symptomatic treatment of patients with FXTAS. Thus, an urgent need for targeted therapeutic intervention strategies based on the disease mechanisms, rather than symptomatic treatment, is warranted.

The initial development of several FXTAS mouse models has significantly contributed to our understanding of the underlying disease mechanisms of FXTAS. Furthermore, these models were very useful to study onset and progression of disease, disease (neuro) pathology, and repeat instability [66-71]. However, none of these initial mouse models could address questions concerning critical periods for intervention or reversibility of FXTAS. In order to answer these questions, and as a proof-of-principle for intervention studies, we have generated an inducible mouse model ([36, 38] and **chapter 3 and 4**). In these mice we could demonstrate that the formation of intranuclear inclusions, the neuropathological hallmark of FXTAS, is only reversible at an early developmental stage. Moreover, stopping expanded CGG repeat RNA expression at a later stage prevents further progression of neuropathology, however, reversibility could not be demonstrated. In addition, in the inducible mice a functional behavioural phenotype could be halted by stopping RNA expression early in disease development ([38] and **chapter 4**). Although it is difficult to extrapolate the results from the overexpressing, inducible mouse model to the human situation, it does suggest that it seems favourable to start treatment in carriers of the PM before the onset of symptoms. Nevertheless, our functional studies in the inducible mouse model indicate that it might also be beneficial to treat symptomatic FXTAS patients to halt or postpone further disease progression. With the current knowledge of the underlying disease mechanisms, several strategies to develop a targeted therapeutic intervention can be envisaged: 1) the use of drug libraries in unbiased screens; 2) removing the genomic expanded CGG repeat; 3) compensating for proteins that are trapped in inclusions; 4) targeting the RNA for degradation; 5) disrupting interactions with RNA binding proteins, and 6) preventing FMRpolyG to be expressed.

Ad 1. An initial, unbiased, approach would be to screen drug libraries in the different animal models of FXTAS. The first screen has already been performed in the fly model for FXTAS. Qurashi, et al., found small molecules, including phospholipase A_2 (PLA_2)-inhibitors, that could ameliorate the toxic effects of the expanded repeat [72]. So far, these PLA_2-inhibitors have not been verified in other cellular and vertebrate models. With the recent introduction of automated, large-scale iPSC-cell culture and differentiating methods it would be interesting to perform an unbiased drug screen in iPSCs from patients with FXTAS or, for example, neural progenitor cells (NPCs). New outcome measures have been described using patient derived iPSCs, including reduced postsynaptic density (PSD) protein 95 protein expression, reduced synaptic puncta density, reduced neurite length, intranuclear ubiquitin- and FMRpolyG-positive inclusions, and disrupted LAP2ß and Lamin B1 nuclear architecture (**chapter 5** and [73]). This approach might also be useful as a personalised medicine method, taking into account the patient's (epi)genetic background.

Ad 2. A strategy to remove the expanded CGG repeat by clustered, regularly interspaced, short palindromic repeat (CRISPR)/CRISPR-associated 9 (Cas9) genome

editing has been demonstrated to be feasible [74, 75]. Successful deletion of the expanded CGG repeat in fragile X-derived iPSCs has been demonstrated, followed by reactivation of the *FMR1* gene by demethylation of the promoter region [76]. In theory, removal of the expanded repeat in premutation cells would prevent both the RNA molecule forming secondary structures, and prevent the expression of stable FMRpolyG proteins. In 2015, the first, very controversial, CRISPR/Cas9 study has been performed in human tripronuclear (3PN) zygotes [77]. Although the authors claimed that they could effectively cleave the endogenous β-globin gene (*HBB*), also off-target effects were reported [77]. This publication raised a public debate about the ethics of human germline editing. I agree with Lanphier and colleagues that at this moment "heritable human genetic modifications pose serious risks, and the therapeutic benefits are tenuous" [78]. Although human genome editing might not be applicable in the (near) future, it is still worthwhile to investigate a proof-of-principle in the KI mouse model for FXTAS. The first *in vivo* studies show that using adeno-associated viral (AAV)-mediated genome editing can reverse gene function in mouse brain by targeting the methyl CpG binding protein (*Mecp2*) gene, which plays an important role in the pathogenesis of Rett syndrome [79].

Ad 3. Rescue of functional protein levels of expanded CGG RNA-binding proteins and other proteins that are trapped in the intranuclear inclusions is another option for therapeutic intervention. [19, 29]. It has been shown that overexpression of Purα or DGCR8 can rescue neuronal cell death in a *Drosophila* model for FXTAS [21, 28]. In neuronal cultures, overexpression of LAP2ß was sufficient to rescue neuronal cell death caused by the toxic C-terminal part of FMRpolyG (**chapter 5**). Although overexpression of proteins trapped in inclusions seems to work in flies and cultured cells, there are some drawbacks regarding protein replacement therapy. To date, over thirty proteins can be found in the intranuclear inclusions. Restoring protein levels of only one of those trapped proteins will probably not be sufficient to prevent or reverse FXTAS. Another point to consider is that correct basal protein levels are necessary in the specific target cells. Inclusions are found in both neurons and astrocytes [80] but different protein levels might be required in the different cell types. Finally, to date, there is no method that can safely deliver proteins to all required target cells, both neurons and astrocytes.

Ad 4. Another approach would be to target the *FMR1* RNA containing the expanded CGG repeat for degradation by using antisense oligonucleotides (AONs) (reviewed in [81]). In animal models of several microsatellite disorders AON-related therapies have been very successful and followed by ongoing clinical trials (reviewed in [82]). Depending on the sequence, backbone, and chemical modifications, these AONs can be used as a way to reduce RNA expression or act as steric hindrance (shielding). Degradation of toxic RNA can be established by gapmers containing a phosphorothioate-modified, nuclease-resistant DNA segment activating RNase H cleavage of the target RNAs. These

gapmers are flanked with 2′-*O*-methyl RNA designed to confer increased nuclease stability and affinity of the AONs to the target RNA ([83] and **chapter 6**). An initial study suggests that it should be possible to target the *FMR1* RNA for RNase H-mediated degradation using mouse embryonic fibroblasts from our inducible mouse model (MEFs) (**chapter 6**). However, these AONs should be tested in more specific cellular and animal models to draw final conclusions about their specificity and efficacy, including better outcome measures (e.g. inclusion formation, FMRpolyG levels, and ultimately animal neuropathology and behaviour).

Ad 5. Another strategy is focused on the use of AONs that shield the CGG hairpin and consequently may prevent RAN translation and/or RNA-binding proteins from being trapped within intranuclear inclusions by the hairpin structure. In initial studies using shielding AONs in FXTAS it has been shown that a fully modified 2′-O-Methyl phosphorothioate is capable of partially reversing a FXTAS-associated splicing defect and reducing FMRpolyG levels in transfected cells [84, 85]. However, these blocking AONs also have an effect on downstream canonical translation when they bind to the RNA containing an expanded CGG repeat. All together this implicates that AONs that use RNase H-mediated degradation or a steric hindrance mechanism, will ultimately result in lower levels of functional fragile X mental retardation protein (FMRP). Lack of FMRP causes fragile X syndrome, the most common inherited form of intellectual disability [86, 87]. FMRP mediates transport and local translation of several target mRNAs at postsynaptic sites in neurons and is important in synaptic plasticity [88]. To date it is unknown whether depletion of FMRP later in life may cause a fragile X syndrome phenotype. A second point to consider is that AONs need to act at a very specific location in the genome, without any off-target effects. Notably the presence of an CGG repeat is not specific for the *FMR1* gene only. The human genome contains several CGG rich domains/genes, thus it can be expected that AONs targeting the CGG repeat can induce off-target effects. Several methods for delivery of AONs to the CNS exists. AONs can be directly delivered into the cerebrospinal fluid through intracerebroventricular (ICV) or intrathecal (IT) injection or infusion using a reservoir that is connected to the ventricles within the brain or spinal cord. Less effective, but also less invasive methods of delivery are systemic delivery and intranasal administration (reviewed in [81]). It has been shown that via direct delivery, AONs were taken up by the vast majority of all neurons and astrocytes [89-91]. Interestingly, AONs that use an RNase H-mediated degradation mechanism, were used in different HD mouse models showing that transient suppression of huntingtin (up to 90%) can be sufficient to ameliorate disease for an extended period of time [89, 92-94]. Similarly, using a single intracerebroventricular (ICV) AON-injection in control mice, it has been shown that *C9orf72* mRNA levels were reduced for up to 18 weeks [45]. In a rat model for ALS caused by a mutation in the *SOD1* gene, it has been shown that the SOD1 protein

can be downregulated by AONs [95, 96]. Thus, in vertebrate models it has been shown that strategies for RNase H-mediated degradation of mRNAs using AONs are very promising. Recently, an AON targeting the *SOD1* gene was used in a phase 1 clinical study using intrathecal delivery. Results of this clinical trial suggest that AONs were well tolerated in patients with SOD1-related familial ALS when administered via an intrathecal infusion [97].

Ad 6. Finally, the use of small chemical compounds that shield the CGG repeat (reviewed in [98]) has great potential to ameliorate FXTAS. Evidence from gel mobility shift assays and spectroscopic methods show that RNA containing an expanded CGG repeat forms hairpin structures with periodically repeating internal loops. The laboratory of Matthew Disney developed several bioactive small molecule probes that target those internal loops [99-102]. The advantage of such a strategy is that it prevents RNA-binding proteins from binding to the expanded CGG repeat and additionally the small molecules will block RAN translation, without having an effect on the downstream translational events. It has been shown in c9FTD/ALS iNeurons (fibroblasts that directly were converted to a neuronal lineage by repressing polypyrimidine-tract-binding protein (PTB1) [103]), that small molecules that bind to the expanded GGGGCC repeat can inhibit RAN translation and foci formation [102]. For FXTAS, we, and others, have obtained similar results (**chapter 6** and [84, 85, 100, 102]). Compounds are effective in cellular models for FXTAS as evidenced by their ability to improve FXTAS-associated pre-mRNA splicing defects, to reduce the size and number of nuclear RNA foci, to reduce the number of both ubiquitin- and FMRpolyG-positive intranuclear inclusions, and to reduce FMRpolyG levels, while not affecting translation of the downstream *FMR1* ORF. Altogether this seems to be a promising therapeutic intervention strategy. Some points to consider are the specificity and toxicity of those compounds. Thus, these compounds need to be tested extensively in *in vivo* models for specificity and toxicity. In my opinion it is essential that potential candidates obtained from studies using *in vitro* models (e.g. primary neurons) need to be followed by an *in vivo* approach. Our inducible mouse model that ubiquitously express RNA containing an expanded CGG repeat (**chapter 3**) is an excellent model to start with. The next step would be to test candidate compounds in our brain specific inducible mouse model (**chapter 4**).

Finally, if preclinical research for a specific targeted treatment for FXTAS (both in vitro and in vivo) has proven successful the process starts to continue research and testing in humans. However, for starting clinical trials there is an urgent need for reliable outcome measures and biomarkers to assess efficacy of treatment. In a c9orf72 study, it was found that c9RAN proteins could be specifically detected in c9FTD/ALS patient cerebrospinal fluid (CSF) and not in healthy controls or ALS patients without c9orf72 mutation [102]. We would like to start a similar approach using an enzyme-linked immunosorbent assay (ELISA) with the newly developed FMRpolyG antibodies described in chapter 2, 4, 5, and

6. As a first step, we may start to detect FMRpolyG in blood and/or CSF in our mouse models at different time points, including before onset of disease, at onset of disease and during progression of disease. These studies may provide information whether FMRpolyG is a reliable prognostic biomarker for onset of disease and/or reliable predictive biomarker for efficacy of targeted treatment. Ultimately, these studies should be performed on human material as well, including blood and CSF.

Concluding remarks

FXTAS is a devastating disease caused by an expanded CGG repeat in the 5'UTR of the *FMR1* gene. In this thesis we report that the RAN translation product, FMRpolyG, is an important trigger to cause (neuro)pathology and behaviour deficits in FXTAS disease models. However, a role of *FMR1* RNA in the pathogenesis of FXTAS cannot be excluded yet. To advance our understanding of the underlying molecular mechanisms of FXTAS it is crucial to generate new cellular and animal models that solely express FMRpolyG. Gaining more mechanistic insight is essential to develop potential targets for future therapeutic intervention studies and to identify new reliable biomarkers. Here, we report that to date the most promising intervention strategy is the use of small chemical compounds that shield the expanded CGG repeat in *FMR1* RNA, to disrupt interactions with RNA-binding proteins, and prevent FMRpolyG to be expressed. In addition, with the recent introduction of automated, large-scale iPSC-cell culture methods and disease relevant outcome measures (e.g. inclusion formation and FMRpolyG levels) it is feasible to conduct intervention studies in a high throughput *in vitro* screening using a human neuronal cellular model. Importantly, drugs that are promising in *in vitro* studies need to be validated in *in vivo* (e.g. mouse) models using reliable outcome measures, including neuropathology, biomarkers, and molecular and behavioural paradigms.

REFERENCES

1. Hagerman, R.J., et al., *Intention tremor, parkinsonism, and generalized brain atrophy in male carriers of fragile X.* Neurology, 2001. **57**(1): p. 127-30.
2. Mirkin, S.M., *Expandable DNA repeats and human disease.* Nature, 2007. **447**(7147): p. 932-40.
3. Orr, H.T. and H.Y. Zoghbi, *Trinucleotide repeat disorders*. Annual Review of Neuroscience, 2007. **30**: p. 575-621.
4. Brouwer, J.R., R. Willemsen, and B.A. Oostra, *Microsatellite repeat instability and neurological disease.* Bioessays, 2009. **31**(1): p. 71-83.
5. Brook, J.D., et al., *Molecular basis of myotonic dystrophy: expansion of a trinucleotide (CTG) repeat at the 3' end of a transcript encoding a protein kinase family member.* Cell, 1992. **68**: p. 799-808.
6. Group, H.s.D.C.R., *A novel gene containing a trinucleotide repeat that is expanded and unstable on Huntington's disease chromosomes. .* Cell, 1993. **72**(6): p. 971-83.
7. Koob, M.D., et al., *An untranslated CTG expansion causes a novel form of spinocerebellar ataxia (SCA8).* Nature Genetics, 1999. **21**(4): p. 379-384.
8. DeJesus-Hernandez, M., et al., *Expanded GGGGCC hexanucleotide repeat in noncoding region of C9ORF72 causes chromosome 9p-linked FTD and ALS.* Neuron, 2011. **72**(2): p. 245-56.
9. Sellier, C., et al., *The multiple molecular facets of fragile X-associated tremor/ataxia syndrome.* J Neurodev Disord, 2014. **6**(1): p. 23.
10. Todd, P.K. and H.L. Paulson, *RNA-mediated neurodegeneration in repeat expansion disorders*. Ann Neurol, 2010. **67**(3): p. 291-300.
11. Zu, T., et al., *Non-ATG-initiated translation directed by microsatellite expansions.* Proc Natl Acad Sci U S A, 2011. **108**(1): p. 260-5.
12. Todd, P.K., et al., *CGG Repeat-Associated Translation Mediates Neurodegeneration in Fragile X Tremor Ataxia Syndrome.* Neuron, 2013. **78**(3): p. 440-455.
13. Ash, P.E., et al., *Unconventional translation of C9ORF72 GGGGCC expansion generates insoluble polypeptides specific to c9FTD/ALS.* Neuron, 2013. **77**(4): p. 639-46.
14. Mori, K., et al., *The C9orf72 GGGGCC repeat is translated into aggregating dipeptide-repeat proteins in FTLD/ALS.* Science, 2013. **339**(6125): p. 1335-8.
15. Usdin, K., *The biological effects of simple tandem repeats: lessons from the repeat expansion diseases.* Genome Res, 2008. **18**(7): p. 1011-9.
16. Tassone, F., et al., *Elevated levels of FMR1 mRNA in carrier males: A new mechanism of involvement in the Fragile-X syndrome.* Am J Hum Genet, 2000. **66**(1): p. 6-15.
17. Kenneson, A., et al., *Reduced FMRP and increased FMR1 transcription is proportionally associated with CGG repeat number in intermediate-length and premutation carriers.* Hum Mol Genet, 2001. **10**(14): p. 1449-1454.
18. Tassone, F., C. Iwahashi, and P.J. Hagerman, *FMR1 RNA withinthe intranuclear inclusions of fragile X-associated Tremor/Ataxia syndrome (FXTAS).* RNA biology, 2004. **1**: p. 103-105.
19. Sellier, C., et al., *Sam68 sequestration and partial loss of function are associated with splicing alterations in FXTAS patients.* Embo J, 2010. **29**: p. 1248-1261.
20. Willemsen, R., E. Mientjes, and B.A. Oostra, *FXTAS: A Progressive Neurologic Syndrome Associated with Fragile X Premutation.* Curr Neurol Neurosci Rep, 2005. **5**(5): p. 405-10.
21. Sellier, C., et al., *Sequestration of DROSHA and DGCR8 by Expanded CGG RNA Repeats Alters MicroRNA Processing in Fragile X-Associated Tremor/Ataxia Syndrome.* Cell Rep, 2013. **3**(3): p. 869-880.
22. Jiang, H., et al., *Myotonic dystrophy type 1 is associated with nuclear foci of mutant RNA, sequestration of muscleblind proteins and deregulated alternative splicing in neurons.* Hum Mol Genet, 2004. **13**(24): p. 3079-88.
23. Mankodi, A., et al., *Myotonic dystrophy in transgenic mice expressing an expanded CUG repeat.* Science, 2000. **289**(5485): p. 1769-73.
24. Daughters, R.S., et al., *RNA gain-of-function in spinocerebellar ataxia type 8.* PLoS Genet, 2009. **5**(8): p. e1000600.
25. Kanadia, R.N., et al., *A muscleblind knockout model for myotonic dystrophy.* Science, 2003. **302**(5652): p. 1978-80.
26. Ho, T.H., et al., *Colocalization of muscleblind with RNA foci is separable from mis-regulation of alternative splicing in myotonic dystrophy.* J Cell Sci, 2005. **118**(Pt 13): p. 2923-33.

27. Sofola, O.A., et al., *RNA-Binding Proteins hnRNP A2/B1 and CUGBP1 Suppress Fragile X CGG Premutation Repeat-Induced Neurodegeneration in a Drosophila Model of FXTAS.* Neuron, 2007. **55**(4): p. 565-71.

28. Jin, P., et al., *Pur alpha Binds to rCGG Repeats and Modulates Repeat-Mediated Neurodegeneration in a Drosophila Model of Fragile X Tremor/Ataxia Syndrome.* Neuron, 2007. **55**(4): p. 556-64.

29. Iwahashi, C.K., et al., *Protein composition of the intranuclear inclusions of FXTAS.* Brain, 2006. **129**(Pt 1): p. 256-271.

30. Qurashi, A., et al., *Nuclear Accumulation of Stress Response mRNAs Contributes to the Neurodegeneration Caused by Fragile X Premutation rCGG Repeats.* PLoS Genet, 2011. **7**(6): p. e1002102.

31. Jin, P., et al., *RNA-Mediated Neurodegeneration Caused by the Fragile X Premutation rCGG Repeats in Drosophila.* Neuron, 2003. **39**(5): p. 739-747.

32. Hokkanen, S., et al., *Lack of Pur-alpha alters postnatal brain development and causes megalencephaly.* Hum Mol Genet, 2012. **21**(3): p. 473-84.

33. Alvarez-Mora, M.I., et al., *MicroRNA expression profiling in blood from fragile X-associated tremor/ataxia syndrome patients.* Genes Brain Behav, 2013. **12**(6): p. 595-603.

34. Tan, H., et al., *MicroRNA-277 Modulates the Neurodegeneration Caused by Fragile X Premutation rCGG Repeats.* PLoS Genet, 2012. **8**(5): p. e1002681.

35. Berman, R.F., et al., *Mouse models of the fragile X premutation and fragile X-associated tremor/ataxia syndrome.* J Neurodev Disord, 2014. **6**(1): p. 25.

36. Hukema, R.K., et al., *Induced expression of expanded CGG RNA causes mitochondrial dysfunction in vivo.* Cell Cycle, 2014. **13**(16): p. 2600-2608.

37. Buijsen, R.A., et al., *FMRpolyG-positive inclusions in CNS and non-CNS organs of a fragile X premutation carrier with fragile X-associated tremor/ataxia syndrome.* Acta Neuropathol Commun, 2014. **2**(1): p. 162.

38. Hukema, R.K., et al., *Reversibility of neuropathology and motor deficits in an inducible mouse model for FXTAS.* Human Molecular Genetics, 2015. **24**(17): p. 4948-4957.

39. Buijsen, R.A., et al., *Presence of inclusions positive for polyglycine containing protein, FMRpolyG, indicates that repeat-associated non-AUG translation plays a role in fragile X-associated primary ovarian insufficiency.* Hum Reprod, 2015.

40. Banez-Coronel, M., et al., *RAN Translation in Huntington Disease.* Neuron, 2015. **88**(4): p. 667-77.

41. Mackenzie, I.R., et al., *Quantitative analysis and clinico-pathological correlations of different dipeptide repeat protein pathologies in C9ORF72 mutation carriers.* Acta Neuropathol, 2015. **130**(6): p. 845-61.

42. Fratta, P., et al., *Homozygosity for the C9orf72 GGGGCC repeat expansion in frontotemporal dementia.* Acta Neuropathol, 2013. **126**(3): p. 401-9.

43. Harms, M.B., et al., *Lack of C9ORF72 coding mutations supports a gain of function for repeat expansions in amyotrophic lateral sclerosis.* Neurobiol Aging, 2013. **34**(9): p. 2234 e13-9.

44. Koppers, M., et al., *C9orf72 ablation in mice does not cause motor neuron degeneration or motor deficits.* Ann Neurol, 2015. **78**(3): p. 426-38.

45. Lagier-Tourenne, C., et al., *Targeted degradation of sense and antisense C9orf72 RNA foci as therapy for ALS and frontotemporal degeneration.* Proceedings of the National Academy of Sciences of the United States of America, 2013. **110**(47): p. E4530-E4539.

46. Donnelly, C.J., et al., *RNA toxicity from the ALS/FTD C9ORF72 expansion is mitigated by antisense intervention.* Neuron, 2013. **80**(2): p. 415-28.

47. Mizielinska, S., et al., *C9orf72 frontotemporal lobar degeneration is characterised by frequent neuronal sense and antisense RNA foci.* Acta Neuropathol, 2013. **126**(6): p. 845-57.

48. Zu, T., et al., *RAN proteins and RNA foci from antisense transcripts in C9ORF72 ALS and frontotemporal dementia.* Proc Natl Acad Sci U S A, 2013. **110**(51): p. E4968-77.

49. Mori, K., et al., *Bidirectional transcripts of the expanded C9orf72 hexanucleotide repeat are translated into aggregating dipeptide repeat proteins.* Acta Neuropathol, 2013. **126**(6): p. 881-93.

50. Mizielinska, S., et al., *C9orf72 repeat expansions cause neurodegeneration in Drosophila through arginine-rich proteins.* Science, 2014. **345**(6201): p. 1192-4.

51. Cho, D.H., et al., *Antisense transcription and heterochromatin at the DM1 CTG repeats are constrained by CTCF.* Mol Cell, 2005. **20**(3): p. 483-9.

52. Moseley, M.L., et al., *Bidirectional expression of CUG and CAG expansion transcripts and intranuclear polyglutamine inclusions in spinocerebellar ataxia type 8.* Nat Genet, 2006. **38**(7): p. 758-69.

53. Ladd, P.D., et al., *An Antisense Transcript Spanning the CGG Repeat Region of FMR1 is Upregulated in Premutation Carriers but Silenced in Full Mutation Individuals*. Hum Mol Genet, 2007. **16**: p. 3174-3187.

54. Pastori, C., et al., *Comprehensive analysis of the transcriptional landscape of the human FMR1 gene reveals two new long noncoding RNAs differentially expressed in Fragile X syndrome and Fragile X-associated tremor/ataxia syndrome*. Human Genetics, 2014. **133**(1): p. 59-67.

55. Khalil, A.M., et al., *A novel RNA transcript with antiapoptotic function is silenced in fragile x syndrome*. PLoS ONE, 2008. **3**(1): p. e1486.

56. Polussa, J., A. Schneider, and R. Hagerman, *Molecular Advances Leading to Treatment Implications for Fragile X Premutation Carriers*. Brain Disord Ther, 2014. **3**.

57. Hagerman, R.J., et al., *Treatment of fragile X-associated tremor ataxia syndrome (FXTAS) and related neurological problems*. Clin Interv Aging, 2008. **3**(2): p. 251-62.

58. Hall, D.A., et al., *Symptomatic treatment in the fragile X-associated tremor/ataxia syndrome*. Movement Disorders, 2006. **21**(10): p. 1741-1744.

59. Weiss, D., et al., *Long-term outcome of deep brain stimulation in fragile X-associated tremor/ataxia syndrome*. Parkinsonism Relat Disord, 2015. **21**(3): p. 310-3.

60. Jacquemont, S., et al., *Aging in individuals with the FMR1 mutation*. Am J Ment Retard, 2004. **109**(2): p. 154-64.

61. Bourgeois, J.A., et al., *A review of fragile X premutation disorders: expanding the psychiatric perspective*. J Clin Psychiatry, 2009. **70**: p. 852-862.

62. Seritan, A.L., et al., *Memantine for fragile X-associated tremor/ataxia syndrome: a randomized, double-blind, placebo-controlled trial*. J Clin Psychiatry, 2014. **75**(3): p. 264-71.

63. Jain, K.K., *Evaluation of memantine for neuroprotection in dementia*. Expert Opin Investig Drugs, 2000. **9**(6): p. 1397-406.

64. Yang, J.C., et al., *Memantine effects on verbal memory in fragile X-associated tremor/ataxia syndrome (FXTAS): a double-blind brain potential study*. Neuropsychopharmacology, 2014. **39**(12): p. 2760-8.

65. Yang, J.C., et al., *Memantine Improves Attentional Processes in Fragile X-Associated Tremor/Ataxia Syndrome: Electrophysiological Evidence from a Randomized Controlled Trial*. Sci Rep, 2016. **6**: p. 21719.

66. Bontekoe, C.J., et al., *Instability of a (CGG)(98) repeat in the Fmr1 promoter*. Hum Mol Genet, 2001. **10**(16): p. 1693-9.

67. Peier, A. and D. Nelson, *Instability of a premutation-sized CGG repeat in FMR1 YAC transgenic mice*. Genomics, 2002. **80**(4): p. 423-432.

68. Willemsen, R., et al., *The FMR1 CGG repeat mouse displays ubiquitin-positive intranuclear neuronal inclusions; implications for the cerebellar tremor/ataxia syndrome*. Hum Mol Genet, 2003. **12**(9): p. 949-59.

69. Entezam, A., et al., *Regional FMRP deficits and large repeat expansions into the full mutation range in a new Fragile X premutation mouse model*. Gene, 2007. **395**: p. 125-134.

70. Hashem, V., et al., *Ectopic expression of CGG containing mRNA is neurotoxic in mammals*. Hum Mol Genet, 2009. **18**: p. 2443-2451.

71. Brouwer, J.R., et al., *CGG-repeat length and neuropathological and molecular correlates in a mouse model for fragile X-associated tremor/ataxia syndrome*. J Neurochem, 2008. **107**: p. 1671-1682.

72. Qurashi, A., et al., *Chemical screen reveals small molecules suppressing fragile X premutation rCGG repeat-mediated neurodegeneration in Drosophila*. Hum Mol Genet, 2012. **21**(9): p. 2068-2075.

73. Liu, J., et al., *Signaling defects in iPSC-derived fragile X premutation neurons*. Human Molecular Genetics, 2012. **21**(17): p. 3795-3805.

74. Cong, L., et al., *Multiplex genome engineering using CRISPR/Cas systems*. Science, 2013. **339**(6121): p. 819-23.

75. Mali, P., K.M. Esvelt, and G.M. Church, *Cas9 as a versatile tool for engineering biology*. Nat Methods, 2013. **10**(10): p. 957-63.

76. Park, C.Y., et al., *Reversion of FMR1 Methylation and Silencing by Editing the Triplet Repeats in Fragile X iPSC-Derived Neurons*. Cell Reports, 2015. **13**(2): p. 234-241.

77. Liang, P., et al., *CRISPR/Cas9-mediated gene editing in human tripronuclear zygotes*. Protein Cell, 2015. **6**(5): p. 363-72.

78. Lanphier, E., et al., *Don't edit the human germ line*. Nature, 2015. **519**(7544): p. 410-1.

79. Swiech, L., et al., *In vivo interrogation of gene function in the mammalian brain using CRISPR-Cas9*. Nat Biotechnol, 2015. **33**(1): p. 102-6.

80. Greco, C.M., et al., *Neuronal intranuclear inclusions in a new cerebellar tremor/ataxia*

syndrome among fragile X carriers. Brain, 2002. **125**(Pt 8): p. 1760-1771.

81. Evers, M.M., L.J. Toonen, and W.M. van Roon-Mom, *Antisense oligonucleotides in therapy for neurodegenerative disorders*. Adv Drug Deliv Rev, 2015. **87**: p. 90-103.

82. McClorey, G. and M.J. Wood, *An overview of the clinical application of antisense oligonucleotides for RNA-targeting therapies*. Curr Opin Pharmacol, 2015. **24**: p. 52-8.

83. Monia, B.P., et al., *Evaluation of 2'-modified oligonucleotides containing 2'-deoxy gaps as antisense inhibitors of gene expression.* J Biol Chem, 1993. **268**(19): p. 14514-22.

84. Tran, T., et al., *Targeting the r(CGG) Repeats That Cause FXTAS with Modularly Assembled Small Molecules and Oligonucleotides*. Acs Chemical Biology, 2014. **9**(4): p. 904-912.

85. Yang, W.Y., et al., *Inhibition of Non-ATG Translational Events in Cells via Covalent Small Molecules Targeting RNA.* Journal of the American Chemical Society, 2015. **137**(16): p. 5336-5345.

86. Bagni, C. and B.A. Oostra, *Fragile X syndrome: From protein function to therapy.* Am J Med Genet A, 2013. **161A**: p. 2809-2821.

87. Willemsen, R., et al., *Timing of the absence of FMR1 expression in full mutation chorionic villi.* Human Genetics, 2002. **110**(6): p. 601-605.

88. Levenga, J., et al., *Ultrastructural analysis of the functional domains in FMRP using primary hippocampal mouse neurons.* Neurobiol Dis, 2009. **35**: p. 241-250.

89. Kordasiewicz, H.B., et al., *Sustained therapeutic reversal of Huntington's disease by transient repression of huntingtin synthesis*. Neuron, 2012. **74**(6): p. 1031-44.

90. Whitesell, L., et al., *Stability, clearance, and disposition of intraventricularly administered oligodeoxynucleotides: implications for therapeutic application within the central nervous system.* Proc Natl Acad Sci U S A, 1993. **90**(10): p. 4665-9.

91. Butler, M., et al., *Spinal distribution and metabolism of 2'-O-(2-methoxyethyl)-modified oligonucleotides after intrathecal administration in rats*. Neuroscience, 2005. **131**(3): p. 705-15.

92. Ostergaard, M.E., et al., *Rational design of antisense oligonucleotides targeting single nucleotide polymorphisms for potent and allele selective suppression of mutant Huntingtin in the CNS*. Nucleic Acids Res, 2013. **41**(21): p. 9634-50.

93. Stanek, L.M., et al., *Antisense oligonucleotide-mediated correction of transcriptional dysregulation is correlated with behavioral benefits in the YAC128 mouse model of Huntington's disease*. J Huntingtons Dis, 2013. **2**(2): p. 217-28.

94. Southwell, A.L., et al., *In vivo evaluation of candidate allele-specific mutant huntingtin gene silencing antisense oligonucleotides*. Mol Ther, 2014. **22**(12): p. 2093-106.

95. Winer, L., et al., *SOD1 in cerebral spinal fluid as a pharmacodynamic marker for antisense oligonucleotide therapy.* JAMA Neurol, 2013. **70**(2): p. 201-7.

96. Smith, R.A., et al., *Antisense oligonucleotide therapy for neurodegenerative disease*. J Clin Invest, 2006. **116**(8): p. 2290-6.

97. Miller, T.M., et al., *An antisense oligonucleotide against SOD1 delivered intrathecally for patients with SOD1 familial amyotrophic lateral sclerosis: a phase 1, randomised, first-in-man study.* Lancet Neurol, 2013. **12**(5): p. 435-42.

98. Childs-Disney, J.L. and M.D. Disney, *Approaches to Validate and Manipulate RNA Targets with Small Molecules in Cells*. Annu Rev Pharmacol Toxicol, 2016. **56**: p. 123-40.

99. Parkesh, R., et al., *Design of a bioactive small molecule that targets the myotonic dystrophy type 1 RNA via an RNA motif-ligand database and chemical similarity searching.* J Am Chem Soc, 2012. **134**(10): p. 4731-42.

100. Disney, M.D., et al., *A Small Molecule That Targets r(CGG)(exp) and Improves Defects in Fragile X-Associated Tremor Ataxia Syndrome*. Acs Chemical Biology, 2012. **7**(10): p. 1711-1718.

101. Lee, M.M., A. Pushechnikov, and M.D. Disney, *Rational and modular design of potent ligands targeting the RNA that causes myotonic dystrophy 2*. ACS Chem Biol, 2009. **4**(5): p. 345-55.

102. Su, Z., et al., *Discovery of a biomarker and lead small molecules to target r(GGGGCC)-associated defects in c9FTD/ALS*. Neuron, 2014. **83**(5): p. 1043-50.

103. Xue, Y., et al., *Direct conversion of fibroblasts to neurons by reprogramming PTB-regulated microRNA circuits*. Cell, 2013. **152**(1-2): p. 82-96.

APPENDIX

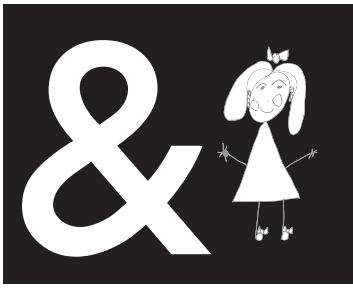

SUMMARY

Fragile X-associated Tremor/Ataxia syndrome (FXTAS), a late-onset monogenetic neurodegenerative disorder, is caused by an CGG-repeat expansion (55-200) in the 5' UTR of the *fragile-X mental retardation 1* gene (*FMR1*). Two disease mechanisms for FXTAS have been proposed. The first hypothesis is an RNA gain-of-function mechanism in which the *FMR1* RNA, containing an expanded CGG repeat, sequesters RNA-binding proteins. Sequestration of RNA-binding proteins into the inclusions might prevent them from exerting their normal function, thereby disturbing cellular function, which in the end might cause neurodegeneration. A second proposed mechanism is a repeat-associated non-AUG-initiated (RAN) protein gain-of-function mechanism in which the sequence upstream of the expanded CGG repeat triggers RAN translation and results in the expression of a cryptic polyglycine-containing protein, FMRpolyG.

Several mouse models have been generated to advance our understanding of the pathogenesis of FXTAS. **Chapter 1** summarizes the findings from studies using these mouse models. The mouse models display a high degree of similarity to premutation carriers with FXTAS, including the presence of elevated levels of *Fmr1* mRNA, decreased levels of FMRP, neurobehavioral deficits, and ubiquitin- and FMRpolyG-positive intranuclear inclusions. These and future mouse models are crucial for preclinical development of therapeutic intervention studies to improve neurological function in FXTAS.

In **chapter 2** we investigated the presence of FMRpolyG-positive intranuclear inclusions in CNS and non-CNS tissues from a premutation carrier with FXTAS. Co-localisation of FMRpolyG and ubiquitin is found in the vast majority of intranuclear inclusions. The presence of FMRpolyG-positive intranuclear inclusions in heart, kidney, adrenal gland and thyroid is consistent with the unexplained medical co-morbidities reported in some patients with FXTAS, including thyroid disease, cardiac arrhythmias, hypertension, migraine, impotence, and neuropathy. This suggests that FMRpolyG expression might also play a role in a toxic protein gain-of-function mechanism in the medical co-morbidities in FXTAS.

To study the pathogenesis of FXTAS and its reversibility, we generated new inducible transgenic mouse models for FXTAS, expressing RNA containing an expanded CGG repeat coupled to eGFP under control of the Tet-On promoter. **In chapter 3** we showed that use of the ubiquitous hnRNP-rtTA driver results in expression in all tissues examined upon doxycycline (dox) administration. Studies with this new inducible mouse model demonstrate that overexpression of RNA, containing an expanded CGG repeat, rather than overexpression of normal sized CGG RNA per se, leads to mitochondrial dysfunction in the liver, resulting in steatosis and apoptosis, and ultimately death of the mice.

The early death of the mice described in chapter 3, hampered the possibility to study the long-term effects of expanded CGG repeat expression in brain. Thus, a new strategy was explored to create bigenic transgenic mice in which exposure to dox induces

expression of either a control size 11CGG or an expanded 90CGG repeat RNA fused to an enhanced green fluorescent protein (eGFP) reporter in the brain of the inducible mice. In **chapter 4** we crossed the new inducible transgenic mice with a brain specific PrP-rtTA driver that further allowed us to study disease progression and possibilities of reversibility. In these mice we could induce the formation of ubiquitin-positive intranuclear inclusions, which also stain positive for the RAN translation product FMRpolyG. Formation of these inclusions is reversible after stopping expression of the RNA at an early developmental stage. Furthermore, we observed a deficit in the compensatory eye movements in these mice, a functional phenotype that could be reduced by stopping expression of the RNA early in disease development. This study showed for the first time the potential of disease reversibility and suggests that early intervention might be beneficial for FXTAS patients.

In **chapter 5** the pathogenic effect of translation of CGG repeats into FMRpolyG is further studied. We showed that a non-canonical ACG codon is the predominant site of initiation. In addition, we could demonstrate that *FMR1* mRNA harbors a small open reading frame (ORF), including the CGG repeat, upstream to the main FMRP ORF. Furthermore, we generated transgenic conditional mouse models expressing either RNA, containing an expanded CGG repeat, including the 5'UTR; or RNA containing an expanded CGG repeat without the 5'UTR. In the first mouse model RNA is produced and translated into FMRpolyG, whereas in the second model RNA is produced, but not translated into FMRpolyG (RNA-only). We found that expression of both FMRpolyG and RNA, containing an expanded CGG repeat, induces neuropathology and behavioural deficits, while RNA-only mice did not display any neuropathology or behavioural deficits. This study proves that FMRpolyG synthesis is required for the formation of inclusions and behavioural deficits in mice. Moreover, we found that (neuro)toxicity of FMRpolyG is mediated by its carboxy-terminus, causing disruption of the nuclear lamina architecture through binding to the LAP2ß protein. Finally, (over)expression of LAP2ß rescued neuronal cell death caused by expression of FMRpolyG.

Chapter 6 describes the generation of new inducible cellular models to study FXTAS. The *in vitro* models are derived from the inducible mice described in Chapter 3. In mouse embryonic fibroblasts, RNA levels can be reduced by RNase H-mediated degradation of the target mRNA. Unfortunately, no obvious pathology (e.g. inclusions) could be found in these cells. In a primary neuronal cell culture, induced expression of RNA, containing an expanded CGG repeat, leads to the formation of ubiquitin- and FMRpolyG-positive inclusions in both neurons and astrocytes. Inclusion formation can be partially prevented by the use of small chemical compounds that have been shown to shield the CGG hairpin in RNA molecules. This may open new avenues for a targeted therapeutic intervention.

In **chapter 7** the findings of the previous chapters are discussed in respect to previously published data.

SAMENVATTING

Fragiele X-geassocieerd tremor/ataxia syndroom (FXTAS) is een monogenetische, neurodegeneratieve aandoening die vaak pas op latere leeftijd tot uiting komt. FXTAS wordt veroorzaakt door een CGG repeat expansie (55-200) in het 5'UTR van het *fragile-X mental retardation 1* (*FMR1*) gen. Er zijn twee mechanismen die de ziekte kunnen veroorzaken. De eerste hypothese is dat *FMR1* boodschapper RNA, met een verlengde repeat, andere RNA bindende eiwitten aantrekt. Deze eiwitten kunnen dan hun normale functie niet meer uitoefenen, wat vervolgens andere cellulaire processen verstoort. Dit zou neurodegeneratie kunnen veroorzaken. Een tweede mechanisme is repeat geassocieerde, niet-AUG geïnitieerde (RAN) translatie. Hierbij wordt de CGG repeat vertaald in een toxisch, polyglycine bevattend eiwit, FMRpolyG.

Verschillende muismodellen zijn gegenereerd om de pathogenese van FXTAS beter te begrijpen. **Hoofdstuk 1** vat de bevindingen die gedaan zijn in de verschillende muismodellen samen. Deze muismodellen vertonen veel overeenkomsten met patiënten met FXTAS, zoals de aanwezigheid van verhoogde levels van *Fmr1* mRNA, verlaagde levels van FMRP, gedragsafwijkingen en ubiquitine- en FMRpolyG-positieve insluitsels. Deze en andere, nog te genereren, muismodellen zijn cruciaal voor de ontwikkeling van preklinische interventie studies om de neurologische functie van patiënten met FXTAS te verbeteren.

In **hoofdstuk 2** onderzoeken we de aanwezigheid van FMRpolyG-positieve, intranucleaire insluitsels in brein en andere organen van een premutatie drager met FXTAS. Co-lokalisatie van FMRpolyG en ubiquitine is gevonden in het merendeel van de insluitsels. De aanwezigheid van FMRpolyG-positieve, intranucleaire insluitsels in hart-, nier-, bijnier- en schildklier-weefsel komt overeen met de onverklaarde, medische co-morbiditeiten die beschreven zijn bij patiënten met FXTAS. Dit suggereert dat de expressie van FMRpolyG een rol speelt in het toxisch eiwit "gain-of-function" mechanisme bij de medische co-morbiditeiten in FXTAS.

Om de pathogenese en reversibiliteit van FXTAS verder te bestuderen hebben we nieuwe, induceerbare, transgene muismodellen ontwikkeld. In **hoofdstuk 3** hebben we gebruik gemaakt van een hnRNP-rtTA driverlijn met expressie van RNA, dat een verlengde CGG herhaling bevat, in alle weefsels. In dit muismodel hebben we aangetoond dat overexpressie van RNA met een verlengde CGG repeat leidt tot mitochondrieel disfunctioneren in de lever van deze muizen. Dit leidt weer tot steatose en apoptose en uiteindelijk gaan deze muizen kort (1 week) na doxycycline (dox) inductie dood. In muizen waarbij we het RNA met slechts 11 CGG herhalingen tot overexpressie brengen zien we geen effect. Dit betekent dat niet overexpressie, maar de lengte van de CGG repeat de onderliggende problemen veroorzaakt.

Omdat de muizen beschreven in hoofdstuk 3 snel na dox inductie dood gaan, kunnen we niet het lange termijn effect in het brein van deze muizen bestuderen. Om dit te

kunnen doen, hebben we een nieuwe strategie ontwikkeld. In **hoofdstuk 4** zijn deze muizen ingekruist met een brein specifieke PrP-rtTA driverlijn. In deze muizen kunnen we onderzoeken hoe de aanmaak van ubiquitine- en FMRpolyG positieve inclusies zich in de tijd ontwikkelt. Verder hebben we gevonden dat de formatie van deze insluitsels reversibel is als de RNA expressie vroeg in het ziekteproces wordt gestopt. In een functionele gedragstest waarbij de oogbeweging wordt geregistreerd, kan dit gedragsfenotype verminderd worden door de RNA expressie vroeg in het ziekteproces te stoppen. Deze studie laat voor het eerst zien dat het ziekteproces in FXTAS muizen omkeerbaar is en suggereert dat een vroege interventie gunstig is voor patiënten met FXTAS.

In **hoofdstuk 5** bestuderen we het pathogene effect van de RAN translatie van de CGG herhaling in FMRpolyG. We hebben aangetoond dat een ACG codon zorgt voor initiatie van de translatie. Verder tonen we aan dat het *FMR1* mRNA een klein open reading frame (ORF) inclusief CGG herhaling bevat, upstream van het FMRP ORF. Daarnaast hebben we nieuwe, conditionele, transgene muismodellen ontwikkeld met en zonder de sequentie die zorgt voor de initiatie van de RAN translatie. Het eerste muismodel produceert RNA dat vertaald wordt in FMRpolyG, terwijl het tweede model alleen RNA produceert (RNA only). In het eerste muismodel dat zowel RNA met een verlengde repeat als FMRpolyG tot expressie brengt ontwikkelen zich neuropathologie en gedragsafwijkingen. Omdat beide niet gevonden worden in het RNA only muismodel, betekent dit dat de synthese van FMRpolyG noodzakelijk is voor zowel inclusie formatie als gedragsafwijkingen. Tenslotte hebben we gevonden dat het LAP2β eiwit bindt aan de carboxy-terminus van FMRpolyG en dat dit zorgt voor verstoring van het kernmembraan. Overexpressie van LAP2β herstelt de neuronale celdood die veroorzaakt wordt door FMRpolyG.

Hoofdstuk 6 beschrijft de generatie van nieuwe induceerbare cellulaire modellen. Deze *in vitro* modellen zijn afgeleid van het induceerbare muismodel beschreven in hoofdstuk 3. In embryonale muizen fibroblasten kunnen RNA levels gereduceerd worden met behulp van antisense oligonucleotiden. In dit celtype is echter geen duidelijke pathologie (bv. inclusie formatie) aanwezig. Daarentegen worden in primaire, hippocampale kweken afgeleid van deze muizen ubiquitine- en FMRpolyG-positieve intranuclaire insluitsels gevonden in zowel neuronen als astrocyten. Door het toevoegen van kleine chemische compounds die binden aan de CGG hairpin structuur in de RNA moleculen kan de vorming van insluitsels gedeeltelijk voorkomen worden. Deze bevindingen openen mogelijkheden voor therapeutische interventie studies om specifiek in te grijpen bij patiënten met FXTAS.

In **hoofdstuk 7** worden de bevindingen van de voorafgaande hoofdstukken in het licht van de bestaande literatuur bediscussieerd.

CURRICULUM VITAE

Personal information

Name:	Ronald Adrianus Maria Buijsen
Date of birth:	January 22nd, 1981
Place of birth:	Bergen op Zoom
e-mail:	rbuijsen@hotmail.com

Professional experience

September 2012 – June 2016

PhD student, Department of Clinical Genetics, Erasmus MC Rotterdam, the Netherlands.
Thesis: Fragile X-associated Tremor/Ataxia Syndrome (FXTAS): RNA or RAN?

June 2007 – September 2012

Research technician, Department of Clinical Genetics, Erasmus MC Rotterdam, the Netherlands.
Project: Experimental approaches towards therapeutic intervention in Fragile X Syndrome (FXS).
Gaining insight in molecular pathways involved in FXS and elucidating the role of the Fragile X mental retardation protein (FMRP) in synaptic transmission and plasticity by investigating neuronal morphology, protein expression and animal behavior using different transgenic mouse lines and cellular models.

Education

October 2006 – June 2007

Intern, Department of Cell biology and Bioinformatics, Erasmus MC Rotterdam, the Netherlands.
Project: Identification of GPCRs in *c. elegans*.

February 2006 – October 2006

Intern, Department of Experimental Cardiology, Erasmus MC Rotterdam, the Netherlands.
Project: Investigate the role of VEGF in heart failure.

2004 – 2007

Study: Bachelor of applied science (BSc) at Avans University, Breda
Major: Biomedical science and laboratory animal science (article 12 Experiments on Animals Act)

LIST OF PUBLICATIONS

Sellier C, **Buijsen RAM**, He F, Jung L, Tropel P, Gaucherot A, Jacobs H, Meziane H, Vincent A, Champy M, Sorg T, Pavlovic G, Wattenhofer-Donze M, Birling M, Eberling P, Ruffenach F, Page A, Anheim M, Martinez-Cerdeno V, Hagerman PJ, Tassone F, Willemsen R, Hukema RK, Viville S, Martinat C, Todd PK, Charlet-Berguerand N. *RAN translation of expanded CGG repeats is pathogenic in Fragile X-associated Tremor/Ataxia Syndrome*. Manuscript in revision for Neuron, 2016.

Buijsen RAM, de Boer H, Severijnen EAWFM, Minneboo M, Verhagen RFM, Schoof M, de Korte V, Berman RF, Charlet-Berguerand N, Wansink DG, Disney MD, Willemsen R, Hukema RK. *Inhibition of the formation of intranuclear inclusions by small chemical compounds in an inducible neuronal cellular model for FXTAS*. Manuscript in preparation.

Buijsen RAM[*], Visser JA[*], Kramer P, Severijnen EA, Gearing M, Charlet-Berguerand N, Sherman SL, Berman RF, Willemsen R, Hukema RK. *Presence of inclusions positive for polyglycine containing protein, FMRpolyG, indicates that repeat-associated non-AUG translation plays a role in fragile X-associated primary ovarian insufficiency.* Hum Reprod. 2016 Jan;31(1):158-68. doi: 10.1093/humrep/dev280. Epub 2015 Nov 3. PubMed PMID: 26537920; PubMed Central PMCID: PMC4677964.

Buijsen RAM[*], Hukema RK[*], Schonewille M[*], Raske C, Severijnen LA, Nieuwenhuizen-Bakker I, Verhagen RF, van Dessel L, Maas A, Charlet-Berguerand N, De Zeeuw CI, Hagerman PJ, Berman RF[#], Willemsen R[#]. *Reversibility of neuropathology and motor deficits in an inducible mouse model for FXTAS*. Hum Mol Genet. 2015 Sep 1;24(17):4948-57. doi: 10.1093/hmg/ddv216. Epub 2015 Jun 9. PubMed PMID: 26060190; PubMed Central PMCID: PMC4527492.

de Esch CE, van den Berg WE, **Buijsen RAM**, Jaafar IA, Nieuwenhuizen-Bakker IM, Gasparini F, Kushner SA, Willemsen R. *Fragile X mice have robust mGluR5-dependent alterations of social behaviour in the Automated Tube Test.* Neurobiol Dis. 2015 Mar;75:31-9. doi: 10.1016/j.nbd.2014.12.021. Epub 2015 Jan 3. PubMed PMID: 25562659.

Buijsen RAM[*], Hukema RK[*], Raske C, Severijnen LA, Nieuwenhuizen-Bakker I, Minneboo M, Maas A, de Crom R, Kros JM, Hagerman PJ, Berman RF[#], Willemsen R[#]. *Induced expression of expanded CGG RNA causes mitochondrial dysfunction in vivo.* Cell Cycle. 2014;13(16):2600-8. doi: 10.4161/15384101.2014.943112. PubMed PMID: 25486200; PubMed Central PMCID: PMC4614669.

Buijsen RAM, Sellier C, Severijnen LA, Oulad-Abdelghani M, Verhagen RF, Berman RF, Charlet-Berguerand N, Willemsen R[#], Hukema RK[#]. *FMRpolyG-positive inclusions in CNS and non-CNS organs of a fragile X premutation carrier with fragile X-associated tremor/ataxia syndrome*. Acta Neuropathol Commun. 2014 Nov 26;2:162. doi: 10.1186/s40478-014-0162-2. PubMed PMID: 25471011; PubMed Central PMCID: PMC4254384.

Berman RF, **Buijsen RAM**, Usdin K, Pintado E, Kooy F, Pretto D, Pessah IN, NelsonDL, Zalewski Z, Charlet-Bergeurand N, Willemsen R, Hukema RK. *Mouse models of the fragile X premutation and fragile X-associated tremor/ataxia syndrome*. J Neurodev Disord. 2014;6(1):25. doi: 10.1186/1866-1955-6-25. Epub 2014 Jul 30. Review. PubMed PMID: 25136376; PubMed Central PMCID: PMC4135345.

Pop AS, Levenga J, de Esch CE, **Buijsen RAM**, Nieuwenhuizen IM, Li T, Isaacs A, Gasparini F, Oostra BA, Willemsen R. *Rescue of dendritic spine phenotype in Fmr1 KO mice with the mGluR5 antagonist AFQ056/Mavoglurant*. Psychopharmacology (Berl). 2014 Mar;231(6):1227-35. doi: 10.1007/s00213-012-2947-y. Epub 2012 Dec 21. PubMed PMID: 23254376.

Gantois I, Pop AS, de Esch CE, **Buijsen RAM**, Pooters T, Gomez-Mancilla B, Gasparini F, Oostra BA, D'Hooge R, Willemsen R. *Chronic administration of AFQ056/Mavoglurant restores social behaviour in Fmr1 knockout mice*. Behav Brain Res. 2013 Feb 15;239:72-9. doi: 10.1016/j.bbr.2012.10.059. Epub 2012 Nov 6. PubMed PMID: 23142366.

Vinueza Veloz MF, **Buijsen RAM**, Willemsen R, Cupido A, Bosman LW, Koekkoek SK, Potters JW, Oostra BA, De Zeeuw CI. *The effect of an mGluR5 inhibitor on procedural memory and avoidance discrimination impairments in Fmr1 KO mice*. Genes Brain Behav. 2012 Apr;11(3):325-31. doi: 10.1111/j.1601-183X.2011.00763.x. Epub 2012 Jan 19. PubMed PMID: 22257369; PubMed Central PMCID: PMC3491868.

Levenga J, de Vrij FM, **Buijsen RAM**, Li T, Nieuwenhuizen IM, Pop A, Oostra BA, Willemsen R. *Subregion-specific dendritic spine abnormalities in the hippocampus of Fmr1 KO mice*. Neurobiol Learn Mem. 2011 May;95(4):467-72. doi: 10.1016/j.nlm.2011.02.009. Epub 2011 Mar 1. PubMed PMID: 21371563.

Levenga J[*], Hayashi S[*], de Vrij FM, Koekkoek SK, van der Linde HC, Nieuwenhuizen I, Song C, **Buijsen RAM**, Pop AS, Gomezmancilla B, Nelson DL, Willemsen R, Gasparini F, Oostra BA. *AFQ056, a new mGluR5 antagonist for treatment of fragile X syndrome*. Neurobiol Dis. 2011 Jun;42(3):311-7. doi: 10.1016/j.nbd.2011.01.022. Epub 2011 Feb 21. PubMed PMID: 21316452.

Levenga J, **Buijsen RAM**, Rifé M, Moine H, Nelson DL, Oostra BA, Willemsen R, de Vrij FM. *Ultrastructural analysis of the functional domains in FMRP using primary hippocampal mouse neurons*. Neurobiol Dis. 2009 Aug;35(2):241-50. doi: 10.1016/j.nbd.2009.05.004. Epub 2009 May 21. PubMed PMID: 19464371; PubMed Central PMCID: PMC2757577.

[*] Co-First authorship

[#] Co-Last authorship

Book Chapter

Foote MM, Careaga M, **Buijsen RAM**, Berman RF, Willemsen R, Hukema RK**.** *Animal Models for FXTAS.The Fragile X-Associated Tremor Ataxia Syndrome (FXTAS),* Springer. In press.

PHD PORTFOLIO

Name PhD student:	Ronald Buijsen
Department:	Clinical Genetics, Erasmus MC
Research School:	Medical Genetics Centre South-West Netherlands (MGC)
PhD-period:	September 1st 2012 – June 22nd 2016
Promotor:	Prof.dr. R. Willemsen
Co-promotor:	Dr. R.K. Hukema

PhD training	Year(s)	Workload (ECTS)
General courses		
Safely working in the laboratory	2012	0.25 ECTS
Laboratory animal science (article 9 experiments on animals act)	2013	3 ECTS
Literature course	2014	2 ECTS
Research integrity	2014	0.3 ECTS
Statistics	2014	2 ECTS
English biomedical writing and communication	2015	3 ECTS
Specific courses		
Introduction to the confocal microscope	2012	0.25 ECTS
PhD teaching program of biomedical science		
– Biochemistry and biophysics	2012	3 ECTS
– Cell and developmental biology	2013	3 ECTS
– Genetics	2013	3 ECTS
Animal handling course (IVC)	2013	0.25 ECTS
MGC Epigenetic regulation in health and disease	2014	0.8 ECTS
Seminars and workshops		
MGC PhD workshop Luxemburg	2013	1 ECTS
MGC PhD workshop Münster	2014	1 ECTS
Fragiele X symposium	2014	0.25 ECTS
MGC PhD workshop Maastricht	2015	1 ECTS
FENS SfN Summer School: Shared mechanisms and specificity in neurodegenerative diseases	2015	2 ECTS
AMIE OIC symposium: Advanced imaging techniques: Today's discoveries, tomorrow's therapies	2015	0.25 ECTS
Fellowsymposium hersenstichting	2015	0.25 ECTS
PhD day: Surviving your PhD!	2015	0.25 ECTS
FXTAS day	2015	0.25 ECTS
Sophia research day	2015	0.25 ECTS
Sophia research day	2016	0.25 ECTS
Various seminars department of clinical genetics	2012-2016	2 ECTS

PhD training	Year(s)	Workload (ECTS)
Presentations		
1st International conference on *FMR1* premutation: Basic mechanisms and clinical involvement	2013	1 ECTS
2nd International conference on *FMR1* premutation: Basic mechanisms and clinical involvement	2015	1 ECTS
MGC PhD workshop Maastricht	2015	0.5 ECTS
FENS SfN Summer School: Shared mechanisms and specificity in neurodegenerative diseases	2015	0.5 ECTS
Group work discussions	2012-2016	4 ECTS
Department of clinical genetics research meeting	2012-2016	2 ECTS
Journal club clinical genetics	2014-2016	1 ECTS
(Inter)national conferences		
NVHG Autumn symposium, Arnhem, The Netherlands	2012	0.5 ECTS
1st International Conference on *FMR1* Premutation: Basic Mechanisms and Clinical Involvement, Perugia, Italy	2013	1 ECTS
NVHG Autumn symposium, Arnhem, The Netherlands	2013	0.25 ECTS
MGC symposium, Rotterdam, The Netherlands	2013	0.25 ECTS
MGC symposium, Rotterdam, The Netherlands	2014	0.25 ECTS
2nd International Conference on *FMR1* Premutation: Basic Mechanisms and Clinical Involvement, Barcelona, Spain	2015	1 ECTS
Translational Neuroscience Network (TN2): From Mechanisms to Therapy in Neurodegeneration, 2015, Amsterdam, The Netherlands	2015	0.25 ECTS
Teaching		
Practical course Junior Med School, Erasmus MC	2012-2014	1 ECTS
Practical course master of neuroscience	2012-2014	1 ECTS
Practical course master of molecular medicine	2012-2014	1 ECTS
Supervising Michelle Minneboo, HLO bachelor thesis, Avans University, Breda	2012-2013	2 ECTS
Supervising Rob Verhagen, HLO bachelor thesis, Avans University, Breda	2013-2014	2 ECTS
Supervising Miriam Schoof, HLO bachelor thesis, Hogeschool Leiden, Leiden	2014-2016	2 ECTS
Supervising Verna de Korte, HLO bachelor thesis, Avans University, Breda	2015-2016	2 ECTS
Institutional Responsibilities		
Organising and chairing journal club for PhD students Department of Clinical Genetics	2014-2016	
Supervisor ML-I laboratory (VMT)	2012-2016	
Contact Person GMO permit Department of Clinical Genetics	2012-2016	

DANKWOORD

Jaaaa, het is zo ver! Mijn "boekje" is af!! Ik heb de afgelopen jaren met heel veel plezier onderzoek mogen doen op de afdeling klinische genetica. In al die jaren heb ik niet alleen heel erg veel geleerd, maar ik heb het ook altijd heel erg naar mijn zin gehad. Het doen van goed onderzoek is een teamsport en daarom wil ik iedereen die mij op wat voor manier dan ook heeft geholpen, bedanken!

Meintje, lieve schat, zonder jou was het nooit gelukt om dit voor elkaar te krijgen. Jij hebt mij altijd gesteund nadat we de beslissing hadden genomen dat ik ging promoveren. Sofie en Wouter, ik vind onderzoek doen geweldig, maar ik vind het nog veel leuker om samen met jullie te knutselen, spelletjes te spelen, te zwemmen, te voetballen en al die andere leuke dingen te doen. Ik ben heel erg trots dat jullie de mooie tekeningen hebben gemaakt die aan het begin van elk hoofdstuk staan. Meintje, Sofie en Wouter, ik hou van jullie! Dan mijn ouders, pa en ma, ik ben jullie heel erg dankbaar dat ik altijd alle mogelijkheden heb gehad om te doen wat ik bedacht had dat ik wilde doen. Ik zal de woorden van pa nooit vergeten: "Ga doen wat je leuk vindt om te doen!" Dat is op het lab zeker gelukt. Ma, ik vind het ontzettend knap hoe je na het overlijden van pa bent doorgegaan. Nu is het mijn beurt om te zeggen dat ik trots op je ben!

Rob en Renate, ik ben heel erg blij geweest met jullie als mijn begeleiders. Vanaf het moment dat ik aangaf dat ik wel OIO wilde worden tot aan het schrijven van mijn thesis zijn jullie altijd enthousiast en positief geweest. Rob, je bent echt de beste promotor die er kan zijn. De deur stond altijd open en ik kon altijd terecht met al mijn (vaak onzinnige) vragen. Op wetenschappelijk gebied heb ik veel van je kunnen leren, maar ik heb ook de vrijheid gehad om zelf projecten en technieken op te pakken en zelfs om af en toe een reeksje te doen. Ook op persoonlijk vlak ben je een voorbeeld voor iedereen. Renate, ik vind het helemaal geweldig dat ik de afgelopen jaren jouw "work husband" mocht zijn. Ik waardeer je eerlijkheid en rechtlijnigheid. De ochtendkoffie was vaak een goed moment om zowel de laatste experimenten als het wereldnieuws door te nemen. Vooral op wetenschappelijk gebied denken we vaak hetzelfde en ik ben zeer trots op wat we, samen met de groep, de laatste jaren hebben bereikt.

Dan mijn paranimfen. Lies-Anne, je bent in al die jaren zowel letterlijk als figuurlijk altijd mijn chauffeur geweest. Niet alleen mocht ik vaak mee naar huis rijden na feestjes, of als de trein toevallig eens een keer niet reed, ook ben je dé expert in kleuringen. Je hebt ontelbaar veel coupes gesneden, kleuringen gedaan en foto's gemaakt, waar ik dan weer gebruik van kon maken. Een van de vele, mooie foto's is te zien op de voorkant van mijn boekje. Ingeborg, de eerste dag dat ik begon als analist klikte het gelijk. Ik heb zo'n beetje alle technieken die je op een lab gebruikt van jou geleerd, met als belangrijkste alles wat komt kijken bij het werken met muizen. Ik vond het heel erg jammer dat je ons lab verliet, maar ik denk dat je als juf helemaal op je plek zit. Guido, wat zou het lab zijn zonder jou? In

de ochtend, voordat iemand anders op het lab aanwezig was, hadden we vaak al van alles en nog wat besproken met een bakje koffie. Ook kon ik altijd terecht voor advies over van alles en nog wat. Verder heb je niet alleen na mijn eerste halve marathon geholpen om mijn veters en schoenen los te maken, ook heb je twee keer als haas gelopen voor de marathon van Rotterdam. Zonder jou was het nog zwaarder geweest.

Nicolas, thank you for being part of the inner committee and flying in to be present at the defense :o)). Chantal, thanks for learning me how to do a proper fluorescent in situ hybridisation. Nicolas and Chantal, thank you for our great collaboration and your support on the articles we have published together!

Graag wil ik ook iedereen van de FXS-FXTAS-FTD-groep bedanken voor alle hulp bij experimenten en de discussies tijdens onze werkbesprekingen. Helen, bedankt voor de neuronenkweken, het kloneren en alle jaren 90 muziek op de radio. Shimriet en Fenne, volgens mij gaat het ook met jullie boekjes helemaal goed komen. Shimriet, wij hebben in elke zitkamer altijd bij elkaar gezeten en elkaar zo vaak kunnen helpen (en soms ook afleiden). Met zoveel data is promoveren geen probleem en ik weet zeker dat je over een aantal jaren een prima klinisch geneticus bent. Fenne, bedankt voor al je input. Ik heb de laatste jaren veel van je geleerd. Ik vind het heel erg knap hoe je in korte tijd zoveel verder bent gekomen met je onderzoek en hoe je nieuwe onderzoeksrichtingen bedenkt en uitvoert. Shami, met jou op het lab valt er altijd wat te lachen. Je werkt pas kort als analist, maar het lijkt alsof je er al jaren zit.

Dan de stagiaires, Michelle, Rob , Miriam en Verna. Bedankt voor de inzet tijdens jullie stage periodes. Ik hoop dat jullie wat geleerd hebben, maar ik heb in ieder geval veel van jullie geleerd. Michelle, ik was heel erg blij dat wij samen konden beginnen aan dit project. Je stage ging zo goed dat je na je stage zelfs kon blijven. Ik vind het mooi om te zien hoe je bent blijven groeien als analist. Rob, je was de eerste op het lab met een goede muzieksmaak en je voelde je op het lab al snel als een vis in het water. Tijdens je stage heb je vooral veel mooie kleuringen gedaan. Miriam, ik vind het knap dat je, ondanks alle tegenslag, toch positief bent gebleven. Verna, vanaf de eerste dag was je erg handig op het lab en ook met je verslag heb je veel indruk gemaakt. Ik weet zeker dat het goed gaat komen met je afstuderen.

Verder wil ik iedereen bedanken die in de fragiel-X groep heeft gewerkt. Ik heb veel met jullie kunnen lachen, maar in al die jaren ook heel erg veel geleerd! Herma, bedankt voor al je advies. Heel erg vaak gevraagd, soms ook ongevraagd. Samen met Lies-Anne heb je mij overgehaald om OIO te worden, bedankt hiervoor! Edwin, eigenlijk zou iedere groep iemand als jou moeten hebben! Niet alleen weet je echt alles op het lab, ook ben je de sfeermaker in welke groep dan ook. Ben, ik heb van jou vooral geleerd om altijd de goede controles mee te nemen. Ik vind het een eer dat je voorzitter wilt zijn bij mijn promotie. Femke, Judith en Josien, jullie enthousiasme voor het onderzoek heeft er voor gezorgd

dat ik me gelijk thuis voelde in groep. Andreea en Celine, jullie hele promotietraject heb ik mee mogen maken. Ik heb altijd met veel plezier met jullie samengewerkt en Andreea, ik vond het een eer om jouw paranimf te zijn. Alan, je zat maar kort bij onze groep, maar vooral de premutatie meeting in Perugia was onvergetelijk. Ook wil ik alle studenten bedanken die stage hebben gelopen binnen onze groep: Sotos (ευχαριστώ), Christina (Knossos), Lisanne, Karin, Tamrat, Adi, Widagdo, Josja, Tracy en Laura-Ashley.

Een lab zou niks zijn zonder vaste krachten waar je op kan terugvallen. Marianne, jij bent eigenlijk de moeder van het lab. Altijd even attent en oprecht geïnteresseerd in iedereen. Bianca, jij hebt altijd de mooiste verhalen over al je verre reizen. Bedankt dat je mij bij alle hardloopwedstrijden weer kon vinden en kon voorzien van water en een banaan. Rachel, de vaste bewoner van het "eiwitlab". Sorry voor alle overlast tijdens de kleuringen. Mark, Leontine en Marian, jullie zijn als functionele unit naar boven verhuisd. Jammer, maar altijd handig als ik weer eens wat moest lenen.

Dan mijn mede-OIO's, samen hebben we ons door alle cursussen en onderwijsverplichtingen heen geslagen. Ook konden we samen onze projecten en het leven als OIO bespreken en ideeën uitwisselen. De PhD workshops in Luxemburg, Münster en Maastricht waren zowel op wetenschappelijk als op sociaal gebied een groot succes. Atze, ik vind het een eer dat ik jouw paranimf mag zijn. Je ligt prima op koers voor je promotie (waar ik nu al naar uit kijk). Ik vind het ontzettend knap wat je in vier jaar samen met Erik op deze, voor jullie groep, nieuwe afdeling hebt opgebouwd. Erik, ik weet zeker dat jij volgend jaar ook een prachtig boekje hebt. Danny, semoga sukses dengan tesismu. Kau adalah ilmuwan Dan ayah yang hebat. Rajendra, tumhari PhD ki samapti ke liye dher sari shubhkamnayein. Katherine, thanks for being my English grammar and spelling checker. Rhiana, bedankt voor je enthousiasme en hulp met het opzetten van de journal club. Roy, jij bent de ideale kamergenoot. Je klaagt echt nooit ergens over. Simone, thanks for answering all my thesis and thesis defense related questions. Alle andere OIO's, bedankt voor jullie gesprekken in de gang/op het lab/bij het koffiezetapparaat.

Suzanne, bedankt dat je aan mij dacht toen er op de 9de een plek vrijkwam als analist. Bedankt ook voor de vele keren dat ik mee mocht rijden. Tjakko en Erwin bedankt dat we het op peil houden van de conditie konden combineren met onofficiële werkbesprekingen. Annelies, bedankt voor je hulp met betrekking tot de ML-I labs en de GGO vergunning. De afgelopen jaren zijn er helaas ook veel goede mensen vertrokken. Christan en Erik, bedankt voor de mooie tijd op het lab. Onze kart en bowling uitjes zal ik niet snel vergeten. E*, jij bent een groot voorbeeld voor iedereen. Je hebt heel veel OIO's verder geholpen met het onderzoek, zonder ook maar een moment aan jezelf te denken. Francesca and Tianna, thanks for being around in the lab.

De vele mensen die altijd klaar staan voor het ondersteunende werk. Zonder jullie zou het lab leven een stuk zwaarder zijn. Jeannette en Bep, bedankt voor het aanmelden van

studenten, het opsturen van pakjes, het doorsturen van e-mailtjes en al het vele andere. Tom en Ruud, bedankt voor alle foto's en het bewerkingen van de vele figuren. Tom, bedankt voor de hulp tijdens het maken van mijn thesis. Je hebt er voor gezorgd dat de figuren er netjes uitzien. Gert en Gert-Jan, je hoefde maar te bellen en jullie stonden altijd gelijk klaar om te helpen of om een probleem op te lossen. Alex en John, bedankt voor de vele µ-injecties. Zonder jullie hulp waren er geen FXTAS muizen geweest en had mijn thesis een stuk korter geweest. Alle dierverzorgsters, Ineke, Sandra, Michelle, Jenny, Charlotte, Kim, Jennifer, Jessica en Jolien. Bedankt voor het geven van dox, het opzetten van breedings en pluggings en het vele andere werk wat jullie hebben gedaan. Marjoleine, bedankt voor de hulp bij alle het OIO regelwerk en cursussen. Koos en Leo, bedankt voor het bestellen en rondbrengen van de pakketjes. Sjozef, Ton, Nils, Mario, Leo en Pim, bedankt voor de technische ondersteuning. Tomassia, bedankt voor het schoonmaken (en bijkletsen).

Prof.dr. Kooy (Frank) en Prof.dr. Kros (Max): bedankt dat jullie in de kleine commissie wilden zitten en dat jullie het manuscript kritisch hebben doorgenomen. Prof.dr. Kremer (Berry) en Dr. Wansink (Rick), bedankt dat jullie de tijd willen nemen om in de grote commissie plaats te nemen.

A big thanks to all our collaborators! Rob (Berman), thanks for all the scientific conversations and support on the articles we have published together. Prof.dr. Disney (Matthew) and Dr. Yang (Wang-Yong), thank you for sharing your compounds. Cecile, your large-scale iPSC-cell culture facility can be a very useful tool in the FXTAS field. Oliver and Monica, good luck with the further characterisation of the inducible mice. Chris en Martijn, bedankt voor de samenwerking betreffende het reversibility paper. Jenny en Piet, bedankt voor al jullie hulp bij het FXPOI paper.

Graag wil ik ook alle familie, vrienden en kennissen bedanken voor de interesse in mijn onderzoek. Vaak heb ik met veel plezier mogen uitleggen wat ik nu precies aan het doen ben in Rotterdam.

Als laatste wil ik graag de Fragiele X Vereniging Nederland en alle premutatiedragers bedanken. De FXTAS dag georganiseerd door de vereniging was een groot succes. Door te praten met de mensen die het aangaat, leer je wat er speelt. Ik hoop dat ik, door een heel klein steentje bij te dragen aan het onderzoek aan FXTAS, geïnteresseerden weer een klein beetje beter kan uitleggen hoe het komt dat premutatiedragers FXTAS ontwikkelen. En dat we met die kennis, in de toekomst, zelfs kunnen werken aan de ontwikkeling van een interventie. Verder zal ik nooit vergeten hoe trots de familie van een overleden patiënt met FXTAS was, dat hun familielid meer inzicht heeft gegeven over het ontstaan van FXTAS. Bedankt!!

Ronald